New Taxa of Marine Ostracods (Anticytherideinae, n. subfam.) from the Upper Cretaceous (Campanian and Maastrichtian) of Mississippi, Alabama and Tennessee, U. S. Gulf Coastal Plain

Terry Markham Puckett[1] and Gene Hunt[2]
[1]*School of Biological, Environmental and Earth Sciences, The University of Southern Mississippi*
118 College Drive, Hattiesburg, Mississippi, 39406, USA
email: Mark.Puckett@usm.edu
[2]*Department of Paleobiology, Smithsonian Institution, 10th St. & Constitution Ave. NW, Washington, DC 20560, USA*

ABSTRACT: This contribution describes new species, genera and a subfamily (Anticytherideinae) of ostracods from the Upper Cretaceous (mid-late Campanian-Maastrichtian) marine deposits of the eastern flank of the Mississippi Embayment. New taxa assigned to the subfamily include *Anticythereis dorsennus* and *A. slipperi*; the new genus *Asculdoracythereis,* which includes the new species *As. asculdora*, *As. invicta*, and *As. pseudoalabamensis*; the new genus *Frodocythereis*, which includes the new species *F. frodoi*; the new genus *Laevipellacythereis*, which includes the new species *L. colossus* and *L. laevipellis*; and the new genus *Tumulocythereis*, which includes the new species *T. incompta*, *T. tiberti*, and *T. tumulus*. Previously described species assigned to the genus *Anticythereis* are re-evaluated, some of which are assigned to one of the new genera. Synapomorphic characters of the new subfamily include a combination of pronounced external post-ocular sulcus with corresponding pair of internal, rimmed inverted platforms and a distinctive "yin-yang" adductor muscle scar pattern.

The taxa display remarkably rapid evolution. The earliest species (*Anticythereis* sp. 1) occurs in the planktonic foraminiferal *Radotruncana calcarata* Taxon Range Zone of mid- to late Campanian age and by the end of the Maastrichtian there are more than 20 species. Most species have very localized occurrences, including several that occur only at a single outcrop. Although species are found on the eastern flank of the Mississippi Embayment and the Atlantic Coastal Plain, none have been observed on the western flank of the Mississippi Embayment. Species have been assigned to the genus *Anticythereis* from other continents (South America, Europe and Africa), but those taxa lack distinctive features of the Anticytherideinae, which is endemic to North America. The group became extinct at the Cretaceous-Paleogene boundary.

Keywords: Late Cretaceous, ostracod, *Anticythereis*, North America, Gulf Coastal Plain

INTRODUCTION

In the 1990's, the first author spoke with Joseph Hazel, ostracod specialist at the Louisiana State University, who indicated an anomalously diverse group of ostracodes assigned to the genus *Anticythereis* that included possibly more than 20 species from the Atlantic Coastal Plain and eastern side of the Mississippi Embayment, many of which were undescribed. The group also appeared to include species that differ only subtly from each other, whereas others differ considerably. Hazel's graduate student, Kasana Pitakpaivan, studied the ostracods of the K-Pg boundary and included images of twelve species that were left in open nomenclature and one that was previously described (*Anticythereis copelandi* Smith, 1978) in her dissertation (Pitakpaivan 1994). Many of these species are very rare and apparently restricted to very small geographic areas; none appear to occur in the Upper Cretaceous deposits of the western side of the Mississippi Embayment and most are restricted to either the Atlantic or Gulf Coastal Plains. Table 1 lists the species names, their original generic assignments, authors, formations where collected, type localities and ages for the species recognized in this study. This geographic restriction has numerous implications, as there have been many species assigned to *Anticythereis* from other parts of the world, including North and West Africa and the Middle East (Al-Furaih 1980; Apostolescu 1961; Barsotti 1963; Carbonnel 1986, 1988; Cronin and Khalifa 1979; Damotte 1982; El-Nady 2002; Gebhardt 1999; Grekoff 1964; Grosdidier 1973, 1979; Honigstein 1984; Honigstein et al. 1985; Ismail and Soliman 1997; Khalifa and Cronin 1979; Masoli 1965; Reyment 1980; Reyment and Reyment 1980; Shahin 2005; van den Bold 1964), South America (Bertels 1973, 1975b, 1975a, 1976, 1977) and Europe (Bosquet 1854; Deroo 1966; van Veen 1936) (Table 2). As detailed herein, most of the key morphological characters, including the anterior hinge element, the pair of inverted platforms corresponding to the inside of the post-ocular sulcus, and muscle scar patterns, are located on the inside of the carapace, yet these features are published for only a few of these species (*A. euglypha* (Bosquet 1854, *A.? inconnexa* Bertels 1973, *A. judaensis* Honigstein 1984, and *A. schilleri* Bertels 1973) and none bear the distinctive suite of features found in the taxa described from North America. It is hypothesized that none of the species described outside of North America will have the same muscle scar patterns as those from North America. Considering only the external morphology, none of the species in Table 2 display the distinctive post-ocular sulcus observed in the North American species. These observations suggest that none of the species

TABLE 1
Species of the Subfamily Anticytherideinae in the North American coastal plains recognized in this study.

Species (original generic assignment and ordered by trivial name)	Generic Assignment This Study	Author	Formation	Type Locality	Age
Anticythereis alabamensis	*Asculdoracythereis*	Smith (1978)	Prairie Bluff Chalk	Lowndes Co., AL	Maastrichtian
Asculdoracythereis asculdora	*Asculdoracythereis*	n. sp.	Providence Sand	Barbour Co., AL	Maastrichtian
Velarocythere cacumenata	*Tumulocythereis*	Brown (1957)	Peedee Formation	Pitt Co., NC	Maastrichtian
Laevipellacythereis colossus	*Laevipellacythereis*	n. sp.	Providence Sand	Barbour Co., AL	Maastrichtian
Anticythereis copelandi	*Frodocythereis*	Smith (1978)	Prairie Bluff Chalk	Lowndes Co., AL	Maastrichtian
Anticythereis dorsennus	*Anticythereis*	n. sp.	Owl Creek Formation	Tippah Co., MS	Maastrichtian
Frodocythereis frodoi	*Frodocythereis*	n. sp.	Owl Creek Formation	Tippah Co., MS	Maastrichtian
Tumulocythereis incompta	*Tumulocythereis*	n. sp.	Owl Creek Formation	Tippah Co., MS	Maastrichtian
Asculdoracythereis invicta	*Asculdoracythereis*	n. sp.	Providence Sand	Barbour Co., AL	Maastrichtian
Laevipellacythereis laevipellis	*Laevipellacythereis*	n. sp.	Owl Creek Formation	Tippah Co., MS	Maastrichtian
Velarocythere legrandi	*Asculdoracythereis*	Brown (1957)	Peedee Formation	Pitt Co., NC	Maastrichtian
Anticythereis lowndesensis	*Asculdoracythereis*	Smith (1978)	Prairie Bluff Chalk	Lowndes Co., AL	Maastrichtian
Carinocythereis (?) priddyi	*Tumulocythereis*	Smith (1978)	Prairie Bluff Chalk	Lowndes Co., AL	Maastrichtian
Asculdoracythereis pseudoalabamensis	*Asculdoracythereis*	n. sp.	Providence Sand	Barbour Co., AL	Maastrichtian
Pseudocythere reticulata	*Anticythereis*	Jennings (1936)	Mt. Laurel and Navesink Fms.	New Jersey	Maastrichtian
Velarocythere scuffletonensis	*Asculdoracythereis*	Brown (1957)	Peedee Formation	Pitt Co., NC	Maastrichtian
Anticythereis slipperi	*Anticythereis*	n. sp.	Ripley Formation	Lowndes Co., AL	late Campanian-Maastrichtian
Tumulocythereis tiberti	*Tumulocythereis*	n. sp.	Owl Creek Formation	Tippah Co., MS	Maastrichtian
Tumulocythereis tumulus	*Tumulocythereis*	n. sp.	Owl Creek Formation	Tippah Co., MS	Maastrichtian
Anticythereis sp. 1	*Anticythereis*	herein, not described	Cusseta Sand	Barbour Co., AL	late Campanian
Asculdoracythereis sp. 1	*Asculdoracythereis*	herein, not described	Owl Creek Formation	Tippah Co., MS	Maastrichtian
Frodocythereis sp. 1	*Frodocythereis*	herein, not described	Coon Creek Formation	Union Co., MS	Maastrichtian
Anticythereis reticulata (=Frodocythereis sp.)	*Frodocythereis*	Van Nieuwenhuise (1976)	Peedee Formation	Florence, Co., South Carolina	Maastrichtian
Lavipellacythereis sp. 1	*Laevipellacythereis*	herein, not described	Coon Creek Formation	Union Co., MS	Maastrichtian
Tumulocythereis sp. 1	*Tumulocythereis*	herein, not described	Ripley Formation	Lowndes Co., AL	Maastrichtian

outside of North America are closely related to the American species and that they evolved from species that pre-existed in those regions and should not be assigned to *Anticythereis*. A planned phylogenetic analysis of the Subfamily Anticytherideinae, described herein to include the North American species, should clarify the relationship of the North American species to those of other continents.

During attempts to determine homologous external ornamentation structures among the species, particularly the presence and configuration of fossae, it became clear that, whereas some species were very similar to each other, others differed considerably and should not be considered to belong to the same genus. All these new genera have synapomorphous characters that indicate that they evolved from the same ancestor (although this is

TABLE 2
Species exclusive of North America that have been assigned to the genus *Anticythereis*.

Species and Original Author and Year (Ordered by Trivial Name)	Author and Year	Age	Location
A. arcana Bertels 1975	Bertels 1975	Maastrichtian	Argentina
A. arcana Bertels 1975	Shahin2005	Paleocene-Eocene	Egypt
A.(?) attenuata Bertels 1975	Bertel, 1975	Maastrichtian	Argentina
A. attitogoensis Apostolescu 1961	Apostolescu, 1961	Eocene	Togo
A. bopaensis Apostolescu 1961	Apostolescu 1961	Paleocene	Togo
A. bopaensis Apostolescu 1961	Barsotti 1963	Paleocene	Libya
A. bopaensis Apostolescu 1961	Reyment 1980	Paleocene	Nigeria
A. bopaensis Apostolescu 1961	Reyment and Reyment 1980	Paleocene	Libya
A. bopaensis Apostolescu 1961	Carbonnel 1986	Paleocene	Senegal
A. bopaensis Apostolescu 1961	Carbonnel 1988	Paleocene	Senegal, Guinea-Bissau
A. culcitosa Apostolescu 1961	Apostolescu 1961	Eocene	Senegal
A. dahomeyi Apostolescu 1961	Apostolescu 1961	Eocene	Togo
A. dahomeyi Apostolescu 1961	Damotte 1982	Eocene	Togo
Cythere euglypha Bosquet 1854	Bosquet 1854	Maastrichtian	Netherlands
Cythere euglypha Bosquet 1854	Deroo 1966	Maastrichtian	Netherlands
Cythereis euglyphoidea van Veen 1936	van Veen 1936	Maastrichtian	Netherlands
Cythereis euglyphoidea van Veen 1937	Deroo 1966	Maastrichtian	Netherlands
A. exigua Apostolescu 1961	Apostolescu 1961	Paleocene	Ivory Coast
"*A.*" GA E 25 Grosdidier 1979	Grosdidier 1979	mid-Cretaceous	Gabon
A. gaensis van den Bold 1964	van den Bold 1964	Santonian	Egypt
A. gaensis van den Bold 1964	Gebhardt 1999	Cenomanian-Coniacian	Egypt
A. gaensis van den Bold 1964	Ismail and Soliman 1997	Cenomanian-Santonian	Egypt
A. heluanensis Bassiouni 1969	Bassiouni 1969	Eocene	Egypt
A. cf. *A. heluanensis* Bassiouni 1970	Cronin and Khalifa 1979	Eocene	Egypt
A. cf. *A. heluanensis* Bassiouni 1970	Khalifa and Cronin 1979	Eocene	Egypt
A.(?) inconnexa Bertels 1973	Bertels 1973	Paleocene	Argentina
A.(?) IR H 32 Grosdidier 1973	Grosdidier 1973	Santonian	Iran
A. judaensis Honigstein 1984	El-Nady 2002	Coniacian-Santonian	Egypt
A. judaensis Honigstein 1984	Honigstein 1984, 1985	early Late Cretaceous	Israel
A. saidi Cronin and Khalifa 1979	Cronin and Khalifa 1979	Eocene	Egypt
A. saitoi Khalifa and Cronin 1979	Khalifa and Cronin 1979	Eocene	Egypt
A. schilleri Bertels 1973	Bertels 1973	Paleocene	Argentina
A. schilleri Bertels 1973	Bertels 1975a	Paleocene	Argentina
A. schilleri Bertels 1973	Bertels 1975b	Paleocene	Argentina
A. schilleri Bertels 1973	Bertels 1976	Paleocene	Argentina
A. schilleri Bertels 1973	Bertels 1977	Paleocene	Argentina
A. seylingi Cronin and Khalifa 1979	Cronin and Khalifa 1979	Eocene	Egypt
A. seylingi Cronin and Khalifa 1979	Khalifa and Cronin 1979	Eocene	Egypt
A. sp. 1 and 2	Masoli 1965	Cenomanian-Turonian	Morocco
A. straba Al-Furaih 1980	Al-Furaih 1980	Eocene	Saudi Arabia
A. TB 1858 Grékoff 1964	Grékoff 1964	Paleocene-lower Eocene	Algeria
A. venusta Bertels 1975	Bertels 1975	Paleocene	Argentina
A. venusta Bertels 1975	Bertels 1977	Paleocene	Argentina

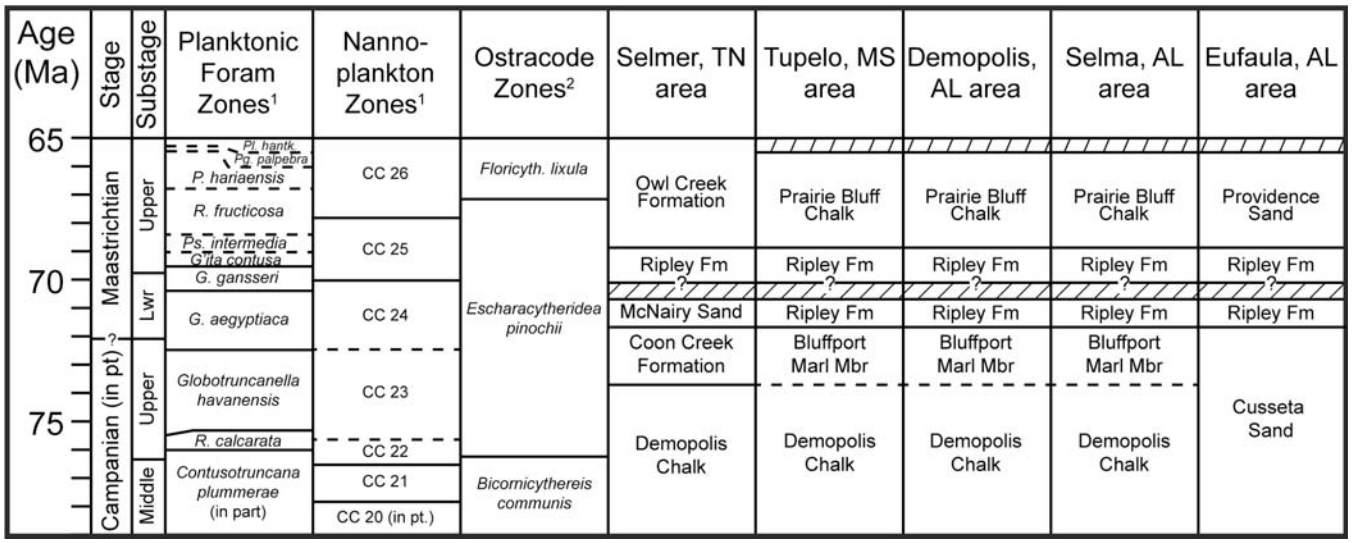

TEXT-FIGURE 1
Chronostratigraphy, biostratigraphy and lithostratigraphy of the late Campanian to Maastrichtian formations on the eastern flank of the Mississippi Embayment. Ages of stages and planktonic foraminiferal biozonation from Gradstein et al. (2020). Ostracod zonations based on Hazel and Brouwers (1982) and Puckett (2005).

yet to be determine by phylogenetic analysis) and should be considered members of the same subfamily. A rarity among the Family Trachyleberididae, the spatial-temporal limits of the group are well defined to be in the late Campanian-Maastrichtian deposits of the Atlantic and northeastern Gulf of Mexico coastal plains. Although complex external morphology is often a characteristic of the Family Trachyleberididae, with well more than 200 genera in the online World Ostracoda Database (Brandão and Karanovic 2021), the range of morphologies displayed by the anticytherideinines in North America is astounding. Also, only four subfamilies of the Trachyleberididae have been recorded in the WOD. This suggests that the level of the subfamily is underutilized for this diverse group and may have paleobiogeographical significance. In the present context, the new subfamily is restricted to the Atlantic and Gulf coastal plains of North America, thus its genetic pool is limited geographically.

The purpose of this paper is to describe a new Subfamily Anticytherideinae; describe four new genera; re-describe the genus *Anticythereis* based on SEM images of the type specimens; re-image and re-describe previously named species that are present in the study area; and present the taxonomic, geographic, and stratigraphic information for each species. Focus is on taxa primarily from samples collected in Tennessee, Mississippi, and Alabama, although reference is made to taxa described from the Atlantic Coastal Plain.

GEOLOGIC SETTING

Species of the Subfamily Anticytherideinae n. gen. occur in the late Campanian and Maastrichtian strata of the U.S. Atlantic and eastern Gulf Coastal Plain sediments (text-fig. 1). The specimens for this study were collected from the eastern flank of the Mississippi Embayment (text-figs 2-4; Appendix 1). Measured sections and sample elevations of two of the most important sections for the new species described herein, the type locality of the Owl Creek Formation in northern Mississippi and an outcrop of the Providence Sand in eastern Alabama, are presented in text-figures 5 and 6, respectively.

The outcropping Upper Cretaceous sediments in the study area overlie a major unconformity. In the northern and central parts (northern Mississippi to central Alabama), the unconformity is angular, with the Upper Cretaceous resting on Devonian rocks and, farther to the south, it rests on Pennsylvanian rocks. In eastern Alabama, the Upper Cretaceous strata rest nonconformably on metamorphic rocks of the Piedmont.

Litho- and biostratigraphic observations of Upper Cretaceous outcrops along the eastern margin of the Mississippi Embayment show three large-scale, unconformity-bound depositional sequences ranging from Santonian through Maastrichtian in age, termed the UZAGC-3.0, UZAGC-4.0 and UZAGC-5.0 sequences (Upper Zuni A-Gulf Coast) by Mancini and others (Mancini and Puckett 2005, Mancini et al. 1996b, Mancini et al. 1995b). Species of Anticytherideinae first appear in the early highstand deposits of the UZAGC-4.0 sequence but reach their greatest diversity in the UZAGC-5.0 sequence. These transgressive-regressive (T-R) cycles are recorded in strata in the Atlantic Coastal Plain, which includes the type locality of the type species from the Mt. Laurel, Navesink and Severn formations of New Jersey and Maryland (Brouwers and Hazel 1978; Gohn 1992; Jennings 1936; Kennedy et al. 2000; Minard et al. 1976; Sugarman et al. 1995), the Peedee Formation in North Carolina (Brown 1957, 1958) and in South Carolina (Swain unpublished; Van Nieuwenhuise and Kames 1976). In contrast to the rich species occurrences on the Atlantic and Gulf coastal plains, the western margin of the Mississippi Embayment in Arkansas and Texas have no record of anticytherideinines.

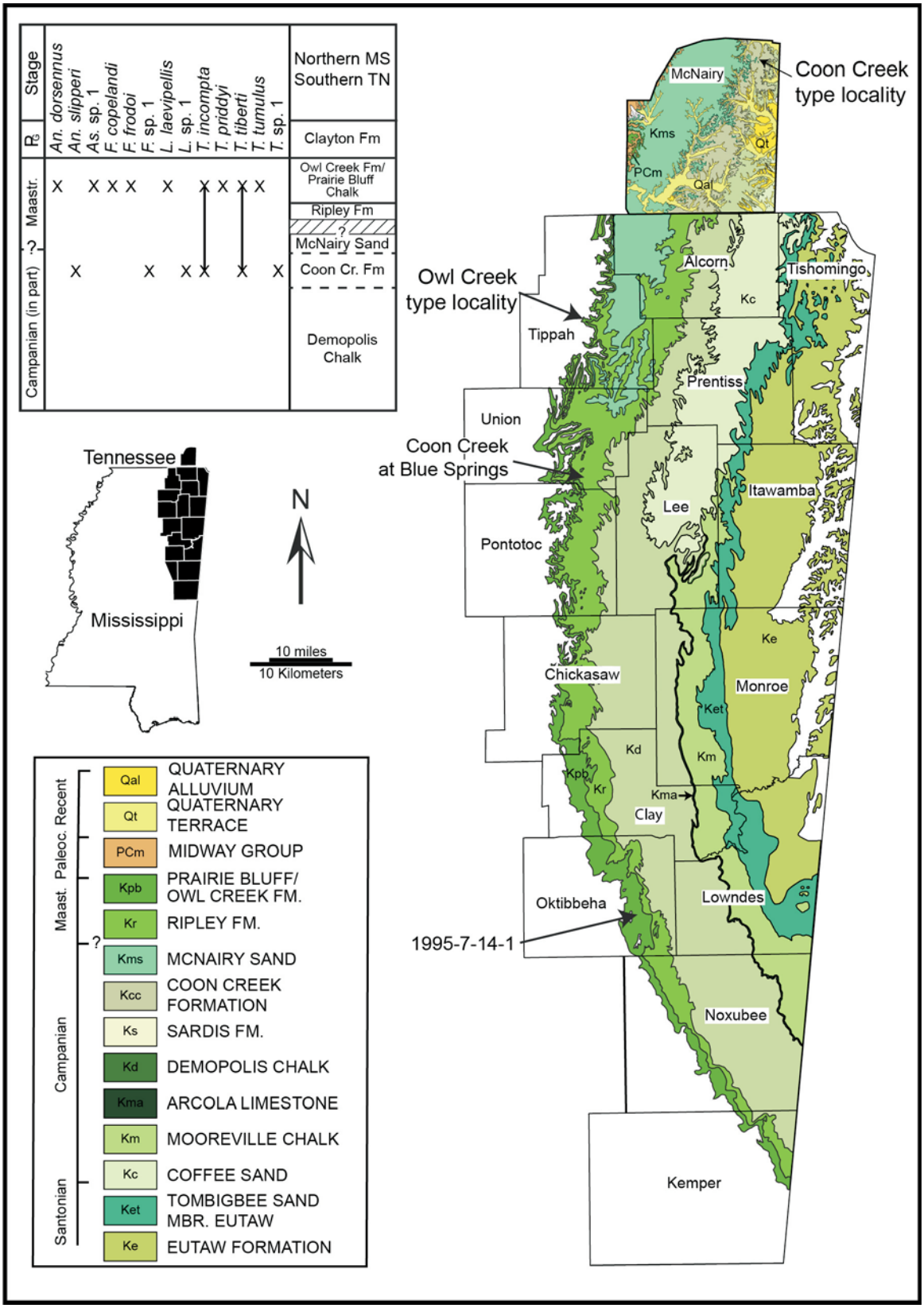

TEXT-FIGURE 2
Geologic map of the Cretaceous formations of northern Mississippi and southern Tennessee showing sample localities and ranges of species of the Subfamily Anticytherideinae n. gen. The Mississippi geologic map is compiled from Thompson (2011) and the geologic map of McNairy County, Tennessee is redrafted from Russell and Parks (1975). The marine tongues of the Demopolis Chalk and Coon Creek Formations are near their updip limit and pinch out into marginal marine and nonmarine facies to the north.

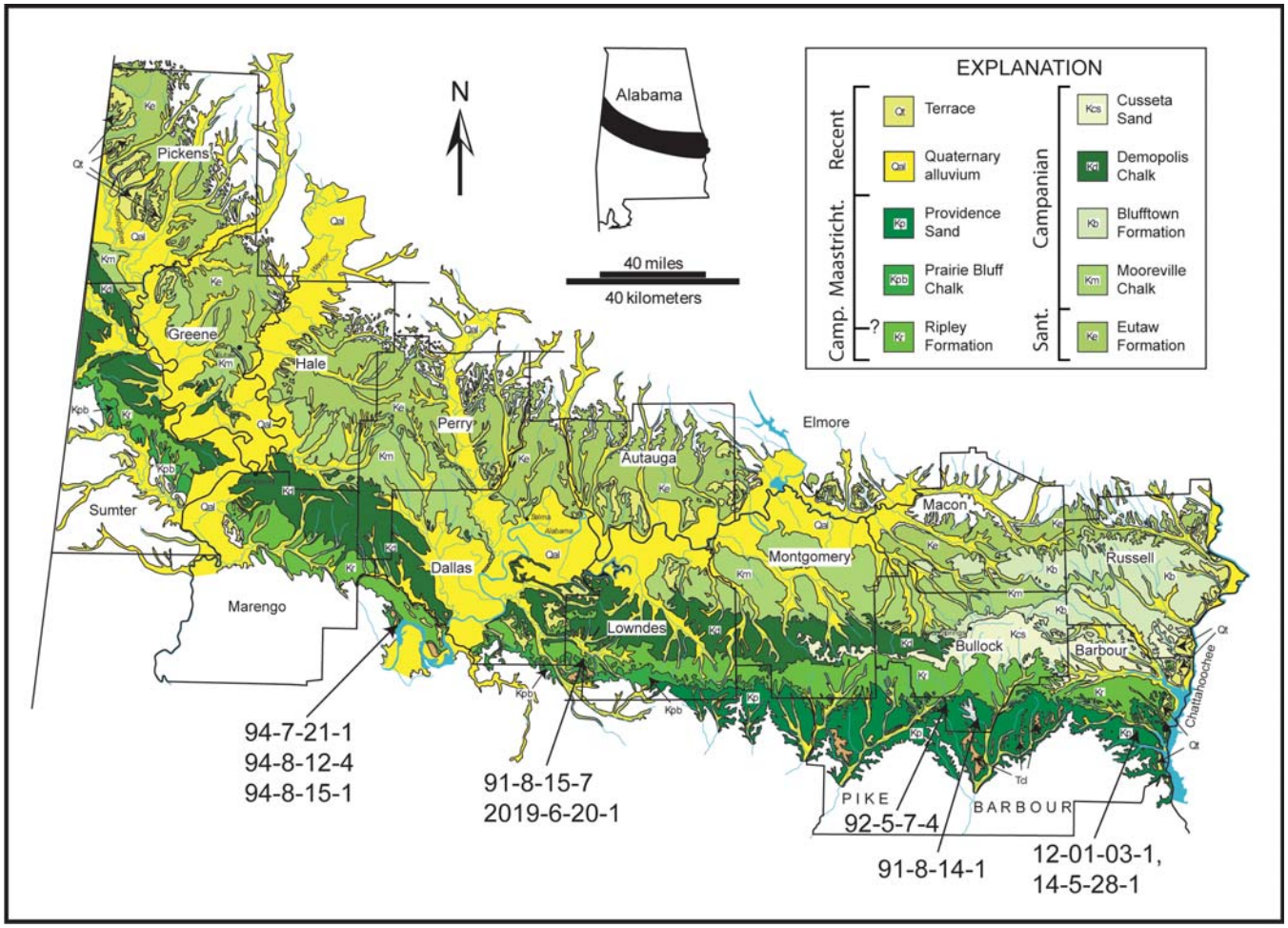

TEXT-FIGURE 3
Geologic map of the Upper Cretaceous formations in Alabama, with sample locations. Map after Osborne et al. (1989). The marine tongues pinch out just to the east of this map in western Georgia.

The biostratigraphy and sequence stratigraphy of the marine Late Cretaceous deposits of northern Mississippi to central Alabama have been studied in detail in outcrop (Hart et al. 2013; Larina et al. 2016; Mancini and Puckett 2005; Mancini et al. 1996b; Mancini et al. 1995a, 1995b; Mancini et al. 1996a; Puckett 1992, 1994, 1995b, 1995a, 1996; Puckett and Mancini 1998). There has been some uncertainty regarding the age of the uppermost Cretaceous deposits, including the Owl Creek Formation and the Prairie Bluff Chalk, due in large part to the absence of key taxa and an unconformity at the top of the Cretaceous. According to several authors (Mancini and Puckett 2005; Mancini et al. 1995b; Mancini et al. 1996a; Puckett 1994, 2005), the uppermost part of the Prairie Bluff Chalk in Lowndes and Wilcox Counties, Alabama, is assigned to the *Racemiguembelina fructicosa* Interval Zone of late, but not latest, Maastrichtian, due to the absence of *Abathomphalus mayaroensis*, *Pseudoguembelina hariaensis*, and *Plummerita hantkeninoides*. Other authors (Habib et al. 1992; Habib et al. 1996; Moshkovitz and Habib 1993) interpreted the absence of these planktonic foraminiferal taxa as due to paleoenvironmental controls, with *A. mayaroensis* in particular being interpreted as a deep-water species which is absent in the relatively shallow water paleoenvironment of the Prairie Bluff. In fact, the latter authors published observations demonstrating that the near-latest Cretaceous calcareous nannofossil zone, the *Micula prinsii* Interval Zone, occurs in the uppermost part of the Prairie Bluff, indicating a latest Maastrichtian age. More recently, Larina et al. (2016) observed rare specimens of *M. prinsii* in the Prairie Bluff Chalk and Owl Creek Formation in several localities in Alabama and Mississippi, as well as the latest Maastrichtian *Discoscaphites iris* ammonoid interval zone. At one outcrop, Moscow Landing, the uppermost Cretaceous strata of the Prairie Bluff Formation are folded and faulted, and thus of different ages along strike in that vicinity. These observations indicate that the amount of time missing at the top of the Cretaceous is variable due mainly to the differential amounts of sediment that were removed during the tsunami associated with the meteorite impact on the Yucatán peninsula.

MORPHOLOGICAL ANALYSES

Important characters in the study of fossil ostracods includes the hinge, muscle scar patterns, type and arrangement of external ornamentation, and nature and arrangement of pore canals, although the importance of particular characters depends on the taxonomic level. Although a phylogenetic analysis is not pre-

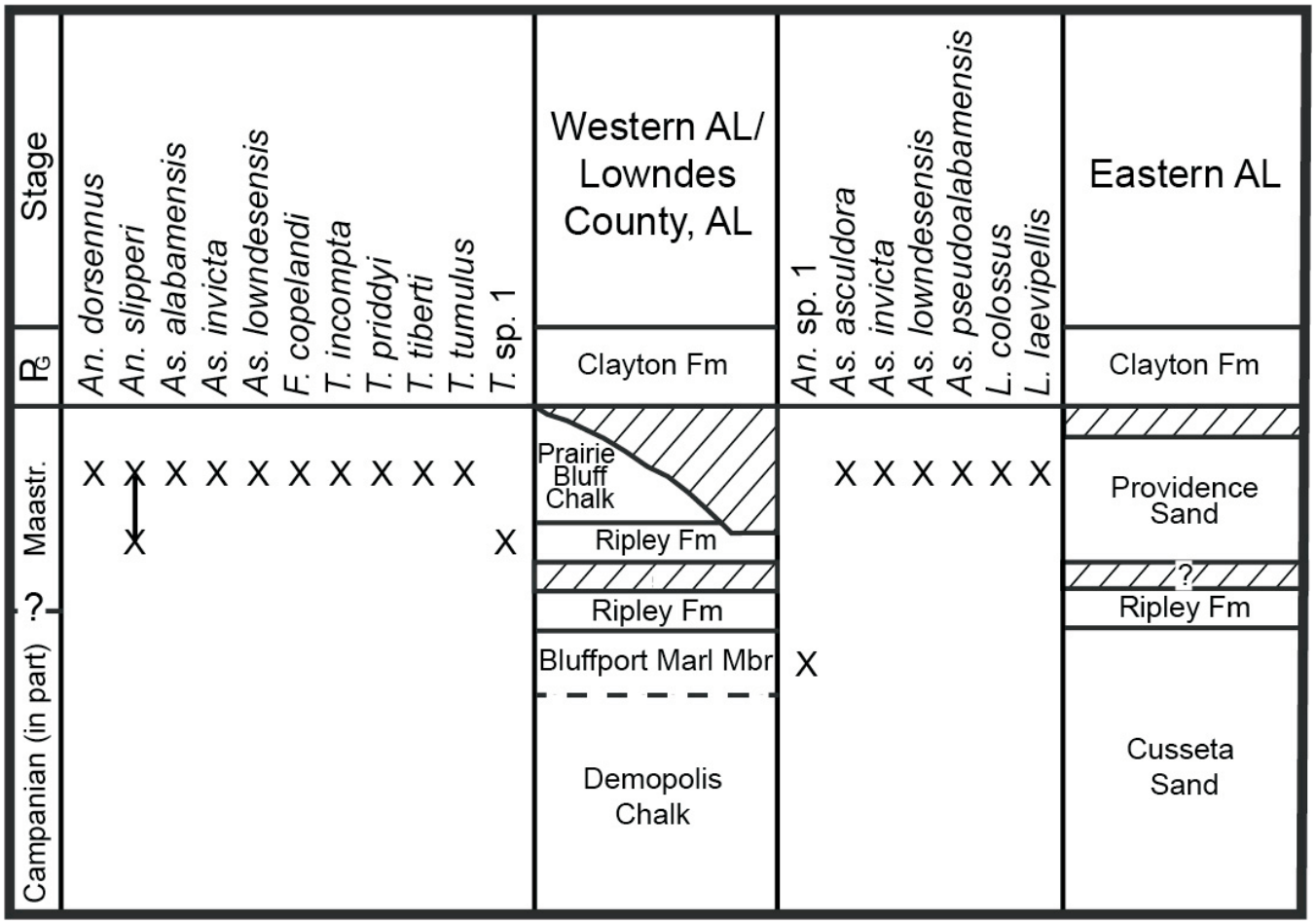

TEXT-FIGURE 4
Geologic ranges of species of the Subfamily Anticytherideinae n. gen. in Alabama.

sented here, there are several characters that are synapomorphic to the groups defined herein, as more fully described in the section on taxonomy. For the Subfamily Anticytherideinae, synapomorphic (distinguishing) characters include the nature of the paramphidont hinge, the muscle scar patterns (with lower three adductor scars forming the shape of a yin and yang symbol), and a pair of fusiform inverted platforms that corresponds to the inside of the post-ocular depression. Distinguishing characters for the genera include the presence or absence of a mid-dorsal hump in outline formed by a post-ocular carina, the presence or absence of lateral lobes, the presence or absence of external reticulate patterns, and the sizes and shapes of the fossae and muri.

In the following discussion and in the systematic descriptions, RV refers to right valve and LV refers to left valve. Fossae refers to a single mesh of the reticulated pattern and muri refers to the walls separating the fossae. Other terms used in the text are defined under "Conventions" below.

Hinge

Species belonging to Anticytherideinae have an amphidont hinge, which is characteristic of the Family Trachyleberididae, although it is not restricted to that family (the Family Hemicytheridae may also possess an amphidont hinge (Athersuch et al. 1989)). Amphidont hinges have a tooth and socket anteriorly in each valve (typically in the RV with anterior tooth and posterior socket) and a tooth or socket posteriorly (typically the tooth is in the RV and the socket is in the LV). Most of the species have a paramphidont hinge in which the anterior and posterior elements are grooved or notched, the median bar is crenulate or smooth, but the anterior LV tooth and corresponding socket in RV are smooth (Benson et al. 1961; Howe and Laurencich 1958) (Pl. 7, figs. 6-8; Pl. 8, fig. 8; Pl. 9, fig. 6; Pl. 10, fig. 6; Pl. 13, fig. 6). In some species, the anterior tooth in the RV (and corresponding socket in LV) tends to be smooth, forming holamphidont hinges (Pl. 11, fig. 6; Pl. 12, fig. 7; Pl. 18, fig. 8), although the grooves may be difficult to see in specimens that are worn or etched. All the species of *Anticythereis*, *Asculdoracythereis* and *Laevipellacythereis* have a paramphidont hinge, both new species of *Frodocythereis* have holamphidont hinges, and all species in *Tumulocythereis* except one (*T. incompta*) have a holamphidont hinge. In the latter species, one specimen (Pl. 15, fig. 6) has a paramphidont hinge and another specimen (Pl. 15, fig. 8) appears to have a holamphidont hinge. Taxonomically, this indicates that the nature of the anterior tooth in RV and corresponding socket in LV, whether crenulate or not, is not a diagnostic character *per se*, even at the species level.

All species of Anticytherideinae display a stepped anterior hinge element in which the tooth (in RV) steps down anteriorly,

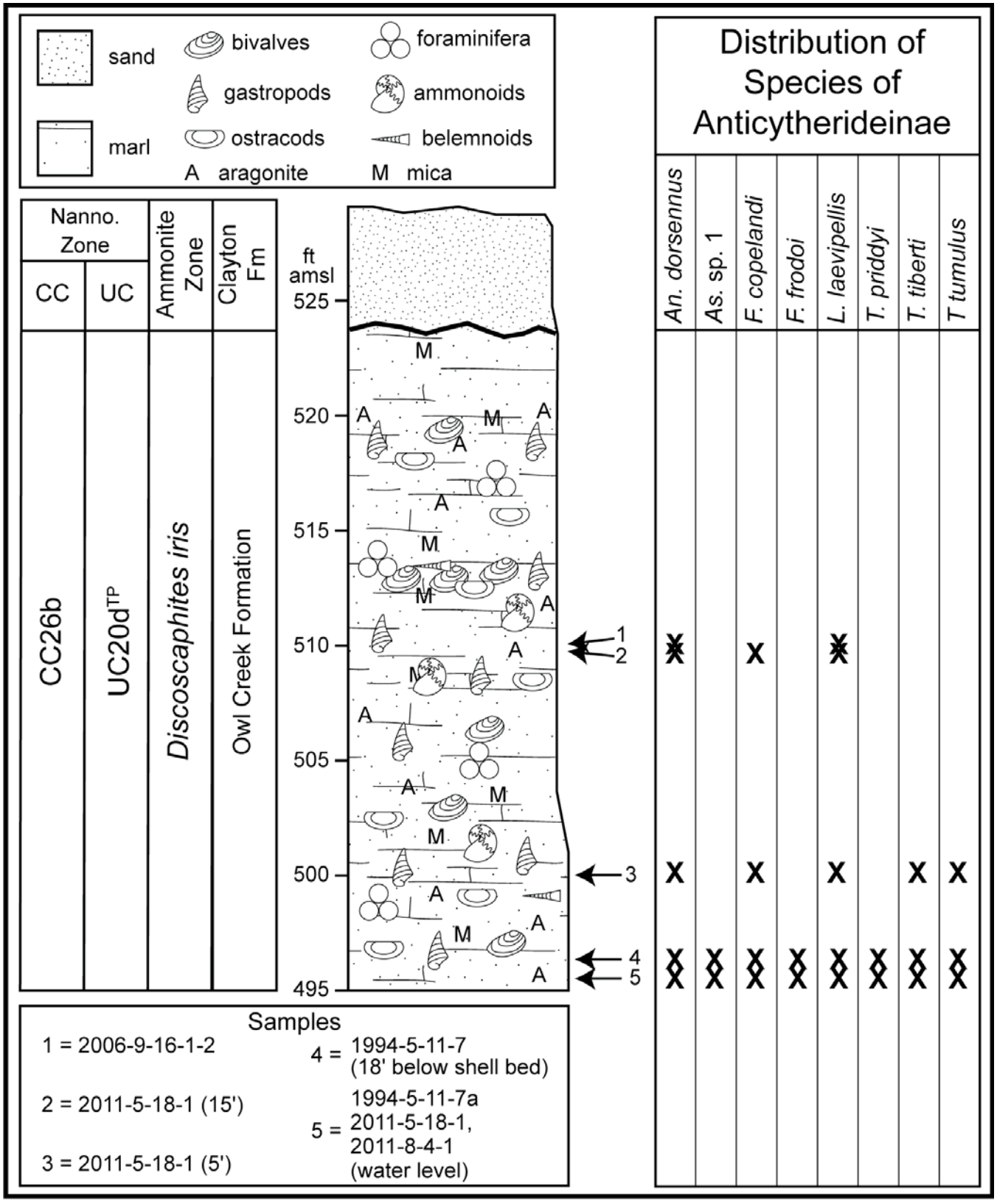

TEXT-FIGURE 5
Measured section, biostratigraphic ages and occurrences of species of the Subfamily Anticytherideinae n. gen. at the type locality of the Owl Creek Formation, Tippah County, Mississippi. Calcareous nannoplankton and ammonoid zonation from Larina et al. (2016).

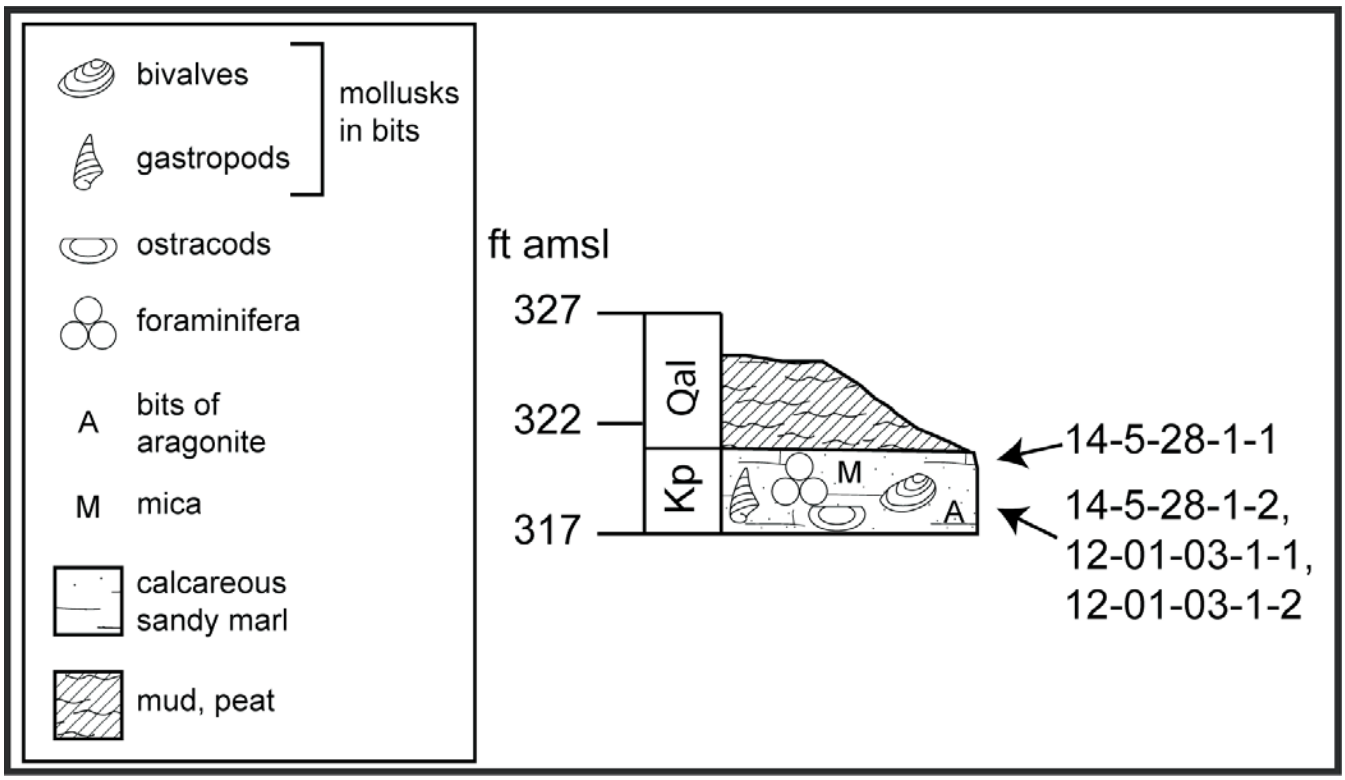

TEXT-FIGURE 6
Measured sections and sample elevations at the Providence Sand at Cheneyhatchee Creek, Barbour County, Alabama.

forming a notched level between the tooth and the selvage (Pl. 8, figs. 8 and 10; Pl. 9, fig. 6; Pl. 10, fig. 6; Pl. 13, fig. 6). Although this hinge feature is not unique to the Anticytherideinae, Triebel (1940) illustrated this feature in *Platycythereis excavata* (Chapman and Sherborn 1893) from the Turonian of Germany, and Bertels (1975a) illustrated it *Trachyleberis noviprinceps* Bertels 1975 of the Maastrichtian of Argentina), the authors are unaware of other taxa in the Late Cretaceous of the U.S. Gulf Coast that have it.

Fossae

One of the outstanding features of the Subfamily Anticytherideinae is the plasticity of the external morphology, ranging from smooth to leopard-like intricacy. This plasticity is manifested mainly in the shape and arrangement of fossae, which are the rounded or polygonal depressions on the outside of the carapace. Taxonomically, it is important to determine whether the patterns are species-specific or if there is some underlying pattern shared by species, i.e., homology. In order to identify homologous structures of the external ornamentation, workers have mapped the fossae and tubercles using an alphanumeric code system, including Pokorný (Pokorný 1969a, 1969b), Liebau (1977) (the original publication was in 1971, but translated and republished in 1977), Benson (1972) and more recently by Hunt (2007) and Huang et al. (2022). Plate 1, figs. 1 and 2 show two examples of the alphanumeric system that Liebau (1977) used to code these structures. Hunt (2007) noted in studying the Recent deep-sea genus *Poseidonamicus* that homologous structures sometimes can be recognized in specific areas of the carapace, but not in others. In general, recognition of homology is facilitated if the structures are adjacent to some reference point such as the central muscle scar field or the carapace margins, or if the pattern is relatively straightforward, such as in vertical lines. Recognition of homologies of fossae is important, as they can provide a framework for determining homology in secondary features, such as normal pore canals.

To aid attempts to homologize ornament features across the disparate morphologies represented in this new subfamily, drawings were prepared in Adobe Illustrator® that include a series of layers for each species, each with drawings of a specific morphologic feature. These layers include: 1.) an SEM image of a specimen used as a base layer; 2.) carapace outline; 3.) fossae outlines; 4.) a layer used to colorize the fossae in an attempt to determine homology; 5.) positions of normal pore canals as viewed from the exterior; 6.) positions of normal canals as viewed from the interior; 7.) estimated positions of fossae not observed in the particular specimen under study (not all normal pore canals were observed on every specimen); 8.) and average positions from both inner and outer views. These drawings are presented in Plates 1 and 2. Layer (4) above was prepared as an attempt to color code the fossae, which was much easier to visualize homologous structures that an alphanumeric code system. Two species studied by Liebau (1977), *Aysegulina ornata* (Bosquet 1847) and *Oertliella horridula* (Bosquet 1854), were used as a guide in mapping the fossae. The alphanumeric code system was converted to a colorized system. The pattern of fossae in these two species was straightforward, as they are located in a series of concentric circles around the central muscle scar field. A similar coding scheme was applied to the species under investigation herein. Repeated efforts at determining homologous fossae among the species were generally unsuccessful, except for the areas along the anterior and posterior margins

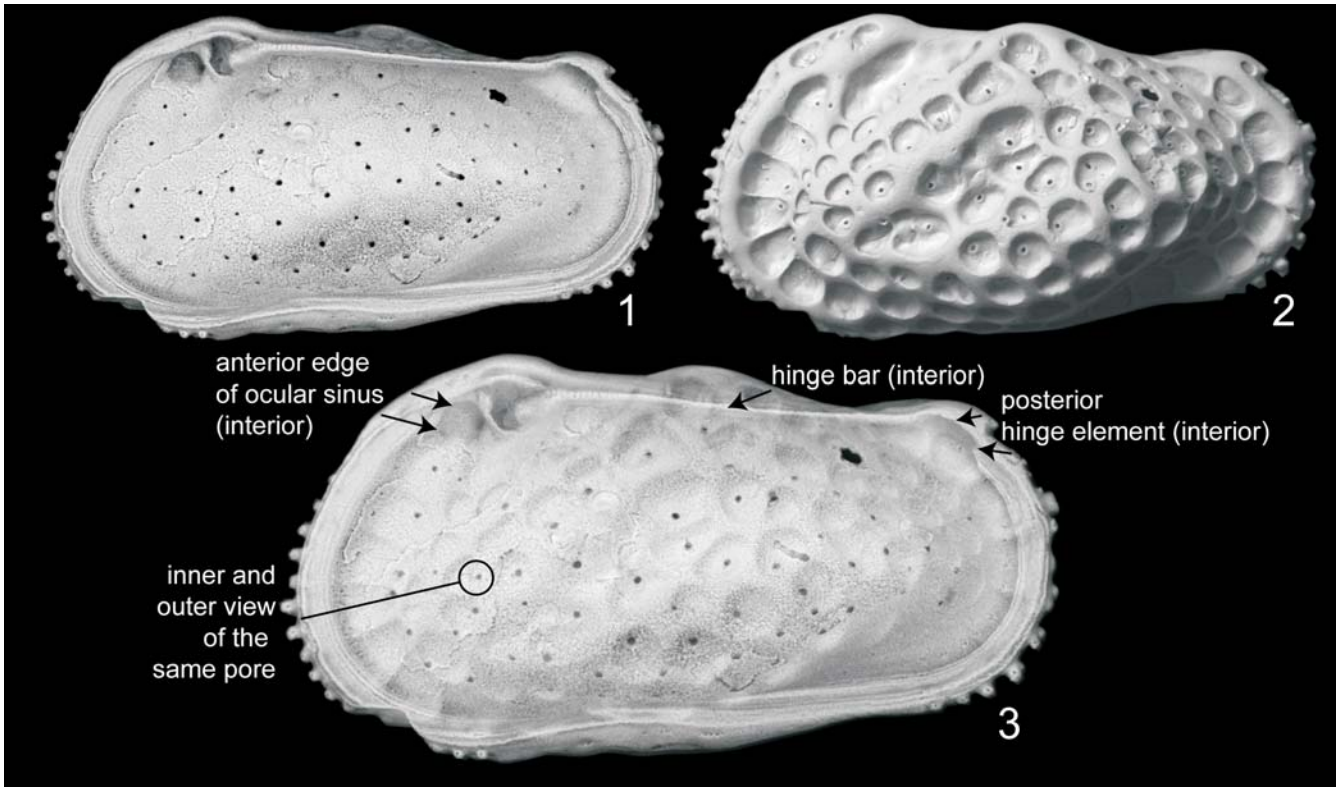

TEXT-FIGURE 7
Interior, exterior, and combined views of *Anticythereis dorsennus* n. sp., specimen 132-13 (see Pl. 5, figs. 2 and 7 and captions for sample information). Note that the interior image (1) has been flipped horizontally.

and the post-ocular depression. Indeed, trying to correlate homologies among the species became an exercise in "make it up as you go along," though further studies may make more progress. These challenges in determining homologies were integral to the decision to define the new genera.

At first glance on Plate 1, the fossae of *Asculdoracythereis invicta* n. gen., n. sp. appear to differ considerably from the other species. Each of the deep longitudinal depressions is subdivided by ghost-like muri into polygons similar to the other species (for example, compare *A. invicta* of Plate 9 to *A. pseudoalabamensis* on Plate 7). Some specimens of *Laevipellacythereis laevipellis* n. gen., n. sp. display vestiges of underlying ornamentation that were obscured by tegmen (Pl. 14, figs. 2 and 4), but these were not mapped on Plate 1.

Normal Pore Canals

Normal pore canals (abbreviated NPC) are openings through which setae (also called sensory bristles) connect the animal's body to the external environment. Puri and Dickau (1969) classified pore canals into four types. Type A is a single, simple pore with a sensory hair (sensillum), and was subdivided into Type A' (without an upraised rim or lip) and Type A" (with a lip). Type B is a sieve plate without a well-defined subcentral pore with a sensillum. Type C is a sieve plate with a pore and sensillum emerging from its center. Type D is a sieve plate with a separate, single pore with sensillum. In this study, a normal pore with a sieve plate is called a sieve-type normal pore canal. The type of NPC was correlated to taxonomic groups, in some cases genera and in others at a higher level; for example, polycopes and cytherellids have Type A', xestoleberids and loxoconchids have Type C, and campylocytherines had Type D NPC. In the present context, the trachyleberids may have a Type A, Type B or a Type C, which may be consistent at the generic or familial level. The possible functions and taxonomic importance of NPC were recently reviewed by Lord et al. (2020). NPC can be classified as either simple, which consist of a tube, or sieve-type, which consist of several openings in a sieve plate. They also recognized that the sieve plates may be sunken below the level of the exterior carapace. The function(s) of NPC were still not well understood. As described by Lord et al. (2020), NPC may function as photoreceptors, chemoreceptors, thermoreceptors, excretory functions, osmoregulation, buoyancy function, secretion organs, stabilization in the substrate, or to control the function of associated tubuli. Sieve-type NPC evolved very early in the history of ostracods; Schallreuter (1977) described a new species (*Miehlkella cribroporata*) with relatively simple sieve-type NPC from the Early Ordovician.

In the anticytherideinines, there is generally a one-to-one correspondence between fossae and NPC, i.e., there is a single NPC within a single fossa, but not all fossae have NPC. Sieve-type NPC almost always are located within the soli of the fossae (Pl. 6, fig. 9; Pl. 8, figs. 7 and 11; Pl. 15, fig. 12), although rarely they are located within muri (Pl. 10, fig. 9; Pl. 16, fig. 4). The sieve pores in the anticytherideinines appear to be three tiered in some species, with a rimmed, doughnut-shaped level below the undercut outer carapace, and the sieve plate with subcentral

pore at the bottom (Pl. 13, fig. 10; Pl. 14, fig. 9; Pl. 15, figs. 9 and 11; Pl. 16, fig. 12). The doughnut-shaped second layer is the solum of the taxa with large fossae (that is, the floor of the fossae). Others are the Type C sieve-type NPC (Pl. 7, fig. 9; Pl. 8, fig. 7; Pl. 9, fig. 11).

To determine if the sieve-type NPCs are homologous among the different species in the anticytherideinines, they were mapped, where possible, based on the availability of both inner and outer views of the same specimen (text-figure 7). This was done because, in some specimens, some of the pores were either obscured by debris, they appeared to be present in inner view but not the outer (some sieve pores were apparently obscured by tegmen, that is, an overgrowth of calcite), or the ornamentation obscured the view from the exterior. To do this, the inner view was flipped horizontally and rotated and resized until a good visual match to the external image of the same was achieved. In some specimens, either the interior or exterior of the same specimens was obscured by debris, and thus different specimens were used. The NPC on species that are smooth (*Laevipella cythereis*) were easily visible in exterior view and an inner view was not necessary.

Dorsal Inverted Platform

One of the distinctive characters of the Subfamily Anticytherideinae is the pair of inverted platform structures that are located just ventral and posterior to the anterior hinge elements, in both the LV and RV (Pl. 7, figs. 7 and 8; Pl. 12, figs. 8 and 8; Pl. 13, fig. 8; Pl. 14, figs. 7 and 8; Pl. 15, fig. 10; Pl. 17, figs. 5-7; Pl. 18, figs. 5-8, 12). This structure corresponds to the inner part of the post-ocular sulcus. There are two parallel structures, one below the other; this secondary structure (th lower one) may be almost as large as the upper one (Pl. 18, fig. 12), whereas in most species, the secondary structure is smaller than the upper and is teardrop-shaped or shaped like the Nike™ logo (Pl. 5, fig. 10; Pl. 7, fig. 7; Pl. 11, fig. 6; Pl. 12, fig. 11; Pl. 14, fig. 8; Pl. 15, fig. 13; Pl. 16, figs. 8-10; Pl. 17, fig. 9; Pl. 18, fig. 12). The larger, upper structure is more acuminate anteriorly and the lower, smaller one is more acuminate posteriorly. Well-preserved specimens show that the lower platform surfaces of both structures are rimmed, whereas the center is recessed (Pl. 7, fig. 7; Pl. 12, fig. 11; Pl. 15, figs. 10 and 13; Pl. 17, fig. 9; Pl. 18, fig. 12). It appears that the stresses applied to this structure during calcification pulled the outer carapace inwards, forming the postocular sulcus.

Sexual Dimorphism

Sexual differences in valve dimensions were investigated following the procedures used by Hunt et al. (2017), who documented sexual dimorphism among cytheroid ostracod species of the Late Cretaceous coastal plain. Valve outlines of all specimens figured herein were digitized using the software TPSDig (Rohlf 2013). Valve size was measured as the area enclosed by the outline, and valve shape (elongation) was measured as the ratio of the major to minor axes of the ellipse that best fit the outline. Both variables were log-transformed prior to plotting. In most cytheroid taxa, the left valve slightly overlaps the right, resulting in right valves that are somewhat smaller and more elongate than left valves. This left-right difference was corrected for by applying the average left-right offset of anticytherideinine species estimated by Hunt et al. (2017). This practice modified right valve measurements by adding 0.076 to log size and subtracting 0.057 from log shape, thus converting them to left-valve equivalents.

Sample sizes of the figured species are generally too low (n = 10) for statistical analysis, and separation between sexes was sometimes ambiguous. The survey of sexual dimorphism in the broader fauna (Hunt et al. 2017) included analysis of several large populations attributable to the species studied herein. When possible, the statistically supported male and female clusters from that study are included here as text-figures to help guide the identification of sexes in the present work.

Muscle Scars

One of the most distinctive characters (synapomorphy) of the new Subfamily Anticytherideinae is the muscle scars pattern, particularly the adductor muscle scars. Terminology for the scars is presented in text-figure 8 and a comparison of the muscle scar patterns of species collected during this study is presented on Plate 3. The single U- or V-shaped frontal scars are typical of the Trachyleberididae (Hazel 1967) and are, in fact, a defining character of the family. The mandibular and dorsal scars are also typical of that family, but the adductor scars are distinctive to the new subfamily. The A-1 scar is elongate in a dorsoanterior-ventroposterior direction and is separated dorsally and slightly posteriorly from the other adductor scars. The A-2, A-3 and A-4 scars are herein described as being similar to a yin and yang symbol, with the A-2 adductor that is bulbous anteriorly, but tapers and curves posteriorly over the lower two adductors; an elongate A-4 scar that is tilted slightly dorsoposteriorly, and a small A-3 scars that is sandwiched between the posterior ends of the A-2 and A-4 scars. These "yin and yang" adductor scars have an overall circular shape.

TAXONOMY

Conventions

The species descriptions in the following section use the following abbreviations and symbols: LV = left valve, RV = right valve, USNM PAL = U. S. National Museum (Smithsonian Institution) Paleobiology Collections, AMNH = American Museum of Natural History. The terminology for the muscle scar patterns is presented in text-figure 8.

The descriptions include terms that may not be familiar to all ostracod specialists, particularly if they do not work with trachyleberids, so some of them are defined below. These terms are described in Kesling (1951), Benson et al. (1961), Sylvester-Bradley and Benson (1971), Horne et al. (2002) and Sames et al. (2010).

Apophysis. An offshoot of the murus leading to a rimmed pore canal.

Caperation. Fine wrinkles on carapace surface. In the present context, most caperation is located in the soli of the fossae.

Celation, *sensu* Sylvester-Bradley and Benson (1971). Development of an outer layer of calcite (tegmen) that overlaps and obscures underlying ornament. Peypouquet et al. (1980) and Peypouquet et al. (1988) used the terms aggradation and degradation to refer to the addition or removal, respectively, of calcite from ostracod carapaces as a phenotypic response to environmental cues, particularly in response to the saturation of calcium carbonate. In the present context, however, no correlation between specific environmental parameters and the degree of calcification is implied, and thus the term celation is applied.

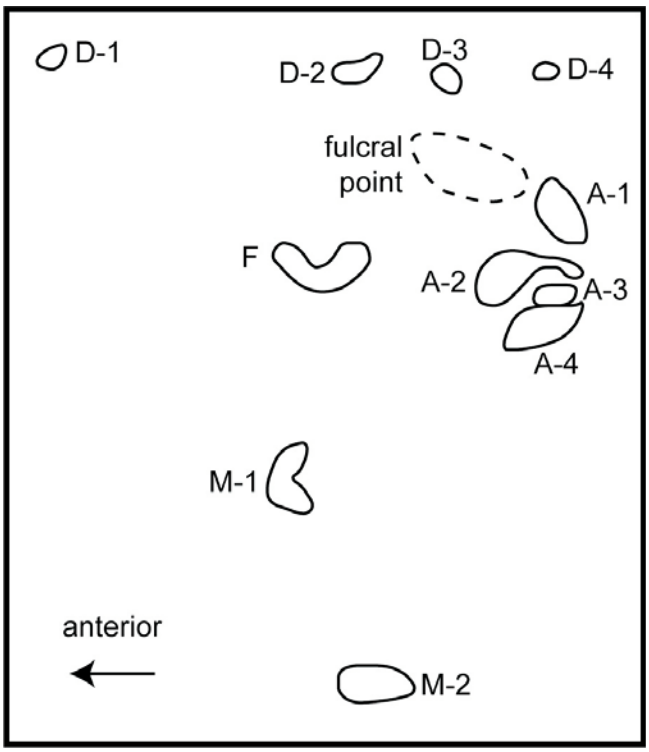

TEXT-FIGURE 8
Terminology for muscle scars on the inside of the ostracod carapace. D = dorsal, A = adductor, F = frontal, M = mandibular. Drawing based on *Frodocythereis frodoi* n. sp., specimen 132-8 (for closeup see Pl. 12, fig. 10).

Equicurvate. Curvature of the anterior or posterior margin in which the greatest extent is at mid-height.

Fossa (plural **fossae**). Single subovate or sub-polygonal mesh of a reticulum.

Foveola (plural **foveolae**). Minute pits in the surface layer of the carapace an order smaller than puncta and fossae.

Fulcral point (or notch). A depression or upraised point where the mandible pivots, which typically overlies the central muscle scar field.

Infracurvate. Curvature of the anterior or posterior margin in which the greatest curvature is below mid-height.

Murus (plural **muri**). The wall of a fossa in a reticulum.

Solum (plural **soli**). The floor of a fossa in a reticulum.

Stragulum (plural **stragula**). Guber and Jaanusson (1964) proposed this term, or stragular process, to refer to a dorsal flap-like overlap of one valve over the other at the cardinal corners (point at which the dorsal margin curves down to the anterior or posterior margin). Guber and Jaanusson proposed the term while studying Ordovician kloedenellid ostracods. The term is not used herein to describe and elevation of the LV above the RV at the terminal hinge elements, but the carapace of the LV does not extend across the RV as they do in the Ordovician taxa.

Supracurvate. Curvature of the anterior or posterior margin in which the greatest curvature is above mid-height.

Tegmen. The secondary layer of calcite produced by celation.

Class OSTRACODA Latreille 1802
Subclass PODOCOPA Sars 1866
Order PODOCOPIDA Sars 1866
Suborder CYTHEROCOPINA Baird 1850
Superfamily CYTHEROIDEA Baird 1850
Family TRACHYLEBERIDIDAE Sylvester-Bradley 1948
Subfamily ANTICYTHERIDEINAE n. subfamily

Type Genus: ***Anticythereis*** van den Bold 1946
Diagnosis: Genera of the Subfamily Anticytherideinae are characterized by a combination of traits that include large, scattered sieve-type normal pore canals with raised rims (Pl. 6, fig. 10; Pl. 4, fig. 9; Pl. 13, fig. 10; Pl. 14, fig. 9; Pl. 15, fig. 12; Pl. 16, fig. 12); a highly sculpted exterior carapace that consists of subrounded or polygonal fossae or a layer of tegmen that obscures ornamentation; a muscle scar pattern with A-2, A-3 and A-4 scars intertwined in a yin-yang symbol with an overall circular shape (Pl. 3); an A-1 scar detached dorsally from others, elliptical and tilted dorsoanteriorly; a post-ocular depression that extends from the dorsal margin to below the ocular sinus; a paramphidont hinge, in RV with a stepped, multilobed anterior tooth and a large, elongate, arcuate posterior tooth tilted diagonally across the dorsoposterior angle (Pl. 8, fig. 10; Pl. 7, fig. 6; Pl. 10, fig. 6; Pl. 15, fig. 10; Pl. 18, fig. 12); complementary sockets in LV; and a pair of inverted, fusiform platforms located anteromedially (arrows point to these structure on Pl. 7, fig. 7; Pl. 13, fig. 6; Pl. 16, fig. 10; Pl. 17, fig. 9; and Pl. 18, fig. 12). A double ogee-shaped structure occurs as an interruption of the selvage at the posterior caudal angle of the RV, with no corresponding structure in the LV (Pl. 7, fig. 8; Pl. 11, fig. 6; Pl. 12, fig. 8; Pl. 13, fig. 6; Pl. 14, fig. 8; Pl. 16, fig. 8; Pl. 18, figs. 6 and 8).

Remarks: This subfamily is restricted to the late Campanian-Maastrichtian of the North American Atlantic and eastern Gulf coastal plains. The following genera are assigned to the new subfamily:

Anticythereis van den Bold, 1946, type species *Anticythereis reticulata* (Jennings 1936)

Asculdoracythereis n. gen., type species *Asculdoracythereis asculdora* n. sp. (Pl. 8)

Frodocythereis n. gen., type species *Frodocythereis frodoi* n. sp. (Pl. 12)

Laevipellacythereis n. gen., type species *Laevipellacythereis laevipellis* n. sp. (Pl. 14)

Tumulocythereis n. gen., type species *Tumulocythereis tumulus* n. sp. (Pl. 18)

Discussions of species' assignments to genera follow the generic descriptions.

Genus ***Anticythereis*** van den Bold 1946

Type Species: *Anticythereis reticulata* (Jennings 1936) (holotype: AMNH-FI 37780A, paratype: AMNH-FI 37780B) (Pl. 4, figs. 1-3; text-fig. 9)

Velarocythere BROWN 1957, p. 20-21, type species *Velarocythere scuffletonensis* Brown 1957 (holotype: USNM PAL 129009, paratypes: USNM PAL 129006, 129007, 129008, 129010).

Amended Diagnosis: Genus of Subfamily Anticytherideinae characterized by a prominent murus that forms a dorsal hump in outline at mid-length that extends above the hinge line, then bends ventroanteriorly behind the post-ocular depression, forming a steep bordering murus. The posterior margin has a distinct marginal carina and is supracurvate in LV and infracurvate in RV.

Remarks: Jennings (1936) named and described a new species he designated as *Pseudocythereis reticulata* that was collected from the Mt. Laurel and Navesink Formations of New Jersey. Biostratigraphic data, including ammonoids, *Exogyra* oysters, calcareous nannoplankton, planktonic foraminifera, and strontium isotopic data indicate that the Mt. Laurel Formation is late Campanian in age and is unconformably overlain by the early Maastrichtian Navesink Formation (Sugarman et al. 1995). Kennedy et al. (2000) observed a Maastrichtian guide fossil, the ammonite *Pachydiscus (Pachydiscus) neubergicus* (Hauer 1858), in a phosphatic bed at the base of the Navesink Formation, indicating an earliest Maastrichtian age. Gamma ray data and field observations indicate that the fossiliferous and quartzose Mt. Laurel Formation represents a highstand systems tract, whereas the finer-grained and fossiliferous Navesink Formation represents a transgressive systems tract. This sequence stratigraphic setting correlates well with the highstand systems tract of the Campanian UZAGC-4.0 depositional sequence and the transgressive systems tract and maximum flooding surface of the Maastrichtian UZAGC-5.0 depositional sequence on the eastern flank of the Mississippi Embayment of Mancini et al. (1996b), with some differences. In the Tennessee-Mississippi-Alabama area, the highstand systems tract of the UZAGC-4.0 sequence continues from the marine Coon Creek Formation into nonmarine sands of the McNairy Sand in northern Mississippi and Tennessee, whereas farther south in eastern Mississippi and central Alabama, the marine Bluffport Marl Member of the Demopolis Chalk grades up-section into the nonmarine Ripley Formation (text-fig. 1). The Mt. Laurel, in contrast, contains marine fossils and was interpreted as upper shoreface deposits, rather than nonmarine (Sugarman et al. 1995). The ill-defined Campanian/Maastrichtian stage boundary, then as today, was interpreted to occur within the time interval represented by the Mt. Laurel-Navesink unconformity. The name *Pseudocythereis* was already used by Skogsberg (1928), so van den Bold (1946) renamed the genus *Anticythereis*, although he did not discuss the genus further.

Brown (1957) named and described *Velarocythere* based on one of his new species, *V. scuffletonensis*, which is characterized generally by even reticulations and low muri. The type specimens of *V. scuffletonensis* have considerable adventitious material, which is why they are not published herein, but can be viewed at the U.S. National Museum Paleobiology Database at URL https://collections.nmnh.si.edu/search/paleo/. Brown stated that *Velarocythere* "shows some affinity to *Anticythereis* van den Bold (*Pseudocythereis* Jennings) but can be separated on the basis of size, hingement, and external shell characteristics," although these differences were not explained. A species Brown described as new (*Velarocythere eikonata*) is considered to be synonymous with Jennings' (1936) type species of *Pseudocythereis reticulata*, thus *Velarocythere* is a junior synonym of *Anticythereis*.

Species: Two new species from the present study are assigned to *Anticythereis*: *A. dorsennus* n. sp. and *A. slipperi* n. sp., in addition to the nominal species, *A. reticulata* (Jennings 1936).

Anticythereis reticulata (Jennings 1936)
Plate 4, figures 1 and 2; Text-fig. 9

Pseudocythereis reticulata JENNINGS 1936. p. 57-58, Pl. 7, figs. 10a-d.
Velarocythere eikonata BROWN 1957. p. 22, Pl. 5, figs. 10-12.– BROWN 1958, p. 64, Pl. 5, fig. 3.
NOT *Anticythereis reticulata* (Jennings 1936).– VAN NIEUWENHUISE 1976, Table 1, Pl. 4, fig. c (= *Frodocythereis* sp.).
Anticythereis reticulata (Jennings 1936).– VAN DEN BOLD, 1946, p. 30. Note: Van den Bold (1946) simply named the new genus *Anticythereis* to accommodate Jennings' species *Pseudocythereis reticulata*, noting that the name *Pseudocythereis* had been used by Skogsberg (1928). See more notes under description of genus.

Type Specimens: The holotype (AMNH-FI 37780A) is a RV broken at the ventroposterior margin, and the paratype (AMNH-FI 37780B) is a well-preserved LV (Pl. 4, figs. 1 and 2). For comparison, Brown's (1957) type specimen of *Velarocythere eikonata* (USNM PAL 129016, a LV) is presented on Pl. 4, fig. 3. This latter specimen has adventitious material on the dorsoanterior 2/3 of the specimen, obscuring morphological details. Nonetheless, the specimens of Brown and those of Jennings are close enough morphologically to consider them to be synonymous.

Diagnosis: None, but Jennings (1936) described the species.

Emended Diagnosis: Carapace characterized by a pair of diagonal costae that extend from a prominent stragulum to below mid-height, anterior of the eye tubercle and parallel to the anterior margin, which then turns sharply ventroposteriorly and becomes more subdued to the mid-posterior region, marking the outline of a prominent sagittal lateral swelling. A deep, elongate sulcus is subjacent to the eye tubercle, wedging anteriorly and down between the eye tubercle, the anterior compressed region, and the prominent anterior diagonal costa. Carapace ornamentation is formed by large, open, rounded fossae with single sieve-type normal pore canals punctuating the sola. Central, elongate, ventroanteriorly oriented sulcus is bordered by prominent lateral costae. Anterior and posterior margins are compressed; posterior margin is with single row of sub-rounded fossae without pits; anterior fossae are larger, sub-rectangular and with thin intervening muri and single sieve-type normal pore canals near the inner margin of the fossae.

Description: The carapace is robust, with the greatest height at the eye tubercles, and with a dorsal shoulder that lies just behind mid-length in outline, closer to the eye tubercle than to the dorsoposterior angle. The anterior and posterior margins are slightly infracurvate. The dorsal profile is sinuous, with a concavity between the greatest height above the eye tubercle to mid-shoulder, then is concave again between the mid-shoulder and dorsoposterior angle. The dorsoposterior angle of the LV is prominent; the angle in the RV is not as distinct and slopes posteriorly. Two rows of denticles are located very close to the anterior and posterior margins. The ventral silhouette is slightly undulatory, with a convexity corresponding to a lateral swelling slightly behind mid-length and is bordered anteriorly and posteriorly by gentle concavities.

The eye tubercles are not prominent, are smooth, and are bordered ventroposteriorly by an elongate, deep sulcus and

ventroanteriorly by a fossa. Circular fossae are located above and on either side of the eye tubercle.

The external ornamentation consists mainly of a combination of carinae, rounded fossae, and sieve-type normal pore canals that punctuate the sola (Pl. 4, fig. 2). Two parallel carinae extend from a prominent dorsal shoulder ventroanteriorly to directly behind the greatest anterior extent of the carapace, then turn ventroposteriorly and less prominently to parallel the ventral margin, in an overall sagittate form. Between these carinae is a sulcus. The region defined by the carinae is inflated relative to the compressed anterior and ventral margins. A smaller carina extends from the eye tubercle to merge with the posterior border of the anterior fossae. Below and posterior of the eye tubercle is a deep, elongate sulcus, the solum of which is punctuated by 1 or 2 pits. Behind the anterior rim is a row of large, sub-rectangular fossae separated by thin, radiating muri; the sola are caperate. Near the posterior margin of each solum is a single sieve-type normal pore canal. Similarly, the compressed area adjacent to the posterior rim has a row of slightly smaller and more rounded fossae that lack pore canals.

Sexually dimorphism was not assessed due to lack of a population to measure. The paratype specimen is plotted with specimens of *A. slipperi* on text-fig. 9.

Internally, the dentition is amphidont (unfortunately, the interior RV of the holotype is damaged and the anterior hinge elements are broken, and thus any grooves that are in paramphidont hinges cannot be observed; the corresponding socket on the LV on the paratype (Pl. 4, fig. 1) does not appear to be grooved). The anterior hinge element in the LV is a vertically elongate socket bordered anteriorly by a slight invagination, dorsally by an arched rim (stragulum), and posteriorly by the subjacent tooth, which is elongated and deflected ventroanteriorly. The median bar in the LV is narrow and straight, crenulate and slightly thicker anteriorly. The posterior socket is elongated ventroposteriorly at ca. 45°. The median groove in the RV is crenulate and very slightly arched and widens near the extremities. The posterior tooth is elongated and angled in the middle. The inner lamella is of uniform width along the anterior, ventral and posterior margins. Pores on the inner surface correspond to the internal openings of the sieve-type normal pore canals on the exterior. A pair of inverted, rimmed, fusiform platforms are located just below and behind the anterior hinge elements; in the LV of the paratype, these platforms are mostly obscured by crystals (arrow on Pl. 4, fig. 1); in the RV of the holotype, however, these platforms can be seen clearly (not illustrated here, but images are available from TMP).

The muscle scar field (Pl. 4, fig. 1) includes a U-shaped F scar that is located at the mid-height of the adductor scars and tilted slightly towards the anterior; there are four adductor scars: the A1 scar is large, ovate, separated dorsoanteriorly from the other adductor scars, and tilted at ca. 30° towards the anterior hinge element; the A-2, A3 and A4 scars are in an overall subcircular shape; the A2 scar is relatively large and is in the shape of boomerang; the A3 scar is small, subcircular, located mid-posteriorly in the adductor group and abuts the A-4 scar; and the A-4 is elongate, tapered on the ends, rises slightly posteriorly, and is with a concavity where it touches the A-3 scar. The mandibular scar is ventroanterior of the central muscle scars, and ovate. The dorsal scars could not be observed on the type specimens due to adventitious material.

Remarks: As Jennings (1936) offered only a brief description and it is the type species of the genus, the species is herein re-described.

This species is very similar to *Anticythereis dorsennus* n. sp. by the presence of a dorsal shoulder near mid-length but differs in being more rounded in lateral outline, by relatively narrower and shallower compressed zone just behind the anterior marginal carina, by the shallower postocular depression, by the less prominent ventroanteriorly oriented carina that extend from the mid-dorsum to behind the ventroanterior angle, and by the greater length of the posterior compressed zone.

Range: Jennings (1936) found his species in the earliest Maastrichtian Navesink Formation of New Jersey and Brown (1957) found *Velarocythere eikonata* in the Peedee Formation in Bladon, Lenoir and Pitt counties, North Carolina.

Anticythereis dorsennus Puckett and Hunt **n. sp.**
Plate 2, figure 8; Plate 3, figure 1; Plate 5, figures 1-11; Text-fig. 10

Etymology: dorsennus, Latin noun meaning humpback or hunchback, in reference to the prominent mid-dorsal hump-shaped carina.

Type Specimen: Holotype: USNM PAL 771796, specimen 132/136-13 (Pl. 5, figs. 2 and 7, male LV), sample 2011-5-18-1 (water level), Maastrichtian Owl Creek Formation, Tippah County, northern Mississippi; paratype: USNM PAL 771797, specimen 132/136-18 (Pl. 5, fig. 4, female LV), sample 2011-8-4-1 (water level), Maastrichtian Owl Creek Formation, Tippah County, Mississippi.

Diagnosis: This species is characterized by a combination of very coarse, deep reticulation; prominent postocular carina that parallels the dorsal margin at mid-length, borders the bottom of the postocular depression to just behind the anterior margin below mid-height, then turns to parallel the anterior and ventral margins, losing its distinction at about 1/3 length; and another very prominent anterior carina, which arises anterior to the eye tubercle, extends parallel to the postocular carina and terminates at the ventral margin. The postocular carina forms a distinctive hump or shoulder at the mid-dorsum in lateral silhouette.

Material: 157 valves

Measurements: Holotype L = 0.748 mm, H = 0.345 mm; paratype L = 0.750 mm, H = 0.369 mm

Description: The carapace is sub-rectangular in lateral outline, and very robust. The dorsal outline is humped, which is formed by the projection of the postocular carina above the hinge line, and curves up at eye tubercle and at the dorsoposterior angle, forming a stragulum; in the LV, the eye tubercle rises prominently above the dorsum, less so in the RV; the anterior margin is broadly curved and infracurvate; the ventral margin is nearly straight, slightly upturned at 1/3 length and is very slightly concave just anterior to the ventroposterior angle; the posterior margin in the LV is broadly and evenly rounded, and equicurvate; in the LV, the posterior margin is broadly rounded in ventral half, and slightly concave in dorsal half; the dorsoposterior angle is broad in the RV, but upraised in the LV.

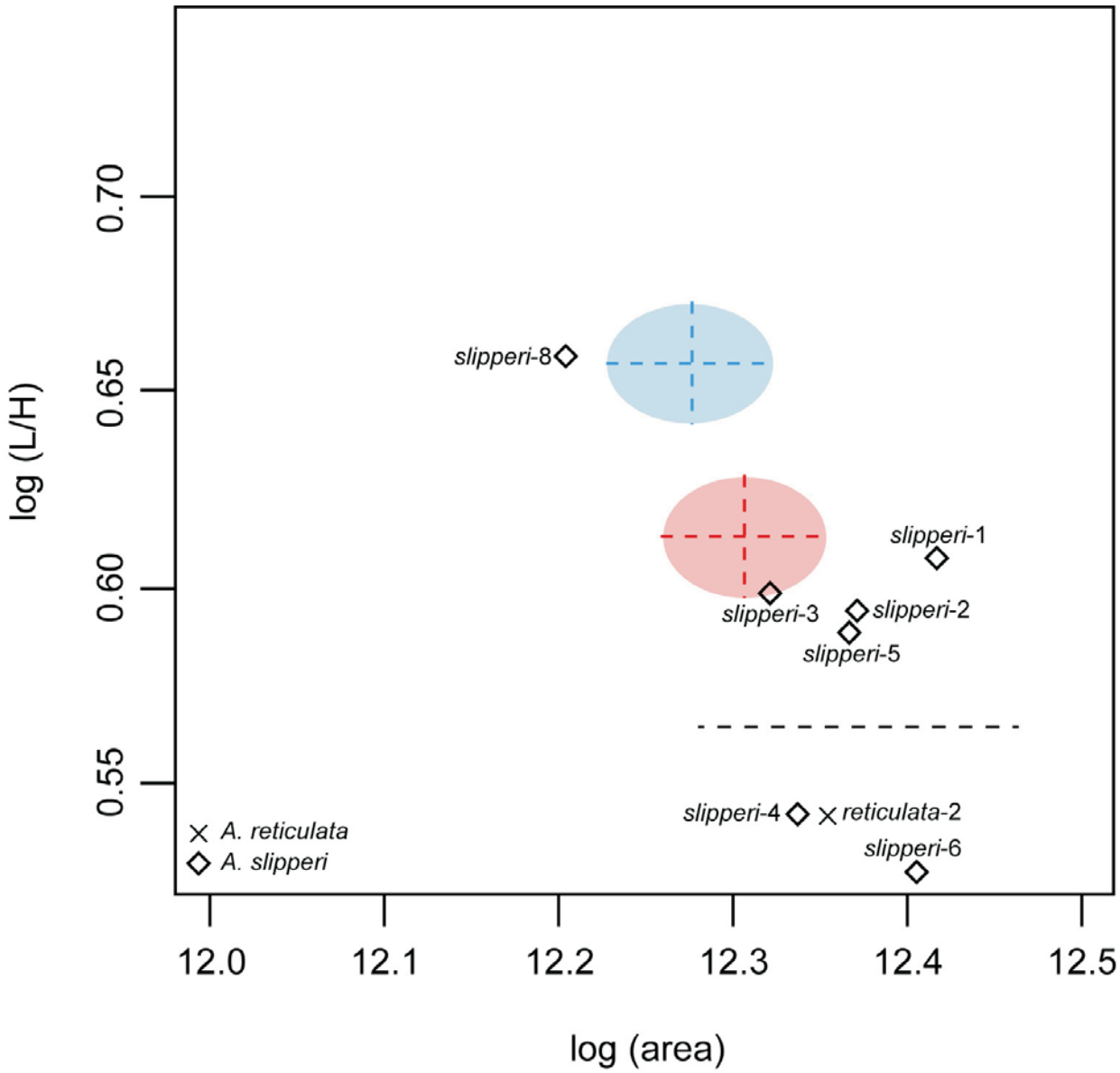

TEXT-FIGURE 9
Size (log area) versus shape (log[L/H]) for *Anticythereis reticulata* and *Anticythereis slipperi*. Dotted line indicates inferred separation between males and females for the specimens figured in this work.

A double row of denticles is located very close to the anterior and posterior margins. The outline in dorsal view is sagittate, with a very narrow marginal zone that steps up to the anterior marginal carina, then narrows slightly to form a bulging lateral outline; the carapace then broadens gently to the greatest width at approximately ¾ length, then tapers to the posterior margin, which is flat. The anterior and posterior marginal zones are compressed, with prominent marginal carinae.

The eye tubercles are distinct, yet do not bulge. The carapace is coarsely reticulate and carinate; a very prominent anterior marginal carina extends from the dorsoanterior angle to the ventroanterior angle, with a fossa on either side of the eye tubercle; a prominent, elongate postocular sulcus extends from the dorsal margin to just below the eye tubercle. Prominent carinae form an arrowhead that points ventroanteriorly; one carina extends ventroanteriorly from the mid-dorsum, where it forms the distinctive hump in outline, turns ventroposteriorly below mid-height, then fades into the venter; a second carina parallels the dorsal carina, begins not quite at the dorsal margin, and terminates at approximately mid-height; a row of sub-rounded to sub-quadrate fossae fills the area between the two carinae, with fossae becoming smaller anteriorly; an anterior carina is parallel and very close to the anterior margin; large, radially-oriented, sub-rectangular fossae are located behind the anterior carina, with intervening thin muri, and with a single rimmed sieve-type normal pore canal at the posterior end of the soli; several relatively small fossae are located between the large sub-rectangular anterior fossae and the prominent lateral carinae; the posterior margin is bordered closely by a ca-

rina, anterior of which are large, subquadrate fossae separated by low muri; a prominent murus extends a short distance ventrally from the eye tubercle. The fossae in the middle and posterior regions of the carapace are generally sub-rounded and become slightly smaller in the posterior region; the intervening muri are robust, with the margins of the fossae being vertical or undercut (Pl. 5, fig. 9); each fossa has a single rimmed sieve-type normal pore canal, which is usually off center. The soli typically are caperate, with radiating wrinkles (Pl. 5, fig. 9). Mural punctation is rare (Pl. 5, fig. 9).

The hinge is paramphidont; the denticulation in the RV (Pl. 5, figs. 6 and 8) includes an anterior, stepped, subtly grooved tooth, with a lower anterior part and an upper taller posterior tooth; a postjacent socket; a straight crenulated groove; and a posterior tooth that is blunt and angled. In the LV (Pl. 5, figs. 5 and 7), the anterior socket has a blunt protuberance at the anterior margin; the narrow subjacent tooth is angled ventroanteriorly, with an overlying low stragulum; the median bar is narrow, straight and crenulate; and the posterior socket, which is angled at ca. 45°, has an overlying stragulum. The selvage and inner margins are distinct, with a narrow vestibule in some specimens; the marginal zone is relatively wide; a double ogee-shaped interruption of the selvage is located at the caudal region (arrow on Pl. 5, fig. 6). Scattered large pits are the inner openings of the sieve-type normal pore canals. The ocular sinus is large and located below and slightly anterior of the anterior hinge element. A pair of rimmed, inverted fusiform platforms are located behind and below the anterior hinge elements that correspond to the interior of the post-ocular sulcus, and both are elongated parallel to the long axis of the carapace; the upper platform is larger and tapers anteriorly; the lower platform is tear-shaped and acuminate posteriorly (Pl. 5, figs. 5-8 and 10-11).

The muscle scars (Pl. 3, fig. 1; Pl. 5, figs. 10 and 11) include a U-shaped F scar; the A-1 is elongate dorsoanteriorly, points towards the anterior hinge elements, is acuminate dorsally, and is located above the posterior ends of the lower adductor scars; the A-2, A-3 and A-4 scars are intertwined in a pattern similar to a yin-yang symbol in an overall circular pattern; the A-2 scar is relatively large, paisley-shaped, and tapers posteriorly above the A-3 scar; the A-3 scar is small, circular, and seated above the posterior margin of the A-4 scar; the A-4 is of intermediate size, is elongate almost horizontally, and has a slight indention where it abuts the A-3 scar; the M-2 is close to the ventral margin, is very narrow and elongate horizontally, and becomes acuminate posteriorly; the M-1 is about half way between the anterior margin of the F scar and the M-2, and is small and nearly circular; there are several dorsal scars, with the D-1 scar being very small and situated well anterior of other scars; the D-2 scar is small and situated directly above the anterior margin of the F scar; a very small, circular D-3 is located directly above the anterior margin of the A-1 scar; and there is a very small, circular scar (D-4?) located farther dorsal of other scars and directly above the posterior margin of the A-1 scar. The fulcral point is arched and situated slightly dorsoanterior of the A-1 scar.

The species is sexually dimorphic, with the males (Pl. 5, fig. 2) being more elongate and the females being more rounded (text-fig. 10). The carapace in the males are not as inflated as the females, with a slightly deeper mid-lateral sulcus.

Remarks: This species is similar to the type species of the genus, *A. reticulata* (Pl. 4, figs. 1 and 2). It differs from that species in being more elongate, by the presence of the two distinctive carinae that extend from the dorsal region to the anterior; by the presence of wider compressed marginal zones; by the sub-rectangular fossae directly behind the anterior rim; and by the less upturned posterior margin.

Range: This species was observed in the Owl Creek Formation of Tippah County, Mississippi and in the Prairie Bluff Formation of Lowndes County, Alabama (text-figs. 2 and 4). Both occurrences are of Maastrichtian age.

Anticythereis slipperi Puckett and Hunt **n. sp.**
Plate 2, figure 7; Plate 3, figure 2; Plate 6, figures 1-10; Text-fig. 9

Etymology: Named in honor of Ian Slipper, who worked at the University of Greenwich and passed away 17 May 2017, for his contributions to the study of Cretaceous ostracods. His works, particularly the studies of the Turonian ostracods of England (Slipper 2019, 2021), are models of meticulous and thorough taxonomic works.

Type Specimens: Holotype USNM PAL 771798, specimen number 148-14 (Pl. 6, fig. 1, female RV), sample 1991-8-15-7, Campanian-Maastrichtian Ripley Formation, Lowndes County, central Alabama; paratype: USNM PAL 771799, specimen number 2011-8-15-1 (15) (pl. 6, fig. 3, male RV), latest Campanian-early Maastrichtian Coon Creek type locality, McNairy County, Tennessee.

Diagnosis: This species is characterized by a supracurvate ventral margin in LV, infracurvate anterior and posterior margins in RV, and a RV with a longitudinal medial sulcus in the central and dorsoposterior region of carapace.

Material: 62 valves and 2 carapaces

Measurements: Holotype L = 0.726 mm, H = 0.410 mm; paratype L = 0.702 mm, H = 0.333 mm.

Description: The carapace is robust. The anterior margins are broadly and evenly rounded; the anteriorly margin of the LV is broadly rounded and slightly infracurvate (Pl. 6, figs. 2 and 4); the posterior margin is broadly rounded and supracurvate; the RV anterior and posterior margins are infracurvate; the posterior margin in the RV is moderately convex in the ventral part, but becomes very slightly concave in the upper part and continues to form a broadly arched dorsum, and has a very weak dorsoposterior angle. The dorsal margin in the LV has stragula above the terminal hinge elements; the dorsal outline of the RV is humped at mid-length due to a carina that protrudes above the hinge line; the ventral outline in the LV is very broadly and evenly rounded, sags and overhangs the ventral margin in lateral view, and curves up in the posterior without a clear ventroposterior angle; the ventral margin in the RV has a gentle concavity at 1/3 length, then becomes broadly convex and curves up to venter. The carapace in dorsal view is sagittate, with compressed margins; the anterior margin is stepped, with a very narrow marginal zone that steps up to the anterior marginal carina, then narrows slightly to form a bulging lateral margin; the greatest width is at circa ¾ length, then narrows to form a compressed posterior margin.

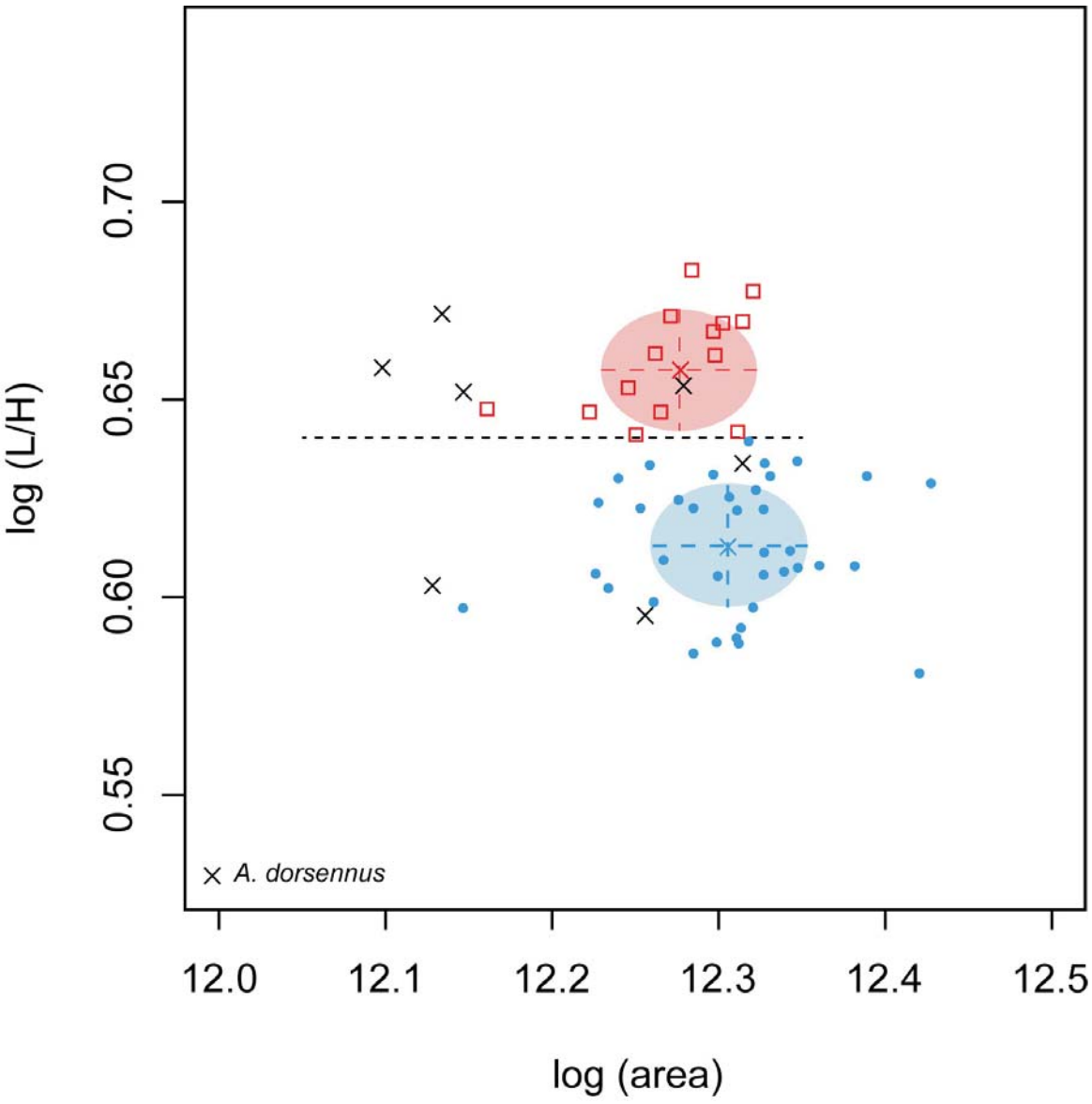

TEXT-FIGURE 10
Size (log area) versus shape (log[L/H]) for *Anticythereis dorsennus*. X's indicate specimens figured herein. Other points are from larger sample of this species analyzed by Hunt et al. (2017, population ANT_RETI-1-2). Blue circles = male and red squares = female clusters from that analysis, with corresponding colors for the 50% probability ellipses. Dotted line indicates inferred separation between males and females for the specimens figured in this work.

The eye tubercles are distinct and slightly elevated. The characteristic postocular sulcus extends from the dorsum slightly anterior of mid-length to directly below the eye tubercle; a strong, upraised carina borders the ventral margin of the postocular sulcus, forms a dorsal apex, and becomes less distinct below the eye tubercle; an anterior carina parallels the anterior margin, with intervening rectangular fossae separated by low muri; behind the anterior carina is a series of quadrate to rectangular fossae separated by low and thin muri, with smooth soli; the central part of the carapace has large, sub-rounded fossae, each with a single rimmed sieve-type normal pore canal; the muri are generally sloped to the soli, but sometimes are undercut (Pl. 6, fig. 10); the soli are caperate in places (Pl. 6, fig. 10); the regions just anterior and posterior to the center have slightly smaller and sub-rounded fossae; fossae in the posterior region become subquadrate, and are separated by low, thin muri; the fossae in the center of the carapace above mid-height are largest and deepest; in the RV, the center part of carapace has a gentle, elongate sulcus generally corresponding to the zone of large fossae, and extends from directly below the eye tubercle to 4/5 length; the muri are sparsely foveolate. Low, blunt denticles are located very close to the anterior and posterior margins.

The hinge is paramphidont; the RV (Pl. 6, fig. 6) has a slightly lobate anterior tooth, with a lower and smoother anterior knob and a taller, grooved posterior knob, and with subjacent socket;

the median groove is robust and crenulate, and widens towards the extremities; an elongate posterior tooth is located at the dorsoposterior angle, is oriented at approximately 45°, and is steeper on the ventral side; the hinge in the LV (Pl. 6, fig. 5) has an anterior socket that extends to below a postjacent blunt tooth, a straight and narrow median bar, and a socket at the dorsoposterior angle. The inner surface has scattered pores that are the inner openings of sieve-type normal pore canals. The marginal zones in the anterior, ventral and posterior regions are wide and have a well-developed duplicature; the selvage and list in the RV correspond to selvage groove in the LV; the ventral margin is slightly upturned just anterior of mid-length; the selvage on the LV is interrupted by a double ogee-shaped structure that lies just above mid-height (the specimen in Pl. 6, fig. 6 is abraded, but other specimens in the authors' collection have this structure preserved). A pair of rimmed, fusiform inverted platforms are located below the anterior end of the medial hinge element (Pl. 6, fig. 6); the upper platform is larger and acuminate anteriorly, whereas the lower platform is smaller and acuminate posteriorly; these platforms correspond in location to the inner surface of the postocular sulcus. A large ocular sinus is located just in front and below the anterior hinge element.

The muscle scars (Pl. 3, fig. 2; Pl. 6, figs. 6 and 7) have a V-shaped F scar; the A-2, A-3 and A-4 adductor scars are intertwined in a characteristic yin-yang symbol, with a large A-2 bulbous in the anterior that tapers across the A-3 scar; the small, elongate A-3 and A-4 scars are very close and nearly fused; the A-1 is offset dorsally and posteriorly from other adductor scars, is elliptical and tilted dorsoanteriorly; a reniform M-1 is directly below the F scar, less than half distance to venter; a small, elongate M-2 is close to the venter and tilted slightly dorsal from horizontal; the D-1 scar is directly below the ocular sinus; a small, circular D-2 is about half distance from D-1 to the F scar; a small, circular D-3 is located above the A-1 scar; the fulcral point is circular and sunken.

The species is sexually dimorphic, with the males being more elongate with strongly supracurvate posterior margins, whereas the females are rounder with less dramatic upturned posterior margin (text-fig. 9). The longitudinal sulcus in the males is better defined than the females, which is more inflated.

Remarks: This species is similar to *A. dorsennus* n. sp. by the mid-dorsal hump in outline, by the downwardly deflected carina along the posterior margin of the postocular depression, by the subcircular fossae that are located across the carapace, and by the more inflated lateral surface. It differs from that species in having a supracurvate posterior margin, rather than equicurvate; by less prominent anterior and posterior marginal carina; by less prominent and sharp-edged anterior carinae; and shallower fossae. It differs from *A. reticulata* (Jennings 1936) by being more elongate and less globose, by narrower muri, and by more polygonal fossae.

Range: This species was found in the type locality of the Coon Creek Formation (latest Campanian-early Maastrichtian) in McNairy County, Tennessee, the Ripley Formation (Maastrichtian) of Sumter, Lowndes and Dallas counties, Alabama, and the Prairie Bluff Chalk (Maastrichtian) of Lowndes County, central Alabama and Oktibbeha County, eastern Mississippi (text-figs. 2 and 4). This is one of the earliest species in the genus in the region. Sixty of the sixty-two specimens were collected from the coeval Coon Creek Formation in southern Tennessee and Ripley Formation of Alabama; the two other occurrences are in the Prairie Bluff Chalk.

Anticythereis sp. 1
Plate 4, figure 11

Material: 7 valves

Remarks: This species has a relatively large, sub-rectangular carapace with a gentle dorsal hump in outline, relatively shallow reticulation of sub-rounded fossae; and two anterior carinae parallel to the anterior margin with intervening sub-rectangular fossae. Unfortunately, this species is quite rare and only seven valves were recovered, in none of which can the internal morphology be observed. For these reasons, this species is left in open nomenclature.

Range: This species was found in a single sample collected from the Cusseta Sand of Barbour County, eastern Alabama (text-fig. 4). This sample is in the planktonic foraminiferal *Radotruncana calcarata* Taxon Range Zone of earliest late Campanian age (Puckett and Mancini 1998), and is therefore the oldest sample that includes anticytherideinines.

Genus ***Asculdoracythereis*** Puckett and Hunt **n. gen.**

Etymology: This genus is named after the type species, *Asculdoracythereis asculdora* n. gen. et sp., in reference to the smooth dorsal outline.

Type Species: *Asculdoracythereis asculdora* gen et sp. nov. (Pl. 1, fig. 4; Pl. 3, fig. 3; Pl. 8, figs. 1-11; Text-fig. 11).

Diagnosis: Species of the genus *Asculdoracythereis* are characterized by a combination of a carapace that is broadly rounded to flattened in dorsal view (i.e., not sulcate or lobate), has a level lateral outline in mid-dorsum, has relatively shallow fossae, and has a polygonal network of sharp-edged muri.

Remarks: Most of the species assigned to the new genus from the present study are from the Providence Sand (Maastrichtian) of eastern Alabama. These species include the nominal species, *As. invicta* n. sp., *As. lowndesensis* (Smith 1978) (also observed in the Prairie Bluff Chalk (Maastrichtian) of central Alabama), and *As. pseudoalabamensis* n. sp. Likewise, *Asculdoracythereis alabamensis* (Smith 1978), which he collected from the Prairie Bluff Formation of central Alabama, should be assigned to this genus. Other species of possible assignment to *Asculdoracythereis* include *Velarocythere scuffletonensis* Brown, 1957 and *V. legrandi* Brown, 1957. The type specimens of the latter two species have adventitious material on them, but SEM images can be viewed *via* the collections database at the U.S. National Museum (search engine found at https://collections.nmnh.si.edu/search/paleo/). The latter two species are from the Peedee Formation (Maastrichtian) of North Carolina. An undescribed species, *As.* sp. 1 (Pl. 4, figs. 9 and 10) which was collected from the Owl Creek Formation of northern Mississippi, is tentatively assigned to the new genus, but was very rare and the details of the interior of the carapace are not known.

The species assigned to *Asculdoracythereis* n. gen. are remarkably similar to each other and can be difficult to distinguish, differing mainly in the shape of the fossae and the presence or absence of carinae. It is also the most diverse genus in the new subfamily and includes at least eight species. The genus was

short-lived, evolving in the Maastrichtian and becoming extinct at the end of the Cretaceous.

Asculdoracythereis alabamensis (Smith 1978)
Plate 7, Figure 3

Anticythereis alabamensis SMITH 1978, p. 555, Pl. 6, fig. 21, Maastrichtian Prairie Bluff Chalk, Lowndes County, Alabama.

Type Specimen: Holotype USMN PAL 255752, female RV (Pl. 7, fig. 3).

Diagnosis: Species characterized by combination of strongly infracurvate anterior margin, laterally swollen carapace, non-reticulate in the posterior, and with fossae arranged concentrically subparallel to carapace outline.

Remarks: Smith (1978) noted that *As. alabamensis* differs from *A. legrandi* (Brown, 1957) in that the latter "has small spines on the anterior end [presumably denticles] and lacks the anterior rim and smooth posterior margin of *As. alabamensis* n. sp." Images of the holotype of *As. alabamensis* (USNM PAL 255753) and of *As. legrandi* (USNM PAL 129011; available for view at the USNM web site for paleobiology collections) show that the anterior margin *A. alabamensis* extends downward more than *As. legrandi*; the anterior rim noted by Smith in the latter species includes sets of carinae parallel to the margins, with four in the anterior and three in the dorsoposterior region. Otherwise, the species are very similar.

This species is very similar to *As. pseudoalabamensis* n. sp. (Pl. 7), but differs in being less elongate, having a more swollen lateral surface, having concentrically arranged fossae, and with a smooth posterior. The muri are relatively low, but that may be a taphonomic artifact of the type specimen. The overall shape is similar to *As. invicta* n. sp., but it lacks the sharp-angled longitudinal carinae of the latter species. Sexual dimorphism unknown, but the figured specimen is plotted on text-fig. 10.

Range: Smith (1978) found this species in the Prairie Bluff Chalk (Maastrichtian) of Lowndes County, Alabama. None were found during this study.

Asculdoracythereis asculdora Puckett and Hunt **n. sp.**
Plate 1, figure 4; Plate 3, figure 3; Plate 8, figures 1-11; Text-fig. 11

Etymology: *a* – meaning without, and *sculdor*, Anglo-Saxon for shoulder.

Type Specimen: Holotype: USNM PAL 771800, specimen 146-1 (Pl. 8, fig. 2, male LV); paratype: USNM PAL 771801, specimen 148-3 (Pl. 8, fig. 4, female LV); both specimens from sample 2012-01-03-1-2, Providence Sand (Maastrichtian), Barbour County, eastern Alabama.

Diagnosis: This species is characterized by a combination of relatively flat lateral surface, sub-rectangular lateral outline, coarse and well-rounded fossae completely covering carapace, almost straight dorsal outline, and relatively shallow post-ocular depression.

Material: 6 carapaces and 82 single valves

Measurements: Holotype L = 0.684 mm, H = 0.339 mm; paratype L = 0.708 mm, H = 0.387.

Description: The carapace is robust; the lateral outline is sub-rectangular; the greatest height is at the anterior dorsal angle, although not prominent; the anterior margin is infracurvate, and is broadly and evenly rounded; the posterior margin of the LV is slightly supracurvate, whereas in the RV it is equicurvate and broadly rounded; the dorsal margin is nearly straight in the LV, but very slightly convex in the RV; the ventral margin is nearly straight in the LV, but slightly concave in the RV, with the typical concavity at 1/3 length; the posterior margin of the LV curves smoothly up from the venter in the males, becoming almost straight vertical up to the dorsoposterior angle, and in the females it is broadly rounded. Small, blunt denticles are located along the ventroanterior and posterior margins. The carapace in dorsal view is broadly bulging, with the greatest width at circa 4/5 length; the marginal zones are conspicuously not compressed, with a very slight indentation just posterior of weak anterior marginal carina.

The eye tubercles are smooth areas just below the dorsoanterior angle, but do not bulge. The post-ocular sulcus is subjacent to the eye tubercle and extends ventroanteriorly from the dorsal margin to slightly anterior of mid-length to terminate well above mid-height. The primary external ornamentation is reticulation across entire carapace; fossae are rounded, ranging from circular to rounded polygonal. There are two rows of fossae parallel to the anterior margin, both being sub-rectangular with long axis parallel to margin, with the dorsal-most fossae becoming acuminate dorsally; the anterior row generally includes 6 fossae, and the second row includes 7; the murus between the first and second row is continuous, with the muri separating the fossae in each row being relatively thin. The fossae in the anterior half are slightly smaller than those in the posterior half and are generally more subcircular, whereas those in posterior half are more sub-rectangular; the fossae along posterior and ventral margins are elongate parallel to the margins; the sola are typically caperate, with stretch marks that radiate away from sieve pores (Pl. 8, figs. 7 and 11); the muri are generally nearly vertical or undercut (Pl. 8, fig. 7). Sieve-type normal pore canals with raised rims are located near center of the fossae, and sometimes with an apophysis; the sieve plates are sunken well below raised rim, and include numerous openings (Pl. 8, fig. 7).

The hinge is paramphidont; the anterior hinge element in the LV (Pl. 8, fig. 3) includes a concentrically grooved socket that extends well below the postjacent tooth; the tooth is elongated ventroanteriorly; the median hinge bar is straight and crenulate; the posterior hinge socket is located at the ventroposterior angle and tilted at circa 45°; the anterior hinge tooth in the RV (Pl. 8, figs. 8 and 10) is stepped, with both parts being vertically grooved; the postjacent socket is deep; the median hinge groove is straight, crenulate, and narrowest in the middle; the posterior tooth arches across the dorsoposterior angle. The selvage, selvage groove, list and inner margins along the anterior, ventral, and posterior margins are with no observable vestibule. There is an interruption of the selvage at the caudal region in the RV that produces a double ogee-shaped structure (slightly damaged in the specimen on Pl. 8, fig. 8), with corresponding smooth area in the LV. A pair of elongate, rimmed, inverted platforms located between the central muscle scar field and the hinge (Pl. 8, figs. 9 and 10), which corresponds to the inside of the postocular sulcus, is observed in some specimens; the smaller, lower platform is slightly forward of the upper, and in most specimens is ill-defined; the anterior end of the upper platform is acuminate anteriorly, whereas the lower platform is

acuminate posteriorly. A large ocular sinus lies just anterior and ventral of the anterior hinge elements (Pl. 8, figs. 8-10).

The muscle scars (Pl. 3, fig. 3; Pl 8, figs. 9 and 10) include a V-shaped F scar tilted slightly forward, with the posterior taller than the anterior; the A-2, A-3 and A-4 scars are arranged in an overall circular pattern and intertwined like a yin-yang symbol; the A-1 scar is oval, tilted anterodorsally, offset vertically from the other adductors and located above the posterior ends of the other adductor scars; a tilted, paisley-shaped A-2 scar tapers across the lower adductor scars; a small, elongate A-3 scar is sandwiched between the posterior ends of the A-2 and A-4 scars; and the A-4 scar is elongate, tilted slightly, and is acuminate ventroanteriorly. An elliptical M-2 scar is located just inside of the ventral margin below and slightly posterior of the F scar, with an intervening elongate and reniform M-1. A depressed fulcral point is located above and slightly anterior of the adductor scars. Four small, circular dorsal scars are located near dorsal margin that extend from anterior of the F scar to directly above the posterior margin of the adductor scars.

The species is sexually dimorphic, with the females having a greater height/length ratio and more inflated than the males (text-fig. 11).

Remarks: Generic synapomorphic characters observed in the species include the rimmed sieve-type normal pore canals on the fossae (Pl. 8, fig. 7); muscle scar pattern with yin-yang-shaped adductor scars (Pl. 3, fig. 3; Pl. 8, fig. 10); a pair of rimmed, inverted, fusiform platforms that correspond to the inside of the postocular sulcus (Pl. 8, figs. 9, 10); and lobate hinge teeth (Pl. 8, fig. 10). The sub-rectangular carapace outline is similar to *As.* sp. 1, but it is larger and includes more numerous and smaller fossae; the posterior margin is smoother and lacks the lobate outline of *A.* sp. 1.

Range: This species has been found only in the Providence Sand (Maastrichtian) of Barbour County, eastern Alabama (text-fig. 4).

Asculdoracythereis invicta Puckett and Hunt **n. sp.**
Plate 1, figure 4; Plate 3, figure 4; Plate 9, figures 1-11; Text-fig. 11

Etymology: invictus, Latin meaning unconquered, strong, in reference to the strong muri and carinae on the carapace.

Type Specimens: Holotype: USNM PAL 771802, specimen 147-10 (Pl. 9, fig. 1, male RV); paratype: USNM PAL 771803, specimen 147-13 (Pl. 9, fig. 4, female LV); both specimens from the Maastrichtian Providence Sand, Barbour County, eastern Alabama.

Diagnosis: Carapace large with a sub-quadrate outline, with strong longitudinal carinae connected by weaker sub-vertical muri; longitudinal carinae converge near ventroanterior margin; muri polygonal, quadrate in centrally inflated region of carapace.

Material: 35 valves and 3 carapaces

Measurements: Holotype L = 1.100 mm, H = 0.524 mm; paratype H = 0.892 mm, paratype L = 0.488 mm.

Description: The carapace is large, robust, and sub-quadrate in lateral outline. The dorsal margin is straight but with protrusions from carinae that extend the silhouette above the margin, and with a prominent peak near mid-length; the anterior margin is broadly and evenly rounded and infracurvate; the ventral margin is very broadly convex in the LV, but in the RV is characteristically concave; the posterior margin in the LV is very broadly rounded, almost straight in the central part, and equicurvate; the RV has a broadly rounded posterior margin in the lower half, is gently concave in the upper half up to a subtle dorsoposterior angle, and is infracurvate. The anterior and posterior margins have a double row of small denticles that are slightly longer at and below mid-height. The carapace in dorsal view is broadly and gently bulged; the anterior margin is blunt, then flares at the anterior marginal carina, then narrows to bulge at the lateral margin; the sides are broad but nearly flat, with the greatest width at approximately 3/4 length, then tapers to a slightly compressed posterior region; the posterior margin is blunt.

The eye tubercle is gentle and not bulged. A distinctive postocular sulcus extends from the dorsal margin at circa 1/3 length, drops below the eye tubercle, then continues parallel to the anterior margin to the venter just behind the marginal carina; a depressed zone behind the marginal carina is subdivided into large, sub-quadrate fossae by thin and low muri; the anterior marginal carina extends from near the dorsal margin just behind dorsoanterior angle and skips across the eye tubercle to parallel the anterior margin to the venter; between the anterior carina and anterior margin is a region with very narrow, sub-rectangular fossae defined by low, thin muri; the posterior marginal zone is compressed, with few, small, blunt tubercles connected by low, thin muri. The middle section of the carapace bulges, is coarsely carinate, with very prominent sub-horizontal carinae and lower, thinner muri tilted slightly anteriorly to form subquadrate fossae; just below the postocular sulcus is a relatively low carina, which is connected at both ends to a second large subjacent carina, which together form a fusiform structure that encloses low, thin interconnecting muri that separate small, subquadrate fossae; these two carinae merge to form a single carina that curves back to parallel the ventral margin; two other carinae in the central area arise from just anterior of the posterior part of the lateral bulge, oriented dorsoanteriorly, to curve ventroanteriorly at 2/3 length, with the dorsal carina curved anterior of the ventral carina to join with a prominent anterior carina where it begins to curve ventroposteriorly; just behind mid-length, a short carina intervenes between the two longitudinal carinae a short distance, beginning just below a curve in dorsal carina to terminate near mid-length; another sub-horizontal carina extends across the bulged part of carapace paralleling the lower of the two mid-carapace carina to join it behind the curve of prominent anterior carinae, forming a fusiform structure; the ventral carina bifurcates posteriorly at 1/3 length, with the resulting two carina paralleling each other; just above the central muscle scar field is a distinctive sub-circular fossa (see arrow on Pl. 9, fig. 2) that interrupts the dorsal longitudinal carina; zones between the lateral carinae are connected by low muri angled slightly anteriorly to form sub-quadrate fossae; in general, the mural walls are tall (particularly at the carinae) (Pl. 9, fig. 11), but rarely undercut; caperation in the soli was not observed. The surface has scattered, rimmed sieve-type normal pore canals; the sieve plates are sunken below level of the soli (Pl. 9, fig. 11); a gentle moat surrounds the pore canals; sieve pores are generally located within the confines of the fossae, but sometimes are located on the sides or even within muri (Pl. 9, fig. 11), although none are located on the prominent carinae.

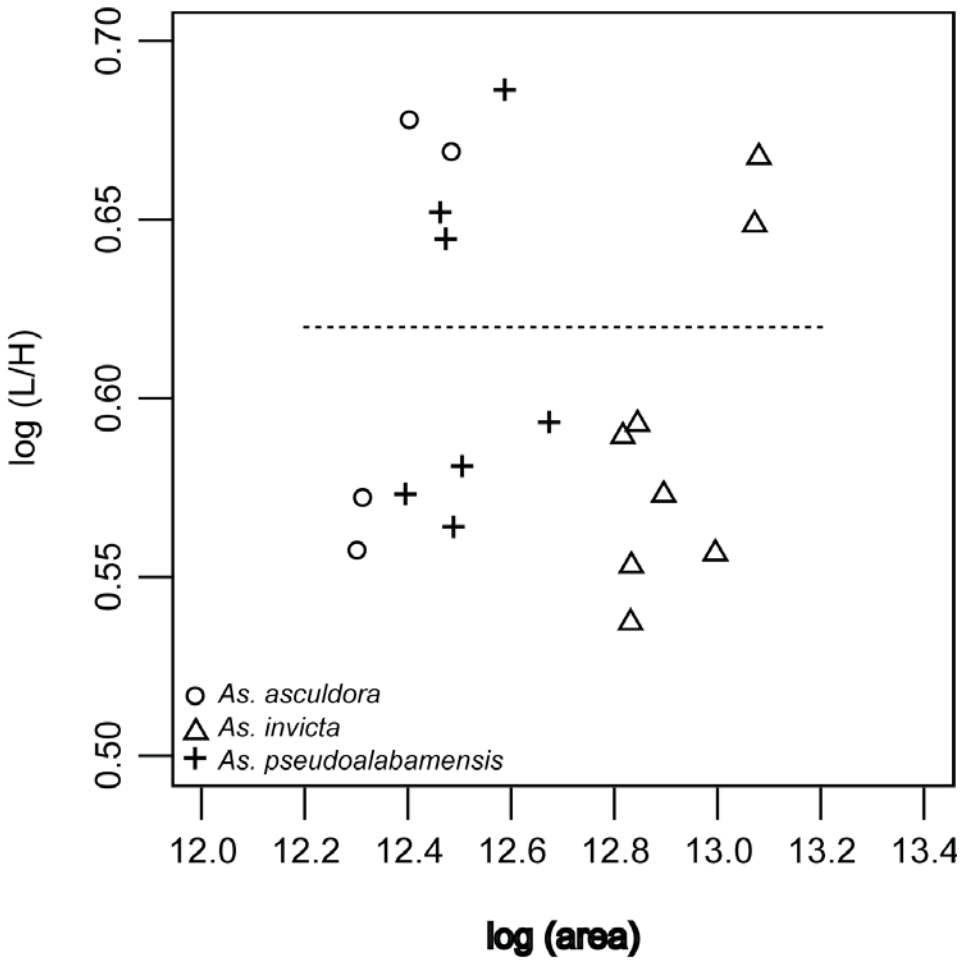

TEXT-FIGURE 11
Size (log area) versus shape (log[L/H]). (A) *Asculdoracythereis asculdora*, *Asculdoracythereis invicta*, and *Asculdoracythereis pseudoalabamensis*. Dotted line indicates inferred separation between males and females for the specimens figured in this work; in this case, the same separation point is inferred for all three species.

The hinge is paramphidont; the RV (Pl. 9, figs. 6 and 8) has a stepped and grooved anterior tooth; the smooth subjacent socket shallows posteriorly; the median groove is straight and crenulate, and widens towards the extremities; the posterior tooth is arched across the dorsoposterior angle and multilobate; in the LV (Pl. 9, figs. 5 and 7), the anterior socket is grooved; the subjacent tooth is tall and narrow; the median bar is straight and crenulated; and the posterior socket is loculate and curves around the dorsoposterior margin. Large pores correspond to the inner openings of the sieve-type normal pore canals. The duplicature is relatively wide. The selvage in the RV is interrupted in the caudal region by a double ogee-shaped structure (Pl. 9, figs. 6 and 8, although the specimen in fig. 6 is abraded), with corresponding area in the LV. A pair of inverted platforms is seated below and just behind the anterior hinge element corresponding to the interior of the postocular sulcus, and are elongate longitudinally (pl. 9, figs. 5-10); well-preserved specimens show the upper platform to be rimmed; the upper platform is acuminate anteriorly, whereas the much smaller lower platform is acuminate posteriorly; the platforms are less distinct in the LV. The ocular sinus is relatively small and opens just below the anterior part of the anterior hinge element (Pl. 9, figs. 5-8).

The muscle scars (Pl. 3, fig. 4; Pl. 9, figs. 9 and 10) have a U-shaped F scar, with the posterior limb being taller than the anterior; the A-1 scar is slightly elliptical, with the long axis oriented dorsoanteriorly, and is detached vertically from other adductor scars; the A-2, A-3 and A-4 scars intertwine like a yin-yang symbol in an overall circular shape; the A-2 scar is bulbous in the anterior part, similar to a paisley shape, then becomes acuminate in the posterior above the A-3 scar; the A-3 scar is small, elongate, and sandwiched between the posterior ends of the A-2 and A-4 scars; the A-4 scar is elongate and oriented slightly ventrally from horizontal; the subcircular M-1 scar lies directly below the F scar, and is slightly more than halfway between the ventral margin and the central muscle scar field; the small, horizontally elongate M-2 scar near venter is directly below the central muscle scar field; there are four small, subcircular dorsal scars; the D-1 scar is below the eye tubercle; the small, circular D-2, D-3 and D-4 scars are located above the central muscle scar field, with the D-3 scar being slightly closer to the D-2 scar; and a raised fulcral point lies between the cen-

tral scar field and the dorsal scars, and is elongate longitudinally.

The species is sexually dimorphic, with the males being more elongate and the females having a greater height/length ratio (text-fig. 11).

Remarks: This species is similar to *As. alabamensis* (Smith 1978) in overall shape, anterior marginal carina and subjacent depressed zone with sub-quadrate fossae formed by low muri; however, the prominent sub-longitudinal carina that converge in the ventroanterior region in the new species and the overall stronger carinae serve to differentiate the two. The overall shape, anterior marginal carina and postjacent depressed area with sub-quadrate fossae are also similar to *As. lowndesensis* (Smith, 1978), but the spinose ornamentation and lack of longitudinal carinae on that species differentiate it from the newly described species.

Range: This species has only been found in the Providence Sand (Maastrichtian) of Barbour County, eastern Alabama (text-fig. 4).

Asculdoracythereis lowndesensis (Smith 1978)
Plate 1, figure 3; Plate 3, figure 5; Plate 10, figures 1-10

Anticythereis lowndesensis SMITH 1978, p. 555-556, Pl. 6, figs. 22-23.

Type Specimens: The type specimens of *A. lowndesensis* were collected from the Prairie Bluff Formation (Maastrichtian) of Lowndes County, central Alabama (Smith 1978). The holotype is USNM PAL 255755, a RV with considerable debris that obscures the details of the carapace. The paratype is USNM PAL 255754, which is a juvenile LV.

Diagnosis: None given, but Smith (1978) described the species.

Emended Diagnosis: Carapace with polygonal, deep fossae, and conspicuous blunt spines that punctuate the muri at or near their junctions, either spinose or knobby. Large, radiating fossae lie behind the anterior marginal rim, and are separated by low, thin muri that forms the wide, nearly flat, infracurvate anterior region.

Material: 79 valves

Remarks: One of the authors (TMP) has collected a topotype specimen (not illustrated) that appears to be identical to the holotype but is much better preserved. The topotype specimen reveals that the upraised pores at mural junctions are spinose, being at least twice as tall as the surrounding muri. In the holotype, these conjunctive spines and spine clusters have been broken. The specimens from eastern Alabama do not appear to have had such long spines, as they do not appear to be broken and are knob-like. Taphonomic control can be seen in well-preserved specimens, where delicate upraised cup- or vase-like structures (Pl. 10, fig. 7) adorn the carapace. Sieve-type normal pore canals are located across the carapace and often pierce the muri (Pl. 10, figs. 7-9). The sieve plates have a central pore that is surrounded by numerous openings and lies below the exterior level of the carapace; they are also depressed in the center like a funnel. One sieve-type normal pore lies directly below a knob-like conjunctive spine (arrow on Pl. 10, fig. 9). The adventitious material on the holotype conceals details of the soli, which are typically caperate, and the muri, which are often undercut (Pl. 10, figs. 7 and 9). As in the holotype, the specimens from eastern Alabama show a prominent knob-like pore conus just above mid-height near the posterior margin (arrow on Pl. 10, fig. 4).

The hinge is paramphidont and well displays the morphology that is typical of the genus (Pl. 10, figs. 5 and 6). The anterior hinge in the RV is stepped and multilobate, and the LV is grooved to accept the tooth. Low stragula rise above the terminal hinge elements of the LV. The muscle scar pattern (Pl. 3, fig. 5; Pl 10, fig. 10) matches other species of the genus, particularly the yin-yang pattern of the A-2, A-3, and A-4 adductor scars, as well as the detached, elliptical, and tilted A-1 scar. There are at least three dorsal muscle scars, with the most anterior being directly below the anterior tooth of the hinge of the RV (Pl. 10, fig. 6). The rimmed, inverted platforms are also present (see Pl. 10, fig. 6 and top of Pl. 10, fig. 10), although the lower one is quite small. The double ogee-shaped interruption of the selvage is present at the posterior extremity of the RV (see Pl. 10, fig. 6, although the structure is slightly abraded).

Range: Smith (1978) reported this species from the Prairie Bluff Formation (Maastrichtian) of Lowndes County, central Alabama, and this study found the species rarely in the Prairie Bluff (same locality as Smith) and Providence Sand of Bullock County, Alabama, but more numerous specimens were picked from the Providence Sand (Maastrichtian) of Barbour County (text-fig. 4).

Asculdoracythereis pseudoalabamensis Puckett and Hunt **n. sp.**
Plate 1, figure 5; Plate 3, figure 6; Plate 7, figures 1-2, 4-11; Text-fig. 11

Etymology: *pseudo*, Latin for false, and *alabamensis*, in reference to *Anticythereis alabamensis* Smith, 1978, to which this species is similar.

Type Specimens: Holotype specimen 147-1, USNM PAL 771804 (Pl. 7, figs. 2, 9), male LV; paratype specimen 147-4, USNM PAL 771805 (Pl. 7, fig. 4), female LV; both specimens from sample 2012-01-03-1-2, Maastrichtian Providence Sand, Barbour County, eastern Alabama.

Diagnosis: This species is characterized by a combination of an evenly reticulate pattern of sub-polygonal fossae across the entire carapace except for the anterior zone, which is a relatively flattened zone of two rows of sub-quadrangular fossae separated by a thin murus; a downwardly-sloped anterior margin well developed on the RV; a thin carina that extends from mid-dorsum, behind the post-ocular depression to die out just above the central muscle scar field; and carinae that are aligned in rows separated by a murus behind the anterior flattened zone in the LV and the ventrolateral region of the RV.

Material: 17 carapaces and 144 valves

Measurements: Holotype L = 1.023 mm, H = 0.530; paratype L = 0.672, H = 0.375 mm.

Description: The carapace is robust and oblong. The greatest height is just behind the eye tubercle at the low anterior stragulum; the anterior margin is infracurvate and the posterior margin of the LV is slightly supracurvate; both margins are broadly rounded. The dorsal margin in external view has a sharp-edged, arching carina that originates just behind postocular sulcus to terminate in front of the dorsoposterior angle; in the LV, the ventral silhouette continues smoothly from

the anterior margin, very broadly rounded, to turn vertical at the blunt posterior margin; in the RV, the venter is characteristically incurved at about 1/3 length so that the margin is hidden behind the carapace in external view; the outline of the ventral to the posterior margins in the RV is broadly rounded up to mid-height, where it curves to form a straight or slightly concave dorsoposterior margin. A double row of denticles is located very close to the anterior and posterior margins. In dorsal view, the carapace is broadly and gently bulged, with a highly compressed marginal zone that steps up to the anterior carina, then tapers at the post-carina sulcus; the main part of the lateral bulge is gentle and broad, with the greatest width located near mid-length; the posterior zone is not compressed and gently narrows to the margin.

The eye tubercle is a distinct, smooth bulge at the dorsoanterior angle. The postocular sulcus is deep and smooth, and continuous from the dorsal margin just in front of mid-length to below the eye tubercle. The anterior region has two rows of large, low rectangular fossae; the rows are separated by a prominent carina that arises from the eye tubercle; the anterior row of fossae is separated from the anterior margin by a low carina that bifurcates immediately in front of the eye tubercle; the second row of fossae is slightly larger than first; both rows have smooth, flat soli; the ornamentation on the lateral, rounded region of carapace has quadrilateral fossae of generally uniform size; the muri are steep, vertical and even undercut in places (Pl. 7, fig. 9), but with rounded soli; some soli are caperate (Pl. 7, fig. 10); sieve-type normal pore canals with raised rims are located within the fossae, usually adjacent to the muri but occasionally are intramural (Pl. 7, fig. 10); the sieve plates are located inside the raised rims, and include a central pore surrounded by numerous smaller openings in concentric rows (Pl. 7, fig. 9). The dorsal carina extends from in front of the dorsoposterior angle to just in front of mid-length, where it turns sharply down behind the postocular sulcus to lose its definition; behind this carina is another depressed zone, so that the intervening carina looks like an arête between glacial valleys.

The hinge is paramphidont (Pl. 7, figs. 5-8); the anterior hinge element in the RV has a stepped tooth (Pl. 7, figs. 6 and 8); the anterior part of the tooth is lower than the subjacent tooth, is angled slightly down from horizontal, is smooth and elongate, and drops off abruptly to the carapace marginal zone and selvage; the subjacent tooth is taller, with shallow vertical grooves; the socket behind the tooth is deep, with a flaring and sharp ventral flange; the median groove is crenulate and has a double row of thin flanges above the crenulations; the posterior tooth in the RV is arched and grooved across the dorsoposterior angle; the anterior hinge socket in the LV is bipartite to accommodate the stepped tooth in the RV, with the anterior being shallow and elongate and the postjacent socket is larger, rounded and deeper; the postjacent tooth is smooth and rounded; the median hinge bar is straight, crenulate, and slightly constricted in middle; and the elongate socket is angled at about 45° across the dorsoposterior angle. The inner carapace wall is punctuated by pores, which are inner openings of sieve-type normal pore canals. The marginal zones have a well-defined duplicature, with selvage, list and flange groove; in the RV, the selvage is interrupted by a double ogee-shaped structure in the caudal region (arrow on Pl. 7, fig. 8); in the LV, there is no corresponding structure; in the LV is the selvage and flange groove; a vestibule is very narrow. Two inverted, fusiform, rimmed, inverted platforms lie in parallel just below and behind the anterior hinge elements corresponding to the interior of the postocular sulcus (arrows on Pl. 7, fig. 7); the dorsal platform is much larger than the one below it, is acuminate anteriorly, and is bluntly rounded at the posterior end; the lower platform is about half the size of upper, is tear-shaped, being acuminate posteriorly and rounded anteriorly. The ocular sinus is located just in front of and below the anterior hinge elements (Pl. 7, figs. 5-8)

The muscle scars (Pl. 3, fig. 6; Pl. 7, fig. 11) have a U-shaped F scar that is slightly higher posteriorly; the A-1 scar is ovate, with long axis about 45°, and is detached vertically and posteriorly from the other adductor scars; the A-2, A-3 and A-4 scars intertwine like a yin-yang symbol in an overall circular pattern; the A-2 scar is paisley-shaped and tapers as it curves over the A-3; the A-3 scar is small, elongate and acuminate anteriorly, and lies at the posterior ends of the A-2 and A-4 scars; the A-4 scar is elongate and tapers anteriorly; the M-1 scar is rounded and is located directly below the F scar about half way to the M-2 scar; the M-2 scar is just inside of the ventral marginal zone, is elongate longitudinally, and is located below the space between the F and adductor scars; the D-1 scar is moated and located directly below the eye tubercle; the D-2 and D-3 scars are small, round, and located above the space between the F and adductor scars; the D-4 scar is small, ovoid, and located above the A-1 scar; the fulcral point is depressed and located above the anterior end of the adductor scars.

The species is sexually dimorphic, with the females being slightly shorter but more rounded, and the males being longer and more elongate (text-fig. 11).

Remarks: This species displays all the characteristics of the genus: a well-defined postocular sulcus; two fusiform inverted platforms that possibly serve for attachment points of dorsal muscles and tendons on the interior of the postocular sulcus; the yin-yang configuration of A-2, A-3 and A-4 scars arranged in overall circular shape; and fossae with large sieve pores with raised rims. It is very similar to *As. alabamensis* Smith, 1978 (Pl. 7, fig. 7) with its infracurvate, compressed anterior zone, well-developed polygonal fossae on lateral surface, ovate depression in the caudal region of the RV, and the hinge. The new species differs from that species by being larger, more elongate, and with fossae that extend to the posterior margin.

Range: This species was found only in the Providence Sand (Maastrichtian) of Barbour County, eastern Alabama (text-fig. 4). Although one of the authors (TMP) has samples from Smith's (1978) type locality, no specimens of *A. alabamensis* were found in them.

Acsuldoracythereis sp. 1
Plate 4, figures 9 and 10

Material: 11 valves

Remarks: This very rare species is characterized by a combination of sub-rectangular lateral outline, a reticulate pattern with sub-rounded fossae, a squared off dorsoposterior region with hummocky projections, and a relatively flat lateral surface that slopes very gently to the posterior, then drops to a slightly compressed posterior margin. Unfortunately, no specimens were found for which the internal features could be observed. It is with uncertainty that this species is included in the genus *Asculdoracythereis*, particularly because of the morphology of the posterior margin and the uncertainty of the internal mor-

phology but is tentatively included because of the presence of a broad and flat lateral surface and reticulation.

Range: Owl Creek Formation (Maastrichtian) of northern Mississippi (text-fig. 2).

Genus ***Frodocythereis*** Puckett and Hunt **n. gen.**

Etymology: This genus is named after the type species, *Frodocythereis frodoi* gen. et sp. nov., in reference to the ring-shaped murus on the lateral surface.

Type Species: *Frodocythereis frodoi* n. sp. nov. (Pl. 2, fig. 5; Pl. 3, fig. 8; Pl. 12, figs. 1-12; Text-fig. 12).

Diagnosis: Species in the genus *Frodocythereis* are characterized by a combination of an overall sub-rectangular shape; very deep, polygonal fossae; a compressed posterior margin; a carina that forms a strong buttress along the ventral border of the post-ocular depression; large, box-like or sub-polygonal fossae below the post-ocular depression; a carina parallel to the dorsal carina but below it; and a relatively wide and flat anterior zone with shallow, radiating muri.

Species: Species that are assigned to the genus *Frodocythereis* include, of course, the type species, found in the Owl Creek Formation (Maastrichtian) of northern Mississippi, *F. copelandi* (Smith, 1978), found in the Owl Creek and Prairie Bluff Chalk of central Alabama, and *F.* sp. 1 of the Coon Creek Formation (latest Campanian-early Maastrichtian) of northern Mississippi. The species identified as *Anticythereis reticulata* (Jennings 1936) by Van Nieuwenhuise and Kames (1976), which is an undescribed new species with very deep fossae and sub-vertical muri, should also be assigned to *Frodocythereis*.

Frodocythereis copelandi (Smith 1978)
Plate 2, figure 6; Plate 3, figure 7; Plate 11, figures 1-11; Text-fig. 12

Anticythereis copelandi SMITH 1978, p. 556, pl. 6, figs. 24-25.

Type Specimens: Holotype USNM PAL 255757 (female RV; Pl. 11, fig. 1), sample 15A; paratype USNM PAL 255756 (RV), sample 14-I both specimens collected from the Prairie Bluff Formation (Maastrichtian), Lowndes County, central Alabama.

Diagnosis: Smith (1978) noted that "*A. copelandi* differs from *A. legrandi* (Brown, 1957) by being more coarsely reticulate and having a different arrangement of surface ornamentation."

Amended Diagnosis: This species is characterized by the following features: carapace relatively small, sub-rectangular in lateral outline; very prominent carinae, with one that nearly encircles the lateral surface of carapace; it rises above the dorsum in the mid- to posterior part of the carapace, angles ventroanteriorly to below mid-height, turns ventroposteriorly to parallel ventral margin, then bends up nearly vertically to complete the loop. A large, box-like fossa is located below the eye tubercle, bordered dorsally by the post-ocular carina; a wide apophysis usually extends a short distance into the fossa, forming an invagination.

Material: 2 carapaces, 245 valves

Remarks: This species displays all of the generic characters, including the postocular depression that extends from the dorsal margin to below the eye tubercle, with the corresponding two inverted platform structures on the inside of the carapace (Pl. 11, figs 5 and 6); the hinge that includes a stepped anterior tooth in the RV (Pl. 11, fig. 6); the yin-yang symbol made by the A-2, A-3 and A-4 muscle scars (Pl. 3, fig. 7; Pl. 11, figs. 9 and 10); the constellation of raised sieve-type normal pore canals (closeup on Pl. 11, fig. 11); and the double ogee-shaped caudal structure on the duplicature at the posterior margin of the LV (Pl. 11, fig. 6, noted by arrow). Sexual dimorphism is observed with the males being more elongate than the females (text-fig. 12).

The holotype (Pl. 11, fig. 1), unfortunately, is partially obscured by debris. The robust muri on the carapace exterior are vertical or undercut (Pl. 11, fig. 11). The raised sieve-type normal pore canals are often connected to the surrounding muri by apophyses, and the soli are often caperate. The lower inverted platform is quite small and the upper one is acuminate anteriorly. This species has compressed anterior and posterior margins with large polygonal fossae and small intervening muri that are observed in other species of the genus, including *A. dorsennus*, *F. frodoi*, *As. alabamensis*, *As. invicta*, and several others.

Range: Smith (1978) described this species from the Prairie Bluff Chalk (Maastrichtian) of Lowndes County, Alabama. In this study, *A. copelandi* was found only in the Owl Creek (Maastrichtian) of northern Mississippi. This species, therefore, has a relatively wide geographic extent, ranging from central Alabama to northern Mississippi (text-figs. 2 and 4).

Frodocythereis rodoi Puckett and Hunt **n. sp.**
Plate 2, figure 5; Plate 3, figure 8; Plate 12, figures 1-12; Text-fig. 12

Etymology: *frodoi,* in reference to Frodo Baggins, the ring bearer in *Lord of the Rings*, and the characteristic ring-shaped murus just in front of the muscle scar on the external surface.

Type Specimens: Holotype: USNM PAL 771806, specimen 134-2 (Pl. 12, figs. 4 and 12, male LV), sample 2011-8-4-1 (water level), Maastrichtian Owl Creek Formation, Tippah County, Mississippi; paratype USNM PAL 771807, specimen 104-6 (Pl. 12, fig. 6, female LV), sample 2011-5-18-1 (water level), Maastrichtian Owl Creek Formation, Tippah County, Mississippi

Diagnosis: Very large fossae, with largest just anterior to center of carapace, with most prominent in shape of ring just below postocular sulcus; steep and well-defined muri; dorsal carina, with subjacent vertical muri; and anterior marginal carina and subjacent rectangular fossae divided by radiating muri.

Material: 118 valves and no carapaces.

Measurements: Holotype L = 0.809 mm, H = 0.393 mm; paratype L = 0.744 mm, H = 0.452 mm.

Description: The carapace is robust; the greatest height is at the eye tubercle; the anterior margins are broadly rounded and infracurvate; the posterior margin of the RV is infracurvate, whereas in the LV it is slightly supracurvate. The dorsal margin is bipartite, with an almost straight anterior part that slopes posteriorly to 1/3 length, then the silhouette becomes hummocky and slightly arched in the posterior part due to the dorsal carina being elevated above the hinge line; the ventral margin in the LV is concave in the anterior part to the mid-length, then is al-

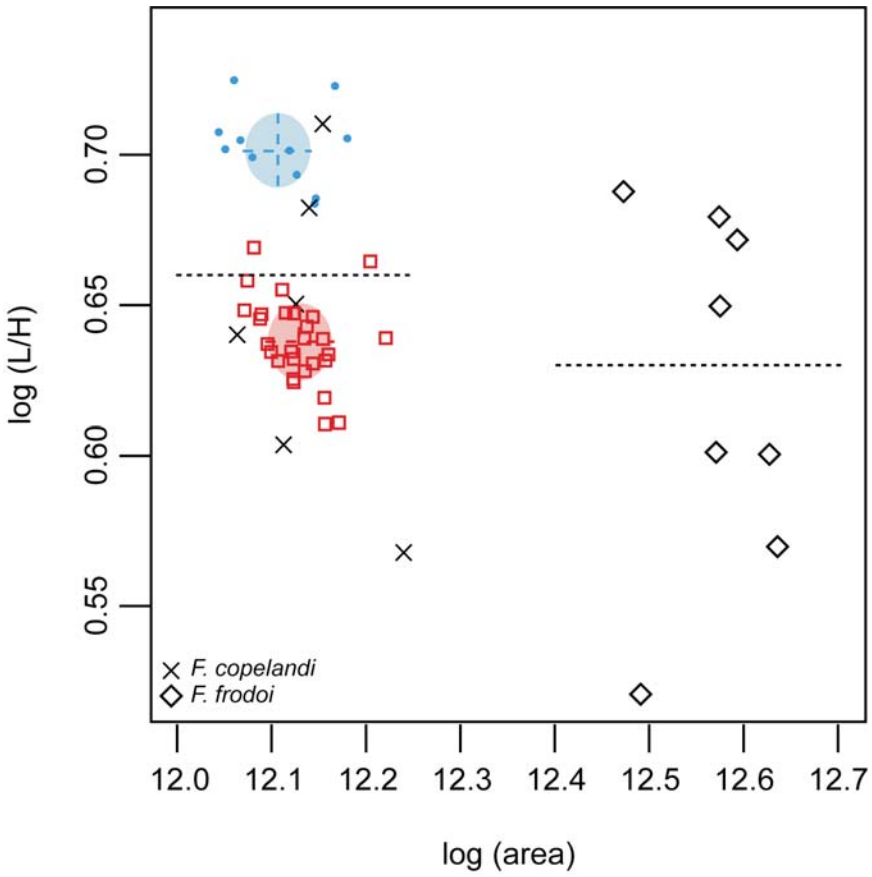

TEXT-FIGURE 12
Size (log area) versus shape (log[L/H]) for *Frodocythereis copelandi* (X) and *Frodocythereis frodoi* (diamonds). Other points are from larger sample of this species analyzed by Hunt et al. (2017, population ANT_COPE-1). Blue circles = male and red squares = female clusters from that analysis, with corresponding colors for the 50% probability ellipses. Dotted line indicates inferred separation between males and females for the specimens figured in this work.

most straight to the ventroposterior margin; the posterior margin in the RV is very bluntly rounded in the ventral part, then straight to a very obtuse dorsoposterior angle; in the LV, the posterior margin is very broadly rounded in ventral part and more curved in dorsal part. A double row of denticles is located very close to the anterior and posterior margins. In dorsal view, the anterior, compressed margin is very narrow, then steps up to the anterior marginal carina, then narrows slightly to the lateral bulge; the lateral margins then rise gently to become nearly flat except for an indentation just in front of mid-length, which corresponds to the sulcus just behind the lateral ring-like carina; the greatest width is just behind this indentation; the posterior margin drops abruptly to form a compressed posterior.

The eye tubercle is high and prominent. A deep postocular sulcus extends from the dorsal margin just anterior of mid-length to below the eye tubercles; the lower boundaries are defined by a prominent carina. The exterior ornamentation consists of a combination of large fossae and prominent muri; an anterior carina extends from the eye tubercle to parallel the anterior margin, becoming closer to the margin ventrally where it disappears at the ventroanterior angle; small, thin, radiating muri extend perpendicularly behind anterior carina and terminate within the sola to form 3-sided rectangular fossae, with muri sometimes connecting the raised sieve-type normal pore canals as apophyses; posterior to the 3-sided anterior fossae is an arc of smooth zone that is continuous from the post-ocular sulcus, continues subparallel to the anterior margin, and terminates at the ventroanterior angle; a prominent; serrated dorsal carina is located in the posterior 2/3 of the dorsum, which connects ventroanteriorly to the lateral ring-like structure in front and slightly above the central muscle scars; a murus extends anteriorly from the lower part of the ring a short distance, then terminates; other large polygonal fossae are located directly below and behind the ring; behind the ring, but not connected to it, is a longitudinal carina, concave up in the anterior part and almost straight and sloping slightly ventrally in the posterior part, that terminates in the flattened posterior region of carapace; four vertical muri extend from the longitudinal carina to the dorsal carina; three large polygonal fossae are located at mid-length and slightly behind, bordered ventrally by two smaller fossae; a prominent concave up carina is located near and parallel to the ventral margin; several rounded fossae are located in the ventral half of carapace; in the LV, a row of square fossae is located between the ventral carina and ventral margin; the posterior part of the RV is flat, but reticulate in LV. There are numerous and scattered sieve-type normal pore canals located mainly in the central part of carapace in both the sola of fossae and in the muri.

Muscle scars are often observed in external view (Pl. 12, figs. 1, 4 and 12).

The hinge is paramphidont (Pl. 12, figs. 7 and 8); the anterior hinge tooth in the RV is stepped, with the lower anterior part that rises to a taller, very gently grooved tooth and subjacent smooth socket; the median groove is straight and crenulate; the posterior tooth is smooth, elongate, and downturned at the dorsoposterior angle; the LV has an anterior grooved socket, a postjacent and smooth tooth, a crenulate median bar, and a smooth posterior socket at the dorsoposterior corner. Internally, the carapace is punctuated by pits that are the inner openings of the sieve-type normal pore canals. The selvage of the RV is split into double-ogee shaped interruption just above mid-height (Pl. 12, fig. 7). A pair of rimmed, inverted platforms are located below and behind the anterior hinge elements (Pl. 12, figs. 7-8 and 11), both of which are elongate parallel to the long axis of the carapace and correspond to the inner part of the postocular sinus; the upper platform is larger than the lower and is acuminate anteriorly, whereas the lower is shaped like a checkmark and acuminate posteriorly. The ocular sinuses are located below and anterior to the anterior hinge elements (Pl. 12, figs. 7 and 8).

The muscle scars (Pl. 3, fig. 8; Pl. 12, figs. 9-11) include dorsal, adductor, frontal and mandibular scars; the F scar lies directly in front of the adductors, in the shape of an open U; a large ovate A-1 scar is located dorsoanteriorly of the other adductor scars and is tilted anterior of vertical; the A-2, A-3 and A-4 scars are intertwined in a yin and yang symbol with an overall circular shape; the A-2 scar is paisley-shaped, with the narrow end that tapers across the A-3 scar; the A-3 scar is small, elongate, and is located at the posterior ends of the A-2 and A4-scars; the A-4 scar is elongate and tilted slightly ventroanteriorly; there are four dorsal scars, nearly all in a horizontal row; the sub-circular D-1 scar is located well in front of others; the reniform D-2 scar lies above the posterior margin of the F scar; the sub-circular D-3 scar lies above the A-1 scar; and the small, sub-circular D-4 scar is located near the posterior end of the adductor scars; the reniform M-1 lies directly below the F scar, with the concave side directed posteriorly; the oval M-2 scar sits well below and posterior of the M1 scar. A pair of rimmed, inverted platforms are located ventroposterior to the anterior hinge element, are somewhat more prominent in RV, and corresponds to the inside of the post-ocular sulcus.

The species is sexually dimorphic, with the males being more elongate and the females being taller and rounder (text-fig. 12).

Remarks: This species is similar to *F. copelandi* (Smith 1978) but differs in being larger; less elongate; with coarser, deeper and fewer fossae; and bears the distinctive ring-like fossa just anterior to the central muscle scar field. It differs from *F.* sp. 1 by having fewer and coarser fossae, being more sub-rectangular and less rounded, and by the presence of the distinctive ring structure.

Range: This species was found only in the Owl Creek Formation (Maastrichtian) type locality in Tippah County, Mississippi, where it occurs abundantly (text-fig. 2).

***Frodocythereis* sp. 1**
Plate 4, Figure 6

Material: 7 valves

Remarks: This species is characterized by very deep, sub-polygonal fossae that extend across the entire carapace except for the postocular depression. The muri are vertical to undercut. The postocular depression forms a saddle along the dorsal margin and bifurcates ventroanteriorly. The anterior marginal depression is separated from the anterior margin by a carina and is subdivided by low and thin muri. It displays all the characters of the subfamily, including sieve-type normal pore canals with raised rims, postocular depression, distinctive muscle scar pattern, stepped anterior tooth in RV, a double ogee-shaped structure at the posterior end of selvage in RV, and a pair of inverted platforms ventroposterior of the anterior hinge element in the RV. It is assigned to *Frodocythereis* n. gen. based on the presence of deep polygonal fossae (except along anterior margin), lack of prominent lobation and compressed posterior margin.

Range: This rare species was found in only one sample (2010-10-22-1(512)) from the latest Campanian-early Maastrichtian Coon Creek Formation of Union County, Mississippi (text-fig. 2).

Genus ***Laevipellacythereis*** Puckett and Hunt **n. gen.**

Etymology: This genus is named after the type species, *Laevipellacythereis laevipellis* n. sp., in reference to the smooth carapace.

Type Species: *Laevipellacythereis laevipellis* gen. et sp. nov. (Pl. 1, fig. 8; Pl. 3, fig. 10; Pl. 14, figs. 1-11; Text-fig. 13).

Diagnosis: The genus *Laevipellacythereis* includes species of the Subfamily to (due to celation) Anticytherideinae that have an almost smooth carapace due celation in which the tegmen has almost completely overgrown any underlying ornamentation (see Sylvester-Bradley and Benson (1971), fig. 30); large, beveled sieve-type normal pore canals surrounded by very small fossae; and subdued lobation.

Species: Species assigned to the genus *Laevipellacythereis* include the type species from the Owl Creek Formation of Maastrichtian age, *L. colossus* n. sp, from the Maastrichtian Providence Sand of eastern Alabama (Pl. 13, figs. 1-11), and *L.* sp. 1 from the latest Campanian-early Maastrichtian Coon Creek Formation of northern Mississippi (Pl. 4, figs. 4-5).

Laevipellacythereis colossus Puckett and Hunt **n. sp.**
Plate 1, figure 7; Plate 3, figure 9; Plate 13, figures 1-11; Text-fig. 13

Etymology: colossus, Latin noun, meaning a large statue, referring to the large size of this species.

Type Specimens: Holotype USNM PAL 771808, specimen 148-7 (Pl. 13, fig. 2, male LV); paratype USNM PAL 771809, specimen 148-9 (Pl. 13, fig. 4, female LV); both specimens from sample 2012-01-03-1-2, Maastrichtian Providence Sand of Barbour County, Alabama

Diagnosis: This species is characterized by the combination of a large, elongate, sub-rectangular carapace; two rows of large fossae parallel to anterior margin, with posterior row forming depression; carapace widest just behind mid-length; and surface punctuated by large, moated sieve pores located within small, shallow fossae.

Material: 11 carapaces and 40 single valves collected from the Providence Sand (Maastrichtian) of Barbour County, eastern Alabama

Measurements: Holotype L = 0.976 mm, H = 0.440 mm; paratype L = 0.827 mm, H = 0.410 mm.

Description: The carapace is large for the genus, and robust. In lateral view, the LV is sub-rectangular, and the RV is oblong, with the greatest height located either at the eye tubercle (RV) or at the dorsolateral swelling just posterior of mid-length (LV). The anterior margin is broadly rounded and infracurvate; the ventral margin undulates in the LV, the RV has the typical podocopid broad concavity at circa 1/3 length; the posterior margin in the LV curves up from the venter rather sharply to form an equicurvate posterior outline; in the RV, the posterior margin curves up broadly from the venter to mid-height, where it sharply becomes concave up to the dorsoposterior angle, which is distinct, to form an infracurvate margin; the dorsal margin is slightly undulatory, with the greatest convexity just behind mid-length. In dorsal view, the carapace is broadly bulged, with a very slight anterior compression, to the greatest width just behind mid-length; the posterior margin is slightly compressed.

The eye tubercle is of low relief, not bulging. A distinct post-ocular depression in the form of a groove extends from just anterior of mid-length to terminate below the eye tubercle; the solum of the post-ocular sulcus is caperate in places (Pl. 13, fig. 4); this sulcus is very deep, and the exterior expression of the internal inverted platform can be seen on some specimens (arrow on Pl. 13, fig. 4). In the relatively larger males, the lateral surface is swollen behind mid-length in upper 2/3 of carapace and forms a dorsal bulge; in the females, the posterior circa 1/5 of the carapace is compressed (Pl. 13, figs. 3 and 4). Two rows of fossae are parallel to the anterior margin; the fossae in the anterior row are generally small, and circular to elongate; the fossae in the second row are elongate parallel to the anterior margin, are separated by thin muri, and form a distinctive, continuous depression. Circular and moated sieve-type normal pore canals always are located in the very small fossae; the sieve plates are sunken below the level of the soli; the soli are rimmed around the sieve pores and may be undercut around their periphery (Pl. 13, fig. 10); the carapace has a small number of foveolae (Pl. 13, fig. 10).

The hinge is paramphidont; the anterior tooth of the RV (Pl. 13, figs. 6 and 8) is stepped and subtly multilobed; the anterior part of the tooth is not as tall and is narrower than the subjacent tooth; a rounded socket is located immediately behind the tooth; the median groove is straight and crenulate, widens towards the extremities, and has a narrow, superjacent groove; the posterior tooth in the RV is elongate and angled across the dorsoposterior angle; the anterior socket in the LV is locellate, the subjacent tooth is rounded, the median bar is straight and crenulate; the posterior socket, which is angled, is located at the dorsoposterior angle; and low stragula are located above the sockets of the LV. The inner margin along the venter upturns at approximately 1/3 length. The marginal zone includes the selvage, selvage groove, inner margin and narrow vestibulum in some specimens; the selvage of the RV is interrupted at the caudal angle by a double ogee-shaped structure (right arrow on Pl. 13, fig. 6). The inner surface of carapace has large, scattered pores that correspond to the inner openings of the sieve-type normal pore canals. Two rimmed, inverted platforms that are elongate parallel to the long axis of the carapace are located ventroposteriorly of interior hinge elements (Pl. 13, figs. 6 (left two arrows) and 8); these platforms correspond to the inner part of the post-ocular depression; the lower platform, which is acuminate anteriorly, is less than half the size of the upper one, which is acuminate posteriorly. The large ocular sinus is located just ventroanterior of the anterior hinge element (Pl. 13, fig. 6).

The F scar is U-shaped (Pl. 3, fig. 9; Pl. 13, figs. 5-9 and 11). The A-1 scar is located above the posterior ends of the other adductor scars and is elongate almost vertically; the A-2 and A-4 scars are intertwined similar to a yin-yang symbol, with the A-2 being bulbous anteriorly and the A-4 tapering anteriorly; the A-3 scar is either very small, missing, or fused with either the A-2 or A-4 scars. The fulcral point is nearly circular, located anterior to the dorsal part of the A-1 scar. The M-1 scar is elongate, tilted slightly anteriorly, and located below the F scar; the M-2 scar is close to the ventral margin, is teardrop shaped, and is acuminate posteriorly. The D-1 scar is located directly below the ocular sinus; the D-2 and D-3 scars are indistinct; no D-4 was observed.

The species is sexually dimorphic, with the females being smaller but more laterally inflated than the males (text-fig. 13).

Remarks: This species is similar to *Laevipellacythereis laevipellis* n. sp. in the lack of reticulation and overall smooth carapace except for distinct sieve-type normal pore canals but differs in the lack of the very broad longitudinal lobes, the presence of the row of elongate fossae parallel to the anterior margin that form a depression, and by the presence of a well-defined, elongate and groove-like postocular sulcus.

Range: This species has been found only in the Providence Sand (Maastrichtian) of Barbour County, eastern Alabama (text-fig. 4).

Laevipellacythereis laevipellis Puckett and Hunt **n. sp.**
Plate 1, figure 8; Plate 3, figure 10; Plate 14, figures 1-11; Text-fig. 13

Etymology: *laevi*, Latin for smooth, and *pellis*, Latin for skin, in reference to the smooth surface.

Type Specimens: Holotype: USNM PAL 771810, specimen 130/135-23 (Pl. 14, fig. 2,female LV); paratype: USNM PAL 771811, specimen 130/135-28 (Pl. 14, fig. 3, male RV); both specimens from sample 2011-8-4-1 (water level), Maastrichtian Owl Creek Formation, Tippah County, northern Mississippi.

Diagnosis: Carapace oblong, surface almost smooth by addition of tegmen, with round sieve-type normal pore canals located inside small, round fossae; four subdued lateral lobes, one along dorsoposterior margin, another at the central muscle scar field, a third, concave up, near the ventral margin, and a subdued lobe parallel to the anterior margin.

Material: 238 valves and 1 carapace

Measurements: Holotype L = 0.762 mm, H = 0.381 mm; paratype L = 0.726 mm, H = 0.333 mm.

Description: The carapace is very robust and oblong; the dorsoanterior outline is slightly concave in the RV and convex in the LV; the anterior margin is broadly rounded and slightly

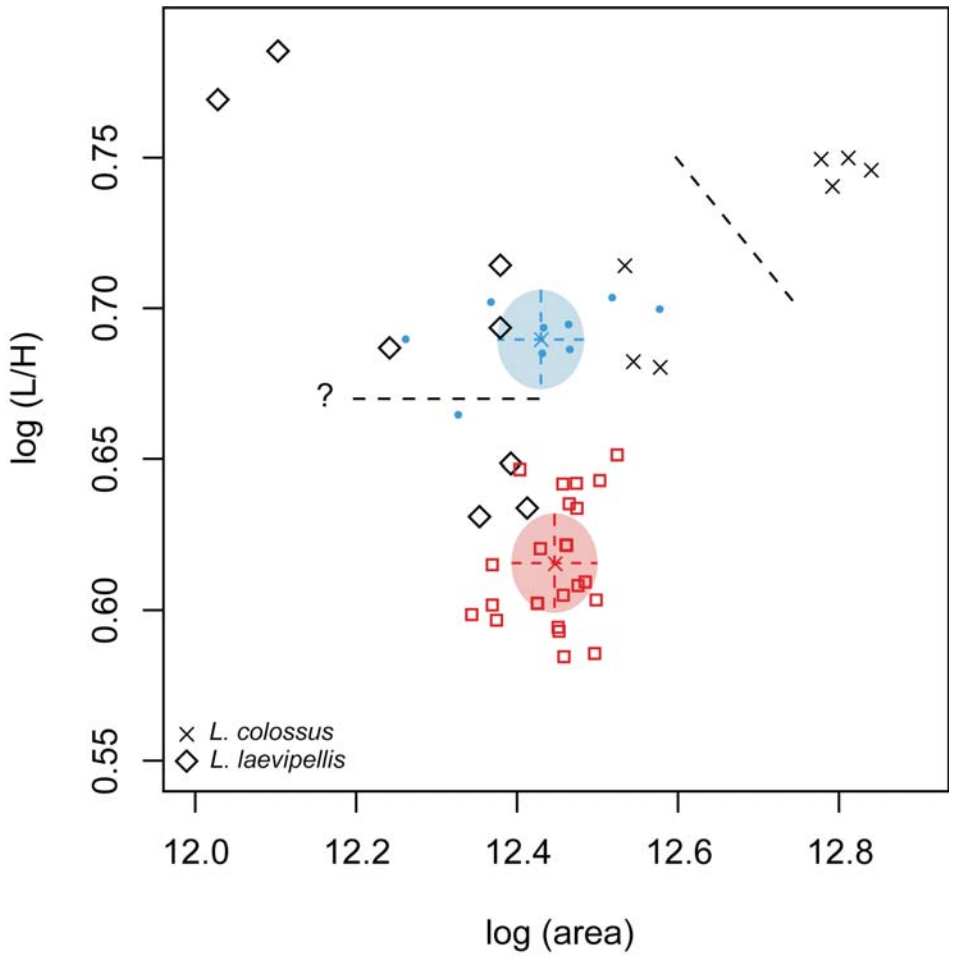

TEXT-FIGURE 13
Size (log area) versus shape (log[L/H]) for *Laevipellacythereis colossus* (X) and *Laevipellacythereis laevipellis* (diamonds). Other points are from larger sample of this species analyzed by Hunt et al. (2017, population ANT_CACU-1-2). Blue circles = male and red squares = female clusters from that analysis, with corresponding colors for the 50% probability ellipses. Dotted line indicates inferred separation between males and females for the specimens figured in this work.

infracurvate; the ventral outline is broadly concave, more so in the RV; the posterior margin in the LV is very broadly rounded, nearly blunt, equicurvate, and becomes nearly straight along the dorsoposterior margin; the ventral part of the posterior margin in the RV is very broadly rounded and the upper part is concave, forming a distinct angle near mid-height; the dorsal silhouette is slightly humped at circa ¾ length due to the bulging of the dorsoposterior lobe above the hinge line. In dorsal view, the carapace has three bulges, each rising progressively higher posteriorly: one just behind the anterior margin, another just in front of mid-length, and the other just behind mid-length; the greatest width is at the third bulge; the anterior and posterior margins are not compressed but rise gently from the ends.

There are four lobes on the lateral part of the carapace: one is dorsoposterior, another is ventral, a third is subcentral, and the fourth is parallel to the anterior margin; the intervening sulci are shallow and more distinct in the males; the dorsoposterior lobe is located at ¾ length and rises above the level of the hinge; the ventral lobe rises gently from the anterior to its maximum height directly below the dorsoposterior lobe; and the subcentral lobe, which is the smallest, corresponds in location to the central muscle scar field.

The eye tubercle is indistinct. The anterior area has very gentle costae that are sub-parallel to the outer margin. The lateral surface is almost smooth except for the small circular fossae that contain the sieve-type normal pore canals; these regions appear to be three-tiered: the external carapace forms the upper tier, which is undercut in many specimens (Pl. 14, fig. 9), the soli of the fossae form the middle tier, and the sieve plate forms the lower tier; the soli surrounding the sieve plate are rimmed.

The hinge is paramphidont (Pl. 14, figs. 5-8); the anterior tooth of the RV has a narrow anterior part that steps up to a taller, multilobate tooth; the subjacent socket is smooth; the median groove is crenulate and widens towards the extremities, and a large posterior tooth that arches across the dorsoposterior angle; the socket in the LV is loculate to accommodate the multilobed complementary tooth; the subjacent tooth is blunt; the median bar is straight, thin and crenulate, and widens very slightly near the posterior terminus; and the posterior socket is loculate, arched across the dorsoposterior angle, and with a ventral rim.

The inner surface is punctuated by scattered pores that correspond to the openings of the sieve-type normal pore canals on the outer surface. The inner margin is relatively wide and distinct; the selvage is a distinct, narrow rim; marginal in-folds are broadest anteriorly and posteriorly. The posterior caudal region of the RV has an interruption of the selvage that forms a double ogee-shaped structure (arrow on Pl. 14, fig. 8), with no complementary structure in the LV. A pair of rimmed internal platforms (Pl. 14, figs. 5, 7 and 8) that corresponds to the inside of the postocular sulcus is located just behind and ventral to the anterior hinge element; the upper platform is larger and acuminate anteriorly and the lower, smaller platform is acuminate posteriorly. The ocular sinus is located just below and anterior to the anterior hinge element.

The muscle scars (Pl. 3, fig. 10; Pl. 14, figs. 6-8 and 10) include a U-shaped F scar, rotated slightly anteriorly; the ovate A-1 scar is oriented at 300° (in RV), acuminate at the upper end, and located above the posterior part of the other adductor scars; the A-2, A-3 and A-4 scars intertwine similar to a yin-yang symbol in the overall form of a circle; the A-2 is large and paisley-shaped, oriented horizontally, and narrows between the A-1 and the lower scars; the A-3 scar is very small and squeezed between the posterior ends of the A-2 and A-4 scars. The A-4 scar is of intermediate size, oblong and oriented at 50° (in LV). A pair of mandibular scars lie directly below the F scar, with the upper, kidney-shaped M-1 being smaller and above the U-shaped M-2, which is close to the ventral margin. The small dorsal scars include one located between the anterior hinge element and the central muscle scars, and a vertical pair located behind the interior platforms (Pl. 14, fig. 7).

Species is sexually dimorphic, with the females more inflated and slightly larger; the males are slimmer, with a very gentle, elongate sulcus along central part of lateral swelling (text-fig. 13).

Remarks: This species differs from the others in the Subfamily Anticytherideinae by having very small, round fossae that encircle the sieve-type normal pore canals. There are, therefore, three tiers at these locations: the outer carapace is the upper tier, which is undercut around the fossae, very narrow soli form the second tier, and the sieve plates form the lower tier.

This species differs from *L. colossus* by being more inflated laterally; by the presence of the four lateral lobes; by having more rounded anterior and posterior margins; and by being very slightly rather than strongly infracurvate. It differs from *Laevipellacythereis* sp. 1, which was found in the Coon Creek Formation of latest Campanian-early Maastrichtian age, by the presence of a smooth and lobate carapace, but differs in having a smooth anterior region, rather than having a depressed line of fossae that parallels the anterior margin and being more elongate.

Range: This species was found in the Owl Creek Formation of Tippah County, Mississippi and in the Providence Sand (both Maastrichtian) of Barbour County, eastern Alabama (text-figs 2 and 4). This is the only species in this study to be found across the field area, ranging from northern Mississippi to eastern Alabama.

***Laevipellacythereis* sp. 1**
Plate 4, figures 7 and 8

Material: Only 9 valves were collected

Remarks: This species is very similar to *Laevipellacythereis colossus* n. gen., n. sp., differing mainly in outline, with a less infracurvate anterior margin, and the carapace is less elongate and more sub-rectangular. As both males and females were collected of both species, the difference between the two species cannot be attributed to sexual dimorphism. It is morphologically intermediate between *L. colossus* and *L. laevipellis*. It is likely that *L.* sp. 1 is the ancestor to both *L. laevipellis* and *L. colossus*.

Range: All specimens were found from a single sample (2010-10-22-1(512)), collected from the latest Campanian-early Maastrichtian Coon Creek Formation of Union County, Mississippi (text-fig. 2).

Genus ***Tumulocythereis*** Puckett and Hunt **n. gen.**

Etymology: This genus is named after the type species, *Tumulocythereis tumulus* sp. nov, in reference to the characteristic lobation of the species.

Type Species: *Tumulocythereis tumulus* n. gen et sp. nov. (Pl. 2, fig. 4; Pl. 3, fig. 14; Pl. 18, figs. 1-14; Text-fig. 15).

Diagnosis: Species of the genus *Tumulocythereis* are characterized by a combination of a diagonal swelling of the carapace that extends from just in front of the dorsoposterior angle to below the subcentral tubercle, with an intervening sulcus; external carapace drops off steeply from lateral swelling to form compressed posterior region; carapace completely reticulated, with subrounded to polygonal fossae.

Species: Species that are assigned to *Tumulocythereis* from this study include the type species from the Owl Creek Formation of northern Mississippi and the Prairie Bluff Chalk from eastern Mississippi and central Alabama, all of Maastrichtian age; *T. priddyi* (Smith 1978) from the Owl Creek Formation and Prairie Bluff Chalk of central Alabama; *T. tiberti* n. sp. from the Coon Creek Formation of northern Mississippi of latest Campanian-earliest Maastrichtian age, the Owl Creek Formation and the Prairie Bluff Chalk; and *T.* sp. 1 from the Coon Creek Formation of northern Mississippi and the Ripley Formation of latest Campanian-Maastrichtian of central Alabama.

Remarks: Species of the genus *Tumulocythereis* differ from species of *Anticythereis* by a more even dorsal outline (without the dorsal shoulder), by the presence of a large ventrolateral lobe, and by the absence of prominent carinae. They differ from species of *Asculdoracythereis* by the presence of lateral lobes and much more inflated carapaces and the smoother dorsal outline uninterrupted by a dorsal carina. They differ from species of *Laevipellacythereis* by the presence of large fossae.

Tumulocythereis incompta Puckett and Hunt **n. sp.**
Plate 2, figure 1; Plate 3, figure 11; Plate 15, figures 1-14; Text-fig. 14

Etymology: incomptus, Latin meaning unadorned, in reference to the lack of reticulation.

Type Specimens: Holotype: USNM PAL 771812, specimen 142-11 (pl. 15, fig. 1, male RV); paratype: USNM PAL 771813, specimen 142-10 (Pl. 15, fig. 3, female RV); both specimens from sample 2011-8-4-1 (water level), Maastrichtian Owl Creek Formation, Tippah County, Mississippi.

Diagnosis: This species is characterized by a relatively smooth carapace except for moderately sized, subcircular fossae associated with sieve pores, very broad muri, and very subtle diagonal sulcus on LV.

Material: 158 valves

Measurements: Holotype L = 0.696 mm, H = 0.309 mm; paratype L = 0.654 mm, H = 0.298 mm.

Description: The carapace is of medium size for the genus, elongate, sub-rectangular, and robust. The greatest height is at the eye tubercle and the greatest length is at or near mid-height. The dorsal outline is slightly undulating, with a hump at the eye tubercle that corresponds to the low stragula; the lateral swelling of the carapace bulges slightly above the hinge behind mid-length; the anterior margin is broadly and evenly rounded and slightly infracurvate; the ventral margin in the RV has the typical concavity at 1/3 length that corresponds to the upturned ventral margin; the ventral margin in the LV is either straight or slightly convex; the posterior margin in the LV is very broadly rounded and equicurvate; in the RV, the ventral half of the posterior margin is very gently convex, but at mid-height, the posterior margin becomes concave to just below the dorsoposterior angle. In dorsal view, the carapace outline rises gently from the anterior margin in a very broad convexity to the greatest width at approximately 4/5 length, then slopes sharply down to the compressed posterior margin.

The eye tubercle is a subtle, smooth area, not bulged. A prominent postocular sulcus extends from just below the dorsal margin to below the eye tubercle, with the dorsal part being horizontal, then bends down below the eye tubercle; in some specimens, the postocular sulcus is broken into sub-rectangular cells defined by apophyses (Pl. 15, fig. 4); a gentle, diagonal sulcus extends from near the dorsal margin behind mid-length, across the middle region to terminate above the ventroanterior angle. The lateral surface of the carapace is almost completely covered by fossae and intervening wide muri; distinctive but small, circular fossa punctuate the smooth zone that is laterally adjacent to the eye tubercle; there is an anterior row of small fossae very close to the anterior margin that is bordered posteriorly by a low carina, with the fossae being slightly elongate parallel to the anterior margin; there is a row of large, sub-rectangular fossae just behind the low anterior carina, with the long axes parallel to the anterior margin; the fossae in the region of the subcentral tubercle are small relative to those behind it; the posterior part of the LV has small, marginal fossae that are very close to the posterior margin and bordered by a low carina, similar to those near the anterior margin; a row of large, subcircular fossae is located in front of the low carina, and extends from the dorsoposterior angle to below the lateral bulge behind mid-length. Sieve-type normal pore canals with raised rims occupy the soli sub-centrally (Pl. 15, figs. 9 and 12), and the margins of the fossae undercut the carapace; the carapace within small fossae appears to be three-tiered, with the upper tier being the muri, the middle tier being the soli, and the lower tier being the sieve plate (Pl. 15. figs. 9 and 11); the sieve pores are uniform in size, despite variation in size of the surrounding fossae; the openings in the sieve plates are of irregular geometry that surround a central opening; in some sieve plates, relatively strong bars connect the central opening to the margins of the plate; the soli are moated, with maximum depth slightly more than half way from the sieve pore rims to the margins (Pl. 15, figs. 9 and 12); the soli display subtle caperation (Pl. 15, fig. 12); the entire lateral surface is punctuated by microstructural tubes within the crystal fabric, with no preferred orientation.

The hinge is paramphidont (Pl. 15, figs. 5-8 and 10); the RV has a stepped anterior tooth, with a low, narrow and lobate anterior part that steps up to a taller multilobate tooth; the postjacent socket is smooth; the median groove is straight, crenulated, and bordered dorsally by a thin bar; the posterior tooth is crenulated and arches across the dorsoposterior angle; in the LV, the anterior socket is grooved in the lower part to accept the complementary tooth; the median bar is crenulate and extends to the dorsal parts of the anterior and posterior sockets; the posterior socket is angled, bordered dorsally by bar and groove, and forms dorsal bulge (stragulum) at the dorsoposterior angle. The anterior, ventral, and posterior margins have a selvage, selvage groove, and list; the ventral margin is typically upturned at 1/3 length; the marginal zone is relatively wide, particularly along the posterior and anterior regions, with no distinct vestibule; the RV has the distinctive double ogee-shaped structure that interrupts the selvage in the caudal region (arrow on Pl. 15, fig. 8), with no corresponding structure in the LV; scattered, large pits in the interior correspond to external sieve-type normal pore canals; the ventroanterior and ventroposterior regions have small, blunt denticles very close to the margins. Two distinctive, elongate, rimmed inverted platforms are located below the anterior part of the median hinge bar (Pl. 15, figs. 10 and 13-14), which may represent attachment points of muscles and tendons; the upper platform is larger and acuminate anteriorly; the upper platform is smaller and acuminate posteriorly. The ocular sinus is at the ventroanterior border of anterior hinge elements.

The muscle scars (Pl. 3, fig. 11; Pl. 15, fig. 14) have a V-shaped F scar; the A-1 scar is elliptical, angled at circa 320° (in RV), and lies above the posterior part of the other adductor scars; the A-2, A-3 and A-4 scars intertwined in the pattern of a yin-yang symbol, with an overall circular shape; the A-2 scar is paisley-shaped, tapers posteriorly over the A-3 scar, and is angled ventroanteriorly; the A-3 scar is small and slightly elongate, and is sandwiched between the posterior ends of the A-2 and A-3 scars; the A-4 scar is elliptical and angled ventroanteriorly; the M-1 scar is located ventrally of the F scar, is elongate and narrow, and is angled ventroposteriorly; the M-2 scar is located near the ventral margin, is narrow and angled ventroposteriorly, and is crescent shaped; the D-1 scar is located below the ocular sinus, is nearly circular and small; the D-2, D-3 and D-4 scars are small, circular, evenly distributed horizontally above the central muscle scar field near dorsal margin; the fulcral point is a depression located in front of the A-1 scar between the adductor scars and the F scar.

The species is sexually dimorphic, with the females being shorter and rounder and the males being more elongate (text-fig. 14). The lateral sulci in the males is slightly deeper than the females, which is more inflated.

Remarks: This species is distinctive in having very wide muri that separate the relatively small, subcircular fossae. Among the species of *Tumulocythereis* n. gen., *T. incompta* is most similar to *T. tumulus*, as *T. priddyi* and *T. tiberti* have well developed reticulation and more elevated lobation. It differs from *T. tumulus* in being less elongate; the anterior and posterior marginal zones are also less compressed. This is the oldest species of the genus and may be the ancestor.

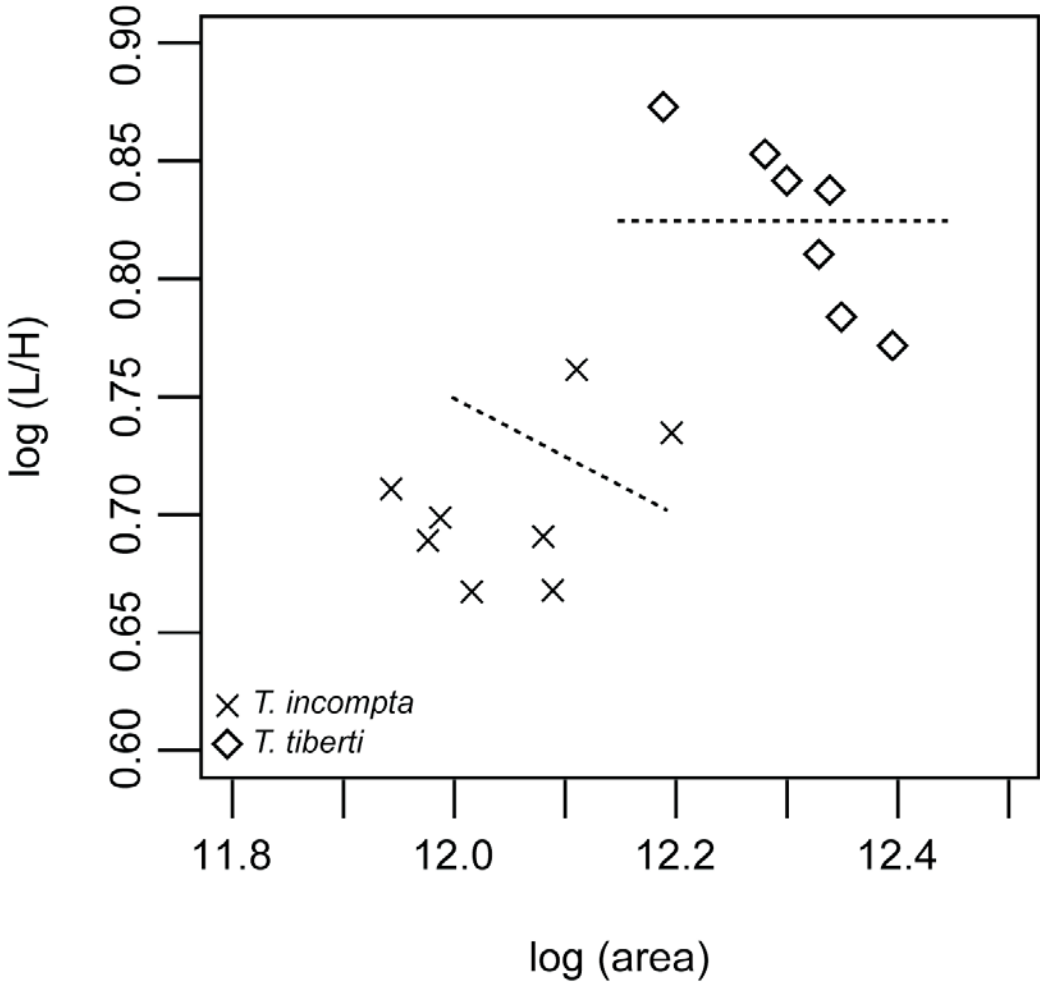

TEXT-FIGURE 14
Size (log area) versus shape (log[L/H]) for *Tumulocythereis incompta* (X) and *Tumulocythereis tiberti* (diamonds). Dotted line indicates inferred separation between males and females for the specimens figured in this work.

Range: This species was found in the Coon Creek Formation (latest Campanian-early Maastrichtian) of northern Mississippi, the Owl Creek Formation (late Maastrichtian) of the type locality in Tippah County, Mississippi, where it may be abundant, and in the Prairie Bluff Chalk (late Maastrichtian) of central Alabama (text-figs 2 and 4).

Tumulocythereis priddyi Smith 1978
Plate 2, figure 3; Plate 3, figure 12; Plate 16, figures 1-13; Text-fig. 15

Carinocythereis (?) *priddyi* SMITH 1978, p. 553-554, pl. 5, figs. 8-10.

Type Specimens: The type specimens were collected from the Prairie Bluff Chalk (Maastrichtian) of Lowndes County, central Alabama. All three type specimens are LVs: holotype (USNM PAL 255717) and paratypes USNM PAL 255718 and USNM PAL 255719 (Pl. 16, fig. 2). Another specimen that is recorded as being from the type locality is catalogued at the USNM PAL as number 642412, which has a broken dorsoposterior margin, and is not illustrated here. In all these specimens, the fossae have considerable adventitious material that obscures their details. Adventitious material covers the ventral and anterior regions of the holotype, which completely obscures the morphology in these regions. Debris also covers the muscle scars in paratype USNM PAL 255418 (not illustrated here).

Diagnosis: None given, but Smith (1978) described the species. Smith stated that the generic assignment was uncertain and suggested that the species may represent a new genus.

Emended Diagnosis: Carapace elongate, sub-rectangular; carapace rises from anterior region to approximately 4/5 length, where it drops off sharply to posterior compressed zone; ventral margin concave in both LV and RV; posterior and anterior margins nearly symmetrical in LV; fossae subrounded, cover entire carapace, with moderately wide muri.

Material: 195 valves

Remarks: The fossae are typically round to highly elliptical; in some case, adjacent fossae seem to have merged, with an apophysis that extends to the raised sieve pores (arrow on Pl. 16, fig. 11), although the single sieve-type normal pore canal within indicates a single, invaginated fossa. The species displays the characters typical of the genus, including the

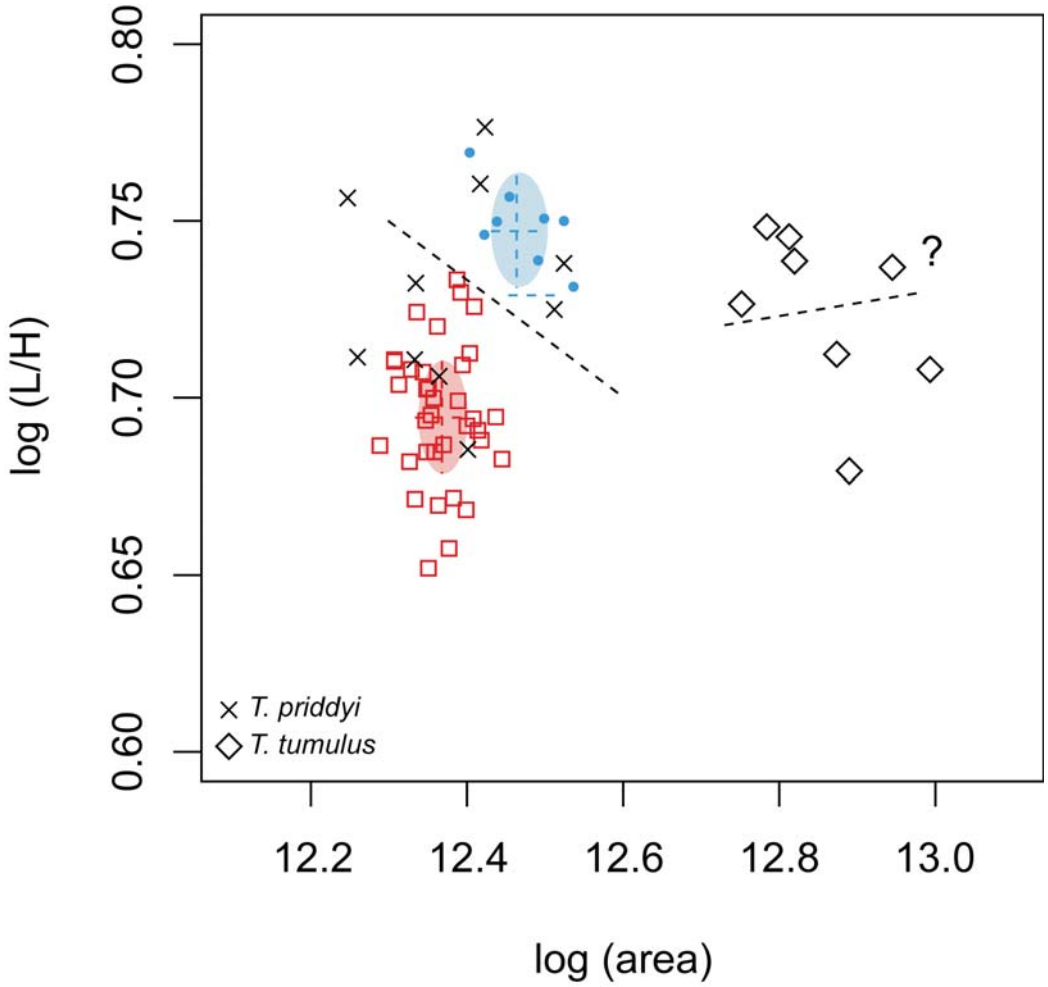

TEXT-FIGURE 15
(A) Size (log area) versus shape (log[L/H]) for *Tumulocythereis priddyi* (X) and *Tumulocythereis tumulus* (diamonds). Other points are from larger sample of this species analyzed by Hunt et al. (2017, population CAR_PRID-1). Blue circles = male and red squares = female clusters from that analysis, with corresponding colors for the 50% probability ellipses.

postocular sulcus that extends from the dorsal margin just anterior of mid-length to below the bulged eye tubercle; the hinge in RV has a stepped anterior tooth, with lower anterior part lobed that steps up to a taller lobed postjacent tooth; the posterior tooth is crenulated and angled arched across the dorsoposterior angle; the selvage is interrupted at the caudal region of the RV by a double ogee-shaped structure (arrow on Pl. 16, fig. 8), with no corresponding structure in the LV; the A-2, A-3 and A-4 scars are intertwined in the shape of yin-yang symbol, with a dorsally offset, elliptical, and tilted A-1. A pair of rimmed, fusiform inverted platforms is located below and ventral of the anterior hinge element, corresponding to the interior of the postocular sulcus, that are possibly related to the attachment point of the inner lamella at the anterior isthmus (arrows on Pl. 16, fig. 10). In this species, the rimmed sieve-type normal pore canals are typically on the margins of fossae, rather than in the center (Pl. 16, fig. 11). Some of the rimmed sieve-type normal pore canals are located on a low murus within a fossa (see arrow on Pl. 16, fig. 11); the small openings of the sieve plate are arranged concentrically around the central opening; the margins of fossae undercut surrounding muri (Pl. 16, figs. 11 and 12). The carapace has foveolate muri, with foveolae being subparallel to the margins of fossae and separated from them by narrow smooth strip (Pl. 16, fig. 11).

T. priddyi is distinctive in being relatively elongate and sub-rectangular. It is very similar to *T. tiberti* n. sp., but is less elongate, less compressed posteriorly, more infracurvate and less constricted vertically near mid-length. It differs from *T. tumulus* in having more dense reticulation, is more sub-rectangular, has more subtle lobation and lacks the strong marginal carinae. The density of the reticulation is variable, with some specimens having narrower intervening muri (i.e., the paratype specimen, Pl. 16, fig. 2) and others having wider intervening muri (Pl. 16, figs. 3-6). Sexual dimorphism is observed with males being more elongate than females (text-fig. 15).

Range: Smith (1978) described this species based on specimens collected from the Prairie Bluff Chalk (Maastrichtian) of Lowndes County, central Alabama. All but one of the specimens collected for this study were from the Owl Creek Forma-

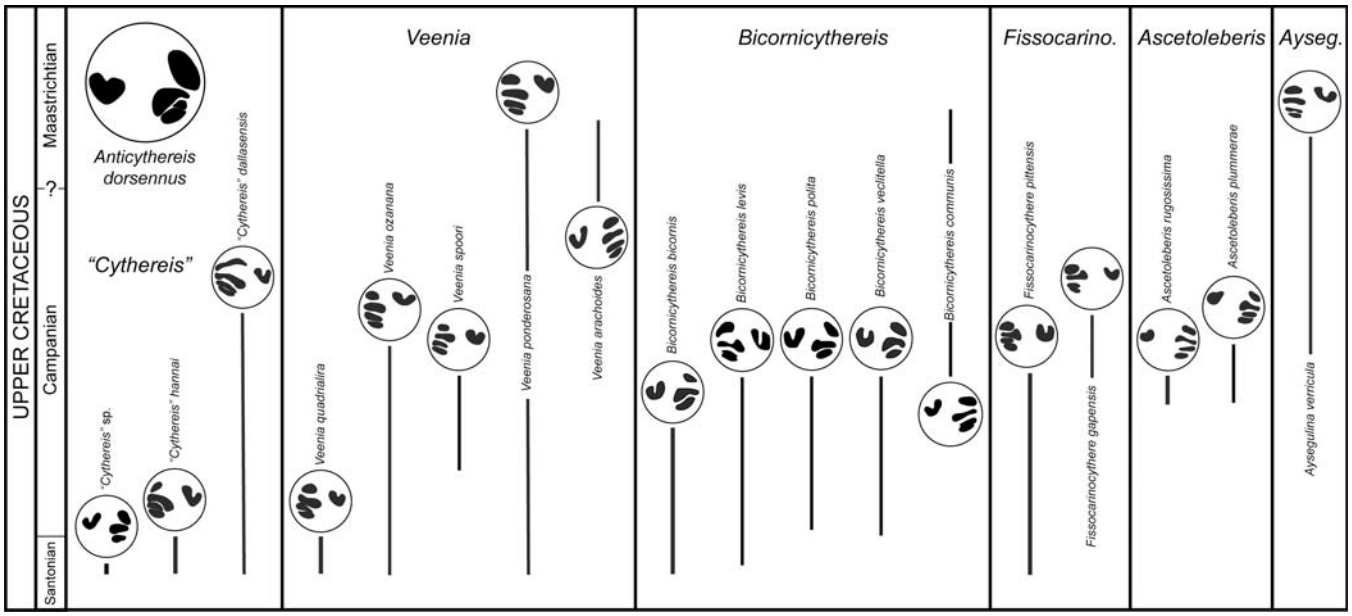

TEXT-FIGURE 16
Comparison of the central muscle scars of representative trachyleberid ostracod species from the U.S. Gulf Coastal Plain. Ranges of the species is based on Puckett (2005) and Puckett (2012). The *Fissocarino* refers to *Fissocarinocythere* and *Ayseg* refers to *Aysegulina*.

tion (Maastrichtian) of Tippah County, northern Mississippi. The lone exception was collected from Smith's type locality (a topotype specimen). This species, therefore, ranges in the Maastrichtian from central Alabama to northern Mississippi and is among the most widespread species of the genus (text-figs. 2 and 4).

Tumulocythereis tiberti Puckett and Hunt **n. sp.**
Plate 2, figure 2; Plate 3, figure 13; Plate 17, figures 1-11; Text-fig. 14

Etymology: Named in honor of Neil Tibert of the University of Mary Washington, who passed away Dec. 20, 2015, for his contributions to the study of Cretaceous ostracods of North America.

Material: 99 valves.

Type Specimens: Holotype: USNM PAL 771814, specimen 130/135-18 (Pl. 17, fig. 3, female RV) from sample 2011-8-4-1 (water level), Maastrichtian Owl Creek Formation, Tippah County, Mississippi.

Diagnosis: Carapace very elongate, medially swollen with dorsal sulcus in the middle in lateral view, widening at the ends; polygonal fossae cover the carapace in leopard-like pattern; carapace highly inflated laterally, rising towards the posterior to drop off abruptly to highly compressed ventroposterior margin, forming a diagonal lobe with median sulcus; configuration of fossae just in front of the central muscle scar field as viewed from outside distinct from rest of carapace, with small, round fossae near the scars and elongate fossae more anteriorly.

Description: The carapace is elongate, with the greatest height at the eye tubercle; the anterior margin is slightly infracurvate and broadly rounded; the posterior margin in the LV is very slightly infracurvate, with an obtusely angled caudal region; the ventroposterior margin in the RV is infracurvate, with an obtuse angle located below mid-height, and a straight dorsoposterior margin. Short, blunt denticles are located just above the margins in the ventroanterior and ventroposterior regions; the venter in the LV of males (Pl. 17, fig. 2) is very slightly concave to about ¾ length where it turns down to form the rounded ventroposterior margin; the dorsal margin is straighter than in the males. In dorsal view, the carapace outline is sagittate; the anterior margin rises to the anterior marginal carina, then tapers at the post-carina sulcus, then rises to the greatest width at approximately 4/5 length; there is a slight bulge at the subcentral tubercle; the posterior margin drops abruptly and convexly from the greatest width to the highly compressed posterior margin.

The eye tubercle is a distinctive smooth area near the dorsoanterior angle but bulges only slightly. There is a very prominent, diagonal, slightly arcuate (concave up) lateral swelling that extends from the dorsoposterior margin and becomes imperceptible near the ventral margin at about 1/3 length; the sub-central tubercle area is on a slight platform; and the posterior part of the carapace behind the lateral swellings is very compressed and forms a nearly vertical step up to the lateral swelling. The external ornamentation is a complex combination of fossae, foveolate muri and rimmed sieve-type normal pore canals. Fossae completely cover the exterior surface; a line of fossae that are subquadrate is located just behind the anterior margin at mid-height that become sub-rectangular near the dorsal and ventral margins; behind that is a line of large subquadrate fossae; the rest of the carapace is generally covered with medium-sized, rounded, polygonal fossae aligned in rows parallel to the outline; the fossae in the subcentral platform are small and more complex, particularly within muscle scar field; muscle scars are often clearly seen in external view (Pl. 17, fig. 11), with muri conforming to the scar outlines. Sola of fossae

are generally smooth but slightly caperate in some fossae (Pl. 17, fig. 7). The muri are foveolated, with foveolae aligned in uni-, bi- and multi-serial rows subparallel to muri (Pl. 17, figs. 8, 10 and 11). Rimmed sieve-type normal pore canals generally are located in the sola of scattered fossae in the central part of carapace but are not present in every fossa.

The hinge is holamphidont (Pl. 17, figs. 5 and 6); the anterior tooth in the RV is stepped, with a lower, grooved anterior part that rises up to a grooved subjacent tooth; the median element is a straight, crenulate groove that widens towards the extremities; the posterior tooth is tilted at circa 45° across the dorsoposterior angle; the LV has an anterior, elongate socket, subjacent and small tooth, straight and crenulate median bar that forms a shelf below the dorsal margin, and a subrounded posterior socket. The inner surface of the carapace is generally smooth except for the openings of the sieve-type normal pore canals; the sieve plate can be observed in internal view in some thin-shelled specimens (Pl. 17, fig. 9). The selvage in the RV is interrupted by a double ogee-shaped structure at the caudal region (which is abraded on the specimen in Pl. 17, fig. 6), with no corresponding structure in the LV. A pair of rimmed, fusiform inverted platforms is located behind and below the anterior hinge elements and directly above the central muscle scar field (arrows on Pl. 17, fig. 9); these platforms are located on the inside of the postocular sulcus; the larger, upper platform is acuminate anteriorly, and the smaller, lower platform is acuminate posteriorly. A large, prominent ocular sinus is subjacent to the anterior hinge element.

The muscle scar field (Pl. 3, fig. 13, Pl. 17, figs. 5-9 and 11) includes an open V-shaped F scar. The adductor set includes a vertical column of four scars; the A-1 scar is ovoid, tilted forward dorsally and lies above the posterior ends of the other adductor scars; the A-2, A-3 and A-4 scars are intertwined like a yin and yang symbol in an overall circular pattern; the A-2 scar is paisley shaped, with the posterior tapering above the A-3 scar; the A-3 scar is very small and circular, and sandwiched between the posterior margins of the A-2 and A-4 scars; the A-4 scar is oblong and points towards the ventroanterior margin. There are two mandibular scars; M-1 lies directly below the F scar in a posteriorly directed parenthesis shape; the M-2 appears to be two small, circular scars that are close to the ventral margin. The dorsal scars include a small subcircular anterior scar (D-1) located directly below the eye tubercle, a pair of small elongate scars (D-2 a and b) that are located behind the tubercle, a small ovoid scar (D-3) that is well back from the D-2 pair, and a small, lower, centrally located sub-rectangular scar (D-4).

The species is sexually dimorphic, with the males being more elongate than the females (text-fig. 14); the ventral margins of the males are more concave than the females (compare Pl. 17, fig. 2 to fig. 4). The males are distinguished from the females also by a constriction in the height of the carapace at mid-length.

PLATE 1

Morphology of fossae and maps of normal pore canals in Anticytherideinae Ostracoda. Note the color scheme that denotes whether the pore was mapped based on an inner view, outer view, combined view (position estimated by mapping a mid-way point between the same pore as viewed from the inside and from the outside), and estimated position based on other specimens.

1 *Oertliella horridula* (Bosquet 1854) showing homologous fossae and conation in upper Maastrichtian tuffaceous chalk of Maastricht from Liebau (1977, fig. 10). Alphanumeric code reflects interpreted homology.

2 *Aysegulina ornata* (Bosquet 1847), coding and locality as above. This species was traditionally placed in the genus *Limburgina* Deroo 1966, but Özdikmen (2010) discovered that the name had previously been used by Laurentiaux (1950) for a genus of Carboniferous insects. Özdikmen then substituted the name *Aysegulina* for *Limburgina*.

3 *Asculdoracythereis lowndesensis* (Smith 1978), LV, based on SEM image of specimen 134-18 (closeup of external morphological features on Pl. 10, fig. 9). Pores mapped on basis of external view only.

4 *Asculdoracythereis asculdora* n. gen., n. sp., LV, based on SEM image of specimen 148-3 (Pl. 8, fig. 4). Pores mapped on basis of external view only.

5 *Asculdoracythereis pseudoalabamensis* n. gen., n. sp., RV, based on SEM image of specimen 147-6 (internal views on Pl. 7, figs. 7 and 8). Pores mapped on basis of external view only.

6 *Asculdoracythereis invicta* n. gen., n. sp., LV, based on SEM images of external view of specimen 147-12 (Pl. 9, figs. 2 and 11) and inner pores (specimen 147-14, Pl. 9, fig. 5).

7 *Laevipellacythereis colossus* n. gen., n. sp., RV, based on SEM images of external view of specimen 148-8 (Pl. 13, figs. 1 and 9).

8 *Laevipellacythereis laevipellis* n. gen., n. sp., LV, based on SEM images of external view of specimen 130-5 (internal view on Pl. 14, fig. 5).

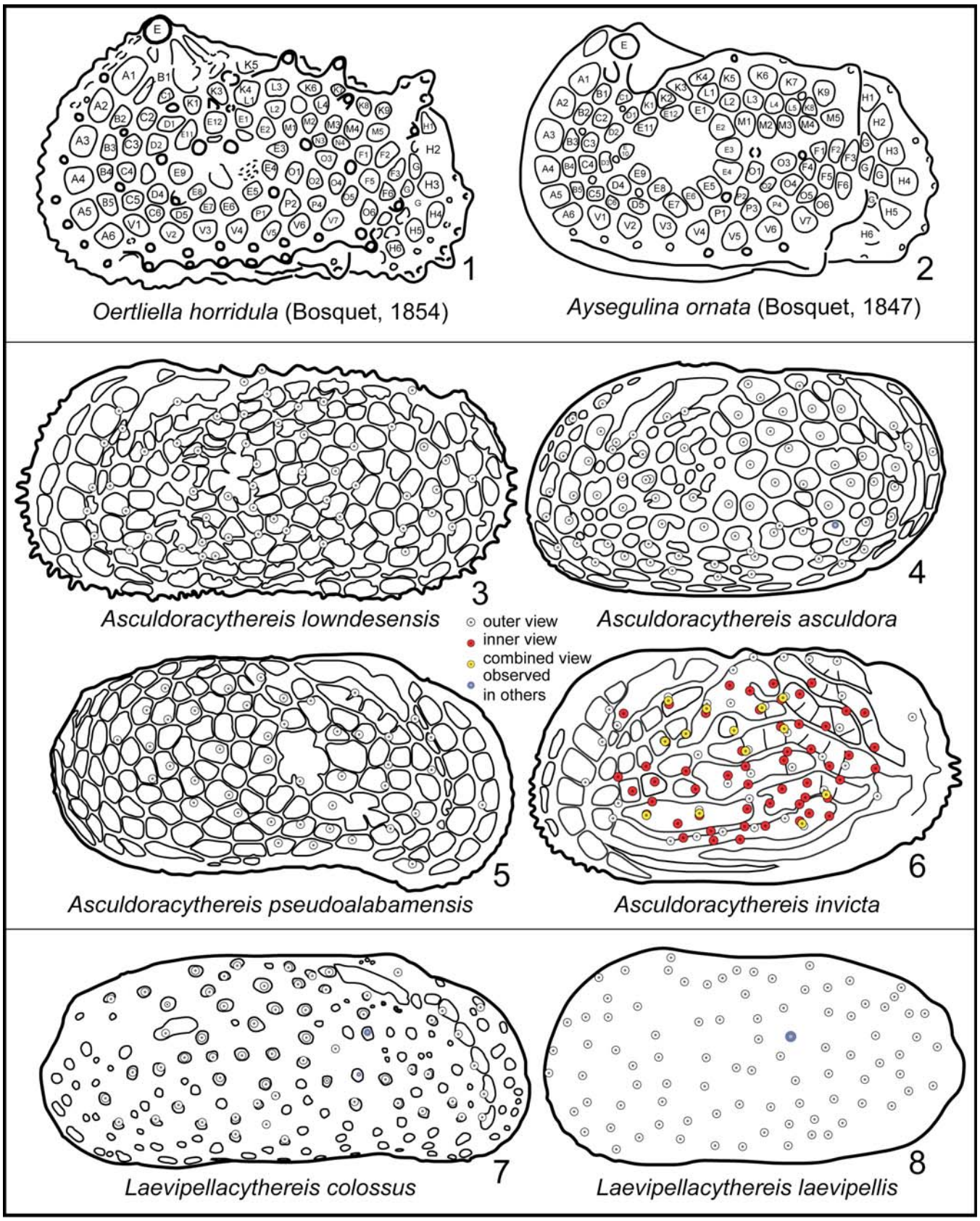
1
Oertliella horridula (Bosquet, 1854)
2
Aysegulina ornata (Bosquet, 1847)
3
Asculdoracythereis lowndesensis
4
Asculdoracythereis asculdora
outer view
inner view
combined view
observed
in others
5
Asculdoracythereis pseudoalabamensis
6
Asculdoracythereis invicta
7
Laevipellacythereis colossus
8
Laevipellacythereis laevipellis

Remarks: This species is distinctive in being highly elongate and constricted medially, creating a sagittate posterior margin, particularly in the LV. The lateral lobes are highly inflated relative to the compressed ventroposterior margin. The reticulation becomes fine and complex above the central muscle scar field, and the muscle scars are often visible in exterior view (Pl. 17, figs. 7-8 and 10). Unfortunately, the carapace of this species is susceptible to breaking, due possibly to a relatively thin carapace and the mid-length constriction. Several specimens were broken in attempts to clean the specimens and during handling. Thus, no paratype has been designated.

Range: This species was observed from the Coon Creek Formation (latest Campanian-early Maastrichtian) of Union County, northern Mississippi, the Owl Creek Formation (late Maastrichtian) type locality in Tippah County, northern Mississippi, and Prairie Bluff Chalk (late Maastrichtian) of Lowndes County, central Alabama (text-figs 2 and 4).

Tumulocythereis tumulus Puckett and Hunt **n. sp.**
Plate 2, figure 4; Plate 3, figure 14; Plate 18, figures 1-14; Text-fig. 15

Etymology: *tumulus*, Latin for mound, barrow, or hillock, in reference to the distinctive lateral swellings of the carapace.

Type Specimens: Holotype: USNM PAL 771815, specimen 143-6 (Pl. 18, figs. 1 and 13, female RV); paratype: USNM PAL 771816, specimen 143-7 (Pl. 18, figs. 4 and 10; male LV); both specimens from sample 2011-5-18-1 (water level), Maastrichtian Owl Creek Formation.

Diagnosis: This species is characterized by three prominent swellings on the lateral carapace: a subcentral tubercle, an arcuate ventral lobe, and a dorsoposterior lobe; the subcentral and dorsoposterior lobes form a shoulder in front of which is the post-ocular depression; the fossae are generally subrounded and with wide muri.

Material: 54 valves

Measurements: Holotype L = 0.738 mm, H = 0.345 mm; paratype L = 0.750 mm, H = 0.369.

Description: The carapace is elongate and robust; the carapace outline is constricted vertically; the anterior margin is broadly and evenly curved, and very slightly infracurvate; the ventral margin is incurved; the posterior margin in the LV is broadly and evenly rounded and slightly supracurvate; the posterior outline in the RV is evenly convex in the lower half, gently concave in the upper half, and angled at mid-height; the dorsal margins are straight, but have stragula above the terminal hinge elements that form a concave mid-dorsum that is eclipsed by the dorsoposterior lobe. There are denticles very close to the ventroanterior and ventroposterior margins. The carapace outline in dorsal view is flat and compressed anteriorly, then rises gently to slight bulge at 1/3 length that corresponds to the subcentral tubercle, drops very slightly at mid-length, then gently rises to the greatest width at approximately 4/5 length that corresponds to the posterior lobe, then drops rapidly and concavely to the compressed posterior zone.

PLATE 2

See Plate 1 for details regarding color coding system for pores.

1 *Tumulocythereis incompta* n. gen., n. sp., RV, based on SEM images of inner and outer views of specimen 141-7, collected from sample 2011-8-4-1 (water level), Owl Creek Formation, Maastrichtian, Tippah County, Mississippi.

2 *Tumulocythereis tiberti* n. gen., n. sp., LV, based on SEM images of inner and outer views of specimen 130/135-9 (closeup of external features on Pl. 17, fig. 10).

3 *Tumulocythereis priddyi* (Smith 1978), RV, based on SEM images of inner and outer views of specimen 130/135-8 (internal view on Pl. 16, fig. 9).

4 *Tumulocythereis tumulus* n. gen., n. sp., LV, based SEM image of external view of specimen 143-18, collected from sample 2011-8-4-1 (water level), Owl Creek Formation, Maastrichtian, Tippah County, Mississippi.

5 *Frodocythereis frodoi* n. gen., n. sp., LV, based on SEM images of external and internal views of specimen 132/136-3, collected from sample 2011-8-4-1 (water level), Owl Creek Formation, Maastrichtian, Tippah County, Mississippi.

6 *Frodocythereis copelandi* (Smith 1978), LV., based on SEM images of external and internal views of specimen 132/136-24 (closeup of muscle scars on Pl. 11, fig. 10).

7 *Anticythereis slipperi* n. sp., LV, based on SEM image of external view of specimen 134-14 (Pl. 6, fig. 2).

8 *Anticythereis dorsennus* n. sp., LV, based on SEM image of external and internal views of specimen 132/136-13 (Pl. 5, figs. 2 and 7).

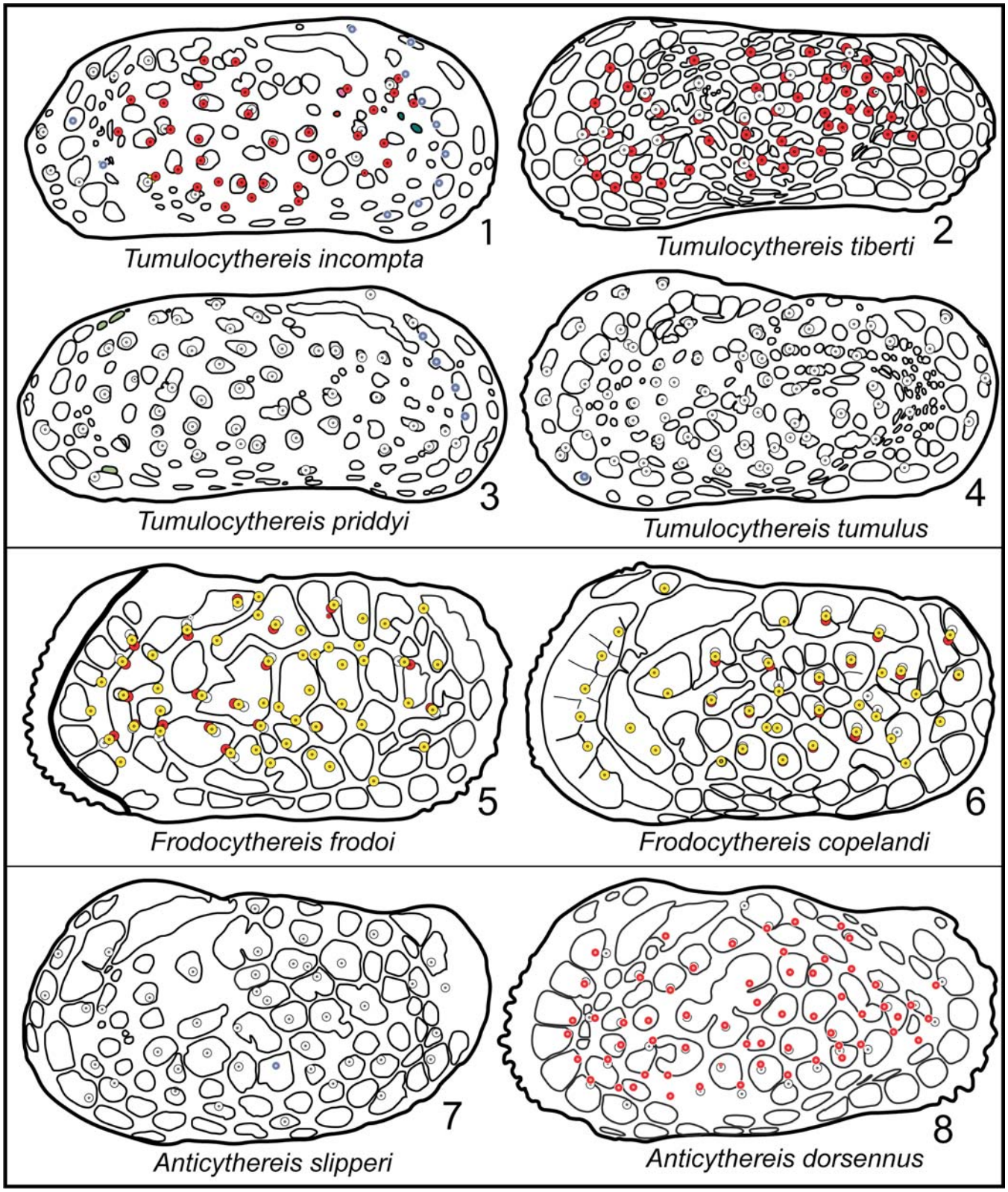
1
Tumulocythereis incompta
2
Tumulocythereis tiberti
3
Tumulocythereis priddyi
4
Tumulocythereis tumulus
5
Frodocythereis frodoi
6
Frodocythereis copelandi
7
Anticythereis slipperi
8
Anticythereis dorsennus

The eye tubercle is a gentle, smooth bulge at the dorsoanterior angle. The external carapace has a combination of large lobes, deep sulci ornamented with fossae of a wide variety of shapes and sizes like a spotted leopard, and wide muri. There are three main lobes: a broad subcentral tubercle is located slightly above and in front of carapace center, a dorsoposterior lobe that extends above the hinge line, and a large arcuate ventrolateral lobe; the subcentral tubercle rises gently from the anterior margin, but drops off more sharply ventrally and posteriorly to the central sulcus; the subcentral tubercle and dorsoposterior lobes are connected by broad ridge; the dorsoposterior lobe terminates just in front of the posterior hinge element; the ventral lobe arises gently out of the anterior region and swells prominently in a curved, concave-up lobe to drop abruptly to the compressed posterior margin below the dorsoposterior lobe; the lower side of the ventral lobe is nearly vertical in lateral view; a broad sulcus is located between the bordering lobes, being horizontal between the dorsal and ventral lobes and curved below the subcentral tubercle to flatten out in the anterior region; a gentle ridge extends downward from the eye tubercle and flattens out in the anterior region. The postocular sulcus is bipartite, with a deeply sculpted, boomerang-shaped sulcus cutting into the thick marginal ridge just below and behind the eye tubercle that points to the lower edge of the eye; this sulcus is floored by shallow, polygonal fossae, with delicate intervening muri (Pl. 18, figs. 3-4); the immediately posterior zone is not quite as deeply sculpted, but curves back to lie immediately below the thick dorsal rim; this latter sulcus cuts deeply into the dorsal rim and the adjacent dorsal lobe, undercutting them. The anterior and posterior margins are thick and prominent and bordered inwardly by equally wide, deeply sculpted regions; within the marginal rims is a single line of 10-11 elongate fossae that extend from just in front of the eye tubercle and continue to the incurved ventral margin; in the RV, a line of elongate fossae ornament the convex ventroposterior margin, but the fossae become small and round along the concave dorsoposterior margin; the fossae behind the anterior rim are deeply sculpted, sub-rectangular, and separated by narrow muri that are tapered in the middle; within each fossa is a single, rimmed sieve-type normal pore canal that is offset towards the center of the carapace (Pl. 18, figs. 1-4), and in some places is connected to the bordering murus by an apophysis (arrow on Pl. 18, fig. 10). The muri that border the fossae are steep and undercut in places (Pl. 18, fig. 14); in some fossae there is a single sieve-type normal pore canal that is surrounded by a moated solum; the sieve plates lie below the level of the soli; the soli are often caperate (arrow on Pl.

PLATE 3

Muscle scar patterns of species of the Subfamily Anticytherideinae. Arrows point anteriorly.
Dashed features represent the fulcral point. Locality information for specimens not given here are in the referenced plate captions.
See text-figure 8 for identification of muscle scars.

1 *Anticythereis dorsennus* n. sp., specimen number 132/136-15, collected from sample 2011-8-4-1 (water level), Maastrichtian Owl Creek Formation, Tippah County, Mississippi.

2 *Anticythereis slipperi* n. sp., specimen number 150-9 (Pl. 6, fig. 7).

3 *Asculdoracythereis asculdora* n. gen., n. sp., specimen 148-5 (Pl. 8, figs. 3 and 9).

4 *Asculdoracythereis invicta* n. gen., n. sp., specimen 147-17 (Pl. 9, figs. 7 and 10).

5 *Asculdoracythereis lowndesensis* (Smith 1978), specimen 146-7 (Pl.10, figs. 5 and 10).

6 *Asculdoracythereis pseudoalabamensis* n. gen., n. sp., specimen 147-7 (Pl. 7, figs. 6 and 11).

7 *Frodocythereis copelandi* (Smith 1978), specimen 132-24 (Pl. 11, fig. 10).

8 *Frodocythereis frodoi* n. gen., n. sp., specimen 132-3, sample 2011-8-4-1 (water level), Maastrichtian Owl Creek Formation, Tippah County, Mississippi.

9 *Laevipellacythereis colossus* n. gen., n. sp., sample 148-11 (Pl. 13, figs. 5 and 11).

10 *Laevipellacythereis laevipellis* n. gen., n. sp., specimen 130-2, sample 2011-5-18-1 (water level), Maastrichtian Owl Creek Formation, Tippah County, Mississippi.

11 *Tumulocythereis incompta* n. gen., n. sp., specimen 145-6 (Pl. 15, figs. 10 and 14).

12 *Tumulocythereis priddyi* (Smith 1978), specimen 133-11, sample 2011-8-4-1 (water level), Maastrichtian Owl Creek Formation, Tippah County, Mississippi.

13 *Tumulocythereis tiberti* n. gen., n. sp., specimen 130-9 (closeup of external surface on Pl. 17, fig. 10).

14 *Tumulocythereis tumulus* n. gen., n. sp., specimen 143-1 (Pl. 18, fig. 13).

15 *Asculdoracythereis pseudoalabamensis* n. gen., n. sp., for reference specimen 147-7 (Pl. 7, figs. 6 and 11).

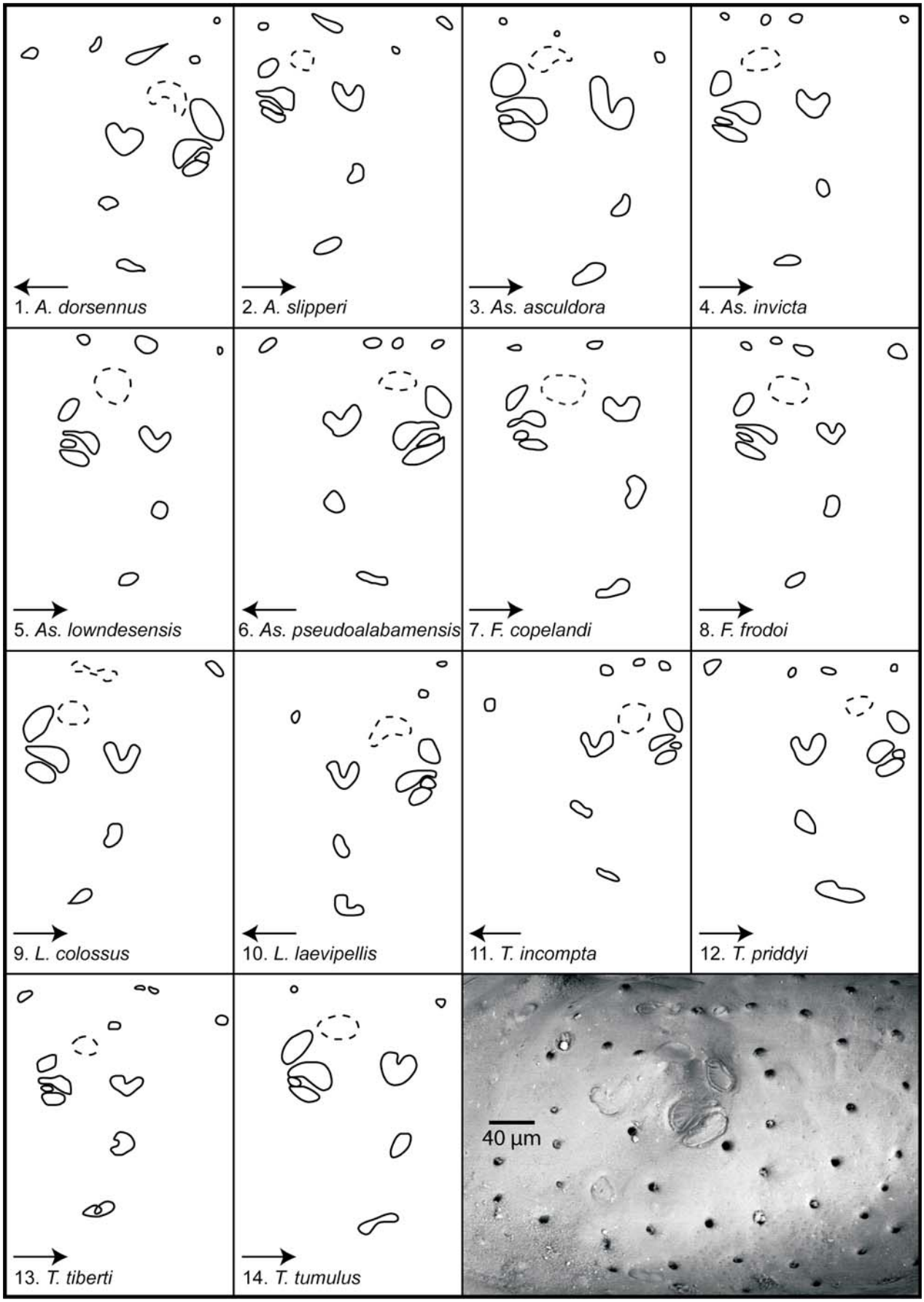
1. A. dorsennus
2. A. slipperi
3. As. asculdora
4. As. invicta
5. As. lowndesensis
6. As. pseudoalabamensis
7. F. copelandi
8. F. frodoi
9. L. colossus
10. L. laevipellis
11. T. incompta
12. T. priddyi
13. T. tiberti
14. T. tumulus
40 µm

18, fig. 11); the fossae on the subcentral tubercle are sparse, small and round; the fossae on the posterior slope are also small and round; most of the fossae in the center of the carapace are of medium size, with wide variety of shapes, and some appear to coalesce, thus forming elongate fossae. The entire carapace except for the fossae is foveolate (Pl. 18, figs. 9-11 and 14).

The hinge is holamphidont (Pl. 18, figs. 5-8 and 12); the anterior tooth in the RV is stepped, with a lower, grooved part in the anterior that steps up posteriorly to a taller tooth and subjacent socket; the middle hinge element is a straight, crenulated groove that widens at the extremities; the posterior tooth is elongate and angled in the middle; the hinge in the LV has a deep anterior socket that extends below the postjacent, vertically elongate tooth; the middle hinge element is a straight crenulate bar; the posterior socket is at the dorsoposterior angle and is tilted ventroposteriorly; low stragula overlie the terminal hinge elements. The inner surface has scattered openings that correspond to the inside of sieve-type normal pore canals. The marginal zone is wide, especially in the anterior; the selvage in the RV is interrupted by a double ogee-shaped structure at the caudal region (Pl. 18, figs. 6 (with arrow) and 8), with no complementary structure in the LV; the anterior selvage has thin, radiating muri that are connected to the anterior margin (Pl. 18, fig. 8). Two parallel, rimmed, fusiform inverted platforms (arrows on Pl. 18, fig. 12) are located just behind and ventral of the anterior hinge elements, with the lower, smaller platform being more acuminate posteriorly and the larger, upper one being more acuminate anteriorly; these structures correspond to the inside of the postocular sulci. The ocular sinus is located just below and anterior of the anterior hinge elements.

The muscle scars (Pl. 3, fig. 14; Pl. 18, figs. 5-8, and 12-13) have a U-shaped F scar that is tilted slightly anteriorly; the A-1 scar is elliptical, tilted slightly dorsoanteriorly from vertical, and is detached above the posterior end of other adductor scars; the A-2, A-3 and A-4 scars are intertwined in a yin-yang symbol with overall circular pattern; the A-2 scar is paisley shaped and curves and tapers over the A-3 scar; the A-3 scar is small, circular, and sandwiched between posterior ends of the A-2 and A-4 scars; the A-4 scar is elongate longitudinally and tilted slightly ventroanteriorly; the M-1 scar is elliptical, points towards the ocular sinus, and lies directly below the F scar; the M-2 scar is below and slightly posterior to the M-1 scar, is very elongate and constricted in the middle; the D-1 scar is elliptical and located directly below the ocular sinus; the D-4 is small, circular, and located above the A-1 scar; the other dorsal scars are small and indistinct; the fulcral point is depressed, slightly elliptical, and located just in front of and above the A-1 scar.

The species is sexually dimorphic, with the males being more elongate than the females (text-fig. 15). The lateral lobes on the males are not as inflated as on the females.

PLATE 4

Type specimens and species of Anticytherideinae left in open nomenclature or described from the Atlantic Coastal Plain
All specimens at same scale. Sexes are uncertain. LV = left valve, RV = right valve

1 Paratype *Anticythereis reticulata* (Jennings 1936), AMNH-FI 37780B, internal LV. Arrow points to inverted platform almost obscured by crystal growth.

2 Same specimen as figure 1.

3 *Anticythereis reticulata* (Jennings, 1936), USNM PAL 129016, Maastrichtian Peedee Formation, Pitt County, North Carolina; this is Brown's (1957) holotype of *Velarocythere eikonata* (USNM PAL 129016).

4 *Tumulocythereis* sp. 1, external LV, specimen 149-1, sample 2019-6-20-1 (185), Maastrichtian Ripley Formation, Lowndes County, Alabama.

5 *Tumulocythereis* sp. 1, external RV, specimen 149-3, sample 2019-6-20-1 (190), Maastrichtian Ripley Formation, Lowndes County, Alabama.

6 *Frodocythereis* sp. 1, external LV, specimen 141-21, sample 2010-10-22-1 (512), latest Campanian-Maastrichtian Coon Creek Formation, Union County, Mississippi.

7 *Laevipellacythereis* sp. 1, external RV, specimen 149-18, sample 2010-10-22-1 (512), latest Campanian-Maastrichtian Coon Creek Formation, Union County, Mississippi.

8 *Laevipellacythereis* sp. 1, external LV, specimen 149-19, sample 2010-10-22-1 (512), latest Campanian-Maastrichtian Coon Creek Formation, Union County, Mississippi.

9 *Asculdoracythereis* sp. 1, external RV, specimen 149-7, sample 2011-5-18-1 (water level), Maastrichtian Owl Creek Formation, Tippah County, Mississippi.

10 *Asculdoracythereis* sp. 1, external LV, specimen 149-9, sample 2011-5-18-1 (water level), Maastrichtian Owl Creek Formation, Tippah County, Mississippi.

11 *Anticythereis* sp. 1, external LV, specimen 149-14, sample 1993-6-11-3 (1), Campanian Cusseta Sand, Barbour County, Alabama.

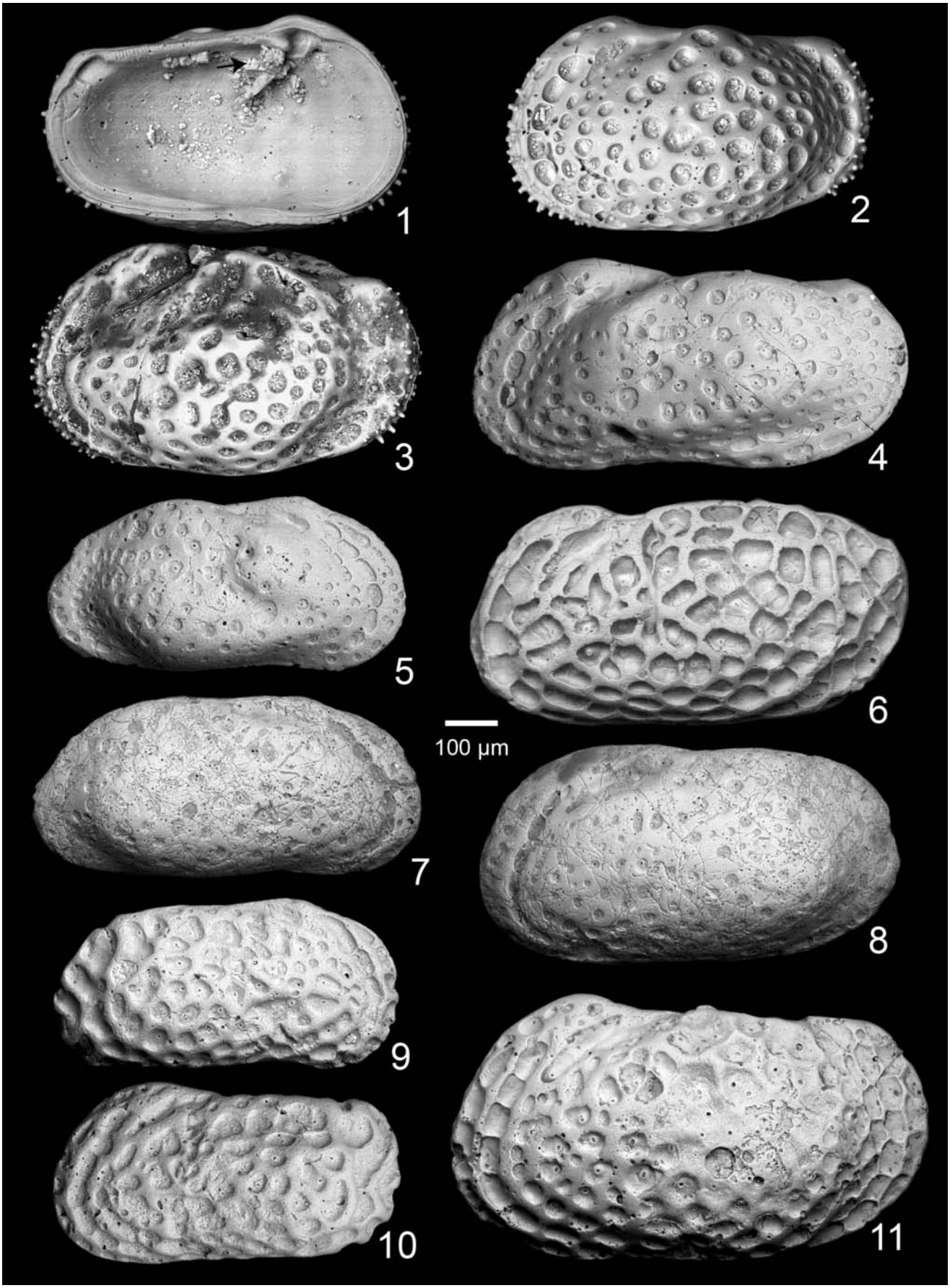
1
2
3
4
5
6
100 µm
7
8
9
10
11

Remarks: This species is relatively thick-shelled and with swollen muri; the carapace is strongly lobate and with marginal carinae; the strongly inflated subcentral tubercle and ventrolateral lobes with intervening sulcus are also distinctive. Among the species of *Tumulocythereis*, it is most similar to *T. incompta* in having broader muri and smaller fossae but has subcircular, rather than polygonal, fossae and is more elongate and constricted medially than *T. incompta*.

Range: This species was found in the Owl Creek Formation type locality, Tippah County, northern Mississippi; in the Prairie Bluff Chalk of Oktibbeha County, eastern Mississippi; and in the Prairie Bluff Chalk of Lowndes County, central Alabama. All samples are of late Maastrichtian age (text-figs. 2 and 4).

Tumulocythereis sp. 1
Plate 4, figures 4-5

Material: 16 valves were collected during this study.

Remarks: This species is very similar to *T. tumulus* n. gen., n. sp., but the lateral outline is less elongate. The posterior margin is more supracurvate and rounded, the anterior lobe is more swollen, the sulcus between the subcentral and ventral lobes is shallower, the anterior and posterior margins are not as compressed, and the subcircular fossae are fewer by the thickened muri.

Range: This species was collected from the Coon Creek Formation of Union County, Mississippi and from the coeval Ripley Formation of Lowndes County, Alabama, both of latest Campanian-early Maastrichtian age. This species could, therefore, be the ancestor of the other species of the genus (text-figs. 2 and 4).

DISCUSSION

Character Evolution and Evolutionary History

Despite many years of study on the Late Cretaceous marine ostracods of the U.S. Gulf Coastal Plain, there remains a considerable amount of work to be done on the taxonomy and systematics of these diverse fossils. This contribution makes several taxonomic proposals to organize and understand many of the species of trachyleberids that occur near the end of the Cretaceous. This section presents some of the taxonomic implications for their study.

The anticytherideinines belong to the Family Trachyleberidae based mainly on their amphidont hinge, presence of ornamentation such as carinae and fossae, and the muscle scar pattern, which includes a single (unsplit) frontal muscle scar and a vertical row of adductor muscle scars. Sylvester-Bradley (1948) originally described the Family Trachyleberidae to include a large number of ornamented ostracods with "…accommodation groove lacking or reduced to a narrow shelf; straight hinge, with subdivided median element; and compressed carapace (especially anteriorly and posteriorly) though sometimes with alae." Sylvester-Bradley (1948) also described the Subfamily Trachyleberinae to include "Ornate Trachyleberidae with compressed sub-rectangular shell, pronounced muscle scar node (='subcentral tubercle' [*sic*]; forms a "muscle scar pit" when viewed from the interior; eye tubercle, posterior and anterior cardinal angles, and posterior and anterior rims. Accommoda-

---

PLATE 5

Anticythereis dorsennus n. sp.
Specimens 1-8 at same scale, as indicated. Scale for figures 9-11 as indicated.
All specimens collected from the Maastrichtian Owl Creek Formation, Tippah County, Mississippi.
LV = left valve, RV = right valve

1 Exterior RV, female, specimen 132/136-21, same figure as 6, 9 and 11, sample 2011-5-18-1 (water level).

2 Holotype (USNM PAL 771796), exterior LV, male, specimen 132/136-13, sample 2011-5-18-1 (water level).

3 Exterior RV, female, specimen 132/136-20, same specimen as figures 8 and 10 sample 2011-5-18-1 (water level).

4 Paratype (USNM PAL 771797), exterior LV, female, specimen 132/136-18, sample 2011-8-4-1 (water level).

5 Interior LV, male, specimen 132/136-14, sample 2011-5-18-1 (water level).

6 Interior RV, male, specimen 132/136-21, same specimen as figures 1, 9 and 11. Arrow points to double ogee-shaped caudal interruption of selvage.

7 Interior LV, same specimen as figure 2.

8 Interior RV, same specimen as figures 3 and 10.

9 Closeup reticulations and sieve pores, same specimen as figures 1 and 6.

10 Closeup muscle scars, RV, same specimen as figure 3 and 8.

11 Closeup muscle scars. RV, same specimen as figures 1, 6 and 9.

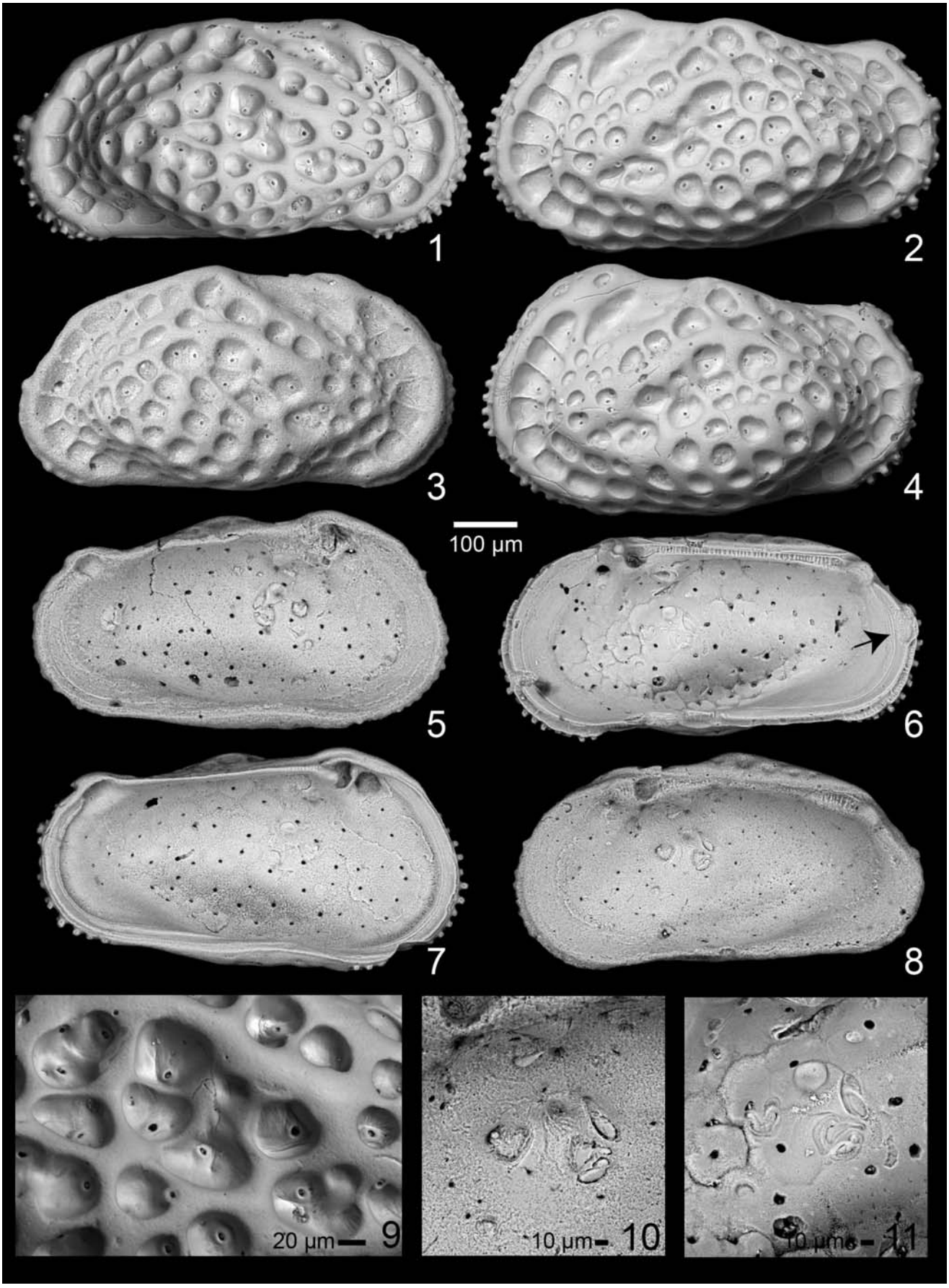
1
2
3
4
100 µm
5
6
7
8
20 µm
9
10 µm
10
10 µm
11

tion groove absent, or present only as a very narrow shelf. No vestibule. Median element of hinge subdivided, smooth or finely denticulate." These definitions included a large number of taxa ranging from the Jurassic to the Recent, and even include taxa, such as *Oligocythereis*, that have a merodont/entomodont hinge. Puri (1953), recognizing that the Family Trachyleberidae included genera that are not closely related to one another, described the Subfamily Hemicytherinae to include genera with a muscle scar pattern consisting of a vertical row of four adductor scars, with additional three or four scars in an oblique row situated anteriorly (i.e., a subdivided frontal scar). Later, van Morkhoven (1963) emended the diagnosis of the Subfamily Trachyleberinae (Family Cytheridae, now Cytheroidea) to put the pattern of the central muscle scars in primary importance: "Central muscle scars consisting of a vertical row of four adductor scars, which are rarely subdivided, and a V-shaped frontal scar." Other diagnostic characters included a wide marginal zone, numerous marginal pore canals, hinge generally amphidont/heterodont (but included some Cretaceous genera with merodont or entomodont hinges), generally well-developed eyespots, heavily calcified carapace that is usually ornamented with strong spines or ridges, and marginal denticulations. Similarly, the Treatise volume on ostracods (Benson et al. 1961) defined the trachyleberids solely on the basis of hard part morphology. Hazel (1967) recognized the importance of the muscle scar patterns in deciphering the phylogenetic history of the trachyleberids and hemicytherids, interpreting the former to be the ancestors of the latter. As more details about the biology of living trachyleberids became known, the soft part morphology was included (Athersuch et al. 1989; Horne et al. 2002).

The paramphidont hinges of the anticytherideinines are not unique to the group, although the combination of the stepped and grooved anterior hinge element and the angled and arched posterior hinge element of the RV are distinctive. In the U.S. Gulf Coastal Plain, species of *Bicornicythereis* also have a stepped anterior hinge element in the RV, although the lower anterior part is not grooved (see Puckett (2009a), Pl. 3, fig. 14, other images unpublished). Species of *Ascetoleberis* also have this knob-like step anterior to the anterior tooth in the RV. Almost all the species described herein have a grooved anterior tooth in the RV (paramphidont), but some appear to be smooth (holamphidont); that may be due, however, to being slightly worn, as the grooves are subtle.

The pattern of the muscle scars, particularly the adductor scars, is one of the most distinctive characters in the new subfamily. Text-figure 16 presents the muscle scar patterns of representative trachyleberid species of the Late Cretaceous of the U.S. Gulf Coast (trachyleberids that are clearly distinctive, such as the brachycytherines, were omitted from the comparison). Whereas all the taxa in text-figure 16 have a single U- or V-shaped frontal scar, most of the taxa have stacked series of four elongate adductor scars (*Ascetoleberis, Aysegulina,* and *Veenia*), rather than the intertwined A-2, A-3 and A-4 scars. The adductor muscle scars of species of *Bicornicythereis* (Puckett 2009a) are the most similar to the new subfamily, although several of the species (*B. bicornis, B. polita* and *B. veclitella*) ap-

---

PLATE 6

Anticythereis slipperi n. sp.

Specimens 1-6, 8 at same scale, as indicated. Scale for figures 7, 9-11 as indicated.

LV = left valve, RV = right valve

1 Exterior RV, presumed male, specimen 148-14, sample 1991-8-15-7, Maastrichtian Ripley Formation, Lowndes County, Alabama.

2 Holotype (USNM PAL 771798), exterior LV, presumed male, specimen 134-14, sample 2011-8-15-1 (15), latest Campanian-Maastrichtian Coon Creek Formation, McNairy County, Tennessee.

3 Paratype (USNM PAL 771799), exterior RV, presumed male, specimen 146-4, sample 2011-8-15-1 (15), latest Campanian-Maastrichtian Coon Creek Formation, McNairy County, Tennessee.

4 Exterior LV, female, specimen 148-18, sample 2010-10-22-1 (512), latest Campanian-Maastrichtian Coon Creek Formation, Union County, Mississippi.

5 Interior LV, presumed male, specimen 150-9, same specimen as figure 7, sample 2019-6-20-1 (180), Maastrichtian Ripley Formation, Lowndes County, Alabama.

6 Interior RV, female, specimen 148-20, sample 2019-6-20-1 (185), Maastrichtian Ripley Formation, Lowndes County, Alabama.

7 Closeup muscle scars, LV, same specimen as figure 5.

8 Exterior LV, male, specimen 134-15, sample 2011-8-15-1 (15), latest Campanian-Maastrichtian Coon Creek Formation, McNairy County, Tennessee.

9 Closeup of muscle scars, reticulation and sieve pores in exterior view, same specimen as figure 1.

10 Closeup reticulation and sieve pores, specimen 148-15, sample 2010-10-22-1 (512), latest Campanian-Maastrichtian Coon Creek Formation, Union County, Mississippi.

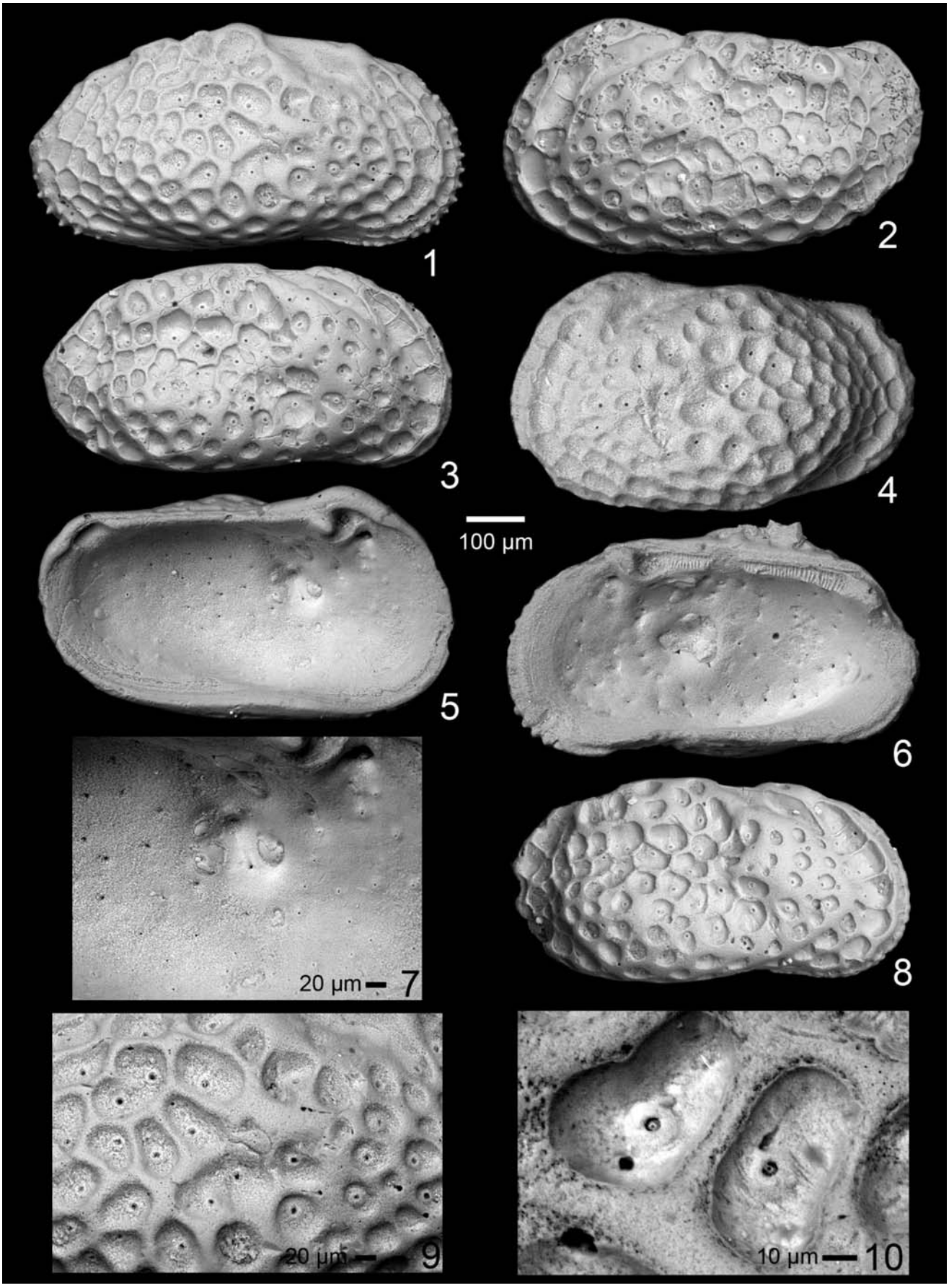
1
2
3
4
100 µm
5
6
20 µm
7
8
20 µm
9
10 µm
10

pear to have only three adductor scars; however, the lowest scar is probably two scars that have fused (in two of the species, *B. communis* and *B. levis*, these can be seen as two scars that are almost fused). The distinctive A-2 scar in *Bicornicythereis*, which bulges anteriorly over the lower scars, is very similar to those of the new subfamily, but the A-3 is either missing, elongate or fused. Puckett and colleagues (Puckett 2009a, Puckett et al. 2016) recognized the close association of paleogeography and distinctive muscle scar patterns in Late Cretaceous trachyleberids and the tremendous amount of information that is conveyed by these patterns. For example, many species in North America, South America, Africa, and Madagascar had been assigned to the genus *Brachycythere.* Puckett (2012) recognized that there is a systematic difference in the muscle scar patterns between those that occur in North America and those that occur elsewhere, as all the species from North America have split second adductor scars, whereas those from elsewhere have a single, elongate second adductor. This difference was the basis of describing a new genus of brachycytherines, *Sapucariella*. Similarly, given an image of the central muscle scar pattern of any of the species described herein, they can be readily assigned to the new genus, and thus are restricted paleogeographically to North America.

Another distinctive character of the new subfamily is the pair of rimmed, fusiform, inverted platforms located on the inside of the carapace that corresponds to the postocular sulcus. As with the muscle scar patterns, this structure is an indication of distinctive soft part morphology, although the exact function is uncertain. It is possible that this structure is an isthmus, which is the area where the inner lamella is connected to the body, or the attachment site for dorsal muscles and tendons that support the soft body and control appendages. Keyser (1990, 2005) described and illustrated both anterior and posterior isthmuses in *Cyprideis torosa* (Jones 1850), and stated that the isthmus is where the connection between the inner epidermal cell layer and the outer epidermal cell layer is lost and the inner cell lining is connected to the body cuticle. Whatever the function was of this structure, the authors are not aware of any other taxa that possess it or any homologous structure.

PLATE 7

Asculdoracythereis pseudoalabamensis n. sp., and *Asculdoracythereis alabamensis* (Smith 1978)
Specimens 1-8 at same scale, as indicated. Scale for figures 9-11 as indicated.
LV = left valve, RV = right valve

1 *Asculdoracythereis pseudoalabamensis*, exterior RV, male, specimen 147-3, sample 2012-01-03-1-2, Maastrichtian Providence Sand, Barbour County, Alabama.

2 Holotype (USNM PAL 771804) *Asculdoracythereis pseudoalabamensis*, exterior LV, male, specimen 147-1, sample 2012-01-03-1-2, Maastrichtian Providence Sand, Barbour County, Alabama.

3 *Asculdoracythereis alabamensis* (Smith 1978) holotype (USNM PAL 255753), exterior RV, male, Maastrichtian Prairie Bluff Formation, Lowndes County, Alabama.

4 Paratype (USNM PAL 771805) *Asculdoracythereis pseudoalabamensis,* exterior LV, female, specimen 147-4, sample 2012-01-03-1-2, Maastrichtian Providence Sand, Barbour County, Alabama.

5 *Asculdoracythereis pseudoalabamensis*, interior LV, female, specimen 147-5, sample 2012-01-03-1-2, Maastrichtian Providence Sand, Barbour County, Alabama.

6 *Asculdoracythereis pseudoalabamensis*, interior RV, female, specimen 147-7, sample 2012-01-03-1-2, Maastrichtian Providence Sand, Barbour County, Alabama.

7 *Asculdoracythereis pseudoalabamensis*, closeup of interior RV, female, specimen 147-6, sample 2012-01-03-1-2, Maastrichtian Providence Sand, Barbour County, Alabama. Note stepped anterior hinge tooth and muscle scars. Arrow on right points to upper inverted platform, arrow on left points to lower platform.

8 *Asculdoracythereis pseudoalabamensis*, same specimen as fig. 7.

9 *Asculdoracythereis pseudoalabamensis*, closeup of sieve-type normal pore canals, same specimen as figure 2.

10 *Asculdoracythereis pseudoalabamensis*, closeup of external ornamentation and muscle scars, same specimen as figure 1.

11 *Asculdoracythereis pseudoalabamensis,* closeup of muscle scars, same specimen as figure 6.

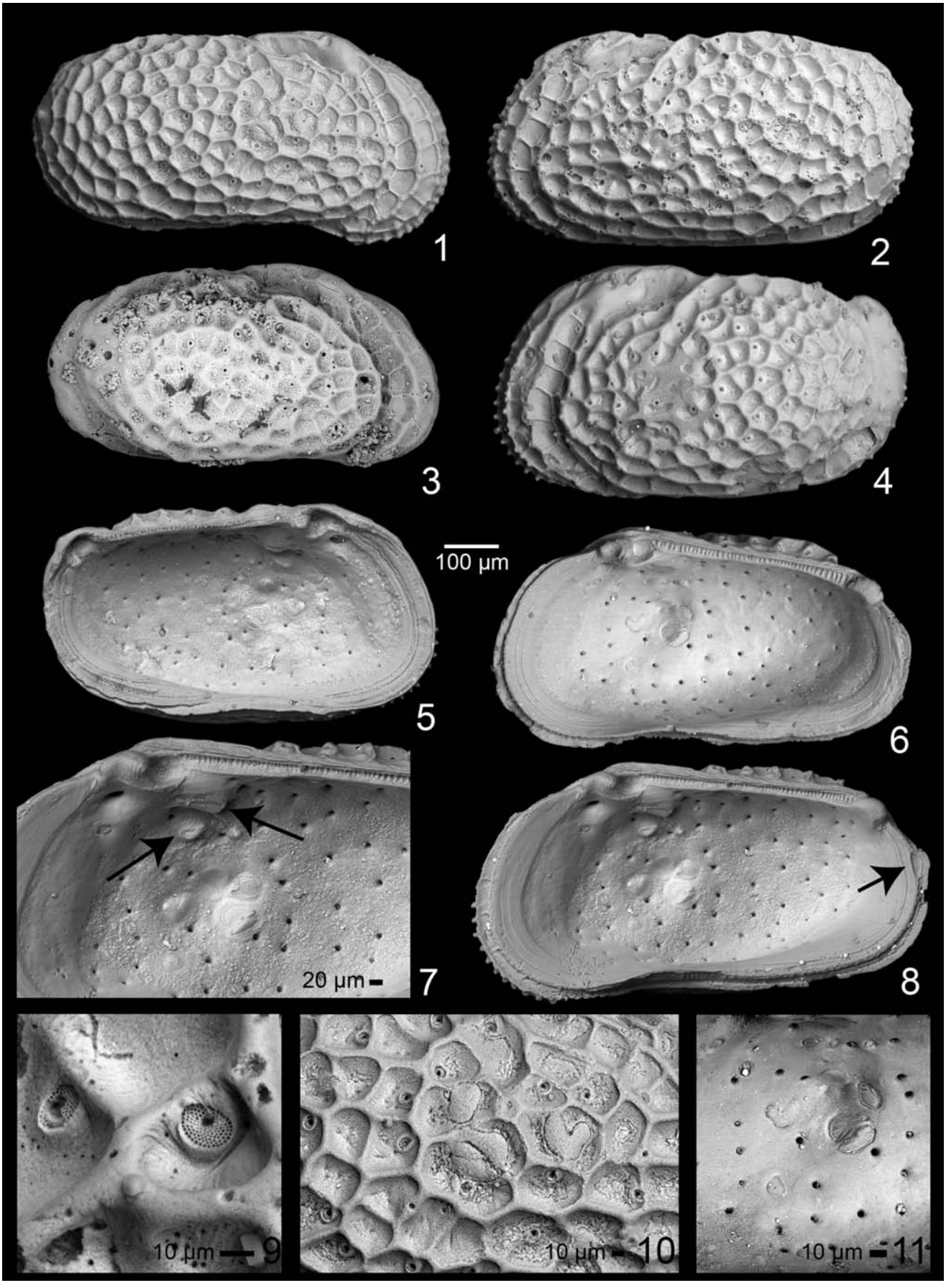
1
2
3
4
100 µm
5
6
20 µm
7
8
10 µm
9
10 µm
10
10 µm
11

All species of the new subfamily have an interruption of the selvage in the RV at the caudal region that is typically shaped like a double ogee or is ovoid (arrows point to this structure on Pl. 5, fig.6; Pl. 7, fig. 8; Pl. 12, fig. 6; Pl. 14, fig. 8; Pl. 15, fig. 8; Pl. 16, fig. 8; and Pl. 18, fig. 6). This structure may be analogous to the posterior siphonate indentations Maddocks (1969) observed in Recent bairdiids, and is the exit for the water that flows over the body of the ostracod so it can breathe with the valves almost closed (Maddocks, personal communication, 2021). This structure is common in the Late Cretaceous ostracods of the U.S. Gulf Coast and has been observed in the following groups:

•brachycytherines, including *Brachycythere asymmetrica* Puckett 1994, *B. crenulata* Crane 1965, *B. plena* Alexander 1934 (Puckett et al. (2016), Pl. 4, fig. 11), *B. rhomboidalis* (Berry 1925), *B. nausiformis* Swain 1952 and *Digmocythere russelli* (Howe and Lea 1936);

•schulerideids (*Schuleridea travisensis* Hazel and Paulson 1964);

•trachyleberids, including species of *Ascetoleberis* (*A. plummeri* (Israelsky 1929) and *A. rugosissima* (Alexander 1929); *Bicornicythereis* (*B. bicornis* (Israelsky 1929); see Puckett (2009a), Pl. 1, fig. 9), *B. communis* (Israelsky 1929); see Puckett (2009a), Pl 5, fig. 6); *B. nodilinea* (Crane 1965), see Puckett (2009a), Pl. 3, fig. 1)); *B. polita* (Crane 1965); see Puckett (2009a), Pl. 3, fig. 12); *Fissocarinocythere* (*F. gapensis* (Alexander 1929) and *F. pidgeoni* (Berry 1925)); *Floricythereis lixula* (Crane 1965); *Planileberis costatana* (Israelsky 1929); *Pterygocythereis (Pterygocythereis) cheethami* Hazel and Paulson 1964; *Praephacorhabdotus pokornyi* (Hazel and Paulson 1964); and *Veenia* (*V. ozanana* (Israelsky 1929); *V. quadrialira* (Swain 1952); *V. spoori* (Israelsky 1929).

All of the aforementioned species have this feature only in the RV; the LV, in contrast, has a flattened area in the caudal region that corresponds to this position (see images in Puckett (2009a), for example, *Bicornicythereis bicornis* (Pl. 1, fig. 9), *B. nodilinea* (Pl. 3, fig. 1), *B. polita* (Pl. 3, fig. 12), *B. communis* (Pl. 5, fig. 6)). This morphology (flattened zone in LV corresponding to the double ogee-shaped structure in RV) is consistent with the interpretation that it is an outlet for water when the valves are nearly closed. The Recent bairdiids have indentations on both valves, however, whereas the anticytherideinines it is only on the RV.

The distribution of the sieve-type normal pore canals and fossae was mapped to answer the following questions: Is there a common pattern for the distribution of the pore canals? Is there a common pattern for some species and not others? If so, what are the taxonomic implications of these patterns? Are there homologous fossae in different species? If so, what are the taxonomic implications? Tsukagoshi and Ikeya (1987) and Tsukagoshi (1990) studied the distribution of normal pore canals in Recent species of *Cythere* to determine their significance in phylogenetics. Tsukagoshi (1990) subdividing the pore canals into five types; types 4 and 5 are pertinent here, as they are sieve-type normal pore canals, differing by Type 4 having a single bristle and Type 5 having a split bristle; the morphology of the sieve pores themselves were approximately the same (in other words, one would not be able to differentiate between Type 4 and Type 5 in fossil material). Tsukagoshi (1990) found that each species has its own distribution of sieve-type normal pore canals, but that these distributions were stable for each species; the distributional patterns for non-sieve-type normal pore canals (that is, simple openings) were stable among closely related species. To make sure that all the normal pore canals were mapped, views from both the inside and outside views were

---

PLATE 8

Asculdoracythereis asculdora n. sp.

Specimens 1-6, 8 at same scale, as indicated. Scale for figures 7, 9-11 as indicated. All specimens from the Maastrichtian Providence Sand of Barbour County, Alabama

LV = left valve, RV = right valve

1 Exterior RV, male, specimen 146-16, sample 2012-01-03-1-2.

2 Holotype (USNM PAL 771800), exterior LV, male, specimen 148-1, sample 2012-01-03-1-2.

3 Interior LV, female, specimen 148-5, sample 2012-01-03-1-2.

4 Paratype (USNM PAL 771801), exterior LV, female, specimen 148-3, sample 2012-01-03-1-2.

5 Exterior RV, A-1 instar, specimen 146-14, sample 2012-01-03-1-2.

6 Exterior LV, A-1 instar, specimen 146-15, sample 2012-01-03-1-2.

7 Closeup showing details of fossae and sieve pores, specimen 146-13, sample 2012-01-03-1-2.

8 Interior RV, male, specimen 146-21, sample 2014-5-28-1-2.

9 Closeup muscle scars, RV, same specimen as figure 3.

10 Closeup muscle scars, same specimen as 8.

11 Closeup fossae and sieve pores, same specimen as figure 6.

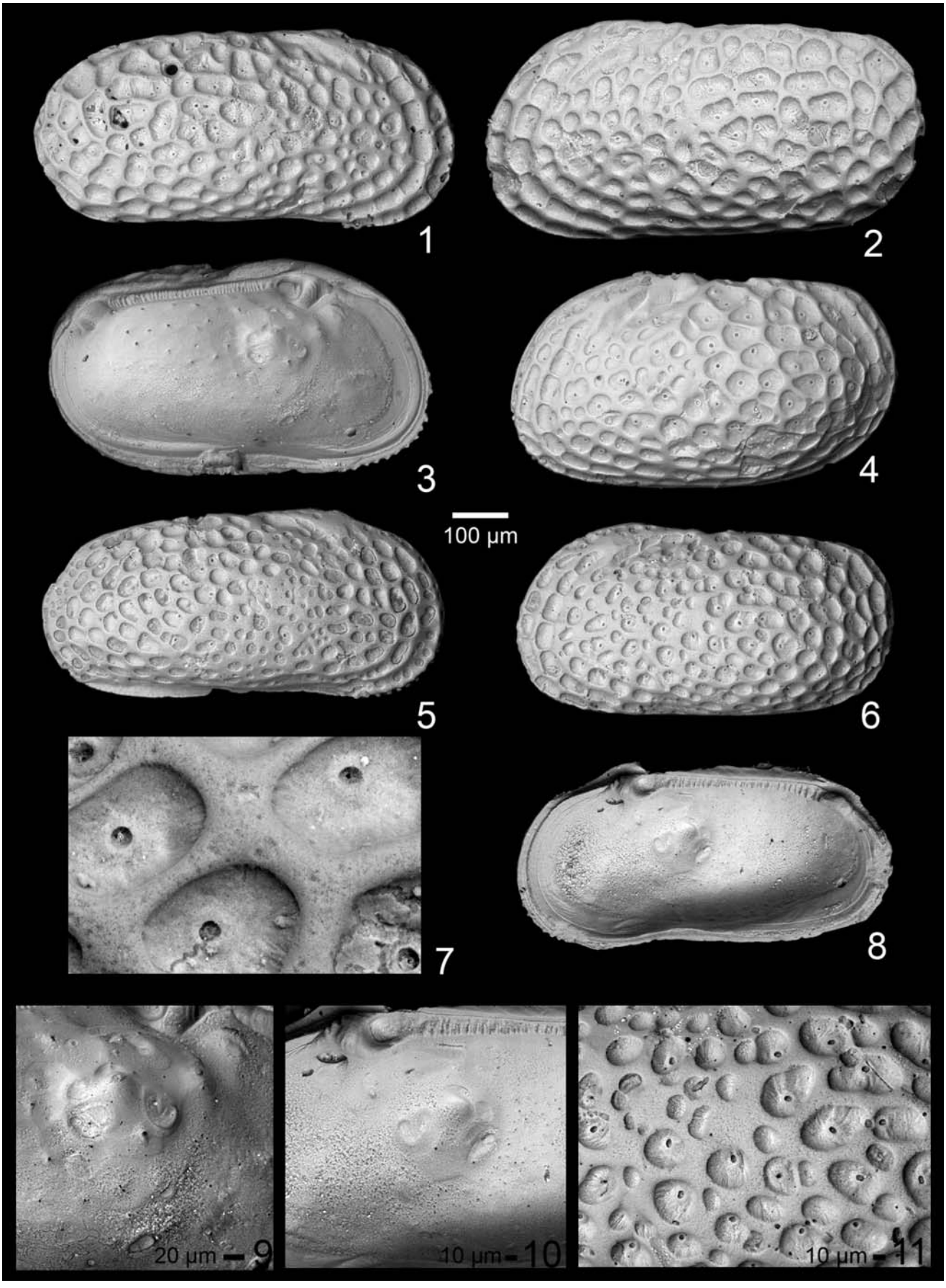
1
2
3
4
100 µm
5
6
7
8
20 µm
9
10 µm
10
10 µm
11

used (Plates 1 and 2) and superimposed on the same images. Each species has a fairly large number of pores, totaling almost 100 in some species. Attempts were made to connect the pores by lines, such as was done by Tsukagoshi (1990), but the patterns seemed to be different for each species. Mapping the sieve-type normal pore canals in the present study indicates that only the pore canals in the anterior and posterior regions could be determined to be homologous and their positions are stable. This indicates that the patterns of distribution of the sieve-type normal pore canals among the species of the anticytherideinines are species specific and cannot be used as a synapomorphic character to unite species within genera.

Similarly, the patterns of fossae were mapped in order to 1.) determine if homologous patterns of fossae could be determined among species, and 2.) assist in recognizing homologous patterns of sieve-type normal pore canals. Okada (Okada 1981, 1982b, 1982a) demonstrated that there is a correlation between epidermal cells and cuticular reticulation of the Recent species *Bicornucythere bisanensis*, with the cells correlating to the fossae and the cell walls corresponding to the muri. Okada (1981) observed the same cell-polygon in species of *Loxoconcha*. Similar correlation has been discovered in other fossil groups as well, including the recent discovery in scalidophoran worms of Cambrian age (Wang et al. 2020). The pattern of reticulation of the ostracods is stable in the last two instars within species, indicating a genetic control (Okada 1981, 1982b, 1982a). Clearly, then, the pattern of reticulation in the species that Liebau (1977) studied, for which he was able to track homologous fossae, must have had a nearly identical arrangement of epicuticle cells, and it was hypothesized that at least some of the species studies herein would have similar patterns as well. Except for the fossae along the anterior and posterior margins, however, the patterns of fossae are unique to each species (Pl. 1 and 2). Even within a species there is variability, and no two specimens are exactly the same, even from the same sample, and the exact patterns are different for females and males; compare, for example, the male on Plate 16, fig. 4 and the female on Plate 16, fig. 6, which were collected at the same level at the same outcrop. These differences indicate the possibility that there are cryptic species among those described herein. In any case, these observations indicate that homologous patterns of fossae and carinae cannot be used as a synapomorphic character to unite species into higher taxa within the anticytherideinines.

Overall, the anticytherideinines first appear in the later Campanian planktonic foraminiferal *Radotruncana calcarata* Taxon Range Zone (*Anticythereis* sp. 1, which was found in the Cusseta Sand of Barbour County, eastern Alabama). *Anticythereis slipperi*, which occurs in the latest Campanian-early Maastrichtian Coon Creek Formation and Ripley Formation of central Alabama, was among the oldest species to occur abundantly. Other species that appear at this level include *Tumulocythereis incompta* and *T. tiberti.* Several other species occurred at this time but were rare and left in open nomenclature (*Frodocythereis* sp. 1, *Laevipellacythereis* sp. 1, *Tumulocythereis* sp. 1). By the Maastrichtian, the subfamily reached its highest diversity, but became extinct at the K/Pg boundary. The ancestors to the subfamily are uncertain. Among the most similar morphologically are the species of *Bicornicythereis*, which has a similar muscle scar pattern and a small knob just anterior to the anterior tooth in the RV. One of those species, *B. communis*, is a long-ranging, widespread and com-

---

PLATE 9

Asculdoracythereis invicta n. sp.

Specimens 1-8 at same scale, as indicated. Scale for figures 9-11 as indicated. All specimens collected from the Maastrichtian Providence Sand of Barbour County, Alabama.

LV = left valve, RV = right valve

1 Holotype (USNM PAL 771802), exterior RV, male, specimen 147-10, sample 2012-01-03-1-2.

2 Exterior LV, female, specimen 147-12, sample 2012-01-03-1-2. Arrow points to distinctive circular fossa.

3 Exterior RV, female, specimen 147-11, sample 2012-01-03-1-2.

4 Paratype (USNM PAL 771803), exterior LV, female, specimen 147-13, sample 2012-01-03-1-2.

5 Interior LV, female, specimen 147-14, sample 2012-01-03-1-2.

6 Interior RV, female, specimen 147-16, sample 2012-01-03-1-2.

7 Interior LV, female, specimen 147-17, sample 2014-5-28-1-2.

8 Interior RV, male, specimen 147-18, sample 2014-5-28-1-2.

9 Closeup muscle scars, same specimen as figure 8.

10 Closeup muscle scars, same specimen as figure 7.

11 Closeup fossae and sieve pores, same specimen as figure 2.

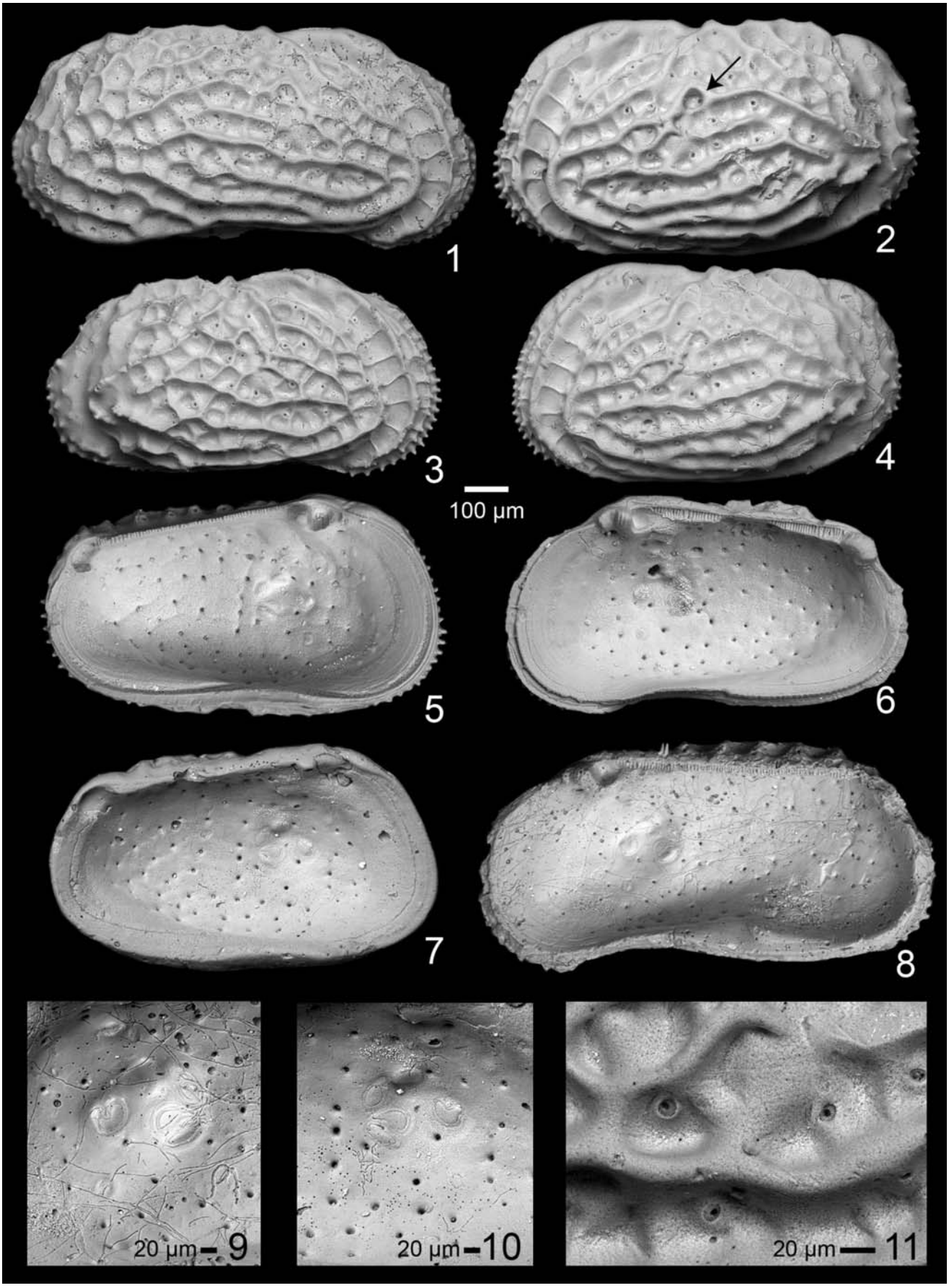
1
2
3
4
100 µm
5
6
7
8
20 µm 9
20 µm 10
20 µm 11

mon species in the Late Cretaceous deposits of the Gulf Coastal Plain and was living at the time of the appearance of the new subfamily. There is no indication, however, of the inverted platforms nor the related extended and deep postocular sulcus in that genus (see images in Puckett (2009a)).

Biogeographic Implications

The results of this study demonstrate that shallow marine, ornamented and sighted ostracods have a remarkable capacity to evolve indigenously. This makes them a powerful group for testing plate tectonic reconstructions and for studying evolutionary patterns uncomplicated by immigration and emigration. The newly defined Subfamily Anticytherideinae is a good example of such endemism, but so are several other genera that are restricted to these Late Cretaceous deposits of the North American coastal plain, including *Acuminobrachycythere, Antibythocypris, Ascetoleberis, Bicornicythereis,* and *Fissocarinocythere*. There are still species in these deposits that are assigned to catch-all genera such as *Cythereis* that should probably be assigned to an as-yet undescribed endemic genera (e.g., *C. caudata* Butler and Jones 1957*,* and *C. hannai* Israelsky 1929). The present study was undertaken to clean up the taxonomy of a relatively large number of species that one of the authors (TMP) has been collecting for many years.

On a regional scale, Puckett et al. (2012) discovered an indigenous shallow marine ostracod fauna from the Maastrichtian of Jamaica, and later discovered a very similar fauna in Chiapas, Mexico (Puckett 2009b, 2013). These observations, plus plate tectonic models, indicate that Jamaica was connected to Chiapas during the Late Cretaceous and rifted away during the Paleocene. On a much larger scale, Seeling et al. (2004) performed cluster analysis, ordination by nonmetric multidimensional scaling analysis and area cladograms on the global occurrences of 218 genera of ostracods from the Campanian to demonstrate an association of genera with paleogeography. The results showed an overall close alignment of generic assemblages with paleogeographic areas. There were, however, some anomalies. For example, Mexico clustered with Middle Eastern countries, Jamaica clustered with West Africa and Brazil, and the U.S. Gulf Coast clustered with European Georgia. A close inspection of that dataset reveals considerable noise in the signal due, in part, to incorrect generic assignments in the original published literature. The analysis also included all known genera in the various regions, including wide-ranging, apparently blind taxa such as *Argilloecia*, *Bairdia, Bythocypris* and many others, and single occurrences of genera at many localities. Deep water is not a barrier to blind taxa like it can be for sighted taxa, so it would not be unexpected for blind taxa to occur on more than one continent, and thus they would not be as useful for determining paleogeography as the sighted taxa that are restricted to shallow water. Genera located at a single locality cannot be used to infer former connectedness of habitats, just as an apomorphic character cannot be used in a phylogenetic analysis to determine relatedness of taxa—synapomorphic characters must be used. Further, and more crucial to the present arguments, there were several genera that were reported from different continents where species had been assigned to inappropriate genera. For example, the genera *Brachycythere* and *Curfsina* were reported from several continents, but analysis of the internal morphology reveals that the muscle scar patterns differ systematically according to region (Puckett 2002, 2009a). One of the authors of this paper (TMP) took the dataset of Seeling et al. (2004), eliminated the blind, ubiquitous genera, and the taxa that occur at a single area, and updated the generic assignments, resulting in a dataset of only 118 genera, and re-ran the analysis. The results show a closer association of genera and paleogeography and eliminated the anomalies. These observa-

---

PLATE 10

Asculdoracythereis lowndesensis (Smith 1978)

Specimens 1-6 at same scale, as indicated. Scale for figures 7-10 as indicated. All specimens collected from the Maastrichtian Providence Sand in Alabama.

LV = left valve, RV = right valve

1 Exterior RV, female, specimen 146-10, sample 2012-01-03-1-2, Barbour County.

2 Exterior LV, female, specimen 146-8 6216, sample 2012-01-03-1-2, Barbour County.

3 Exterior RV, male, specimen 134-17, sample 1991-8-14-1, Bullock County.

4 Exterior LV, female, specimen 146-11, sample 2014-5-28-1-1, Barbour County.

5 Interior LV, female, specimen 146-7, sample 2012-01-03-1-2, Barbour County.

6 Interior RV, male, specimen 146-5, sample 2012-01-03-1-2, Barbour County.

7 Closeup elevated pores, specimen 146-9, sample 2012-01-03-1-2, Barbour County.

8 Closeup muscle scars, external view RV, same specimen as figure 3.

9 Closeup sieve pores and ornamentation, specimen 134-18, sample 1991-8-14-1, Bullock County. Arrow points to knob-like conjunctive spine.

10 Closeup muscle scars, LV, same specimen as figure 5.

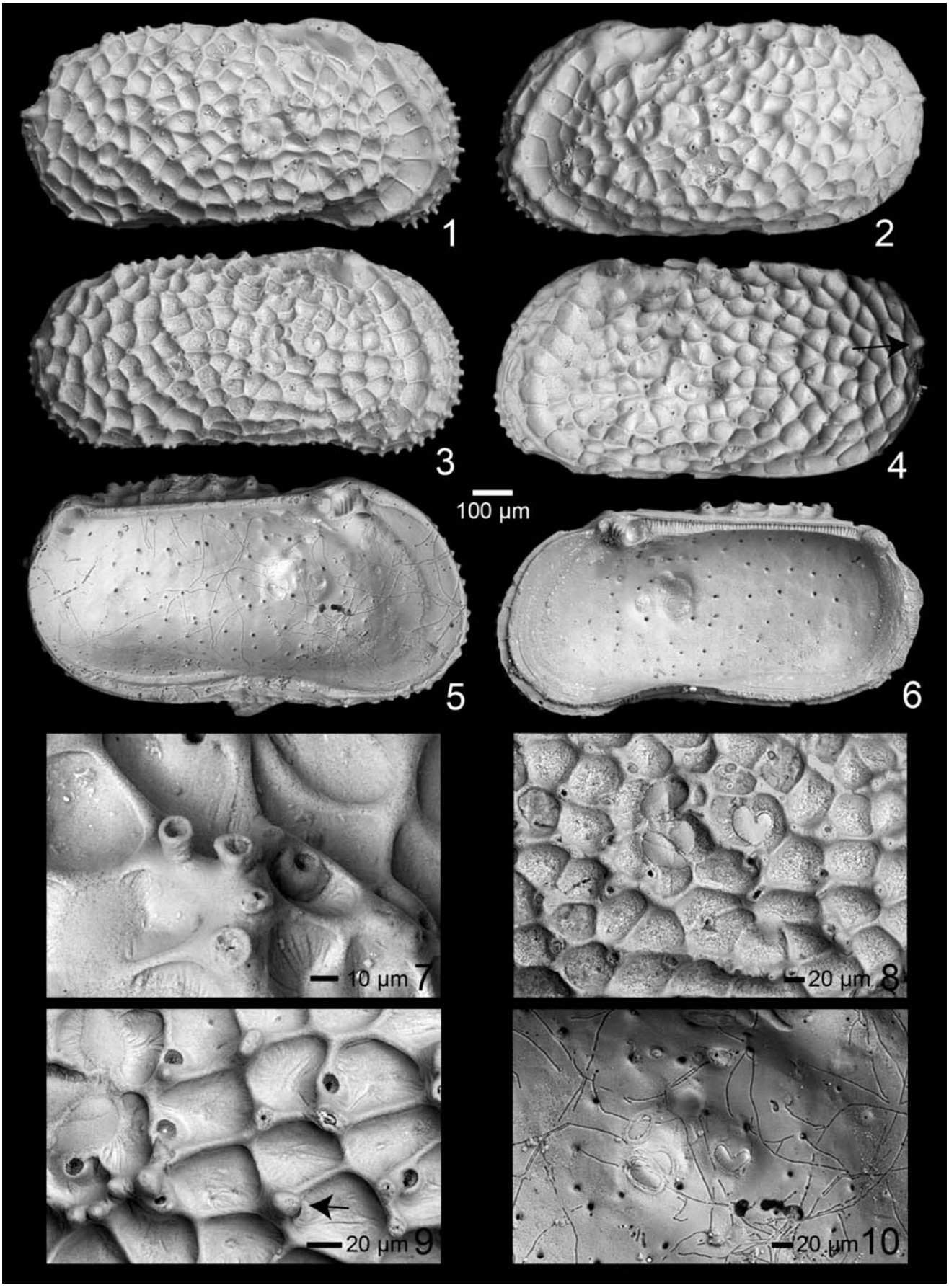
1
2
3
4
100 µm
5
6
10 µm 7
20 µm 8
20 µm 9
20 µm 10

tions indicate that uncritically assigning shallow marine, sighted ostracods from different continents to the same genera undermines their use in paleogeographic studies, including plate tectonics, and should, therefore, be regarded as an opportunity for re-evaluation. As indicated in this discussion, the internal features, particularly the central muscle scars, are critical for accurate assignment of species to genera. Ideally, a phylogenetic analysis combining character cladograms and area cladograms, such as discussed by Lieberman (2000), would result in viable hypotheses regarding the evolution of the faunas through time.

Another implication of the present study is the rapidity with which ostracods can evolve and diversify. Several species have been observed only at a single outcrop, despite sampling of coeval deposits elsewhere. Species of the Subfamily Anticytherideinae first appear in eastern Alabama in the Cusseta Sand (planktonic foraminiferal *Radotruncana calcarata* Taxon Range Zone, early part of the Upper Campanian) and diversify relatively slowly until the Maastrichtian, when their numbers surge to more than 20 species. Its high Maastrichtian diversity did not protect the subfamily from the Cretaceous-Paleogene mass extinction, which marked the end of this clade after approximately 10 million years of evolution.

ACKNOWLEDGMENTS

The authors are grateful to several individuals who contributed to this work. Rosalie Maddocks, Professor at the University of Houston, is sincerely thanked for informative discussions on many aspects of ostracod morphology and biology; her review of the manuscript resulted in vast improvements. Bushra Hussaini, Senior Museum Specialist at the American Museum of Natural History, is thanked for the loan of the type specimens of *Pseudocythereis reticulata* Jennings 1936. Michael Blanton, Research Associate/Team Leader at the University of Southern Mississippi School of Polymer Science and Engineering, is thanked for the extensive use of the Zeiss scanning electron microscope. Amy Stephenson, then undergraduate student at the University of North Alabama, is thanked for picking many specimens and for field assistance. Molly Pasco-Pranger, Associate Professor and Chair of Classics, University of Mississippi, is thanked for her help with the Latin names. Conner and Nathan Puckett are thanked for their assistance in the field.

PLATE 11

Frodocythereis copelandi (Smith 1978)

Specimens 1-7 at same scale, as indicated. Scale for figures 8-11 as indicated.

LV = left valve, RV = right valve

1 Holotype (USNM PAL 255757), exterior RV, female, sample 15A, Maastrichtian Prairie Bluff Formation, Lowndes County, Alabama.

2 Exterior LV, female, specimen 132/136-28, sample 2011-5-18-1 (water level), Maastrichtian Owl Creek Formation, Tippah County, Mississippi.

3 Exterior RV, female, specimen 143-22, sample 2011-8-4-1 (water level), Maastrichtian Owl Creek Formation, Tippah County, Mississippi.

4 Exterior LV, female, specimen 132/136-23, sample 2011-5-18-1 (water level), Maastrichtian Owl Creek Formation, Tippah County, Mississippi.

5 Interior LV, male, specimen 132/136-27, sample 2011-8-4-1 (water level), Maastrichtian Owl Creek Formation, Tippah County, Mississippi.

6 Interior RV, male, specimen 142-9, sample 2011-5-18-1 (water level), Maastrichtian Owl Creek Formation, Tippah County, Mississippi.

7 Exterior RV, male, specimen 28-6a, sample 1994-8-12-4b, Maastrichtian Prairie Bluff Chalk, Lowndes County, Alabama.

8 Closeup external valve, specimen 142-17, sample 2011-8-4-1 (water level), Maastrichtian Owl Creek Formation, Tippah County, Mississippi.

9 Closeup muscle scars, RV, specimen 132/136-26, sample 2011-8-4-1 (water level), Maastrichtian Owl Creek Formation, Tippah County, Mississippi.

10 Closeup muscle scars, LV, specimen 132/136-24, sample 2011-8-4-1 (water level), Maastrichtian Owl Creek Formation, Tippah County, Mississippi.

11 Closeup fossae, punctation and sieve pore, specimen 103-2, sample 2011-5-18-1 (water level), Maastrichtian Owl Creek Formation, Tippah County, Mississippi.

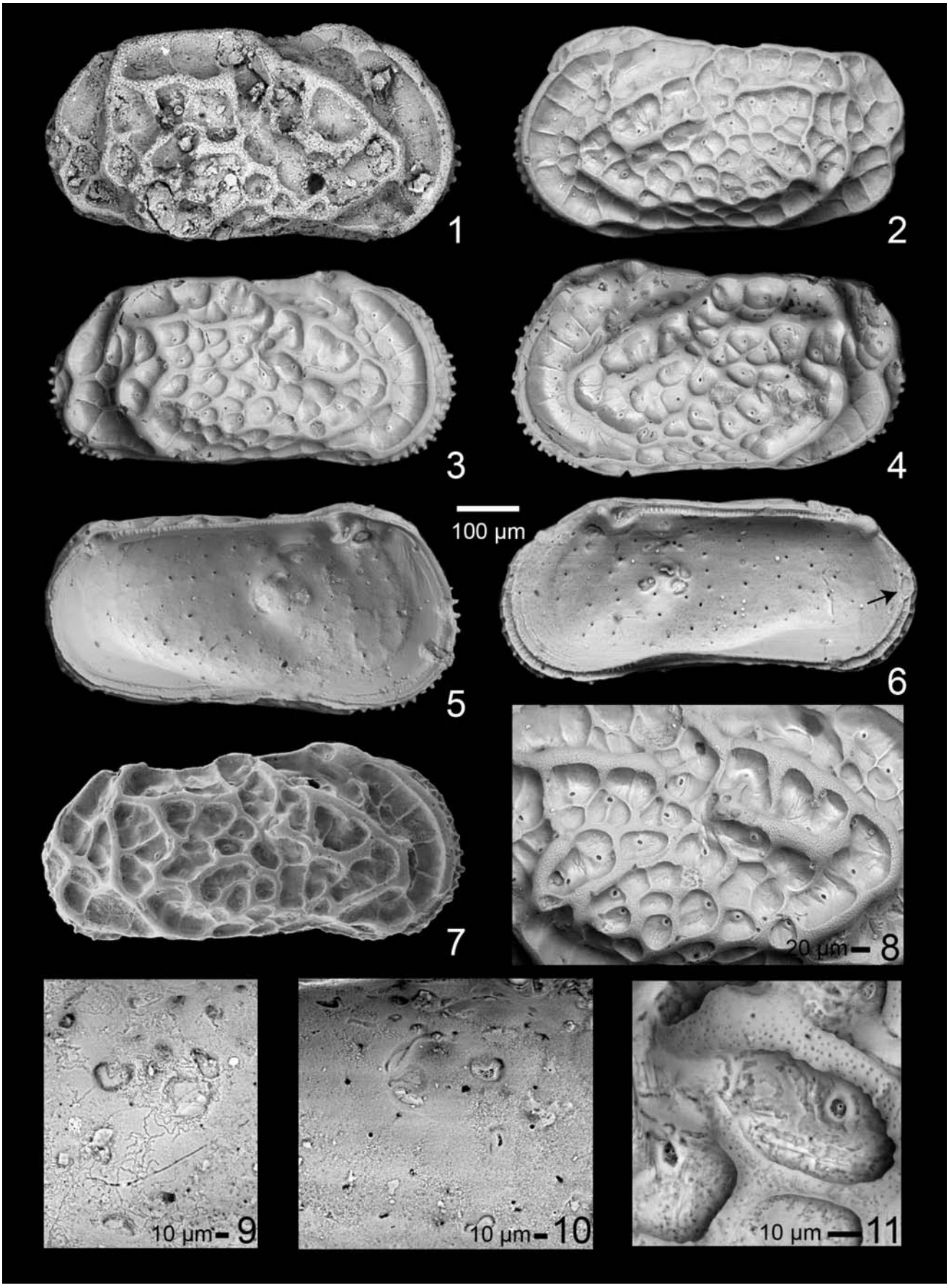
1
2
3
4
100 µm
5
6
7
20 µm
8
10 µm
9
10 µm
10
10 µm
11

REFERENCES

AL-FURAIH, A. A. F., 1980. *Upper Cretaceous and lower Tertiary Ostracoda (Superfamily Cytheracea) from Saudi Arabia.* University of Riyadh, 211 pp.

APOSTOLESCU, V., 1961. Contribution a l'étude paléontoloque (Ostracodes) et stratigraphique des bassins Crétacé et Tertiares de l'Afrique occidentale. *Revue de l'Institut Français du Pétrole,* 16: 779–867.

ATHERSUCH, J., HORNE, D. J. and WHITTAKER, J. E., 1989. *Marine and Brackish Water Ostracods,* London: E.J. Brill.

BAIRD, W., 1850. *The Natural History of the British Entomostraca,* London: The Ray Society.

BARSOTTI, G., 1963. Paleocenic ostracods of Libya (Sirte Basin) and their wide African distribution. *Revue de l'Institut Français du Pétrole,* 18: 1520–1535.

BENSON, R. H., 1972. The *Bradleya* problem, with descriptions of two new psychorospheric genera, *Agrenocythere* and *Poseidonamicus* (Ostracoda: Crustacea). *Smithsonian Contributions to Paleobiology,* 12: 1–138.

BENSON, R. H., BERDAN, J. M., VAN DEN BOLD, W. A. and MOORE, R. C., 1961. *Treatise on Invertebrate Paleontology: Part Q: Crustacea, Ostracoda,* Lawrence, Geological Society of America, 422 pp.

BERTELS, A., 1973. Ostracodes of the type locality of the lower Tertiary (lower Danian) Rocanian Stage and Roca Formation of Argentina. *Micropaleontology,* 19: 308–340.

———, 1975a. Upper Cretaceous (middle Maastrichtian) ostracodes of Argentina. *Micropaleontology,* 21: 97–130.

———, 1975b. Ostracode ecology during the Upper Cretaceous and Cenozoic in Argentina. In: Swain, F. M., Kornicker, L. S. and Lundin, R. F. Eds. *Biology and Paleobiology of Ostracoda, Bulletins of American Paleontology.* Ithaca: Paleontological Research Institute, 317–351.

———, 1976. Evolutionary lineages of some Upper Cretaceous and Tertiary ostracodes of Argentina. *Abhandlungen und Verhandlungen des naturwissenschaftlichen Vereins Hamburg (NF), Supplement,* 18/19: 175–190.

———, 1977. Cretaceous Ostracoda—South Atlantic. In: Swain, F. M. Ed. *Stratigraphic Micropaleontology of Atlantic Basins and Borderlands.* Amsterdam: Elsevier. Developments in Palaeontology and Stratigraphy, 6: 271–303.

BOSQUET, J., 1854. Les crustacés fossiles du terrain crétacé du Limbourg. *Verhandelingen uitgegeven door de Commis sie belast met het vervaardigen eener geologische beschrijving en kaart van Nederland,* 2: 1–127.

BRANDÃO, S. and KARANOVIC, I., 2021. *World Ostracoda Database* [Online]. Available: http://www.marinespecies.org/ostracoda [Accessed 2021-02-02].

BROUWERS, E. and HAZEL, J. E., 1978. Ostracoda and correlation of the Severn Formation (Navarroan; Maestrichtian) of Maryland. *Society of Economic Paleontologists and Mineralogists, Paleontological Monograph,* 1: 1–52.

PLATE 12

Frodocythereis frodoi n. sp.
Specimens 1-8 at same scale, as indicated. Scale for figures 9-12 as indicated.
All specimens collected from the Maastrichtian Owl Creek Formation type locality, Tippah County, Mississippi.
LV = left valve, RV = right valve

1 Exterior RV, female, specimen 132-4, sample 2011-8-4-1 (water level).

2 Exterior LV, female, specimen 29-12, sample 94-5-11-7a.

3 Exterior RV, female, specimen 134-10, sample 2011-8-4-1 (water level).

4 Holotype (USNM PAL 771806), exterior LV, male, specimen 134-2, sample 2011-8-4-1 (water level).

5 Exterior RV, male, specimen 132-9, sample 2011-5-18-1 (water level).

6 Paratype (USNM PAL 771807), exterior LV, female, specimen 104-6, sample 2011-5-18-1 (water level).

7 Interior RV, male, specimen 134-4, sample 2011-8-4-1 (water level).

8 Interior LV, male, specimen 134-1, sample 2011-8-4-1 (water level).

9 Closeup muscle scars, LV, same specimen as figure 8.

10 Closeup muscle scars, RV, specimen 134-8, sample 2011-8-4-1 (water level).

11 Closeup muscle scars, RV, same specimen as figure 7. Note the pair of inverted platforms near the top of the image.

12 Closeup of muscle scars, exterior view, same specimen as figure 4.

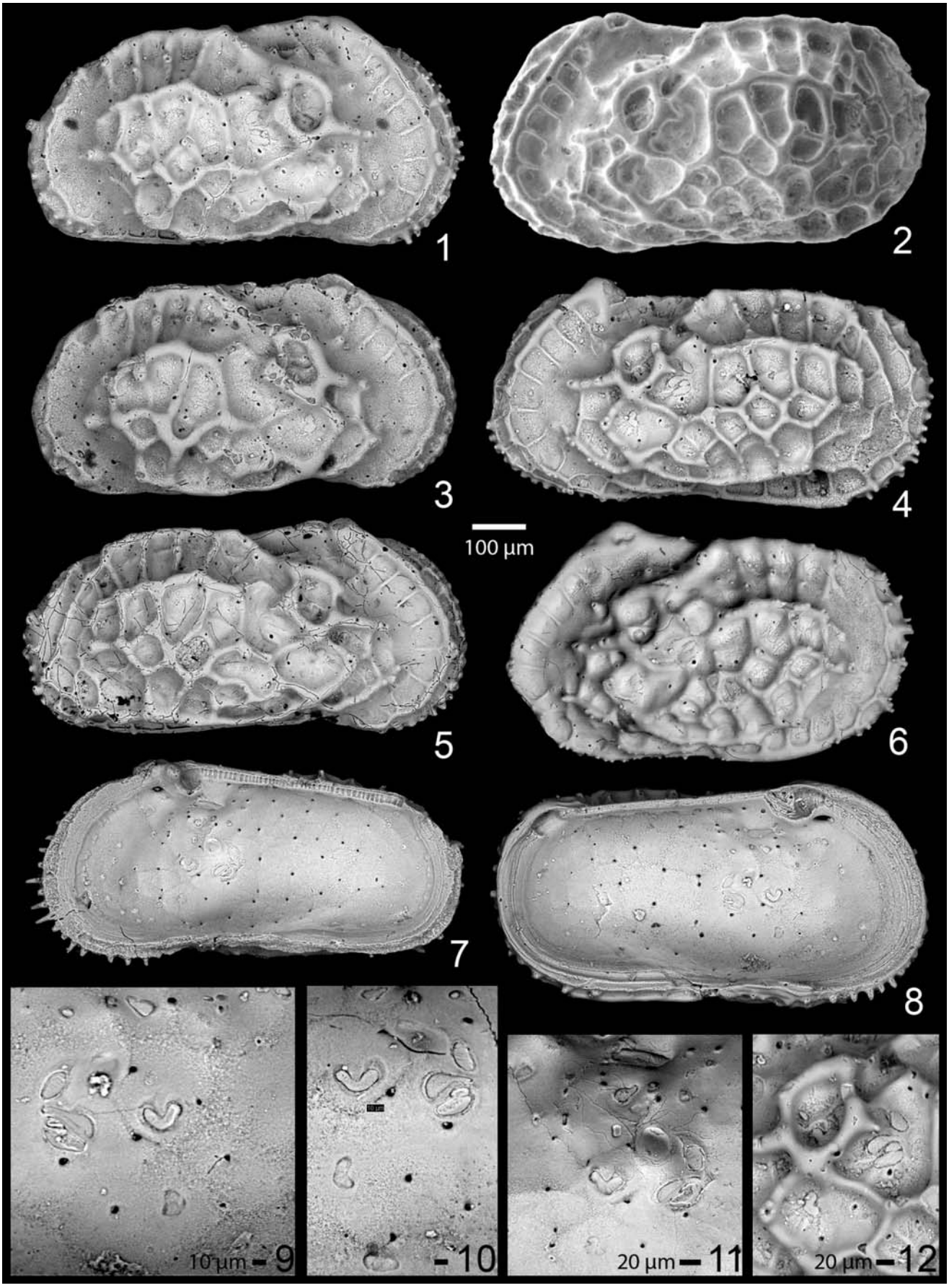
1
2
3
4
100 µm
5
6
7
8
10 µm
9
10
20 µm
11
20 µm
12

BROWN, P. M., 1957. Upper Cretaceous Ostracoda from North Carolina. *North Carolina Department of Conservation and Development, Division of Mineral Resources, Bulletin,* 70: 1–28.

———, 1958. Well logs from the Coastal Plain of North Carolina. *North Carolina Department of Conservation and Development, Division of Mineral Resources, Bulletin*, 72: 1–68.

CARBONNEL, G., 1986. Ostracodes Tertiaires (Paléogène a Néogène) du bassin sénégalo-guinéen. *Documents du Bureau de Recherches Géologiques et Minières,* 101: 33–243.

———, 1988. Les écozones d'ostracodes paléogènes dans les bassins côtiers d'Afrique (Togo, Guinée-Bissau, Sénégal, Mauritanie): un révélateur biogéographique. *Newsletters on Stratigraphy,* 20: 59–72.

CRONIN, T. M. and KHALIFA, H., 1979. Middle and Late Eocene Ostracoda from Gebel El Mereir, Nile Valley, Egypt. *Micropaleontology,* 25: 397–411.

DAMOTTE, R., 1982. Ostracodes Maestrichtiens et Paléocenes du Togo. *Cahiers de Micropaléontologie,* 2: 47–63.

DEROO, G., 1966. Cytheracea (Ostracodes) du Maastrichtien de Maastricht (Pays-Bas) et des régions voisines; résultats stratigraphiques de leur étude. *Mededelingen Van de Geologische Stichting, Serie C, Uitgevers-Maatschappij "Ernst Van Aest", Maastricht,* 2: 1–197.

EL-NADY, H., 2002. Upper Cretaceous ostracods from northeastern Sinai, Egypt: taxonomy and paleobiogeography. *Revue de Paléobiologie, Genève,* 21: 587–638.

GALE, A. S., MUTTERLOSE, J. and BATENBURG, S., 2020. The Cretaceous Period. In: Gradstein, F. M., Ogg, J. G., Schmitz, M. D. and Ogg, G. M. Eds. *Geologic Time Scale 2020.* Amsterdam: Elsevier, 1023–1086.

GEBHARDT, H., 1999. Cenomanian to Coniacian biogeography and migration of North and West African ostracods. *Cretaceous Research,* 20: 215–229.

GOHN, G. S., 1992. Distribution of selected Campanian and Maastrichtian Ostracoda in stratigraphic test holes of the New Jersey Coastal Plain. *U. S. Geological Survey Open File Report, 92-399*: 1–25.

GREKOFF, N., 1964. Étude biostratigraphique des Ostracodes du Crétacé et de l'Eocène inférieur d'Algerie. In: Pétrole, I. F. D. Ed., *Branche Recherche et Exploitation du Pétrole Division Géologie.*

GROSDIDIER, E., 1973. Associations d'Ostracodes de Crétacé d'Iran. *Revue de l'Institut Français du Pétrole,* 28: 131–169.

––––––, 1979. Principaux ostracodes marins de l'intervalle Aptien-Turonien du Gabon (Afrique occidentale). *Bulletin des Centres de Recherches Exploration-Production Elf-Aquitaine,* 3: 1–35.

GUBER, A. L. and JAANUSSON, V., 1964. Ordovician ostracodes with posterior domiciliar dimorphism. *Uppsala University, Geological Institutions Bulletin,* 43: 1–41.

HABIB, D., MOSHKOVITZ, S. and KRAMER, C., 1992. Dinoflagellate and calcareous nannofossil response to sea-level changes in Cretaceous-Tertiary boundary sections. *Geology,* 20: 165–168.

HABIB, D., OLSSON, R. K., LIU, C. and MOSHKOVITZ, S., 1996. High-resolution biostratigraphy of sea-level low, biotic extinction, and chaotic sedimentation at the Cretaceous-Tertiary boundary in Alabama, north of the Chixculub crater. In: Ryder, G., Fastovsky, D. E. and Gartner, S. Eds. *The Cretaceous-Tertiary Event and Other Catastrophes in Earth History.* Boulder: Geological Society of America, 243–252.

HART, M. B., HARRIES, P. J. and CÁRDENAS, A. L., 2013. The Cretaceous/Paleogene boundary events in the Gulf Coast: comparisons

---

PLATE 13

Laevipellacythereis colossus n. sp.
Specimens 1-6, 8 at same scale, as indicated. Scale for figures 7, 9-11 as indicated.
All specimens from sample 2012-01-03-1-2, Maastrichtian Providence Sand of Barbour County, Alabama.
LV = left valve, RV = right valve

1 Exterior RV, male, specimen 148-8.

2 Holotype (USNM PAL 771808), exterior LV, male, specimen 148-7.

3 Interior LV, female, specimen 148-10.

4 Paratype (USNM PAL 771809), exterior LV, female, specimen 148-9. Arrow points to outline of upper internal inverted platform as seen on the exterior of the carapace.

5 Interior LV, male, specimen 148-11.

6 Interior RV, male, specimen 148-13. Left arrows point to upper and lower inverted platforms and right arrow points to interruption of selvage at caudal region.

7 Closeup muscle scars, same specimen as figure 8.

8 Interior RV, female, specimen 148-12.

9 Closeup muscle scars, exterior view, RV, same specimen as figure 1.

10 Closeup sieve pores, RV, same specimen as figure 3.

11 Closeup muscle scars, LV, same specimen as figure 5.

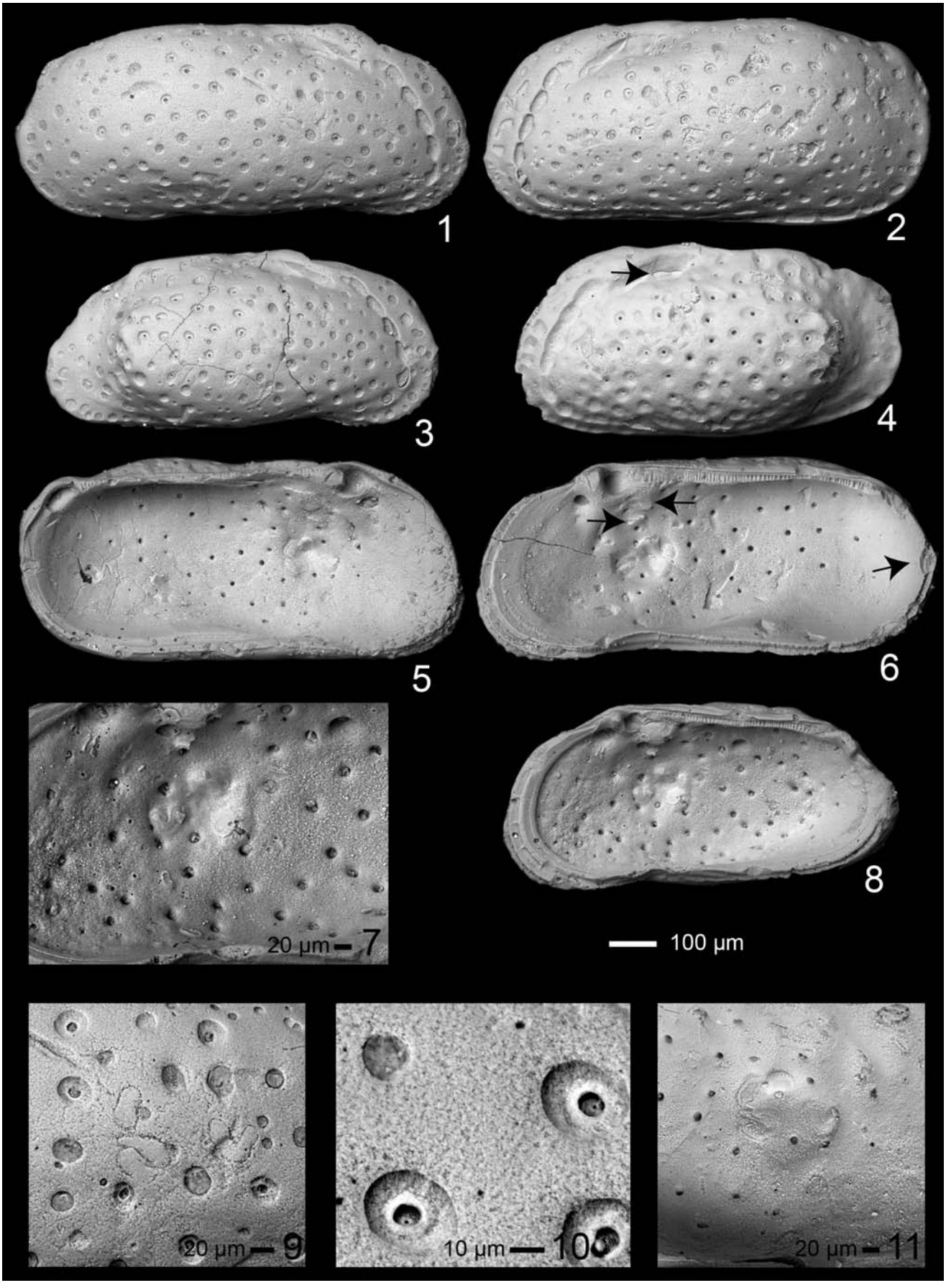
1
2
3
4
5
6
8
20 µm
7
100 µm
20 µm
9
10 µm
10
20 µm
11

between Alabama and Texas. *Transactions of the Gulf Coast Association of Geological Societies,* 63: 235–255.

HAZEL, J. E., 1967. Classification and distribution of the Recent Hemicytheridae and Trachyleberididae (Ostracoda) off northeastern North America. *U.S. Geological Survey Professional Paper,* 564: 1–49.

HAZEL, J. E. and BROUWERS, E. M., 1982. Biostratigraphic and chronostratigraphic distribution of ostracodes in the Coniacian-Maastrichtian (Austinian-Navarroan) in the Atlantic and Gulf Coastal Provinces. *Guidebook of excursions and related papers for the 8th International Symposium on Ostracoda*, 166–198.

HONIGSTEIN, A., 1984. Senonian ostracodes from Israel. *Geological Survey of Israel, Bulletin,* 78: 1–48.

HONIGSTEIN, A., RAAB, M. and ROSENFELD, A., 1985. Manual of Cretaceous ostracodes from Israel. *Geological Survey of Israel, Special Publication,* 5: 1–25.

HORNE, D. J., COHEN, A. and MARTENS, K., 2002. Taxonomy, morphology and biology of Quaternary and living Ostracoda. *Geophysical Monograph,* 131, The Ostracoda: Applications on Quaternary Research, 5–139.

HOWE, H. V. and LAURENCICH, L., 1958. *Introduction to the Study of Cretaceous Ostracoda,* Baton Rouge: Louisiana State University Press, 1–536.

HUANG, H.-H. M., YASUHARA, M., CRONIN, T. M., HISAYO, O. and HUNT, G., 2022. *Poseidonamicus* (Ostracoda) from the North Atlantic Ocean. *Micropaleontology,* 68: 257–271.

HUNT, G., 2007. Morphology, ontogeny, and phylogenetics of the Genus *Poseidonamicus* (Ostracoda: Thaerocytherinae). *Journal of Paleontology,* 81: 607–631.

HUNT, G., FERNANDES MARTINS, J., PUCKETT, T. M., LOCKWOOD, R., SWADDLE, J. P., HALL, C. M. S. and STEDMAN, J., 2017. Sexual dimorphism and sexual selection in cytheroidean ostracodes from the Late Cretaceous of the U.S. Gulf Coastal Plain. *Paleobiology,* 43: 620–641.

ISMAIL, A. A. and SOLIMAN, S. I., 1997. Cenomanian-Santonian foraminifera and ostracodes from Horus Well-1, North Western Desert, Egypt. *Micropaleontology,* 43: 165–183.

JENNINGS, P. H., 1936. A microfauna from the Monmouth and basal Rancocas Groups of New Jersey. *Bulletins of American Paleontology,* 23: 1–77.

KENNEDY, W. J., LANDMAN, N. H., COBBAN, W. A. and JOHNSON, R. O., 2000. Additions to the ammonite fauna of the Upper Cretaceous Navesink Formation of New Jersey. *American Museum Novitates*, 1–30.

KESLING, R. V., 1951. Terminology of ostracod carapaces. *Contributions from the Museum of Paleontology University of Michigan,* 9: 93–171.

KEYSER, D., 1990. Morphological changes and function of the inner lamella of podocopid Ostracoda. In: Whatley, R. and Maybury, C. Eds. *Ostracoda and Global Events.* London: Chapman and Hall, 401–410.

———, 2005. Histological peculiarities of the noding process in *Cyprideis torosa* (Jones) (Crustacea, Ostracoda). *Hydrobiologia,* 538: 95–106.

PLATE 14

Laevipellacythereis laevipellis n. sp.

Specimens 1-8 at same scale, as indicated. Scale for figures 9-11 as indicated.

All specimens collected from the type locality of the Maastrichtian Owl Creek Formation, Tippah County, Mississippi.

LV = left valve, RV = right valve

1 Exterior RV, female, specimen 130/135-22, sample 2011-8-4-1 (water level).

2 Holotype (USNM PAL 771810), exterior LV, female, specimen 130/135-23, sample 2011-8-4-1 (water level).

3 Paratype (USNM PAL 771811), exterior RV, male, specimen 130/135-28, sample 2011-8-4-1 (water level).

4 Exterior LV, male, specimen 130/135-10, possible juvenile, sample 2011-5-18-1 (water level).

5 Interior LV, female, specimen 130/135-5, sample 2011-5-18-1 (water level).

6 Interior RV, female, specimen 130/135-6, sample 2011-5-18-1 (water level).

7 Interior LV, male, specimen 130/135-7, possible juvenile, sample 2011-8-4-1 (water level).

8 Interior RV, male, specimen 130/135-20, sample 2011-8-4-1 (water level). Arrow points to interruption of selvage at caudal region.

9 Closeup sieve pores, specimen 130/135-31, sample 2011-8-4-1 (water level).

10 Closeup muscle scars, specimen 130/135-8, sample 2011-8-4-1 (water level).

11 Closeup sieve pore, same specimen as figure 6.

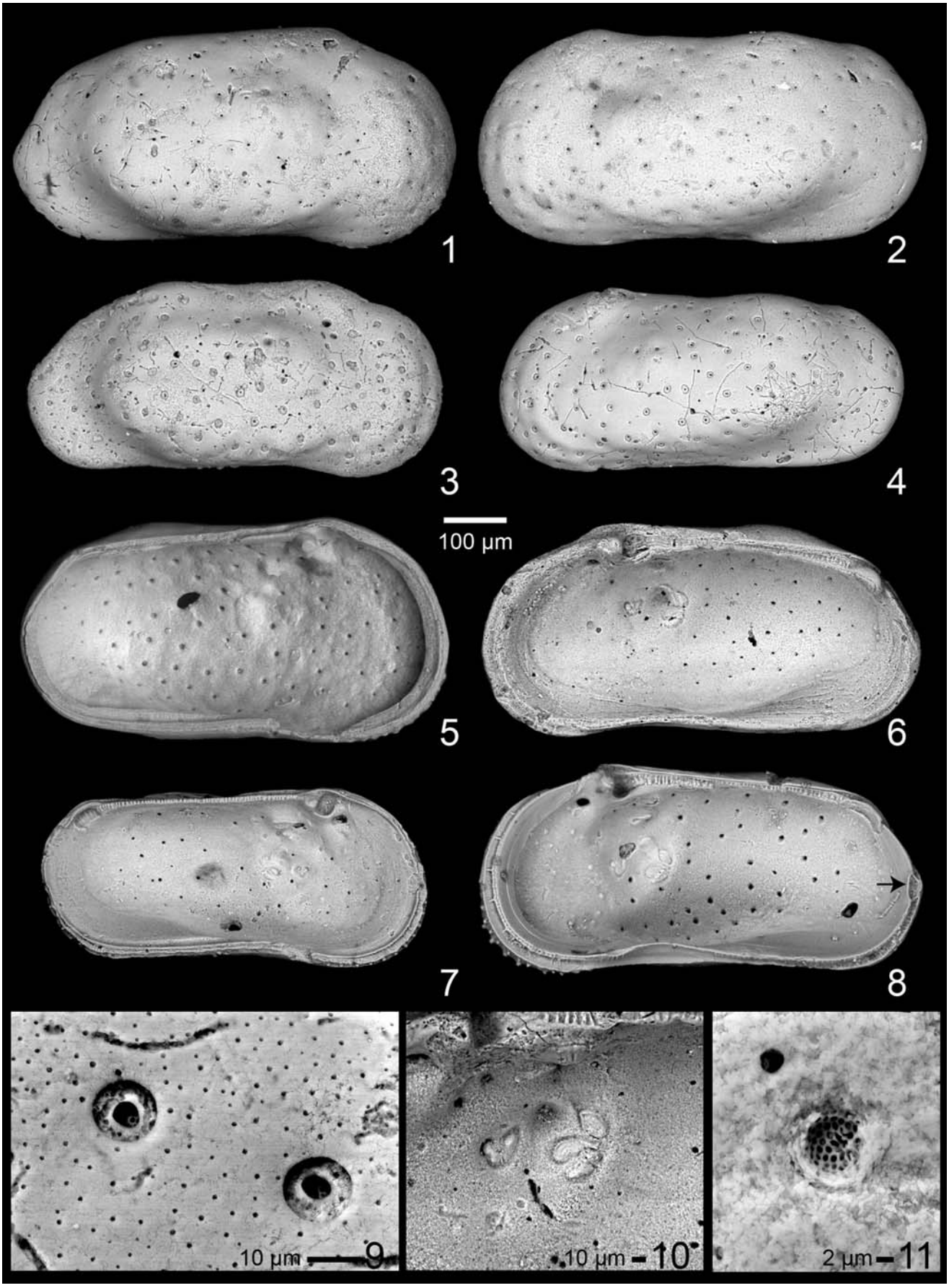
1
2
3
4
100 µm
5
6
7
8
10 µm
9
10 µm
10
2 µm
11

KHALIFA, H. and CRONIN, T. M., 1979. Ostracodes de l'Éocène moyen de El Sheikh Fadl, est de Beni Mazar, Haute-Égypte. *Revue de Micropaléontologie,* 22: 172–185.

LARINA, E., GARB, M., LANDMAN, N., DASTAS, N., THIBAULT, N., EDWARDS, L., PHILLIPS, G., ROVELLI, R., MYERS, C. and NAUJOKAITYTE, J., 2016. Upper Maastrichtian ammonite biostratigraphy of the Gulf Coastal Plain (Mississippi Embayment USA). *Cretaceous Research,* 60: 128–151.

LATREILLE, P. A., 1802. Histoire naturelle, générale et particulière des Crustacés et des Insectes. *Histoire des Cypris et des Cytherées,* 8: 232–254.

LAURENTIAUX, C., 1950. Les insectes Houillers du Limbourg hollandais. *Mededelingen Van de Geologische Stichting, Serie C, Uitgevers-Maatschappij "Ernst Van Aest", Maastricht,* 4: 13–22.

LIEBAU, A., 1977. *Homologous sculpture patterns in Trachyleberididae and related ostracods,* Belgrade: Nolit Publishing House.

LIEBERMAN, B. S., 2000. *Paleobiogeography: Using Fossils to Study Global Change, Plate Tectonics, and Evolution,* New York: Kluwer Academic/Plenum Publishers.

LORD, A. R., CABRAL, M. C. and DANIELOPOL, D. L., 2020. Sieve-type normal pore canals in Jurassic ostracods: A review with description of a new genus. *Acta Palaeontologica Polonica,* 65: 313–349.

MADDOCKS, R. F., 1969. Revision of Recent Bairdiidae (Ostracoda). *United States National Museum Bulletin,* 295: 1–126.

MANCINI, E. A. and PUCKETT, T. M., 2005. Jurassic and Cretaceous transgressive-regressive (T-R) cycles, northern Gulf of Mexico, USA. *Stratigraphy,* 2: 31–48.

MANCINI, E. A., TEW, B. H. and PUCKETT, T. M., 1996a. Comparison of Upper Cretaceous and Paleocene depositional sequences in the eastern Gulf Coastal Plain. *Transactions of the Gulf Coast Association of Geological Societies,* 46: 281–286.

MANCINI, E. A., PUCKETT, T. M. and TEW, B. H., 1996b. Integrated biostratigraphic and sequence stratigraphic framework for Upper Cretaceous strata of the eastern Gulf Coastal Plain. *Cretaceous Research,* 17: 645–669.

MANCINI, E. A., PUCKETT, T. M., TEW, B. H. and SMITH, C. C., 1995a. Upper Cretaceous sequence stratigraphy of the Missis-

PLATE 15

Tumulocythereis incompta n. sp.
Specimens 1-8 at same scale, as indicated. Scale for figures 9-14 as indicated.
LV = left valve, RV = right valve

1 Holotype (USNM PAL 771812), exterior RV, male, specimen 142-11, sample 2011-8-4-1 (water level), Maastrichtian Owl Creek Formation, Tippah County, Alabama.

2 Exterior LV, female, specimen 134-19, 2010-10-22-1 (505), Maastrichtian Coon Creek Formation, Tippah County, Mississippi.

3 Paratype (USNM PAL 771813), exterior RV, female, specimen 142-10, sample 2011-8-4-1, latest Campanian-Maastrichtian Owl Creek Formation, Tippah County, Mississippi.

4 Exterior LV, female, specimen 141-9, sample 2011-8-4-1 (water level), Maastrichtian Owl Creek Formation, Tippah County, Mississippi.

5 Interior LV, female, same specimen as figure 4.

6 Interior RV, female, specimen 145-4, sample 1994-5-11-7a, Maastrichtian Owl Creek Formation, Tippah County, Mississippi.

7 Interior LV, male, specimen 145-5, sample 2011-8-4-1, Maastrichtian Owl Creek Formation, Tippah County, Mississippi.

8 Interior RV, male, specimen 142-9, sample 2011-8-4-1 (water level), Maastrichtian Owl Creek Formation, Tippah County, Mississippi. Arrow points to interruption of selvage at caudal region.

9 Closeup sieve pores, specimen 145-10, sample 2011-5-18-1 (water level), Maastrichtian Owl Creek Formation, Tippah County, Mississippi.

10 Closeup hinge area, specimen 145-6, sample 2011-8-4-1, Maastrichtian Owl Creek Formation, Tippah County, Mississippi.

11 Closeup sieve pores, specimen 145-7, sample 1994-5-11-7 (18' below shell bed), Maastrichtian Owl Creek Formation, Tippah County, Mississippi.

12 Closeup fossae and sieve pores, same specimen as figure 3.

13 Closeup muscle scars, same specimen as figure 7.

14 Closeup muscle scars, same specimen as figure 10.

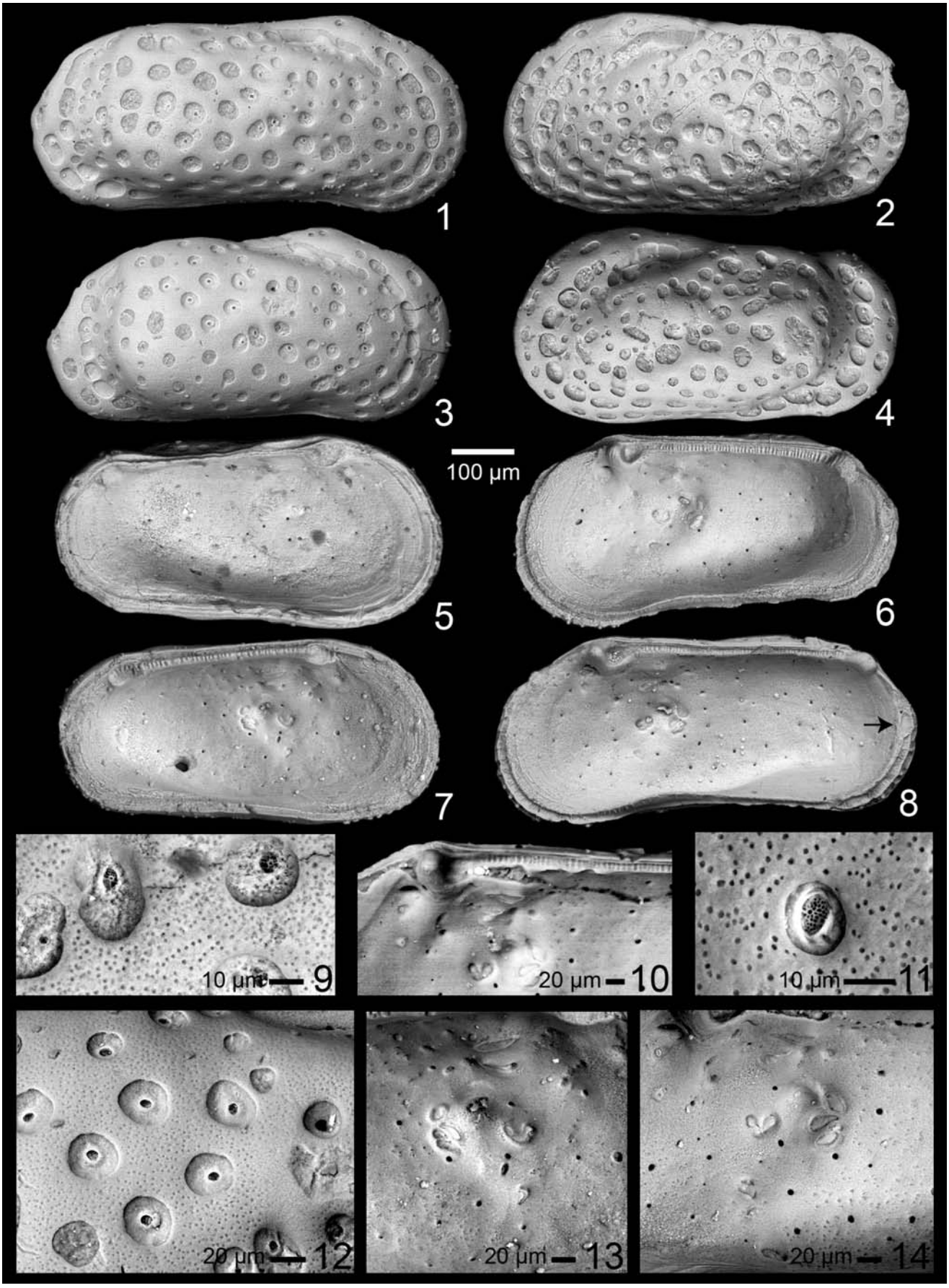
1
2
3
4
100 µm
5
6
7
8
10 µm
9
20 µm
10
10 µm
11
20 µm
12
20 µm
13
20 µm
14

sippi-Alabama area. *Transactions of the Gulf Coast Association of Geological Societies,* 44: 377–384.

———, 1995b. Upper Cretaceous sequence stratigraphy of the Mississippi-Alabama area. *Transactions of the Gulf Coast Association of Geological Societies,* 45: 377–384.

MASOLI, M., 1965. Sur quelques ostracodes fossiles Mésozoiques (Crétacé) du Bassin Côtier de Tarfaya (Maroc méridional). *Bulletin du Bureau de recherches géologiques et minières, Memoire*, 32: 119–128.

MINARD, J. P., SOHL, N. F. and OWENS, J. P., 1976. Re-introduction of the Severn Formation (Upper Cretaceous) to replace Monmouth Formation in Maryland. *U.S. Geological Survey Bulletin,* 1435-A: 132–133.

MOSHKOVITZ, S. and HABIB, D., 1993. Calcareous nannofossil and dinoflagellate stratigraphy of the Cretaceous-Tertiary boundary, Alabama and Georgia. *Micropaleontology,* 39: 167–191.

OKADA, Y., 1981. Development of cell arrangement in ostracod carapaces. *Paleobiology,* 7: 276–280.

———, 1982a. Ultrastructure and pattern of the carapace of *Bicornucythere bisanensis* (Ostracoda, Crustacea). In: Hanai, T. Ed. *Studies on Japanese Ostraoda.* Tokyo: University of Tokyo Press, 229–267.

———, 1982b. Structure and cuticle formation of the reticulated carapace of the ostracode *Bicornucythere bisanensis*. *Lethaia,* 15: 85–101.

OSBORNE, W. E., SZABO, M., COPELAND, C. W., JR. and NEATHERY, T. L., 1989. Geologic Map of Alabama. Tuscaloosa: Geological Survey of Alabama.

ÖZDIKMEN, H., 2010. Substitute names for three genera of Ostracoda (Crustacea). *Munis Entomology & Zoology,* 5: 315–316.

PEYPOUQUET, J.-P., DUCASSE, O., GAYET, J. and PRATVEIL, L., 1980. "Agradation et dégradation" des tests d'ostracodes. Intéret pour la connaissance de l'évolution paléohydrologique des domaines margino-littoraux carbonates. *Actes Réunion "Cristallisation-Déformation-Dissolution des carbonates*, 357–369.

PEYPOUQUET, J.-P., CARBONEL, P., DUCASSE, O., TÖLDERER-FARMER, M. and LÉTÉ, C., 1988. Environmentally cued polymorphism of ostracods. *Developments in Palaeontology and Stratigraphy,* 11: 1003–1019.

PITAKPAIVAN, K., 1994. *Ostracoda of the latest Cretaceous and earliest Tertiary of the Gulf Coastal Plain: biostratigraphy, paleoenvironments and systematics*. unpublished Ph.D. dissertation, Louisiana State University.

PLATE 16

Tumulocythereis priddyi (Smith 1978)

Specimens 1-10 at same scale, as indicated. Scale for figures 11-13 as indicated.

LV = left valve, RV = right valve

1 Exterior RV, male, specimen 130/135-16, sample 2011-8-4-1 (water level), Maastrichtian Owl Creek Formation, Tippah County, Mississippi.

2 Paratype (USNM PAL 255719), sex uncertain, sample 15A, Maastrichtian Prairie Bluff Formation, Lowndes County, Alabama.

3 Exterior RV, female, specimen 143-20, sample 2011-8-4-1 (water level), Maastrichtian Owl Creek Formation, Tippah County, Mississippi.

4 Exterior LV, male, specimen 104-11, sample 2011-5-18-1 (5'), Maastrichtian Owl Creek Formation, Tippah County, Mississippi.

5 Exterior RV, female, specimen 133/137-13, sample 2011-8-4-1 (water level), Maastrichtian Owl Creek Formation, Tippah County, Mississippi.

6 Exterior LV, female, specimen 133/137-6, sample 2011-8-4-1 (water level), Maastrichtian Owl Creek Formation, Tippah County, Mississippi.

7 Interior LV, male, specimen 143-12, sample 2011-8-4-1 (water level), Maastrichtian Owl Creek Formation, Tippah County, Mississippi.

8 Interior RV, male, specimen 145-16, sample 2011-8-4-1 (water level), Maastrichtian Owl Creek Formation, Tippah County, Mississippi. Arrow points to interruption of selvage at caudal region.

9 Interior LV, female, specimen 133/137-8, sample 2011-8-4-1 (water level), Maastrichtian Owl Creek Formation, Tippah County, Mississippi.

10 Interior RV, male, specimen 143-14, sample 2011-8-4-1 (water level), Maastrichtian Owl Creek Formation, Tippah County, Mississippi. Arrows point to upper and lower fusiform inverted platforms.

11 Closeup fossae, specimen 142-13, sample 2011-8-4-1 (water level), Maastrichtian Owl Creek Formation, Tippah County, Mississippi.

12 Closeup sieve pore, same specimen as figure 7.

13 Closeup muscle scars, specimen 103-15, sample 2011-5-18-1 (water level), Maastrichtian Owl Creek Formation, Tippah County, Mississippi.

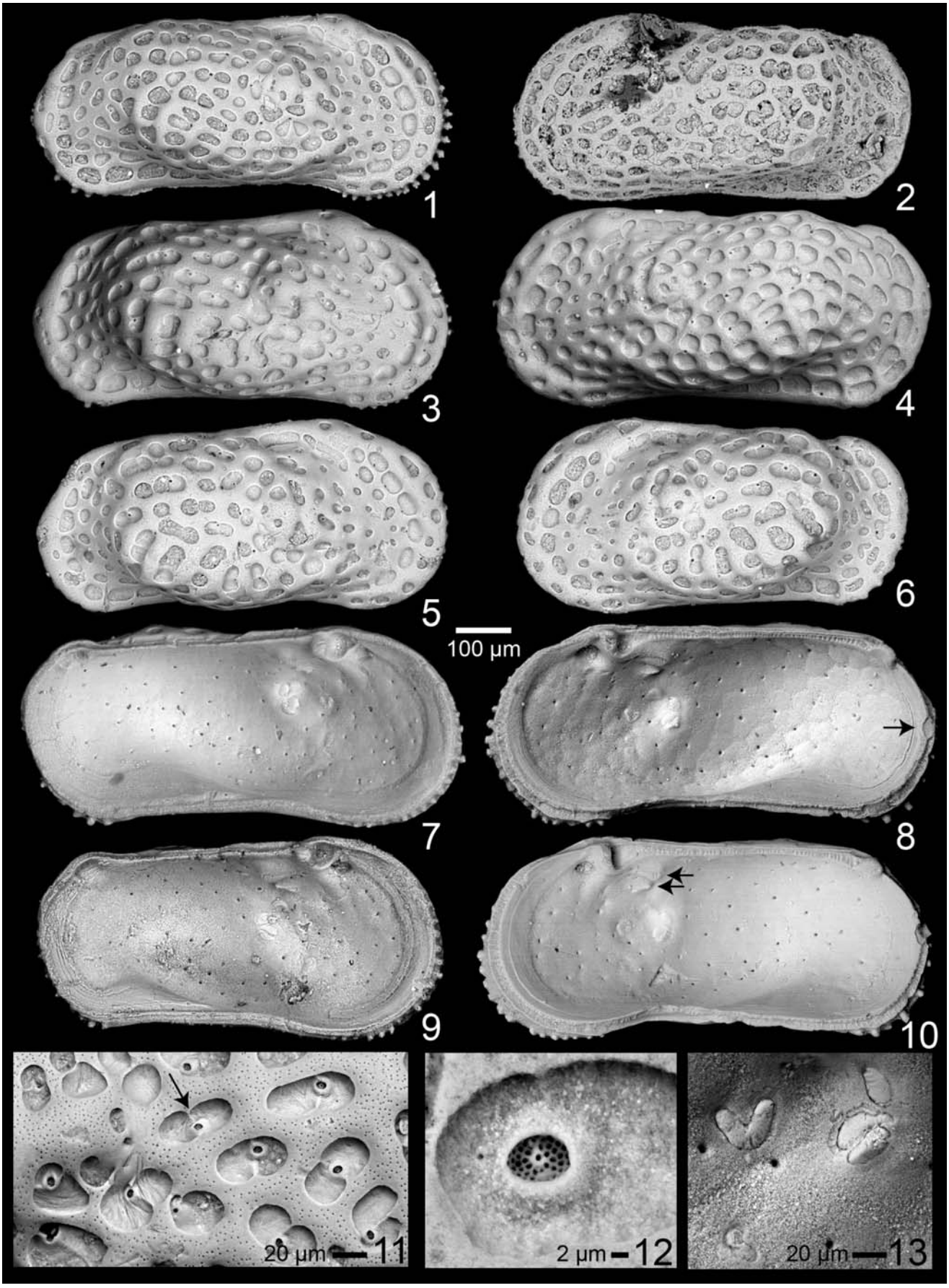
1
2
3
4
5
6
100 µm
7
8
9
10
20 µm
11
2 µm
12
20 µm
13

POKORNÝ, V., 1969a. The Genus *Radimella* Pokorný 1969 (Ostracoda, Crustacea). *Acta Universitatis Carolinae,* 4: 293–334.

———, 1969b. *Radimella*, gen. n.: a new genus of the Hemicytherinae (Ostracoda, Crustacea). *Acta Universitatis Carolinae,* 4: 359–373.

PUCKETT, T. M., 1992. Distribution of ostracodes in the Upper Cretaceous (late Santonian through middle Maastrichtian) of Alabama and Mississippi. *Transactions of the Gulf Coast Association of Geological Societies,* 42: 613–631.

———, 1994. Planktonic foraminiferal and ostracode biostratigraphy of upper Santonain through lower Maastrichtian strata in central Alabama. *Transactions of the Gulf Coast Association of Geological Societies,* 44: 585–595.

———, 1995a. Upper Cretaceous ostracode paleoecology, SE USA. In: Ríha, J. Ed. *Ostracoda and Biostratigraphy.* Rotterdam: A.A. Balkema, 141–151.

———, 1995b. Planktonic foraminiferal and ostracode biostratigraphy of lat Santonian through early Maastrichtian strata in Dallas County, Alabama. *Geological Survey of Alabama Bulletin,* 164: 1–59.

———, 1996. Ecologic atlas of Upper Cretaceous ostracodes of Alabama. *Geological Survey of Alabama Monograph,* 14: 1–176.

———, 2002. Systematics and paleobiogeography of brachycytherine Ostracoda. *Micropaleontology,* 48, supplement no. 2: 1–87.

———, 2005. Santonian-Maastrichtian planktonic foraminiferal and ostracode biostratigraphy of the northern Gulf Coastal Plain, USA. *Stratigraphy,* 2: 117–146.

———, 2009a. On the global distribution of Late Cretaceous ostracodes: the Genus *Bicornicythereis* (n. gen.), with notes on *Curfsina*. *Micropaleontology,* 55: 345–364.

———, 2009b. On the relationship between plate tectonics and phylogeny in ostracodes. *North American Micropaleontological Section—SEPM, Geologic Problem Solving with Microfossils II.* Houston: SEPM.

———, 2012. Paleogeographic significance of muscle scars in global populations of Late Cretaceous ostracodes. *Micropaleontology,* 58: 259–271.

———, 2013. Ostracodes and plate tectonics: a case from the latest Cretaceous of the Caribbean region. *North American Micropaleontological Section—SEPM, Geological Problem Solving with Mircofossils III.* Houston: SEPM.

PUCKETT, T. M. and MANCINI, E. A., 1998. Planktonic foraminiferal *Globotruncanita calcarata* total range zone: its significance and importance to chronostratigraphic correlation in the Gulf Coastal Plain, USA. *Journal of Foraminiferal Research,* 28: 124–134.

PUCKETT, T. M., COLIN, J.-P. and MITCHELL, S., 2012. New species and genera of Ostracoda from the Maastrichtian (Late Cretaceous) of Jamaica. *Micropaleontology,* 58: 397–455.

PUCKETT, T. M., ANDREU, B. and COLIN, J.-P., 2016. The evolution of the Brachycytheride Ostracoda in the context of the breakup of Pangea. *Revue de Micropaléontologie,* 59: 97–167.

PURI, H. S., 1953. The ostracode genus *Hemicythere* and its allies. *Journal of the Washington Academy of Sciences,* 43: 169–179.

PLATE 17

Tumulocythereis tiberti n. sp.
Specimens 1-7 at same scale, as indicated. Scale for figures 8-11 as indicated.
All specimens collected from the type locality of the Maastrichtian Owl Creek Formation, Tippah County, Mississippi.
LV = left valve, RV = right valve

1 Exterior RV, female, specimen 130/135-13, sample 2011-5-18-1 (water level).

2 Exterior LV, male, specimen 130/135-14, sample 2011-5-18-1 (water level).

3 Holotype (USNM PAL 771814), exterior RV, female, specimen 130/135-18, sample 2011-5-18-1 (water level).

4 Exterior LV, presumed female, specimen 103-13, sample 2011-5-8-1 (water level).

5 Interior LV, female, specimen 142-2, sample 2011-8-4-1 (water level).

6 Interior RV, female, specimen 150-6, sample 2011-8-4-1 (water level).

7 Interior LV, presumed male, specimen 130-12, sample 2011-5-18-1 (water level).

8 Closeup muscle scars, external view, same specimen as figure 1.

9 Closeup of muscle scars, LV, specimen 142-1, sample 2011-8-4-1 (water level). Arrows point to fusiform inverted platforms.

10 Closeup of sieve pore and punctation, specimen 130/135-9, sample 2011-5-8-1 (water level).

11 Closeup external ornamentation, specimen 151-6, sample 2011-8-4-1 (water level).

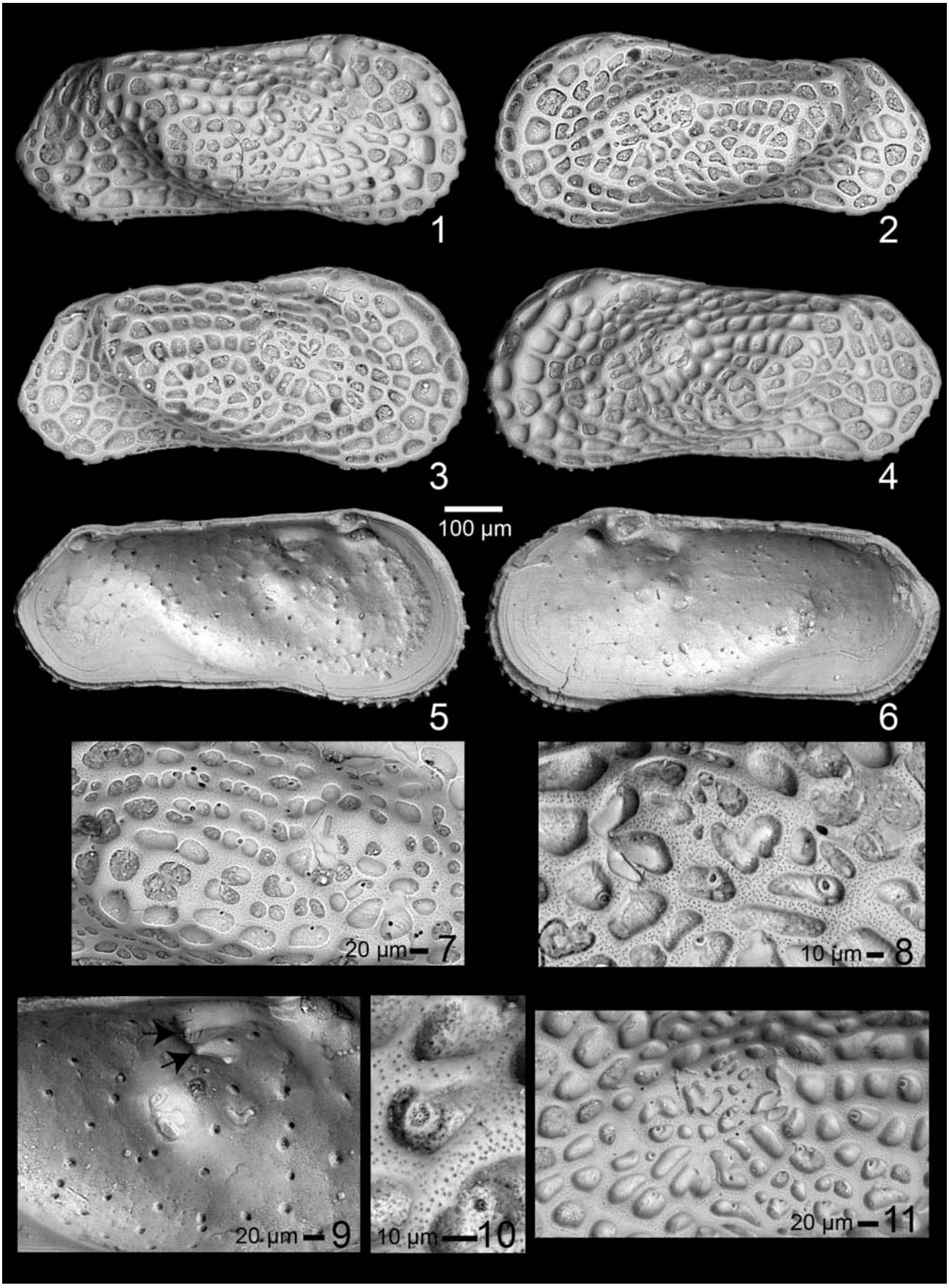
1
2
3
4
100 µm
5
6
20 µm
7
10 µm
8
20 µm
9
10 µm
10
20 µm
11

PURI, H. S. and DICKAU, B. E., 1969. Use of normal pores in taxonomy of Ostracoda. *Transactions of the Gulf Coast Association of Geological Societies,* 29: 353–367.

REYMENT, R. A., 1980. Biogeography of the Saharan Cretaceous and Paleocene epicontinental transgressions. *Cretaceous Research,* 1: 299–327.

REYMENT, R. A. and REYMENT, E. R., 1980. The Palaeocene trans-Saharan transgression and its ostracod fauna. In: Salem, M. J. and Busrewil, M. T. Eds. *The Geology of Libya.* London: Academic Press, 245–254.

ROHLF, F. J., 2013. tpsDIG. 2.17 ed. SUNY Stoneybrook.

RUSSELL, E. E. and PARKS, W. S., 1975. Stratigraphy of the outcropping Upper Cretaceous, Paleocene, and Lower Eocene in western Tennessee including description of younger fluvial deposits. *Tennesse Geological Survey Bulletin*, 76: 1–111.

SAMES, B., WHATLEY, R. and SCHUDACK, M., 2010. *Praecypridea*: A new non-marine ostracod genus from the Jurassic and Early Cretaceous of Europe, North and South America, and Africa. *Journal of Micropalaeontology,* 29: 163–176.

SARS, G. O., 1866. Oversigt af Norges marine Ostracoder. *Forhandlinger i Videnskabs-Selskabet,* 1965, 1–130.

SCHALLREUTER, R. E. L., 1977. On *Miehlkella cribroporata* Schallreuter gen. et sp. nov. *A Stereo-Atlas of Ostracod Shells,* 4: 9–16.

SEELING, J., COLIN, J.-P. and FAUTH, G., 2004. Global Campanian (Upper Cretaceous) ostracod paleobiogeography. *Palaeogeography, Palaeoclimatology, Palaeoecology,* 213: 379–398.

SHAHIN, A., 2005. Maastrichtian to middle Eocene ostracodes from Sinai, Egypt: systematics, biostratigraphy and paleobiogeography. *Revue de Paléobiologie,* 24: 749–779.

SKOGSBERG, K. J. T., 1928. Studies on marine ostracods. Part 2. External morphology of the genus *Cythereis* with descriptions of twenty-one new species. *Occasional Papers California Academy of Science,* 15: 1–155.

SLIPPER, I., 2019. Ostracoda from the Turonian of South-East England. Part 1. *Monographs of the Palaeontographical Society,* 655: 1–75.

———, 2021. Ostracoda from the Turonian of South-East England Part 2. Cytherocopina. *Monographs of the Palaeontological Society,* 657: 47–168.

SMITH, J. K., 1978. Ostracoda of the Prairie Bluff Chalk, Upper Cretaceous (Maestrichtian) and the Pine Barren Member of the Clayton Formation, lower Paleocene (Danian) from exposures along Alabama State Highway 263 in Lowndes County, Alabama. *Transactions of the Gulf Coast Association of Geological Societies,* 28: 539–580.

SUGARMAN, P. J., MILLER, K. G., BUKRY, D. and FEIGENON, M. D., 1995. Uppermost Campanian-Maastrichtian strontium isotopic, biostratigraphic, and sequence stratigraphic framework of the New

---

PLATE 18

Tumulocythereis tumulus n. sp.
Specimens 1-8 at same scale, as indicated. Scale for figures 9-14 as indicated.
All specimens collected from sample 2011-5-18-1 (water level), Maastrichtian Owl Creek Formation
LV = left valve, RV = right valve

1 Holotype (USNM PAL 771815), exterior RV, female, specimen 143-6.

2 Exterior LV, male, specimen 143-11.

3 Exterior RV, presumed male, specimen 103-14.

4 Paratype (USNM PAL 771816), exterior LV, presumed male, specimen 143-7.

5 Interior LV, same specimen as figure 2.

6 Interior RV, female, specimen 143-4. Arrow points to interruption of selvage at caudal region.

7 Interior LV, male, specimen 143-2.

8 Interior RV, female, specimen 143-13.

9 Closeup sieve pore, specimen 143-10.

10 Closeup fossae, same specimen as figure 4. Arrow points to apophysis extending across fossa.

11 Closeup fossae and punctation, specimen 143-17. Note caperate solum (arrow), undercut muri, and apophyses connecting invaginations of muri to puckered sieve-type normal pore canals (upper left of image).

12 Closeup hinge and inverted platform, same specimen as figure 8. Note two fusiform inverted platforms (arrows).

13 Closeup muscle scars LV, specimen 143-1, sample 2011-5-18-1.

14 Closeup fossae and punctation, same specimen as figure 1. Note apophysis extending into fossa (arrow).

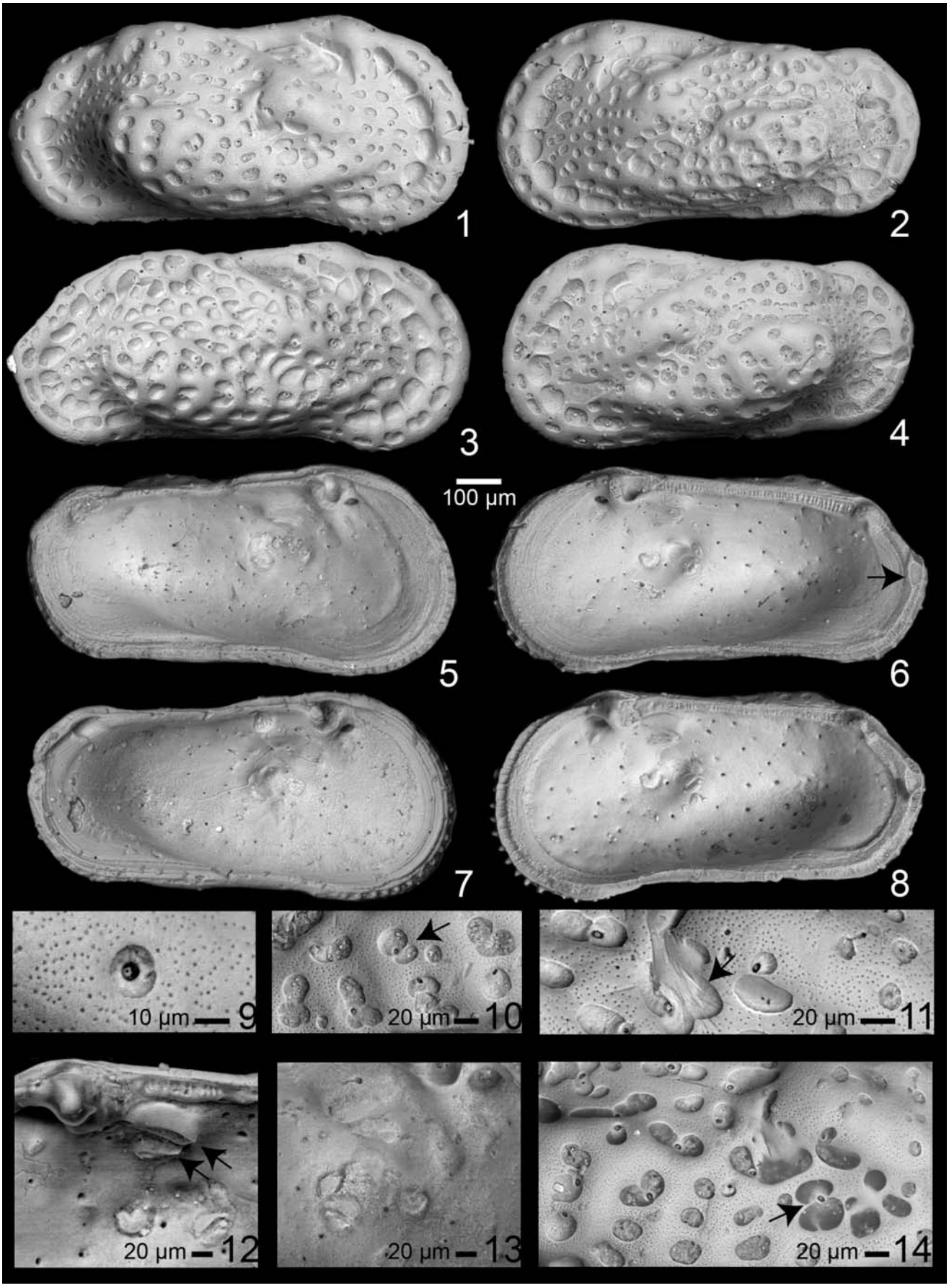
1
2
3
4
100 µm
5
6
7
8
10 µm
9
20 µm
10
20 µm
11
20 µm
12
20 µm
13
20 µm
14

Jersey coastal plain. *Geological Society of America Bulletin,* 107: 19–37.

SWAIN, F. M., unpublished. *Biostratigraphy of Cretaceous Ostracoda from wells in South Carolina* [Online]. Available: http://www.geo.umn.edu/people/profs/swain/ostra_scarolina.pdf [Accessed 2 July 2008].

SYLVESTER-BRADLEY, P. C., 1948. The ostracode genus *Cythereis*. *Journal of Paleontology,* 22: 792–797.

SYLVESTER-BRADLEY, P. C. and BENSON, R. H., 1971. Terminology for surface features in ornate ostracodes. *Lethaia,* 4: 249–286.

THOMPSON, D. E., 2011. Geologic Map of Mississippi. Jackson, MS: Mississippi Department of Environmental Quality.

TRIEBEL, E., 1940. Die Ostracoden der deutschen Kreide. III. Cytherideinae und Cytherinae aus der Unteren Kreide. *Senckenbergiana,* 22: 160–227.

TSUKAGOSHI, A., 1990. Ontogenetic change of distributional patterns of pore systems in *Cythere* species and its phylogenetic significance. *Lethaia,* 23: 225–241.

TSUKAGOSHI, A. and IKEYA, N., 1987. The ostracod genus *Cythere* O. F. Müller, 1785 and its species. *Transactions and Proceedings of the Palaeontological Society of Japan,* 148: 197–222.

VAN DEN BOLD, W. A., 1946. *Contribution to the Study of Ostracoda, with special reference to the Tertiary and Cretaceous microfauna of the Caribbean region,* Amsterdam: J. H. DeBussy.

———, 1964. Ostracoden aus der Oberkreide von Abu Rawash, Ägypten. *Palaeontographica Abteilung, Stuttgart,* 123: 111–136.

VAN MORKHOVEN, F. P. C. M., 1963. *Post-Paleozoic Ostracoda,* Amsterdam: Elsevier Publishing Company, 1–478.

VAN NIEUWENHUISE, D. and KAMES, W. H., 1976. Lithology and ostracode assemblages of the Peedee Formation at Burches Ferry, South Carolina. *South Carolina Division of Geology, Geologic Note,* 20: 73–87.

VAN VEEN, J. E., 1936. Die Cytheridae der Maastrichter Tuffkreide und der Kunrader Korallenkalkes von süd-Limburg. IV. Die gattungen *Cythereis, Archicythereis* und *Cytherideis*. *Natuurjistorisch Maandblad, Jaargang,* 25: 131–168.

WANG, D., VANNIER, J., YANG, X.-G., SUN, J., SUN, Y.-F., HAO, W.-J., TANG, Q.-Q., LIU, P. and HAN, J., 2020. Cuticular pattern replicates the pattern of epidermal cells in lowermost Cambrian scalidophoran worms. *Proceedings of the Royal Society B,* 287: 20200470.

APPENDIX 1
Sample localities.

Coon Creek Fm										
StationNumber	SampleID	Section	Tnship	Range	County	State	Quad	lat	long	Comments
2011-8-15-1	11-8-15-1 (15)	C. E/2 sec. 7	04S	04E	McNairy	TN	Ripley	35° 20' 04"	88° 25' 50"	Coon Creek type locality approximately 4.4 mile WSW of Milledgeville, TN, on west-facing bluff on Coon Creek. Sample collected approximately 15 ft above water level (very shallow).
2010-10-22-1	10-10-22-1 (505)	NW1/4 sec. 16	08S	04E	Union	MS	Sherman	34° 25' 32"	88° 53' 01"	"Blue Springs" section about 5 miles ENE of Tupelo. Section is large exposure about 1/4 mile NW of intersection of MS HWY 178 and HWY 9. Sample collected at elevation approximately 505 a.m.s.l.
Owl Creek Formation										
StationNumber	SampleID	Section	Tnship	Range	County	State	Quad	lat	long	Comments
94-5-11-7	94-5-11-7a	C. E/2 sec. 7	04S	04E	Tippah	MS	Ripley	34° 44' 53"	88° 54' 42"	Owl Creek type locality; sample collected from water level in lower part of section.
94-5-11-7	94-5-11-7 (18' below shell bed)	C. E/2 sec. 7	04S	04E	Tippah	MS	Ripley	34° 44' 53"	88° 54' 42"	Owl Creek type locality; sample collected 18 feet below shell bed in Owl Creek Formation.
2011-5-18-1	11-5-18-1 (water level)	C. E/2 sec. 7 C. E/2 sec.	04S	04E	Tippah	MS	Ripley	34° 44' 53"	88° 54' 42"	Owl Creek type locality; sample collected from water level in lower part of section.
2011-5-18-1	11-5-18-1 (5 ft)	C. E/2 sec. 7	04S	04E	Tippah	MS	Ripley	34° 44' 53"	88° 54' 42"	Owl Creek type locality; sample collected from 5 ft above water level in lower part of section.
2011-5-18-1	11-5-18-1 (15 ft)	C. E/2 sec. 7	04S	04E	Tippah	MS	Ripley	34° 44' 53"	88° 54' 42"	Owl Creek type locality; sample collected from 15 ft above water level in lower part of section.
2011-8-4-1	11-8-4-1 (water level)	C. E/2 sec. 7	04S	04E	Tippah	MS	Ripley	34° 44' 53"	88° 54' 42"	Owl Creek type locality. Sample collected from water level at main section.
Prairie Bluff Formation										
StationNumber	SampleID	Section	Tnship	Range	County	State	Quad	lat	long	Comments
94-8-12-4	94-8-12-4b	SW 1/4 sec. 15	13E	12N	Lowndes	AL	Braggs	32° 00' 37"	86° 45' 20"	Sample collected about 24 feet above road surface.
Providence Sand										
StationNumber	SampleID	Section	Tnship	Range	County	State	Quad	lat	long	Comments
91-8-14-1	91-8-14-1	NW 1/4 sec. 25	01N	23E	Bullock	AL	Perote	31° 54' 07"	85° 42' 08"	Sample collected from road cut on east side of Alabama Highway 29, approximately 1200 feet south of bridge over Double Creek, near base of hill, approximately 20 feet above elevation of bridge. Elevation of bottom of section 365 ft. a.m.s.l.

APPENDIX 1
Sample localities, continued.

2012-01-03-1	2012-01-03-1 (1)	SE 1/4 SE 1/4 sec. 15	10N	28E	Barbour	AL	Eufaula South	31° 50' 26"	85° 13' 16"	Same section as 14-5-28-1, collected on north-facing bank of Cheneyhatchee Creek.
2014-5-28-1	2014-5-28-1 (1)	SE 1/4 SE 1/4 sec. 15	10N	28E	Barbour	AL	Eufaula South	31° 50' 26"	85° 13' 16"	Same section as 12-01-03-1. Elevation of bottom of section 195 ft. a.m.s.l.
Ripley Formation										
StationNumber	SampleID	Section	Tnship	Range	County	State	Quad	lat	long	Comments
91-8-15-7	91-8-15-7	NC 1/2 sec. 26	13N	12E	Lowndes	AL	Braggs	32° 04' 34"	86° 49' 48"	Sample collected directly under bridge over Dry Cedar Creek approximately 2 feet above bottom of creek at ~ 168 ft. a.m.s.l., in lower Ripley Formation.
2019-6-20-1	2019-6-20-1 (180)	S.C. NE/4 sec. 25	13N	13E	Lowndes	AL	Braggs	32° 04' 20"	86° 48' 44"	Upper part of Ripley Fm. ~25-30 ft section, but could only reach 15 ft for samples. Elevation of bottom of section approximately 175 ft a.m.s.l. Sample collected from 180 ft a.m.s.l.
2019-6-20-1	2019-6-20-1 (185)	S.C. NE/4 sec. 25	13N	13E	Lowndes	AL	Braggs	3°2 04' 20"	86° 48' 44"	Upper part of Ripley Fm.. ~25-30 ft section, but could only reach 15 ft for samples. Elevation of bottom of section approximately 175 ft amsl. Sample collected from 185 ft a.m.s.l.
2019-6-20-1	2019-6-20-1 (190)	S.C. NE/4 sec. 25	13N	13E	Lowndes	AL	Braggs	32° 04' 20"	86° 48' 44"	Upper part of Ripley Fm. ~25-30 ft section, but could only reach 15 ft for samples. Elevation of bottom of section approximately 175 ft amsl. Sample collected from 190 ft a.m.s.l.

pore at the bottom (Pl. 13, fig. 10; Pl. 14, fig. 9; Pl. 15, figs. 9 and 11; Pl. 16, fig. 12). The doughnut-shaped second layer is the solum of the taxa with large fossae (that is, the floor of the fossae). Others are the Type C sieve-type NPC (Pl. 7, fig. 9; Pl. 8, fig. 7; Pl. 9, fig. 11).

To determine if the sieve-type NPCs are homologous among the different species in the anticytherideinines, they were mapped, where possible, based on the availability of both inner and outer views of the same specimen (text-figure 7). This was done because, in some specimens, some of the pores were either obscured by debris, they appeared to be present in inner view but not the outer (some sieve pores were apparently obscured by tegmen, that is, an overgrowth of calcite), or the ornamentation obscured the view from the exterior. To do this, the inner view was flipped horizontally and rotated and resized until a good visual match to the external image of the same was achieved. In some specimens, either the interior or exterior of the same specimens was obscured by debris, and thus different specimens were used. The NPC on species that are smooth (*Laevipella cythereis*) were easily visible in exterior view and an inner view was not necessary.

Dorsal Inverted Platform

One of the distinctive characters of the Subfamily Anticytherideinae is the pair of inverted platform structures that are located just ventral and posterior to the anterior hinge elements, in both the LV and RV (Pl. 7, figs. 7 and 8; Pl. 12, figs. 8 and 8; Pl. 13, fig. 8; Pl. 14, figs. 7 and 8; Pl. 15, fig. 10; Pl. 17, figs. 5-7; Pl. 18, figs. 5-8, 12). This structure corresponds to the inner part of the post-ocular sulcus. There are two parallel structures, one below the other; this secondary structure (th lower one) may be almost as large as the upper one (Pl. 18, fig. 12), whereas in most species, the secondary structure is smaller than the upper and is teardrop-shaped or shaped like the Nike™ logo (Pl. 5, fig. 10; Pl. 7, fig. 7; Pl. 11, fig. 6; Pl. 12, fig. 11; Pl. 14, fig. 8; Pl. 15, fig. 13; Pl. 16, figs. 8-10; Pl. 17, fig. 9; Pl. 18, fig. 12). The larger, upper structure is more acuminate anteriorly and the lower, smaller one is more acuminate posteriorly. Well-preserved specimens show that the lower platform surfaces of both structures are rimmed, whereas the center is recessed (Pl. 7, fig. 7; Pl. 12, fig. 11; Pl. 15, figs. 10 and 13; Pl. 17, fig. 9; Pl. 18, fig. 12). It appears that the stresses applied to this structure during calcification pulled the outer carapace inwards, forming the postocular sulcus.

Sexual Dimorphism

Sexual differences in valve dimensions were investigated following the procedures used by Hunt et al. (2017), who documented sexual dimorphism among cytheroid ostracod species of the Late Cretaceous coastal plain. Valve outlines of all specimens figured herein were digitized using the software TPSDig (Rohlf 2013). Valve size was measured as the area enclosed by the outline, and valve shape (elongation) was measured as the ratio of the major to minor axes of the ellipse that best fit the outline. Both variables were log-transformed prior to plotting. In most cytheroid taxa, the left valve slightly overlaps the right, resulting in right valves that are somewhat smaller and more elongate than left valves. This left-right difference was corrected for by applying the average left-right offset of anticytherideinine species estimated by Hunt et al. (2017). This practice modified right valve measurements by adding 0.076 to log size and subtracting 0.057 from log shape, thus converting them to left-valve equivalents.

Sample sizes of the figured species are generally too low (n = 10) for statistical analysis, and separation between sexes was sometimes ambiguous. The survey of sexual dimorphism in the broader fauna (Hunt et al. 2017) included analysis of several large populations attributable to the species studied herein. When possible, the statistically supported male and female clusters from that study are included here as text-figures to help guide the identification of sexes in the present work.

Muscle Scars

One of the most distinctive characters (synapomorphy) of the new Subfamily Anticytherideinae is the muscle scars pattern, particularly the adductor muscle scars. Terminology for the scars is presented in text-figure 8 and a comparison of the muscle scar patterns of species collected during this study is presented on Plate 3. The single U- or V-shaped frontal scars are typical of the Trachyleberididae (Hazel 1967) and are, in fact, a defining character of the family. The mandibular and dorsal scars are also typical of that family, but the adductor scars are distinctive to the new subfamily. The A-1 scar is elongate in a dorsoanterior-ventroposterior direction and is separated dorsally and slightly posteriorly from the other adductor scars. The A-2, A-3 and A-4 scars are herein described as being similar to a yin and yang symbol, with the A-2 adductor that is bulbous anteriorly, but tapers and curves posteriorly over the lower two adductors; an elongate A-4 scar that is tilted slightly dorsoposteriorly, and a small A-3 scars that is sandwiched between the posterior ends of the A-2 and A-4 scars. These "yin and yang" adductor scars have an overall circular shape.

TAXONOMY

Conventions

The species descriptions in the following section use the following abbreviations and symbols: LV = left valve, RV = right valve, USNM PAL = U. S. National Museum (Smithsonian Institution) Paleobiology Collections, AMNH = American Museum of Natural History. The terminology for the muscle scar patterns is presented in text-figure 8.

The descriptions include terms that may not be familiar to all ostracod specialists, particularly if they do not work with trachyleberids, so some of them are defined below. These terms are described in Kesling (1951), Benson et al. (1961), Sylvester-Bradley and Benson (1971), Horne et al. (2002) and Sames et al. (2010).

Apophysis. An offshoot of the murus leading to a rimmed pore canal.

Caperation. Fine wrinkles on carapace surface. In the present context, most caperation is located in the soli of the fossae.

Celation, *sensu* Sylvester-Bradley and Benson (1971). Development of an outer layer of calcite (tegmen) that overlaps and obscures underlying ornament. Peypouquet et al. (1980) and Peypouquet et al. (1988) used the terms aggradation and degradation to refer to the addition or removal, respectively, of calcite from ostracod carapaces as a phenotypic response to environmental cues, particularly in response to the saturation of calcium carbonate. In the present context, however, no correlation between specific environmental parameters and the degree of calcification is implied, and thus the term celation is applied.

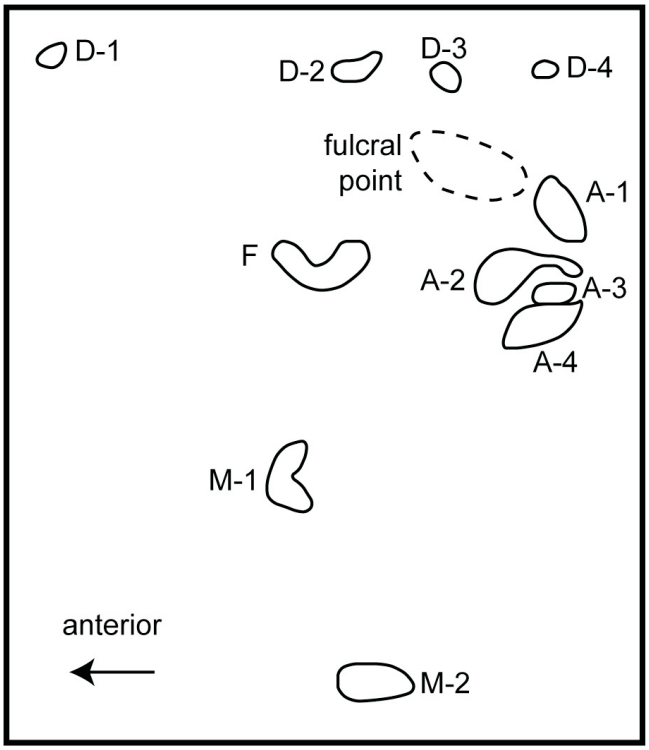

TEXT-FIGURE 8
Terminology for muscle scars on the inside of the ostracod carapace. D = dorsal, A = adductor, F = frontal, M = mandibular. Drawing based on *Frodocythereis frodoi* n. sp., specimen 132-8 (for closeup see Pl. 12, fig. 10).

Equicurvate. Curvature of the anterior or posterior margin in which the greatest extent is at mid-height.

Fossa (plural **fossae**). Single subovate or sub-polygonal mesh of a reticulum.

Foveola (plural **foveolae**). Minute pits in the surface layer of the carapace an order smaller than puncta and fossae.

Fulcral point (or notch). A depression or upraised point where the mandible pivots, which typically overlies the central muscle scar field.

Infracurvate. Curvature of the anterior or posterior margin in which the greatest curvature is below mid-height.

Murus (plural **muri**). The wall of a fossa in a reticulum.

Solum (plural **soli**). The floor of a fossa in a reticulum.

Stragulum (plural **stragula**). Guber and Jaanusson (1964) proposed this term, or stragular process, to refer to a dorsal flap-like overlap of one valve over the other at the cardinal corners (point at which the dorsal margin curves down to the anterior or posterior margin). Guber and Jaanusson proposed the term while studying Ordovician kloedenellid ostracods. The term is not used herein to describe and elevation of the LV above the RV at the terminal hinge elements, but the carapace of the LV does extend across the RV as they do in the Ordovician taxa.

Supracurvate. Curvature of the anterior or posterior margin in which the greatest curvature is above mid-height.

Tegmen. The secondary layer of calcite produced by celation.

Class OSTRACODA Latreille 1802
Subclass PODOCOPA Sars 1866
Order PODOCOPIDA Sars 1866
Suborder CYTHEROCOPINA Baird 1850
Superfamily CYTHEROIDEA Baird 1850
Family TRACHYLEBERIDIDAE Sylvester-Bradley 1948
Subfamily ANTICYTHERIDEINAE n. subfamily

Type Genus: ***Anticythereis*** van den Bold 1946
Diagnosis: Genera of the Subfamily Anticytherideinae are characterized by a combination of traits that include large, scattered sieve-type normal pore canals with raised rims (Pl. 6, fig. 10; Pl. 4, fig. 9; Pl. 13, fig. 10; Pl. 14, fig. 9; Pl. 15, fig. 12; Pl. 16, fig. 12); a highly sculpted exterior carapace that consists of subrounded or polygonal fossae or a layer of tegmen that obscures ornamentation; a muscle scar pattern with A-2, A-3 and A-4 scars intertwined in a yin-yang symbol with an overall circular shape (Pl. 3); an A-1 scar detached dorsally from others, elliptical and tilted dorsoanteriorly; a post-ocular depression that extends from the dorsal margin to below the ocular sinus; a paramphidont hinge, in RV with a stepped, multilobed anterior tooth and a large, elongate, arcuate posterior tooth tilted diagonally across the dorsoposterior angle (Pl. 8, fig. 10; Pl. 7, fig. 6; Pl. 10, fig. 6; Pl. 15, fig. 10; Pl. 18, fig. 12); complementary sockets in LV; and a pair of inverted, fusiform platforms located anteromedially (arrows point to these structure on Pl. 7, fig. 7; Pl. 13, fig. 6; Pl. 16, fig. 10; Pl. 17, fig. 9; and Pl. 18, fig. 12). A double ogee-shaped structure occurs as an interruption of the selvage at the posterior caudal angle of the RV, with no corresponding structure in the LV (Pl. 7, fig. 8; Pl. 11, fig. 6; Pl. 12, fig. 8; Pl. 13, fig. 6; Pl. 14, fig. 8; Pl. 16, fig. 8; Pl. 18, figs. 6 and 8).

Remarks: This subfamily is restricted to the late Campanian-Maastrichtian of the North American Atlantic and eastern Gulf coastal plains. The following genera are assigned to the new subfamily:

Anticythereis van den Bold, 1946, type species *Anticythereis reticulata* (Jennings 1936)

Asculdoracythereis n. gen., type species *Asculdoracythereis asculdora* n. sp. (Pl. 8)

Frodocythereis n. gen., type species *Frodocythereis frodoi* n. sp. (Pl. 12)

Laevipellacythereis n. gen., type species *Laevipellacythereis laevipellis* n. sp. (Pl. 14)

Tumulocythereis n. gen., type species *Tumulocythereis tumulus* n. sp. (Pl. 18)

Discussions of species' assignments to genera follow the generic descriptions.

Genus ***Anticythereis*** van den Bold 1946

Type Species: *Anticythereis reticulata* (Jennings 1936) (holotype: AMNH-FI 37780A, paratype: AMNH-FI 37780B) (Pl. 4, figs. 1-3; text-fig. 9)

Velarocythere BROWN 1957, p. 20-21, type species *Velarocythere scuffletonensis* Brown 1957 (holotype: USNM PAL 129009, paratypes: USNM PAL 129006, 129007, 129008, 129010).

Amended Diagnosis: Genus of Subfamily Anticytherideinae characterized by a prominent murus that forms a dorsal hump in outline at mid-length that extends above the hinge line, then bends ventroanteriorly behind the post-ocular depression, forming a steep bordering murus. The posterior margin has a distinct marginal carina and is supracurvate in LV and infracurvate in RV.

Remarks: Jennings (1936) named and described a new species he designated as *Pseudocythereis reticulata* that was collected from the Mt. Laurel and Navesink Formations of New Jersey. Biostratigraphic data, including ammonoids, *Exogyra* oysters, calcareous nannoplankton, planktonic foraminifera, and strontium isotopic data indicate that the Mt. Laurel Formation is late Campanian in age and is unconformably overlain by the early Maastrichtian Navesink Formation (Sugarman et al. 1995). Kennedy et al. (2000) observed a Maastrichtian guide fossil, the ammonite *Pachydiscus (Pachydiscus) neubergicus* (Hauer 1858), in a phosphatic bed at the base of the Navesink Formation, indicating an earliest Maastrichtian age. Gamma ray data and field observations indicate that the fossiliferous and quartzose Mt. Laurel Formation represents a highstand systems tract, whereas the finer-grained and fossiliferous Navesink Formation represents a transgressive systems tract. This sequence stratigraphic setting correlates well with the highstand systems tract of the Campanian UZAGC-4.0 depositional sequence and the transgressive systems tract and maximum flooding surface of the Maastrichtian UZAGC-5.0 depositional sequence on the eastern flank of the Mississippi Embayment of Mancini et al. (1996b), with some differences. In the Tennessee-Mississippi-Alabama area, the highstand systems tract of the UZAGC-4.0 sequence continues from the marine Coon Creek Formation into nonmarine sands of the McNairy Sand in northern Mississippi and Tennessee, whereas farther south in eastern Mississippi and central Alabama, the marine Bluffport Marl Member of the Demopolis Chalk grades up-section into the nonmarine Ripley Formation (text-fig. 1). The Mt. Laurel, in contrast, contains marine fossils and was interpreted as upper shoreface deposits, rather than nonmarine (Sugarman et al. 1995). The ill-defined Campanian/Maastrichtian stage boundary, then as today, was interpreted to occur within the time interval represented by the Mt. Laurel-Navesink unconformity. The name *Pseudocythereis* was already used by Skogsberg (1928), so van den Bold (1946) renamed the genus *Anticythereis*, although he did not discuss the genus further.

Brown (1957) named and described *Velarocythere* based on one of his new species, *V. scuffletonensis*, which is characterized generally by even reticulations and low muri. The type specimens of *V. scuffletonensis* have considerable adventitious material, which is why they are not published herein, but can be viewed at the U.S. National Museum Paleobiology Database at URL https://collections.nmnh.si.edu/search/paleo/. Brown stated that *Velarocythere* "shows some affinity to *Anticythereis* van den Bold (*Pseudocythereis* Jennings) but can be separated on the basis of size, hingement, and external shell characteristics," although these differences were not explained. A species Brown described as new (*Velarocythere eikonata*) is considered to be synonymous with Jennings' (1936) type species of *Pseudocythereis reticulata*, thus *Velarocythere* is a junior synonym of *Anticythereis*.

Species: Two new species from the present study are assigned to *Anticythereis*: *A. dorsennus* n. sp. and *A. slipperi* n. sp., in addition to the nominal species, *A. reticulata* (Jennings 1936).

Anticythereis reticulata (Jennings 1936)
Plate 4, figures 1 and 2; Text-fig. 9

Pseudocythereis reticulata JENNINGS 1936. p. 57-58, Pl. 7, figs. 10a-d.
Velarocythere eikonata BROWN 1957. p. 22, Pl. 5, figs. 10-12.– BROWN 1958, p. 64, Pl. 5, fig. 3.
NOT *Anticythereis reticulata* (Jennings 1936).– VAN NIEUWENHUISE 1976, Table 1, Pl. 4, fig. c (= *Frodocythereis* sp.).
Anticythereis reticulata (Jennings 1936).– VAN DEN BOLD, 1946, p. 30. Note: Van den Bold (1946) simply named the new genus *Anticythereis* to accommodate Jennings' species *Pseudocythereis reticulata*, noting that the name *Pseudocythereis* had been used by Skogsberg (1928). See more notes under description of genus.

Type Specimens: The holotype (AMNH-FI 37780A) is a RV broken at the ventroposterior margin, and the paratype (AMNH-FI 37780B) is a well-preserved LV (Pl. 4, figs. 1 and 2). For comparison, Brown's (1957) type specimen of *Velarocythere eikonata* (USNM PAL 129016, a LV) is presented on Pl. 4, fig. 3. This latter specimen has adventitious material on the dorsoanterior 2/3 of the specimen, obscuring morphological details. Nonetheless, the specimens of Brown and those of Jennings are close enough morphologically to consider them to be synonymous.

Diagnosis: None, but Jennings (1936) described the species.

Emended Diagnosis: Carapace characterized by a pair of diagonal costae that extend from a prominent stragulum to below mid-height, anterior of the eye tubercle and parallel to the anterior margin, which then turns sharply ventroposteriorly and becomes more subdued to the mid-posterior region, marking the outline of a prominent sagittal lateral swelling. A deep, elongate sulcus is subjacent to the eye tubercle, wedging anteriorly and down between the eye tubercle, the anterior compressed region, and the prominent anterior diagonal costa. Carapace ornamentation is formed by large, open, rounded fossae with single sieve-type normal pore canals punctuating the sola. Central, elongate, ventroanteriorly oriented sulcus is bordered by prominent lateral costae. Anterior and posterior margins are compressed; posterior margin is with single row of sub-rounded fossae without pits; anterior fossae are larger, sub-rectangular and with thin intervening muri and single sieve-type normal pore canals near the inner margin of the fossae.

Description: The carapace is robust, with the greatest height at the eye tubercles, and with a dorsal shoulder that lies just behind mid-length in outline, closer to the eye tubercle than to the dorsoposterior angle. The anterior and posterior margins are slightly infracurvate. The dorsal profile is sinuous, with a concavity between the greatest height above the eye tubercle to mid-shoulder, then is concave again between the mid-shoulder and dorsoposterior angle. The dorsoposterior angle of the LV is prominent; the angle in the RV is not as distinct and slopes posteriorly. Two rows of denticles are located very close to the anterior and posterior margins. The ventral silhouette is slightly undulatory, with a convexity corresponding to a lateral swelling slightly behind mid-length and is bordered anteriorly and posteriorly by gentle concavities.

The eye tubercles are not prominent, are smooth, and are bordered ventroposteriorly by an elongate, deep sulcus and

ventroanteriorly by a fossa. Circular fossae are located above and on either side of the eye tubercle.

The external ornamentation consists mainly of a combination of carinae, rounded fossae, and sieve-type normal pore canals that punctuate the sola (Pl. 4, fig. 2). Two parallel carinae extend from a prominent dorsal shoulder ventroanteriorly to directly behind the greatest anterior extent of the carapace, then turn ventroposteriorly and less prominently to parallel the ventral margin, in an overall sagittate form. Between these carinae is a sulcus. The region defined by the carinae is inflated relative to the compressed anterior and ventral margins. A smaller carina extends from the eye tubercle to merge with the posterior border of the anterior fossae. Below and posterior of the eye tubercle is a deep, elongate sulcus, the solum of which is punctuated by 1 or 2 pits. Behind the anterior rim is a row of large, sub-rectangular fossae separated by thin, radiating muri; the sola are caperate. Near the posterior margin of each solum is a single sieve-type normal pore canal. Similarly, the compressed area adjacent to the posterior rim has a row of slightly smaller and more rounded fossae that lack pore canals.

Sexually dimorphism was not assessed due to lack of a population to measure. The paratype specimen is plotted with specimens of *A. slipperi* on text-fig. 9.

Internally, the dentition is amphidont (unfortunately, the interior RV of the holotype is damaged and the anterior hinge elements are broken, and thus any grooves that are in paramphidont hinges cannot be observed; the corresponding socket on the LV on the paratype (Pl. 4, fig. 1) does not appear to be grooved). The anterior hinge element in the LV is a vertically elongate socket bordered anteriorly by a slight invagination, dorsally by an arched rim (stragulum), and posteriorly by the subjacent tooth, which is elongated and deflected ventroanteriorly. The median bar in the LV is narrow and straight, crenulate and slightly thicker anteriorly. The posterior socket is elongated ventroposteriorly at ca. 45°. The median groove in the RV is crenulate and very slightly arched and widens near the extremities. The posterior tooth is elongated and angled in the middle. The inner lamella is of uniform width along the anterior, ventral and posterior margins. Pores on the inner surface correspond to the internal openings of the sieve-type normal pore canals on the exterior. A pair of inverted, rimmed, fusiform platforms are located just below and behind the anterior hinge elements; in the LV of the paratype, these platforms are mostly obscured by crystals (arrow on Pl. 4, fig. 1); in the RV of the holotype, however, these platforms can be seen clearly (not illustrated here, but images are available from TMP).

The muscle scar field (Pl. 4, fig. 1) includes a U-shaped F scar that is located at the mid-height of the adductor scars and tilted slightly towards the anterior; there are four adductor scars: the A1 scar is large, ovate, separated dorsoanteriorly from the other adductor scars, and tilted at ca. 30° towards the anterior hinge element; the A-2, A3 and A4 scars are in an overall subcircular shape; the A2 scar is relatively large and is in the shape of boomerang; the A3 scar is small, subcircular, located mid-posteriorly in the adductor group and abuts the A-4 scar; and the A-4 is elongate, tapered on the ends, rises slightly posteriorly, and is with a concavity where it touches the A-3 scar. The mandibular scar is ventroanterior of the central muscle scars, and ovate. The dorsal scars could not be observed on the type specimens due to adventitious material.

Remarks: As Jennings (1936) offered only a brief description and it is the type species of the genus, the species is herein re-described.

This species is very similar to *Anticythereis dorsennus* n. sp. by the presence of a dorsal shoulder near mid-length but differs in being more rounded in lateral outline, by relatively narrower and shallower compressed zone just behind the anterior marginal carina, by the shallower postocular depression, by the less prominent ventroanteriorly oriented carina that extend from the mid-dorsum to behind the ventroanterior angle, and by the greater length of the posterior compressed zone.

Range: Jennings (1936) found his species in the earliest Maastrichtian Navesink Formation of New Jersey and Brown (1957) found *Velarocythere eikonata* in the Peedee Formation in Bladon, Lenoir and Pitt counties, North Carolina.

Anticythereis dorsennus Puckett and Hunt **n. sp.**
Plate 2, figure 8; Plate 3, figure 1; Plate 5, figures 1-11; Text-fig. 10

Etymology: dorsennus, Latin noun meaning humpback or hunchback, in reference to the prominent mid-dorsal hump-shaped carina.

Type Specimen: Holotype: USNM PAL 771796, specimen 132/136-13 (Pl. 5, figs. 2 and 7, male LV), sample 2011-5-18-1 (water level), Maastrichtian Owl Creek Formation, Tippah County, northern Mississippi; paratype: USNM PAL 771797, specimen 132/136-18 (Pl. 5, fig. 4, female LV), sample 2011-8-4-1 (water level), Maastrichtian Owl Creek Formation, Tippah County, Mississippi.

Diagnosis: This species is characterized by a combination of very coarse, deep reticulation; prominent postocular carina that parallels the dorsal margin at mid-length, borders the bottom of the postocular depression to just behind the anterior margin below mid-height, then turns to parallel the anterior and ventral margins, losing its distinction at about 1/3 length; and another very prominent anterior carina, which arises anterior to the eye tubercle, extends parallel to the postocular carina and terminates at the ventral margin. The postocular carina forms a distinctive hump or shoulder at the mid-dorsum in lateral silhouette.

Material: 157 valves

Measurements: Holotype L = 0.748 mm, H = 0.345 mm; paratype L = 0.750 mm, H = 0.369 mm

Description: The carapace is sub-rectangular in lateral outline, and very robust. The dorsal outline is humped, which is formed by the projection of the postocular carina above the hinge line, and curves up at eye tubercle and at the dorsoposterior angle, forming a stragulum; in the LV, the eye tubercle rises prominently above the dorsum, less so in the RV; the anterior margin is broadly curved and infracurvate; the ventral margin is nearly straight, slightly upturned at 1/3 length and is very slightly concave just anterior to the ventroposterior angle; the posterior margin in the LV is broadly and evenly rounded, and equicurvate; in the LV, the posterior margin is broadly rounded in ventral half, and slightly concave in dorsal half; the dorsoposterior angle is broad in the RV, but upraised in the LV.

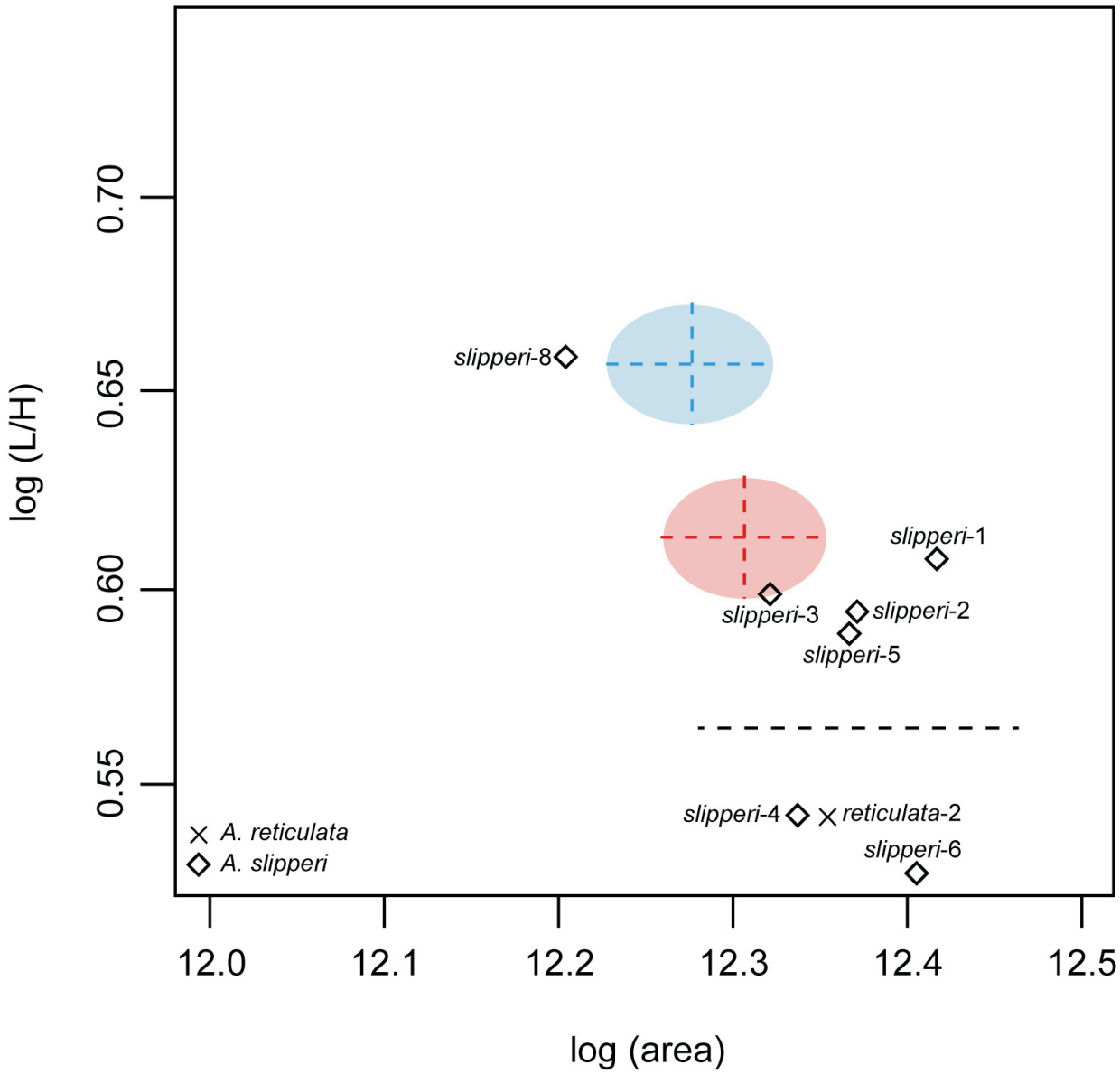

TEXT-FIGURE 9
Size (log area) versus shape (log[L/H]) for *Anticythereis reticulata* and *Anticythereis slipperi*. Dotted line indicates inferred separation between males and females for the specimens figured in this work.

A double row of denticles is located very close to the anterior and posterior margins. The outline in dorsal view is sagittate, with a very narrow marginal zone that steps up to the anterior marginal carina, then narrows slightly to form a bulging lateral outline; the carapace then broadens gently to the greatest width at approximately ¾ length, then tapers to the posterior margin, which is flat. The anterior and posterior marginal zones are compressed, with prominent marginal carinae.

The eye tubercles are distinct, yet do not bulge. The carapace is coarsely reticulate and carinate; a very prominent anterior marginal carina extends from the dorsoanterior angle to the ventroanterior angle, with a fossa on either side of the eye tubercle; a prominent, elongate postocular sulcus extends from the dorsal margin to just below the eye tubercle. Prominent carinae form an arrowhead that points ventroanteriorly; one carina extends ventroanteriorly from the mid-dorsum, where it forms the distinctive hump in outline, turns ventroposteriorly below mid-height, then fades into the venter; a second carina parallels the dorsal carina, begins not quite at the dorsal margin, and terminates at approximately mid-height; a row of sub-rounded to sub-quadrate fossae fills the area between the two carinae, with fossae becoming smaller anteriorly; an anterior carina is parallel and very close to the anterior margin; large, radially-oriented, sub-rectangular fossae are located behind the anterior carina, with intervening thin muri, and with a single rimmed sieve-type normal pore canal at the posterior end of the soli; several relatively small fossae are located between the large sub-rectangular anterior fossae and the prominent lateral carinae; the posterior margin is bordered closely by a ca-

rina, anterior of which are large, subquadrate fossae separated by low muri; a prominent murus extends a short distance ventrally from the eye tubercle. The fossae in the middle and posterior regions of the carapace are generally sub-rounded and become slightly smaller in the posterior region; the intervening muri are robust, with the margins of the fossae being vertical or undercut (Pl. 5, fig. 9); each fossa has a single rimmed sieve-type normal pore canal, which is usually off center. The soli typically are caperate, with radiating wrinkles (Pl. 5, fig. 9). Mural punctation is rare (Pl. 5, fig. 9).

The hinge is paramphidont; the denticulation in the RV (Pl. 5, figs. 6 and 8) includes an anterior, stepped, subtly grooved tooth, with a lower anterior part and an upper taller posterior tooth; a postjacent socket; a straight crenulated groove; and a posterior tooth that is blunt and angled. In the LV (Pl. 5, figs. 5 and 7), the anterior socket has a blunt protuberance at the anterior margin; the narrow subjacent tooth is angled ventroanteriorly, with an overlying low stragulum; the median bar is narrow, straight and crenulate; and the posterior socket, which is angled at ca. 45°, has an overlying stragulum. The selvage and inner margins are distinct, with a narrow vestibule in some specimens; the marginal zone is relatively wide; a double ogee-shaped interruption of the selvage is located at the caudal region (arrow on Pl. 5, fig. 6). Scattered large pits are the inner openings of the sieve-type normal pore canals. The ocular sinus is large and located below and slightly anterior of the anterior hinge element. A pair of rimmed, inverted fusiform platforms are located behind and below the anterior hinge elements that correspond to the interior of the post-ocular sulcus, and both are elongated parallel to the long axis of the carapace; the upper platform is larger and tapers anteriorly; the lower platform is tear-shaped and acuminate posteriorly (Pl. 5, figs. 5-8 and 10-11).

The muscle scars (Pl. 3, fig. 1; Pl. 5, figs. 10 and 11) include a U-shaped F scar; the A-1 is elongate dorsoanteriorly, points towards the anterior hinge elements, is acuminate dorsally, and is located above the posterior ends of the lower adductor scars; the A-2, A-3 and A-4 scars are intertwined in a pattern similar to a yin-yang symbol in an overall circular pattern; the A-2 scar is relatively large, paisley-shaped, and tapers posteriorly above the A-3 scar; the A-3 scar is small, circular, and seated above the posterior margin of the A-4 scar; the A-4 is of intermediate size, is elongate almost horizontally, and has a slight indention where it abuts the A-3 scar; the M-2 is close to the ventral margin, is very narrow and elongate horizontally, and becomes acuminate posteriorly; the M-1 is about half way between the anterior margin of the F scar and the M-2, and is small and nearly circular; there are several dorsal scars, with the D-1 scar being very small and situated well anterior of other scars; the D-2 scar is small and situated directly above the anterior margin of the F scar; a very small, circular D-3 is located directly above the anterior margin of the A-1 scar; and there is a very small, circular scar (D-4?) located farther dorsal of other scars and directly above the posterior margin of the A-1 scar. The fulcral point is arched and situated slightly dorsoanterior of the A-1 scar.

The species is sexually dimorphic, with the male (Pl. 5, fig. 2) being more elongate and the female being more rounded (text-fig. 10). The carapace in the male are not as inflated as the female, with a slightly deeper mid-lateral sulcus.

Remarks: This species is similar to the type species of the genus, *A. reticulata* (Pl. 4, figs. 1 and 2). It differs from that species in being more elongate, by the presence of the two distinctive carinae that extend from the dorsal region to the anterior; by the presence of wider compressed marginal zones; by the sub-rectangular fossae directly behind the anterior rim; and by the less upturned posterior margin.

Range: This species was observed in the Owl Creek Formation of Tippah County, Mississippi and in the Prairie Bluff Formation of Lowndes County, Alabama (text-figs. 2 and 4). Both occurrences are of Maastrichtian age.

Anticythereis slipperi Puckett and Hunt **n. sp.**
Plate 2, figure 7; Plate 3, figure 2; Plate 6, figures 1-10; Text-fig. 9

Etymology: Named in honor of Ian Slipper, who worked at the University of Greenwich and passed away 17 May 2017, for his contributions to the study of Cretaceous ostracods. His works, particularly the studies of the Turonian ostracods of England (Slipper 2019, 2021), are models of meticulous and thorough taxonomic works.

Type Specimens: Holotype USNM PAL 771798, specimen number 148-14 (Pl. 6, fig. 1, female RV), sample 1991-8-15-7, Campanian-Maastrichtian Ripley Formation, Lowndes County, central Alabama; paratype: USNM PAL 771799, specimen number 2011-8-15-1 (15) (pl. 6, fig. 3, male RV), latest Campanian-early Maastrichtian Coon Creek type locality, McNairy County, Tennessee.

Diagnosis: This species is characterized by a supracurvate ventral margin in LV, infracurvate anterior and posterior margins in RV, and a RV with a longitudinal medial sulcus in the central and dorsoposterior region of carapace.

Material: 62 valves and 2 carapaces

Measurements: Holotype L = 0.726 mm, H = 0.410 mm; paratype L = 0.702 mm, H = 0.333 mm.

Description: The carapace is robust. The anterior margins are broadly and evenly rounded; the anteriorly margin of the LV is broadly rounded and slightly infracurvate (Pl. 6, figs. 2 and 4); the posterior margin is broadly rounded and supracurvate; the RV anterior and posterior margins are infracurvate; the posterior margin in the RV is moderately convex in the ventral part, but becomes very slightly concave in the upper part and continues to form a broadly arched dorsum, and has a very weak dorsoposterior angle. The dorsal margin in the LV has stragula above the terminal hinge elements; the dorsal outline of the RV is humped at mid-length due to a carina that protrudes above the hinge line; the ventral outline in the LV is very broadly and evenly rounded, sags and overhangs the ventral margin in lateral view, and curves up in the posterior without a clear ventroposterior angle; the ventral margin in the RV has a gentle concavity at 1/3 length, then becomes broadly convex and curves up to venter. The carapace in dorsal view is sagittate, with compressed margins; the anterior margin is stepped, with a very narrow marginal zone that steps up to the anterior marginal carina, then narrows slightly to form a bulging lateral margin; the greatest width is at circa ¾ length, then narrows to form a compressed posterior margin.

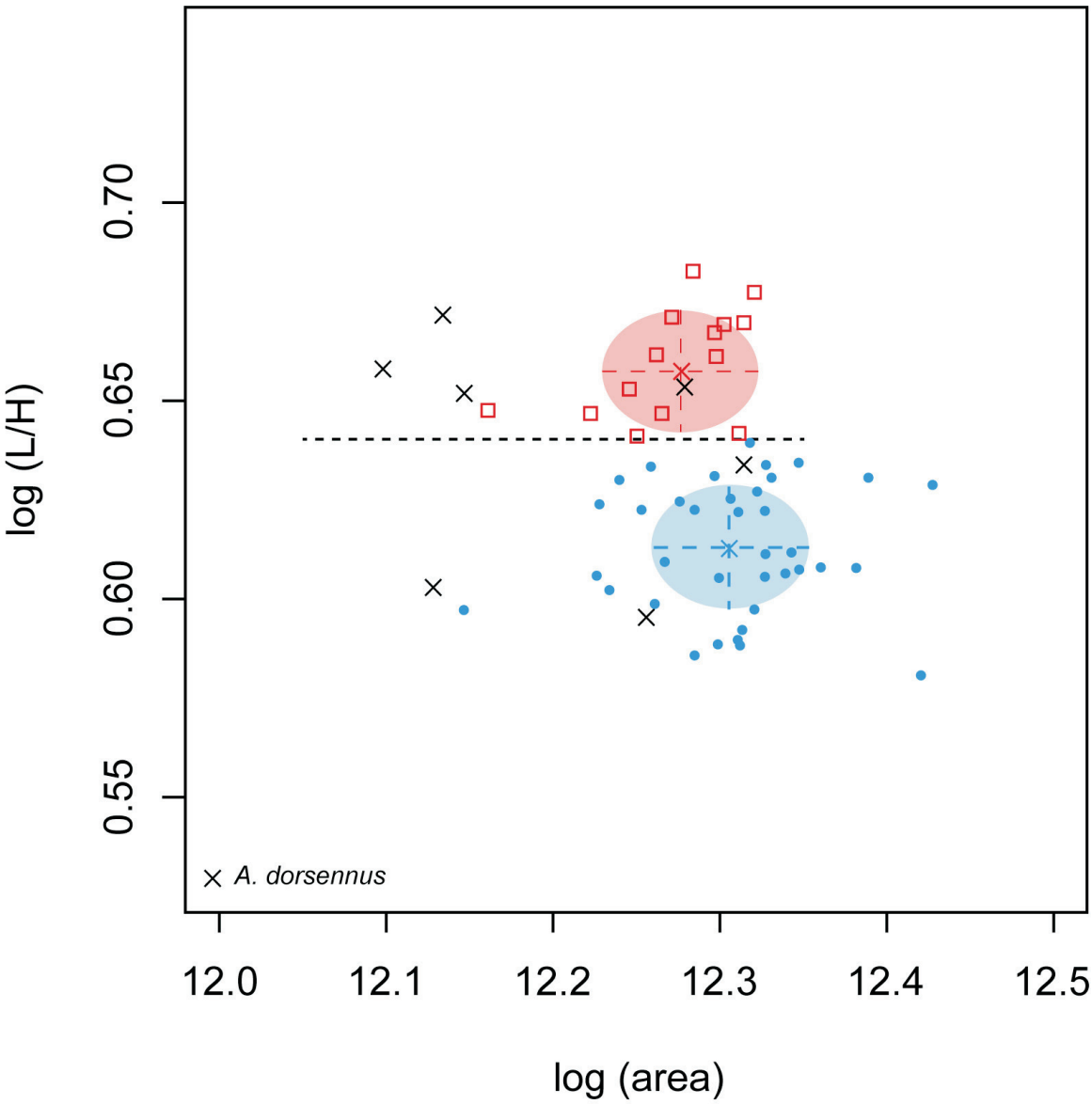

TEXT-FIGURE 10
Size (log area) versus shape (log[L/H]) for *Anticythereis dorsennus*. X's indicate specimens figured herein. Other points are from larger sample of this species analyzed by Hunt et al. (2017, population ANT_RETI-1-2). Blue circles = male and red squares = female clusters from that analysis, with corresponding colors for the 50% probability ellipses. Dotted line indicates inferred separation between males and females for the specimens figured in this work.

The eye tubercles are distinct and slightly elevated. The characteristic postocular sulcus extends from the dorsum slightly anterior of mid-length to directly below the eye tubercle; a strong, upraised carina borders the ventral margin of the postocular sulcus, forms a dorsal apex, and becomes less distinct below the eye tubercle; an anterior carina parallels the anterior margin, with intervening rectangular fossae separated by low muri; behind the anterior carina is a series of quadrate to rectangular fossae separated by low and thin muri, with smooth soli; the central part of the carapace has large, sub-rounded fossae, each with a single rimmed sieve-type normal pore canal; the muri are generally sloped to the soli, but sometimes are undercut (Pl. 6, fig. 10); the soli are caperate in places (Pl. 6, fig. 10); the regions just anterior and posterior to the center have slightly smaller and sub-rounded fossae; fossae in the posterior region become subquadrate, and are separated by low, thin muri; the fossae in the center of the carapace above mid-height are largest and deepest; in the RV, the center part of carapace has a gentle, elongate sulcus generally corresponding to the zone of large fossae, and extends from directly below the eye tubercle to 4/5 length; the muri are sparsely foveolate. Low, blunt denticles are located very close to the anterior and posterior margins.

The hinge is paramphidont; the RV (Pl. 6, fig. 6) has a slightly lobate anterior tooth, with a lower and smoother anterior knob and a taller, grooved posterior knob, and with subjacent socket;

the median groove is robust and crenulate, and widens towards the extremities; an elongate posterior tooth is located at the dorsoposterior angle, is oriented at approximately 45°, and is steeper on the ventral side; the hinge in the LV (Pl. 6, fig. 5) has an anterior socket that extends to below a postjacent blunt tooth, a straight and narrow median bar, and a socket at the dorsoposterior angle. The inner surface has scattered pores that are the inner openings of sieve-type normal pore canals. The marginal zones in the anterior, ventral and posterior regions are wide and have a well-developed duplicature; the selvage and list in the RV correspond to selvage groove in the LV; the ventral margin is slightly upturned just anterior of mid-length; the selvage on the LV is interrupted by a double ogee-shaped structure that lies just above mid-height (the specimen in Pl. 6, fig. 6 is abraded, but other specimens in the authors' collection have this structure preserved). A pair of rimmed, fusiform inverted platforms are located below the anterior end of the medial hinge element (Pl. 6, fig. 6); the upper platform is larger and acuminate anteriorly, whereas the lower platform is smaller and acuminate posteriorly; these platforms correspond in location to the inner surface of the postocular sulcus. A large ocular sinus is located just in front and below the anterior hinge element.

The muscle scars (Pl. 3, fig. 2; Pl. 6, figs. 6 and 7) have a V-shaped F scar; the A-2, A-3 and A-4 adductor scars are intertwined in a characteristic yin-yang symbol, with a large A-2 bulbous in the anterior that tapers across the A-3 scar; the small, elongate A-3 and A-4 scars are very close and nearly fused; the A-1 is offset dorsally and posteriorly from other adductor scars, is elliptical and tilted dorsoanteriorly; a reniform M-1 is directly below the F scar, less than half distance to venter; a small, elongate M-2 is close to the venter and tilted slightly dorsal from horizontal; the D-1 scar is directly below the ocular sinus; a small, circular D-2 is about half distance from D-1 to the F scar; a small, circular D-3 is located above the A-1 scar; the fulcral point is circular and sunken.

The species is sexually dimorphic, with the male being more elongate with strongly supracurvate posterior margins, whereas the female are rounder with less dramatic upturned posterior margin (text-fig. 9). The longitudinal sulcus in the male is better defined than the female, which is more inflated.

Remarks: This species is similar to *A. dorsennus* n. sp. by the mid-dorsal hump in outline, by the downwardly deflected carina along the posterior margin of the postocular depression, by the subcircular fossae that are located across the carapace, and by the more inflated lateral surface. It differs from that species in having a supracurvate posterior margin, rather than equicurvate; by less prominent anterior and posterior marginal carina; by less prominent and sharp-edged anterior carinae; and shallower fossae. It differs from *A. reticulata* (Jennings 1936) by being more elongate and less globose, by narrower muri, and by more polygonal fossae.

Range: This species was found in the type locality of the Coon Creek Formation (latest Campanian-early Maastrichtian) in McNairy County, Tennessee, the Ripley Formation (Maastrichtian) of Sumter, Lowndes and Dallas counties, Alabama, and the Prairie Bluff Chalk (Maastrichtian) of Lowndes County, central Alabama and Oktibbeha County, eastern Mississippi (text-figs. 2 and 4). This is one of the earliest species in the genus in the region. Sixty of the sixty-two specimens were collected from the coeval Coon Creek Formation in southern Tennessee and Ripley Formation of Alabama; the two other occurrences are in the Prairie Bluff Chalk.

Anticythereis sp. 1
Plate 4, figure 11

Material: 7 valves

Remarks: This species has a relatively large, sub-rectangular carapace with a gentle dorsal hump in outline, relatively shallow reticulation of sub-rounded fossae; and two anterior carinae parallel to the anterior margin with intervening sub-rectangular fossae. Unfortunately, this species is quite rare and only seven valves were recovered, in none of which can the internal morphology be observed. For these reasons, this species is left in open nomenclature.

Range: This species was found in a single sample collected from the Cusseta Sand of Barbour County, eastern Alabama (text-fig. 4). This sample is in the planktonic foraminiferal *Radotruncana calcarata* Taxon Range Zone of earliest late Campanian age (Puckett and Mancini 1998), and is therefore the oldest sample that includes anticytherideinines.

Genus ***Asculdoracythereis*** Puckett and Hunt **n. gen.**

Etymology: This genus is named after the type species, *Asculdoracythereis asculdora* n. gen. et sp., in reference to the smooth dorsal outline.

Type Species: *Asculdoracythereis asculdora* gen et sp. nov. (Pl. 1, fig. 4; Pl. 3, fig. 3; Pl. 8, figs. 1-11; Text-fig. 11).

Diagnosis: Species of the genus *Asculdoracythereis* are characterized by a combination of a carapace that is broadly rounded to flattened in dorsal view (i.e., not sulcate or lobate), has a level lateral outline in mid-dorsum, has relatively shallow fossae, and has a polygonal network of sharp-edged muri.

Remarks: Most of the species assigned to the new genus from the present study are from the Providence Sand (Maastrichtian) of eastern Alabama. These species include the nominal species, *As. invicta* n. sp.*, As. lowndesensis* (Smith 1978) (also observed in the Prairie Bluff Chalk (Maastrichtian) of central Alabama), and *As. pseudoalabamensis* n. sp. Likewise, *Asculdoracythereis alabamensis* (Smith 1978), which he collected from the Prairie Bluff Formation of central Alabama, should be assigned to this genus. Other species of possible assignment to *Asculdoracythereis* include *Velarocythere scuffletonensis* Brown, 1957 and *V. legrandi* Brown, 1957. The type specimens of the latter two species have adventitious material on them, but SEM images can be viewed *via* the collections database at the U.S. National Museum (search engine found at https://collections.nmnh.si.edu/search/paleo/). The latter two species are from the Peedee Formation (Maastrichtian) of North Carolina. An undescribed species, *As.* sp. 1 (Pl. 4, figs. 9 and 10) which was collected from the Owl Creek Formation of northern Mississippi, is tentatively assigned to the new genus, but was very rare and the details of the interior of the carapace are not known.

The species assigned to *Asculdoracythereis* n. gen. are remarkably similar to each other and can be difficult to distinguish, differing mainly in the shape of the fossae and the presence or absence of carinae. It is also the most diverse genus in the new subfamily and includes at least eight species. The genus was

short-lived, evolving in the Maastrichtian and becoming extinct at the end of the Cretaceous.

Asculdoracythereis alabamensis (Smith 1978)
Plate 7, Figure 3

Anticythereis alabamensis SMITH 1978, p. 555, Pl. 6, fig. 21, Maastrichtian Prairie Bluff Chalk, Lowndes County, Alabama.

Type Specimen: Holotype USMN PAL 255752, female RV (Pl. 7, fig. 3).

Diagnosis: Species characterized by combination of strongly infracurvate anterior margin, laterally swollen carapace, non-reticulate in the posterior, and with fossae arranged concentrically subparallel to carapace outline.

Remarks: Smith (1978) noted that *As. alabamensis* differs from *A. legrandi* (Brown, 1957) in that the latter "has small spines on the anterior end [presumably denticles] and lacks the anterior rim and smooth posterior margin of *As. alabamensis* n. sp." Images of the holotype of *As. alabamensis* (USNM PAL 255753) and of *As. legrandi* (USNM PAL 129011; available for view at the USNM web site for paleobiology collections) show that the anterior margin *A. alabamensis* extends downward more than *As. legrandi*; the anterior rim noted by Smith in the latter species includes sets of carinae parallel to the margins, with four in the anterior and three in the dorsoposterior region. Otherwise, the species are very similar.

This species is very similar to *As. pseudoalabamensis* n. sp. (Pl. 7), but differs in being less elongate, having a more swollen lateral surface, having concentrically arranged fossae, and with a smooth posterior. The muri are relatively low, but that may be a taphonomic artifact of the type specimen. The overall shape is similar to *As. invicta* n. sp., but it lacks the sharp-angled longitudinal carinae of the latter species. Sexual dimorphism unknown, but the figured specimen is plotted on text-fig. 10.

Range: Smith (1978) found this species in the Prairie Bluff Chalk (Maastrichtian) of Lowndes County, Alabama. None were found during this study.

Asculdoracythereis asculdora Puckett and Hunt **n. sp.**
Plate 1, figure 4; Plate 3, figure 3; Plate 8, figures 1-11; Text-fig. 11

Etymology: *a* – meaning without, and *sculdor*, Anglo-Saxon for shoulder.

Type Specimen: Holotype: USNM PAL 771800, specimen 146-1 (Pl. 8, fig. 2, male LV); paratype: USNM PAL 771801, specimen 148-3 (Pl. 8, fig. 4, female LV); both specimens from sample 2012-01-03-1-2, Providence Sand (Maastrichtian), Barbour County, eastern Alabama.

Diagnosis: This species is characterized by a combination of relatively flat lateral surface, sub-rectangular lateral outline, coarse and well-rounded fossae completely covering carapace, almost straight dorsal outline, and relatively shallow post-ocular depression.

Material: 6 carapaces and 82 single valves

Measurements: Holotype L = 0.684 mm, H = 0.339 mm; paratype L = 0.708 mm, H = 0.387.

Description: The carapace is robust; the lateral outline is sub-rectangular; the greatest height is at the anterior dorsal angle, although not prominent; the anterior margin is infracurvate, and is broadly and evenly rounded; the posterior margin of the LV is slightly supracurvate, whereas in the RV it is equicurvate and broadly rounded; the dorsal margin is nearly straight in the LV, but very slightly convex in the RV; the ventral margin is nearly straight in the LV, but slightly concave in the RV, with the typical concavity at 1/3 length; the posterior margin of the LV curves smoothly up from the venter in the male, becoming almost straight vertical up to the dorsoposterior angle, and in the female it is broadly rounded. Small, blunt denticles are located along the ventroanterior and posterior margins. The carapace in dorsal view is broadly bulging, with the greatest width at circa 4/5 length; the marginal zones are conspicuously not compressed, with a very slight indentation just posterior of weak anterior marginal carina.

The eye tubercles are smooth areas just below the dorsoanterior angle, but do not bulge. The post-ocular sulcus is subjacent to the eye tubercle and extends ventroanteriorly from the dorsal margin to slightly anterior of mid-length to terminate well above mid-height. The primary external ornamentation is reticulation across entire carapace; fossae are rounded, ranging from circular to rounded polygonal. There are two rows of fossae parallel to the anterior margin, both being sub-rectangular with long axis parallel to margin, with the dorsal-most fossae becoming acuminate dorsally; the anterior row generally includes 6 fossae, and the second row includes 7; the murus between the first and second row is continuous, with the muri separating the fossae in each row being relatively thin. The fossae in the anterior half are slightly smaller than those in the posterior half and are generally more subcircular, whereas those in posterior half are more sub-rectangular; the fossae along posterior and ventral margins are elongate parallel to the margins; the sola are typically caperate, with stretch marks that radiate away from sieve pores (Pl. 8, figs. 7 and 11); the muri are generally nearly vertical or undercut (Pl. 8, fig. 7). Sieve-type normal pore canals with raised rims are located near center of the fossae, and sometimes with an apophysis; the sieve plates are sunken well below raised rim, and include numerous openings (Pl. 8, fig. 7).

The hinge is paramphidont; the anterior hinge element in the LV (Pl. 8, fig. 3) includes a concentrically grooved socket that extends well below the postjacent tooth; the tooth is elongated ventroanteriorly; the median hinge bar is straight and crenulate; the posterior hinge socket is located at the ventroposterior angle and tilted at circa 45°; the anterior hinge tooth in the RV (Pl. 8, figs. 8 and 10) is stepped, with both parts being vertically grooved; the postjacent socket is deep; the median hinge groove is straight, crenulate, and narrowest in the middle; the posterior tooth arches across the dorsoposterior angle. The selvage, selvage groove, list and inner margins along the anterior, ventral, and posterior margins are with no observable vestibule. There is an interruption of the selvage at the caudal region in the RV that produces a double ogee-shaped structure (slightly damaged in the specimen on Pl. 8, fig. 8), with corresponding smooth area in the LV. A pair of elongate, rimmed, inverted platforms located between the central muscle scar field and the hinge (Pl. 8, figs. 9 and 10), which corresponds to the inside of the postocular sulcus, is observed in some specimens; the smaller, lower platform is slightly forward of the upper, and in most specimens is ill-defined; the anterior end of the upper platform is acuminate anteriorly, whereas the lower platform is

acuminate posteriorly. A large ocular sinus lies just anterior and ventral of the anterior hinge elements (Pl. 8, figs. 8-10).

The muscle scars (Pl. 3, fig. 3; Pl 8, figs. 9 and 10) include a V-shaped F scar tilted slightly forward, with the posterior taller than the anterior; the A-2, A-3 and A-4 scars are arranged in an overall circular pattern and intertwined like a yin-yang symbol; the A-1 scar is oval, tilted anterodorsally, offset vertically from the other adductors and located above the posterior ends of the other adductor scars; a tilted, paisley-shaped A-2 scar tapers across the lower adductor scars; a small, elongate A-3 scar is sandwiched between the posterior ends of the A-2 and A-4 scars; and the A-4 scar is elongate, tilted slightly, and is acuminate ventroanteriorly. An elliptical M-2 scar is located just inside of the ventral margin below and slightly posterior of the F scar, with an intervening elongate and reniform M-1. A depressed fulcral point is located above and slightly anterior of the adductor scars. Four small, circular dorsal scars are located near dorsal margin that extend from anterior of the F scar to directly above the posterior margin of the adductor scars.

The species is sexually dimorphic, with the female having a greater height/length ratio and more inflated than the male (text-fig. 11).

Remarks: Generic synapomorphic characters observed in the species include the rimmed sieve-type normal pore canals on the fossae (Pl. 8, fig. 7); muscle scar pattern with yin-yang-shaped adductor scars (Pl. 3, fig. 3; Pl. 8, fig. 10); a pair of rimmed, inverted, fusiform platforms that correspond to the inside of the postocular sulcus (Pl. 8, figs. 9, 10); and lobate hinge teeth (Pl. 8, fig. 10). The sub-rectangular carapace outline is similar to *As.* sp. 1, but it is larger and includes more numerous and smaller fossae; the posterior margin is smoother and lacks the lobate outline of *A.* sp. 1.

Range: This species has been found only in the Providence Sand (Maastrichtian) of Barbour County, eastern Alabama (text-fig. 4).

Asculdoracythereis invicta Puckett and Hunt **n. sp.**
Plate 1, figure 4; Plate 3, figure 4; Plate 9, figures 1-11; Text-fig. 11

Etymology: invictus, Latin meaning unconquered, strong, in reference to the strong muri and carinae on the carapace.

Type Specimens: Holotype: USNM PAL 771802, specimen 147-10 (Pl. 9, fig. 1, male RV); paratype: USNM PAL 771803, specimen 147-13 (Pl. 9, fig. 4, female LV); both specimens from the Maastrichtian Providence Sand, Barbour County, eastern Alabama.

Diagnosis: Carapace large with a sub-quadrate outline, with strong longitudinal carinae connected by weaker sub-vertical muri; longitudinal carinae converge near ventroanterior margin; muri polygonal, quadrate in centrally inflated region of carapace.

Material: 35 valves and 3 carapaces

Measurements: Holotype L = 1.100 mm, H = 0.524 mm; paratype H = 0.892 mm, paratype L = 0.488 mm.

Description: The carapace is large, robust, and sub-quadrate in lateral outline. The dorsal margin is straight but with protrusions from carinae that extend the silhouette above the margin, and with a prominent peak near mid-length; the anterior margin is broadly and evenly rounded and infracurvate; the ventral margin is very broadly convex in the LV, but in the RV is characteristically concave; the posterior margin in the LV is very broadly rounded, almost straight in the central part, and equicurvate; the RV has a broadly rounded posterior margin in the lower half, is gently concave in the upper half up to a subtle dorsoposterior angle, and is infracurvate. The anterior and posterior margins have a double row of small denticles that are slightly longer at and below mid-height. The carapace in dorsal view is broadly and gently bulged; the anterior margin is blunt, then flares at the anterior marginal carina, then narrows to bulge at the lateral margin; the sides are broad but nearly flat, with the greatest width at approximately 3/4 length, then tapers to a slightly compressed posterior region; the posterior margin is blunt.

The eye tubercle is gentle and not bulged. A distinctive postocular sulcus extends from the dorsal margin at circa 1/3 length, drops below the eye tubercle, then continues parallel to the anterior margin to the venter just behind the marginal carina; a depressed zone behind the marginal carina is subdivided into large, sub-quadrate fossae by thin and low muri; the anterior marginal carina extends from near the dorsal margin just behind dorsoanterior angle and skips across the eye tubercle to parallel the anterior margin to the venter; between the anterior carina and anterior margin is a region with very narrow, sub-rectangular fossae defined by low, thin muri; the posterior marginal zone is compressed, with few, small, blunt tubercles connected by low, thin muri. The middle section of the carapace bulges, is coarsely carinate, with very prominent sub-horizontal carinae and lower, thinner muri tilted slightly anteriorly to form subquadrate fossae; just below the postocular sulcus is a relatively low carina, which is connected at both ends to a second large subjacent carina, which together form a fusiform structure that encloses low, thin interconnecting muri that separate small, subquadrate fossae; these two carinae merge to form a single carina that curves back to parallel the ventral margin; two other carinae in the central area arise from just anterior of the posterior part of the lateral bulge, oriented dorsoanteriorly, to curve ventroanteriorly at 2/3 length, with the dorsal carina curved anterior of the ventral carina to join with a prominent anterior carina where it begins to curve ventroposteriorly; just behind mid-length, a short carina intervenes between the two longitudinal carinae a short distance, beginning just below a curve in dorsal carina to terminate near mid-length; another sub-horizontal carina extends across the bulged part of carapace paralleling the lower of the two mid-carapace carina to join it behind the curve of prominent anterior carinae, forming a fusiform structure; the ventral carina bifurcates posteriorly at 1/3 length, with the resulting two carina paralleling each other; just above the central muscle scar field is a distinctive sub-circular fossa (see arrow on Pl. 9, fig. 2) that interrupts the dorsal longitudinal carina; zones between the lateral carinae are connected by low muri angled slightly anteriorly to form sub-quadrate fossae; in general, the mural walls are tall (particularly at the carinae) (Pl. 9, fig. 11), but rarely undercut; caperation in the soli was not observed. The surface has scattered, rimmed sieve-type normal pore canals; the sieve plates are sunken below level of the soli (Pl. 9, fig. 11); a gentle moat surrounds the pore canals; sieve pores are generally located within the confines of the fossae, but sometimes are located on the sides or even within muri (Pl. 9, fig. 11), although none are located on the prominent carinae.

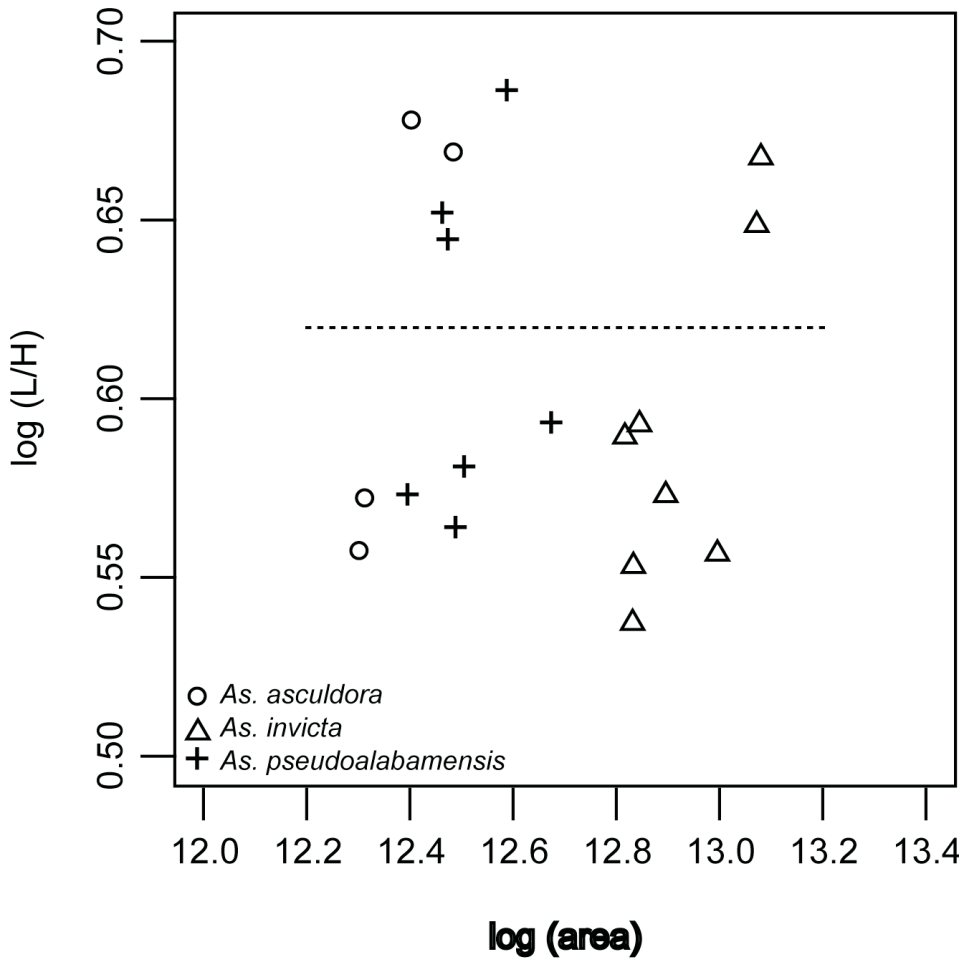

TEXT-FIGURE 11
Size (log area) versus shape (log[L/H]). (A) *Asculdoracythereis asculdora*, *Asculdoracythereis invicta*, and *Asculdoracythereis pseudoalabamensis*. Dotted line indicates inferred separation between males and females for the specimens figured in this work; in this case, the same separation point is inferred for all three species.

The hinge is paramphidont; the RV (Pl. 9, figs. 6 and 8) has a stepped and grooved anterior tooth; the smooth subjacent socket shallows posteriorly; the median groove is straight and crenulate, and widens towards the extremities; the posterior tooth is arched across the dorsoposterior angle and multilobate; in the LV (Pl. 9, figs. 5 and 7), the anterior socket is grooved; the subjacent tooth is tall and narrow; the median bar is straight and crenulated; and the posterior socket is loculate and curves around the dorsoposterior margin. Large pores correspond to the inner openings of the sieve-type normal pore canals. The duplicature is relatively wide. The selvage in the RV is interrupted in the caudal region by a double ogee-shaped structure (Pl. 9, figs. 6 and 8, although the specimen in fig. 6 is abraded), with corresponding area in the LV. A pair of inverted platforms is seated below and just behind the anterior hinge element corresponding to the interior of the postocular sulcus, and are elongate longitudinally (pl. 9, figs. 5-10); well-preserved specimens show the upper platform to be rimmed; the upper platform is acuminate anteriorly, whereas the much smaller lower platform is acuminate posteriorly; the platforms are less distinct in the LV. The ocular sinus is relatively small and opens just below the anterior part of the anterior hinge element (Pl. 9, figs. 5-8).

The muscle scars (Pl. 3, fig. 4; Pl. 9, figs. 9 and 10) have a U-shaped F scar, with the posterior limb being taller than the anterior; the A-1 scar is slightly elliptical, with the long axis oriented dorsoanteriorly, and is detached vertically from other adductor scars; the A-2, A-3 and A-4 scars intertwine like a yin-yang symbol in an overall circular shape; the A-2 scar is bulbous in the anterior part, similar to a paisley shape, then becomes acuminate in the posterior above the A-3 scar; the A-3 scar is small, elongate, and sandwiched between the posterior ends of the A-2 and A-4 scars; the A-4 scar is elongate and oriented slightly ventrally from horizontal; the subcircular M-1 scar lies directly below the F scar, and is slightly more than halfway between the ventral margin and the central muscle scar field; the small, horizontally elongate M-2 scar near venter is directly below the central muscle scar field; there are four small, subcircular dorsal scars; the D-1 scar is below the eye tubercle; the small, circular D-2, D-3 and D-4 scars are located above the central muscle scar field, with the D-3 scar being slightly closer to the D-2 scar; and a raised fulcral point lies between the cen-

tral scar field and the dorsal scars, and is elongate longitudinally.

The species is sexually dimorphic, with the male being more elongate and the female having a greater height/length ratio (text-fig. 11).

Remarks: This species is similar to *As. alabamensis* (Smith 1978) in overall shape, anterior marginal carina and subjacent depressed zone with sub-quadrate fossae formed by low muri; however, the prominent sub-longitudinal carina that converge in the ventroanterior region in the new species and the overall stronger carinae serve to differentiate the two. The overall shape, anterior marginal carina and postjacent depressed area with sub-quadrate fossae are also similar to *As. lowndesensis* (Smith, 1978), but the spinose ornamentation and lack of longitudinal carinae on that species differentiate it from the newly described species.

Range: This species has only been found in the Providence Sand (Maastrichtian) of Barbour County, eastern Alabama (text-fig. 4).

Asculdoracythereis lowndesensis (Smith 1978)
Plate 1, figure 3; Plate 3, figure 5; Plate 10, figures 1-10

Anticythereis lowndesensis SMITH 1978, p. 555-556, Pl. 6, figs. 22-23.

Type Specimens: The type specimens of *A. lowndesensis* were collected from the Prairie Bluff Formation (Maastrichtian) of Lowndes County, central Alabama (Smith 1978). The holotype is USNM PAL 255755, a RV with considerable debris that obscures the details of the carapace. The paratype is USNM PAL 255754, which is a juvenile LV.

Diagnosis: None given, but Smith (1978) described the species.

Emended Diagnosis: Carapace with polygonal, deep fossae, and conspicuous blunt spines that punctuate the muri at or near their junctions, either spinose or knobby. Large, radiating fossae lie behind the anterior marginal rim, and are separated by low, thin muri that forms the wide, nearly flat, infracurvate anterior region.

Material: 79 valves

Remarks: One of the authors (TMP) has collected a topotype specimen (not illustrated) that appears to be identical to the holotype but is much better preserved. The topotype specimen reveals that the upraised pores at mural junctions are spinose, being at least twice as tall as the surrounding muri. In the holotype, these conjunctive spines and spine clusters have been broken. The specimens from eastern Alabama do not appear to have had such long spines, as they do not appear to be broken and are knob-like. Taphonomic control can be seen in well-preserved specimens, where delicate upraised cup- or vase-like structures (Pl. 10, fig. 7) adorn the carapace. Sieve-type normal pore canals are located across the carapace and often pierce the muri (Pl. 10, figs. 7-9). The sieve plates have a central pore that is surrounded by numerous openings and lies below the exterior level of the carapace; they are also depressed in the center like a funnel. One sieve-type normal pore lies directly below a knob-like conjunctive spine (arrow on Pl. 10, fig. 9). The adventitious material on the holotype conceals details of the soli, which are typically caperate, and the muri, which are often undercut (Pl. 10, figs. 7 and 9). As in the holotype, the specimens from eastern Alabama show a prominent knob-like pore conus just above mid-height near the posterior margin (arrow on Pl. 10, fig. 4).

The hinge is paramphidont and well displays the morphology that is typical of the genus (Pl. 10, figs. 5 and 6). The anterior hinge in the RV is stepped and multilobate, and the LV is grooved to accept the tooth. Low stragula rise above the terminal hinge elements of the LV. The muscle scar pattern (Pl. 3, fig. 5; Pl 10, fig. 10) matches other species of the genus, particularly the yin-yang pattern of the A-2, A-3, and A-4 adductor scars, as well as the detached, elliptical, and tilted A-1 scar. There are at least three dorsal muscle scars, with the most anterior being directly below the anterior tooth of the hinge of the RV (Pl. 10, fig. 6). The rimmed, inverted platforms are also present (see Pl. 10, fig. 6 and top of Pl. 10, fig. 10), although the lower one is quite small. The double ogee-shaped interruption of the selvage is present at the posterior extremity of the RV (see Pl. 10, fig. 6, although the structure is slightly abraded).

Range: Smith (1978) reported this species from the Prairie Bluff Formation (Maastrichtian) of Lowndes County, central Alabama, and this study found the species rarely in the Prairie Bluff (same locality as Smith) and Providence Sand of Bullock County, Alabama, but more numerous specimens were picked from the Providence Sand (Maastrichtian) of Barbour County (text-fig. 4).

Asculdoracythereis pseudoalabamensis Puckett and Hunt **n. sp.**
Plate 1, figure 5; Plate 3, figure 6; Plate 7, figures 1-2, 4-11; Text-fig. 11

Etymology: *pseudo*, Latin for false, and *alabamensis*, in reference to *Anticythereis alabamensis* Smith, 1978, to which this species is similar.

Type Specimens: Holotype specimen 147-1, USNM PAL 771804 (Pl. 7, figs. 2, 9), male LV; paratype specimen 147-4, USNM PAL 771805 (Pl. 7, fig. 4), female LV; both specimens from sample 2012-01-03-1-2, Maastrichtian Providence Sand, Barbour County, eastern Alabama.

Diagnosis: This species is characterized by a combination of an evenly reticulate pattern of sub-polygonal fossae across the entire carapace except for the anterior zone, which is a relatively flattened zone of two rows of sub-quadrangular fossae separated by a thin murus; a downwardly-sloped anterior margin well developed on the RV; a thin carina that extends from mid-dorsum, behind the post-ocular depression to die out just above the central muscle scar field; and carinae that are aligned in rows separated by a murus behind the anterior flattened zone in the LV and the ventrolateral region of the RV.

Material: 17 carapaces and 144 valves

Measurements: Holotype L = 1.023 mm, H = 0.530; paratype L = 0.672, H = 0.375 mm.

Description: The carapace is robust and oblong. The greatest height is just behind the eye tubercle at the low anterior stragulum; the anterior margin is infracurvate and the posterior margin of the LV is slightly supracurvate; both margins are broadly rounded. The dorsal margin in external view has a sharp-edged, arching carina that originates just behind postocular sulcus to terminate in front of the dorsoposterior angle; in the LV, the ventral silhouette continues smoothly from

the anterior margin, very broadly rounded, to turn vertical at the blunt posterior margin; in the RV, the venter is characteristically incurved at about 1/3 length so that the margin is hidden behind the carapace in external view; the outline of the ventral to the posterior margins in the RV is broadly rounded up to mid-height, where it curves to form a straight or slightly concave dorsoposterior margin. A double row of denticles is located very close to the anterior and posterior margins. In dorsal view, the carapace is broadly and gently bulged, with a highly compressed marginal zone that steps up to the anterior carina, then tapers at the post-carina sulcus; the main part of the lateral bulge is gentle and broad, with the greatest width located near mid-length; the posterior zone is not compressed and gently narrows to the margin.

The eye tubercle is a distinct, smooth bulge at the dorsoanterior angle. The postocular sulcus is deep and smooth, and continuous from the dorsal margin just in front of mid-length to below the eye tubercle. The anterior region has two rows of large, low rectangular fossae; the rows are separated by a prominent carina that arises from the eye tubercle; the anterior row of fossae is separated from the anterior margin by a low carina that bifurcates immediately in front of the eye tubercle; the second row of fossae is slightly larger than first; both rows have smooth, flat soli; the ornamentation on the lateral, rounded region of carapace has quadrilateral fossae of generally uniform size; the muri are steep, vertical and even undercut in places (Pl. 7, fig. 9), but with rounded soli; some soli are caperate (Pl. 7, fig. 10); sieve-type normal pore canals with raised rims are located within the fossae, usually adjacent to the muri but occasionally are intramural (Pl. 7, fig. 10); the sieve plates are located inside the raised rims, and include a central pore surrounded by numerous smaller openings in concentric rows (Pl. 7, fig. 9). The dorsal carina extends from in front of the dorsoposterior angle to just in front of mid-length, where it turns sharply down behind the postocular sulcus to lose its definition; behind this carina is another depressed zone, so that the intervening carina looks like an arête between glacial valleys.

The hinge is paramphidont (Pl. 7, figs. 5-8); the anterior hinge element in the RV has a stepped tooth (Pl. 7, figs. 6 and 8); the anterior part of the tooth is lower than the subjacent tooth, is angled slightly down from horizontal, is smooth and elongate, and drops off abruptly to the carapace marginal zone and selvage; the subjacent tooth is taller, with shallow vertical grooves; the socket behind the tooth is deep, with a flaring and sharp ventral flange; the median groove is crenulate and has a double row of thin flanges above the crenulations; the posterior tooth in the RV is arched and grooved across the dorsoposterior angle; the anterior hinge socket in the LV is bipartite to accommodate the stepped tooth in the RV, with the anterior being shallow and elongate and the postjacent socket is larger, rounded and deeper; the postjacent tooth is smooth and rounded; the median hinge bar is straight, crenulate, and slightly constricted in middle; and the elongate socket is angled at about 45° across the dorsoposterior angle. The inner carapace wall is punctuated by pores, which are inner openings of sieve-type normal pore canals. The marginal zones have a well-defined duplicature, with selvage, list and flange groove; in the RV, the selvage is interrupted by a double ogee-shaped structure in the caudal region (arrow on Pl. 7, fig. 8); in the LV, there is no corresponding structure; in the LV is the selvage and flange groove; a vestibule is very narrow. Two inverted, fusiform, rimmed, inverted platforms lie in parallel just below and behind the anterior hinge elements corresponding to the interior of the postocular sulcus (arrows on Pl. 7, fig. 7); the dorsal platform is much larger than the one below it, is acuminate anteriorly, and is bluntly rounded at the posterior end; the lower platform is about half the size of upper, is tear-shaped, being acuminate posteriorly and rounded anteriorly. The ocular sinus is located just in front of and below the anterior hinge elements (Pl. 7, figs. 5-8)

The muscle scars (Pl. 3, fig. 6; Pl. 7, fig. 11) have a U-shaped F scar that is slightly higher posteriorly; the A-1 scar is ovate, with long axis about 45°, and is detached vertically and posteriorly from the other adductor scars; the A-2, A-3 and A-4 scars intertwine like a yin-yang symbol in an overall circular pattern; the A-2 scar is paisley-shaped and tapers as it curves over the A-3; the A-3 scar is small, elongate and acuminate anteriorly, and lies at the posterior ends of the A-2 and A-4 scars; the A-4 scar is elongate and tapers anteriorly; the M-1 scar is rounded and is located directly below the F scar about half way to the M-2 scar; the M-2 scar is just inside of the ventral marginal zone, is elongate longitudinally, and is located below the space between the F and adductor scars; the D-1 scar is moated and located directly below the eye tubercle; the D-2 and D-3 scars are small, round, and located above the space between the F and adductor scars; the D-4 scar is small, ovoid, and located above the A-1 scar; the fulcral point is depressed and located above the anterior end of the adductor scars.

The species is sexually dimorphic, with the female being slightly shorter but more rounded, and the male being longer and more elongate (text-fig. 11).

Remarks: This species displays all the characteristics of the genus: a well-defined postocular sulcus; two fusiform inverted platforms that possibly serve for attachment points of dorsal muscles and tendons on the interior of the postocular sulcus; the yin-yang configuration of A-2, A-3 and A-4 scars arranged in overall circular shape; and fossae with large sieve pores with raised rims. It is very similar to *As. alabamensis* Smith, 1978 (Pl. 7, fig. 7) with its infracurvate, compressed anterior zone, well-developed polygonal fossae on lateral surface, ovate depression in the caudal region of the RV, and the hinge. The new species differs from that species by being larger, more elongate, and with fossae that extend to the posterior margin.

Range: This species was found only in the Providence Sand (Maastrichtian) of Barbour County, eastern Alabama (text-fig. 4). Although one of the authors (TMP) has samples from Smith's (1978) type locality, no specimens of *A. alabamensis* were found in them.

Acsuldoracythereis sp. 1
Plate 4, figures 9 and 10

Material: 11 valves

Remarks: This very rare species is characterized by a combination of sub-rectangular lateral outline, a reticulate pattern with sub-rounded fossae, a squared off dorsoposterior region with hummocky projections, and a relatively flat lateral surface that slopes very gently to the posterior, then drops to a slightly compressed posterior margin. Unfortunately, no specimens were found for which the internal features could be observed. It is with uncertainty that this species is included in the genus *Asculdoracythereis*, particularly because of the morphology of the posterior margin and the uncertainty of the internal mor-

phology but is tentatively included because of the presence of a broad and flat lateral surface and reticulation.

Range: Owl Creek Formation (Maastrichtian) of northern Mississippi (text-fig. 2).

Genus ***Frodocythereis*** Puckett and Hunt **n. gen.**

Etymology: This genus is named after the type species, *Frodocythereis frodoi* gen. et sp. nov., in reference to the ring-shaped murus on the lateral surface.

Type Species: *Frodocythereis frodoi* n. sp. nov. (Pl. 2, fig. 5; Pl. 3, fig. 8; Pl. 12, figs. 1-12; Text-fig. 12).

Diagnosis: Species in the genus *Frodocythereis* are characterized by a combination of an overall sub-rectangular shape; very deep, polygonal fossae; a compressed posterior margin; a carina that forms a strong buttress along the ventral border of the post-ocular depression; large, box-like or sub-polygonal fossae below the post-ocular depression; a carina parallel to the dorsal carina but below it; and a relatively wide and flat anterior zone with shallow, radiating muri.

Species: Species that are assigned to the genus *Frodocythereis* include, of course, the type species, found in the Owl Creek Formation (Maastrichtian) of northern Mississippi, *F. copelandi* (Smith, 1978), found in the Owl Creek and Prairie Bluff Chalk of central Alabama, and *F.* sp. 1 of the Coon Creek Formation (latest Campanian-early Maastrichtian) of northern Mississippi. The species identified as *Anticythereis reticulata* (Jennings 1936) by Van Nieuwenhuise and Kames (1976), which is an undescribed new species with very deep fossae and sub-vertical muri, should also be assigned to *Frodocythereis*.

Frodocythereis copelandi (Smith 1978)
Plate 2, figure 6; Plate 3, figure 7; Plate 11, figures 1-11; Text-fig. 12

Anticythereis copelandi SMITH 1978, p. 556, pl. 6, figs. 24-25.

Type Specimens: Holotype USNM PAL 255757 (female RV; Pl. 11, fig. 1), sample 15A; paratype USNM PAL 255756 (RV), sample 14-I both specimens collected from the Prairie Bluff Formation (Maastrichtian), Lowndes County, central Alabama.

Diagnosis: Smith (1978) noted that "*A. copelandi* differs from *A. legrandi* (Brown, 1957) by being more coarsely reticulate and having a different arrangement of surface ornamentation."

Amended Diagnosis: This species is characterized by the following features: carapace relatively small, sub-rectangular in lateral outline; very prominent carinae, with one that nearly encircles the lateral surface of carapace; it rises above the dorsum in the mid- to posterior part of the carapace, angles ventroanteriorly to below mid-height, turns ventroposteriorly to parallel ventral margin, then bends up nearly vertically to complete the loop. A large, box-like fossa is located below the eye tubercle, bordered dorsally by the post-ocular carina; a wide apophysis usually extends a short distance into the fossa, forming an invagination.

Material: 2 carapaces, 245 valves

Remarks: This species displays all of the generic characters, including the postocular depression that extends from the dorsal margin to below the eye tubercle, with the corresponding two inverted platform structures on the inside of the carapace (Pl. 11, figs 5 and 6); the hinge that includes a stepped anterior tooth in the RV (Pl. 11, fig. 6); the yin-yang symbol made by the A-2, A-3 and A-4 muscle scars (Pl. 3, fig. 7; Pl. 11, figs. 9 and 10); the constellation of raised sieve-type normal pore canals (closeup on Pl. 11, fig. 11); and the double ogee-shaped caudal structure on the duplicature at the posterior margin of the LV (Pl. 11, fig. 6, noted by arrow). Sexual dimorphism is observed with the male being more elongate than the female (text-fig. 12).

The holotype (Pl. 11, fig. 1), unfortunately, is partially obscured by debris. The robust muri on the carapace exterior are vertical or undercut (Pl. 11, fig. 11). The raised sieve-type normal pore canals are often connected to the surrounding muri by apophyses, and the soli are often caperate. The lower inverted platform is quite small and the upper one is acuminate anteriorly. This species has compressed anterior and posterior margins with large polygonal fossae and small intervening muri that are observed in other species of the genus, including *A. dorsennus*, *F. frodoi*, *As. alabamensis*, *As. invicta*, and several others.

Range: Smith (1978) described this species from the Prairie Bluff Chalk (Maastrichtian) of Lowndes County, Alabama. In this study, *A. copelandi* was found only in the Owl Creek (Maastrichtian) of northern Mississippi. This species, therefore, has a relatively wide geographic extent, ranging from central Alabama to northern Mississippi (text-figs. 2 and 4).

Frodocythereis frodoi Puckett and Hunt n. sp.
Plate 2, figure 5; Plate 3, figure 8; Plate 12, figures 1-12; Text-fig. 12

Etymology: *frodoi,* in reference to Frodo Baggins, the ring bearer in *Lord of the Rings*, and the characteristic ring-shaped murus just in front of the muscle scar on the external surface.

Type Specimens: Holotype: USNM PAL 771806, specimen 134-2 (Pl. 12, figs. 4 and 12, male LV), sample 2011-8-4-1 (water level), Maastrichtian Owl Creek Formation, Tippah County, Mississippi; paratype USNM PAL 771807, specimen 104-6 (Pl. 12, fig. 6, female LV), sample 2011-5-18-1 (water level), Maastrichtian Owl Creek Formation, Tippah County, Mississippi

Diagnosis: Very large fossae, with largest just anterior to center of carapace, with most prominent in shape of ring just below postocular sulcus; steep and well-defined muri; dorsal carina, with subjacent vertical muri; and anterior marginal carina and subjacent rectangular fossae divided by radiating muri.

Material: 118 valves and no carapaces.

Measurements: Holotype L = 0.809 mm, H = 0.393 mm; paratype L = 0.744 mm, H = 0.452 mm.

Description: The carapace is robust; the greatest height is at the eye tubercle; the anterior margins are broadly rounded and infracurvate; the posterior margin of the RV is infracurvate, whereas in the LV it is slightly supracurvate. The dorsal margin is bipartite, with an almost straight anterior part that slopes posteriorly to 1/3 length, then the silhouette becomes hummocky and slightly arched in the posterior part due to the dorsal carina being elevated above the hinge line; the ventral margin in the LV is concave in the anterior part to the mid-length, then is al-

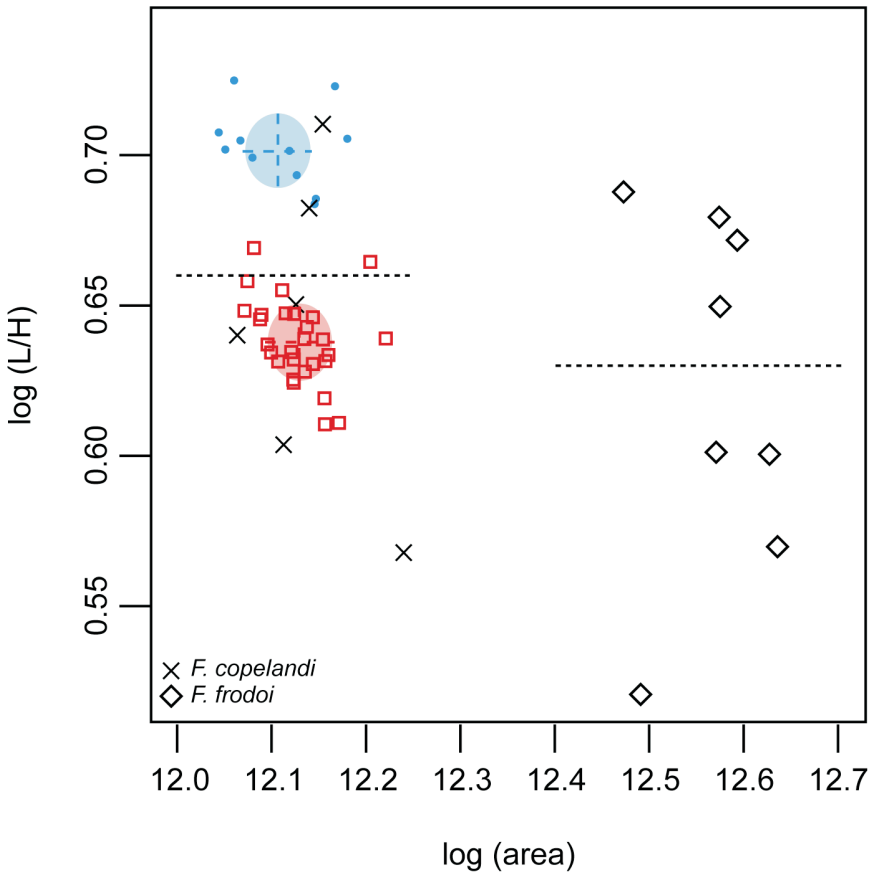

TEXT-FIGURE 12
Size (log area) versus shape (log[L/H]) for *Frodocythereis copelandi* (X) and *Frodocythereis frodoi* (diamonds). Other points are from larger sample of this species analyzed by Hunt et al. (2017, population ANT_COPE-1). Blue circles = male and red squares = female clusters from that analysis, with corresponding colors for the 50% probability ellipses. Dotted line indicates inferred separation between males and females for the specimens figured in this work.

most straight to the ventroposterior margin; the posterior margin in the RV is very bluntly rounded in the ventral part, then straight to a very obtuse dorsoposterior angle; in the LV, the posterior margin is very broadly rounded in ventral part and more curved in dorsal part. A double row of denticles is located very close to the anterior and posterior margins. In dorsal view, the anterior, compressed margin is very narrow, then steps up to the anterior marginal carina, then narrows slightly to the lateral bulge; the lateral margins then rise gently to become nearly flat except for an indentation just in front of mid-length, which corresponds to the sulcus just behind the lateral ring-like carina; the greatest width is just behind this indentation; the posterior margin drops abruptly to form a compressed posterior.

The eye tubercle is high and prominent. A deep postocular sulcus extends from the dorsal margin just anterior of mid-length to below the eye tubercles; the lower boundaries are defined by a prominent carina. The exterior ornamentation consists of a combination of large fossae and prominent muri; an anterior carina extends from the eye tubercle to parallel the anterior margin, becoming closer to the margin ventrally where it disappears at the ventroanterior angle; small, thin, radiating muri extend perpendicularly behind anterior carina and terminate within the sola to form 3-sided rectangular fossae, with muri sometimes connecting the raised sieve-type normal pore canals as apophyses; posterior to the 3-sided anterior fossae is an arc of smooth zone that is continuous from the post-ocular sulcus, continues subparallel to the anterior margin, and terminates at the ventroanterior angle; a prominent; serrated dorsal carina is located in the posterior 2/3 of the dorsum, which connects ventroanteriorly to the lateral ring-like structure in front and slightly above the central muscle scars; a murus extends anteriorly from the lower part of the ring a short distance, then terminates; other large polygonal fossae are located directly below and behind the ring; behind the ring, but not connected to it, is a longitudinal carina, concave up in the anterior part and almost straight and sloping slightly ventrally in the posterior part, that terminates in the flattened posterior region of carapace; four vertical muri extend from the longitudinal carina to the dorsal carina; three large polygonal fossae are located at mid-length and slightly behind, bordered ventrally by two smaller fossae; a prominent concave up carina is located near and parallel to the ventral margin; several rounded fossae are located in the ventral half of carapace; in the LV, a row of square fossae is located between the ventral carina and ventral margin; the posterior part of the RV is flat, but reticulate in LV. There are numerous and scattered sieve-type normal pore canals located mainly in the central part of carapace in both the sola of fossae and in the muri.

Muscle scars are often observed in external view (Pl. 12, figs. 1, 4 and 12).

The hinge is paramphidont (Pl. 12, figs. 7 and 8); the anterior hinge tooth in the RV is stepped, with the lower anterior part that rises to a taller, very gently grooved tooth and subjacent smooth socket; the median groove is straight and crenulate; the posterior tooth is smooth, elongate, and downturned at the dorsoposterior angle; the LV has an anterior grooved socket, a postjacent and smooth tooth, a crenulate median bar, and a smooth posterior socket at the dorsoposterior corner. Internally, the carapace is punctuated by pits that are the inner openings of the sieve-type normal pore canals. The selvage of the RV is split into double-ogee shaped interruption just above mid-height (Pl. 12, fig. 7). A pair of rimmed, inverted platforms are located below and behind the anterior hinge elements (Pl. 12, figs. 7-8 and 11), both of which are elongate parallel to the long axis of the carapace and correspond to the inner part of the postocular sinus; the upper platform is larger than the lower and is acuminate anteriorly, whereas the lower is shaped like a checkmark and acuminate posteriorly. The ocular sinuses are located below and anterior to the anterior hinge elements (Pl. 12, figs. 7 and 8).

The muscle scars (Pl. 3, fig. 8; Pl. 12, figs. 9-11) include dorsal, adductor, frontal and mandibular scars; the F scar lies directly in front of the adductors, in the shape of an open U; a large ovate A-1 scar is located dorsoanteriorly of the other adductor scars and is tilted anterior of vertical; the A-2, A-3 and A-4 scars are intertwined in a yin and yang symbol with an overall circular shape; the A-2 scar is paisley-shaped, with the narrow end that tapers across the A-3 scar; the A-3 scar is small, elongate, and is located at the posterior ends of the A-2 and A4-scars; the A-4 scar is elongate and tilted slightly ventroanteriorly; there are four dorsal scars, nearly all in a horizontal row; the sub-circular D-1 scar is located well in front of others; the reniform D-2 scar lies above the posterior margin of the F scar; the sub-circular D-3 scar lies above the A-1 scar; and the small, sub-circular D-4 scar is located near the posterior end of the adductor scars; the reniform M-1 lies directly below the F scar, with the concave side directed posteriorly; the oval M-2 scar sits well below and posterior of the M1 scar. A pair of rimmed, inverted platforms are located ventroposterior to the anterior hinge element, are somewhat more prominent in RV, and corresponds to the inside of the post-ocular sulcus.

The species is sexually dimorphic, with the male being more elongate and the female being taller and rounder (text-fig. 12).

Remarks: This species is similar to *F. copelandi* (Smith 1978) but differs in being larger; less elongate; with coarser, deeper and fewer fossae; and bears the distinctive ring-like fossa just anterior to the central muscle scar field. It differs from *F.* sp. 1 by having fewer and coarser fossae, being more sub-rectangular and less rounded, and by the presence of the distinctive ring structure.

Range: This species was found only in the Owl Creek Formation (Maastrichtian) type locality in Tippah County, Mississippi, where it occurs abundantly (text-fig. 2).

***Frodocythereis* sp. 1**
Plate 4, Figure 6

Material: 7 valves

Remarks: This species is characterized by very deep, sub-polygonal fossae that extend across the entire carapace except for the postocular depression. The muri are vertical to undercut. The postocular depression forms a saddle along the dorsal margin and bifurcates ventroanteriorly. The anterior marginal depression is separated from the anterior margin by a carina and is subdivided by low and thin muri. It displays all the characters of the subfamily, including sieve-type normal pore canals with raised rims, postocular depression, distinctive muscle scar pattern, stepped anterior tooth in RV, a double ogee-shaped structure at the posterior end of selvage in RV, and a pair of inverted platforms ventroposterior of the anterior hinge element in the RV. It is assigned to *Frodocythereis* n. gen. based on the presence of deep polygonal fossae (except along anterior margin), lack of prominent lobation and compressed posterior margin.

Range: This rare species was found in only one sample (2010-10-22-1(512)) from the latest Campanian-early Maastrichtian Coon Creek Formation of Union County, Mississippi (text-fig. 2).

Genus ***Laevipellacythereis*** Puckett and Hunt **n. gen.**

Etymology: This genus is named after the type species, *Laevipellacythereis laevipellis* n. sp., in reference to the smooth carapace.

Type Species: *Laevipellacythereis laevipellis* gen. et sp. nov. (Pl. 1, fig. 8; Pl. 3, fig. 10; Pl. 14, figs. 1-11; Text-fig. 13).

Diagnosis: The genus *Laevipellacythereis* includes species of the Subfamily to Anticytherideinae that have an almost smooth carapace due celation in which the tegmen has almost completely overgrown any underlying ornamentation (see Sylvester-Bradley and Benson (1971), fig. 30); large, beveled sieve-type normal pore canals surrounded by very small fossae; and subdued lobation.

Species: Species assigned to the genus *Laevipellacythereis* include the type species from the Owl Creek Formation of Maastrichtian age, *L. colossus* n. sp, from the Maastrichtian Providence Sand of eastern Alabama (Pl. 13, figs. 1-11), and *L.* sp. 1 from the latest Campanian-early Maastrichtian Coon Creek Formation of northern Mississippi (Pl. 4, figs. 4-5).

Laevipellacythereis colossus Puckett and Hunt **n. sp.**
Plate 1, figure 7; Plate 3, figure 9; Plate 13, figures 1-11; Text-fig. 13

Etymology: colossus, Latin noun, meaning a large statue, referring to the large size of this species.

Type Specimens: Holotype USNM PAL 771808, specimen 148-7 (Pl. 13, fig. 2, male LV); paratype USNM PAL 771809, specimen 148-9 (Pl. 13, fig. 4, female LV); both specimens from sample 2012-01-03-1-2, Maastrichtian Providence Sand of Barbour County, Alabama

Diagnosis: This species is characterized by the combination of a large, elongate, sub-rectangular carapace; two rows of large fossae parallel to anterior margin, with posterior row forming depression; carapace widest just behind mid-length; and surface punctuated by large, moated sieve pores located within small, shallow fossae.

Material: 11 carapaces and 40 single valves collected from the Providence Sand (Maastrichtian) of Barbour County, eastern Alabama

Measurements: Holotype L = 0.976 mm, H = 0.440 mm; paratype L = 0.827 mm, H = 0.410 mm.

Description: The carapace is large for the genus, and robust. In lateral view, the LV is sub-rectangular, and the RV is oblong, with the greatest height located either at the eye tubercle (RV) or at the dorsolateral swelling just posterior of mid-length (LV). The anterior margin is broadly rounded and infracurvate; the ventral margin undulates in the LV, the RV has the typical podocopid broad concavity at circa 1/3 length; the posterior margin in the LV curves up from the venter rather sharply to form an equicurvate posterior outline; in the RV, the posterior margin curves up broadly from the venter to mid-height, where it sharply becomes concave up to the dorsoposterior angle, which is distinct, to form an infracurvate margin; the dorsal margin is slightly undulatory, with the greatest convexity just behind mid-length. In dorsal view, the carapace is broadly bulged, with a very slight anterior compression, to the greatest width just behind mid-length; the posterior margin is slightly compressed.

The eye tubercle is of low relief, not bulging. A distinct post-ocular depression in the form of a groove extends from just anterior of mid-length to terminate below the eye tubercle; the solum of the post-ocular sulcus is caperate in places (Pl. 13, fig. 4); this sulcus is very deep, and the exterior expression of the internal inverted platform can be seen on some specimens (arrow on Pl. 13, fig. 4). In the relatively larger male, the lateral surface is swollen behind mid-length in upper 2/3 of carapace and forms a dorsal bulge; in the female, the posterior circa 1/5 of the carapace is compressed (Pl. 13, figs. 3 and 4). Two rows of fossae are parallel to the anterior margin; the fossae in the anterior row are generally small, and circular to elongate; the fossae in the second row are elongate parallel to the anterior margin, are separated by thin muri, and form a distinctive, continuous depression. Circular and moated sieve-type normal pore canals always are located in the very small fossae; the sieve plates are sunken below the level of the soli; the soli are rimmed around the sieve pores and may be undercut around their periphery (Pl. 13, fig. 10); the carapace has a small number of foveolae (Pl. 13, fig. 10).

The hinge is paramphidont; the anterior tooth of the RV (Pl. 13, figs. 6 and 8) is stepped and subtly multilobed; the anterior part of the tooth is not as tall and is narrower than the subjacent tooth; a rounded socket is located immediately behind the tooth; the median groove is straight and crenulate, widens towards the extremities, and has a narrow, superjacent groove; the posterior tooth in the RV is elongate and angled across the dorsoposterior angle; the anterior socket in the LV is locellate, the subjacent tooth is rounded, the median bar is straight and crenulate; the posterior socket, which is angled, is located at the dorsoposterior angle; and low stragula are located above the sockets of the LV. The inner margin along the venter upturns at approximately 1/3 length. The marginal zone includes the selvage, selvage groove, inner margin and narrow vestibulum in some specimens; the selvage of the RV is interrupted at the caudal angle by a double ogee-shaped structure (right arrow on Pl. 13, fig. 6). The inner surface of carapace has large, scattered pores that correspond to the inner openings of the sieve-type normal pore canals. Two rimmed, inverted platforms that are elongate parallel to the long axis of the carapace are located ventroposteriorly of interior hinge elements (Pl. 13, figs. 6 (left two arrows) and 8); these platforms correspond to the inner part of the post-ocular depression; the lower platform, which is acuminate anteriorly, is less than half the size of the upper one, which is acuminate posteriorly. The large ocular sinus is located just ventroanterior of the anterior hinge element (Pl. 13, fig. 6).

The F scar is U-shaped (Pl. 3, fig. 9; Pl. 13, figs. 5-9 and 11). The A-1 scar is located above the posterior ends of the other adductor scars and is elongate almost vertically; the A-2 and A-4 scars are intertwined similar to a yin-yang symbol, with the A-2 being bulbous anteriorly and the A-4 tapering anteriorly; the A-3 scar is either very small, missing, or fused with either the A-2 or A-4 scars. The fulcral point is nearly circular, located anterior to the dorsal part of the A-1 scar. The M-1 scar is elongate, tilted slightly anteriorly, and located below the F scar; the M-2 scar is close to the ventral margin, is teardrop shaped, and is acuminate posteriorly. The D-1 scar is located directly below the ocular sinus; the D-2 and D-3 scars are indistinct; no D-4 was observed.

The species is sexually dimorphic, with the female being smaller but more laterally inflated than the male (text-fig. 13).

Remarks: This species is similar to *Laevipellacythereis laevipellis* n. sp. in the lack of reticulation and overall smooth carapace except for distinct sieve-type normal pore canals but differs in the lack of the very broad longitudinal lobes, the presence of the row of elongate fossae parallel to the anterior margin that form a depression, and by the presence of a well-defined, elongate and groove-like postocular sulcus.

Range: This species has been found only in the Providence Sand (Maastrichtian) of Barbour County, eastern Alabama (text-fig. 4).

Laevipellacythereis laevipellis Puckett and Hunt **n. sp.**
Plate 1, figure 8; Plate 3, figure 10; Plate 14, figures 1-11; Text-fig. 13

Etymology: *laevi*, Latin for smooth, and *pellis*, Latin for skin, in reference to the smooth surface.

Type Specimens: Holotype: USNM PAL 771810, specimen 130/135-23 (Pl. 14, fig. 2,female LV); paratype: USNM PAL 771811, specimen 130/135-28 (Pl. 14, fig. 3, male RV); both specimens from sample 2011-8-4-1 (water level), Maastrichtian Owl Creek Formation, Tippah County, northern Mississippi.

Diagnosis: Carapace oblong, surface almost smooth by addition of tegmen, with round sieve-type normal pore canals located inside small, round fossae; four subdued lateral lobes, one along dorsoposterior margin, another at the central muscle scar field, a third, concave up, near the ventral margin, and a subdued lobe parallel to the anterior margin.

Material: 238 valves and 1 carapace

Measurements: Holotype L = 0.762 mm, H = 0.381 mm; paratype L = 0.726 mm, H = 0.333 mm.

Description: The carapace is very robust and oblong; the dorsoanterior outline is slightly concave in the RV and convex in the LV; the anterior margin is broadly rounded and slightly

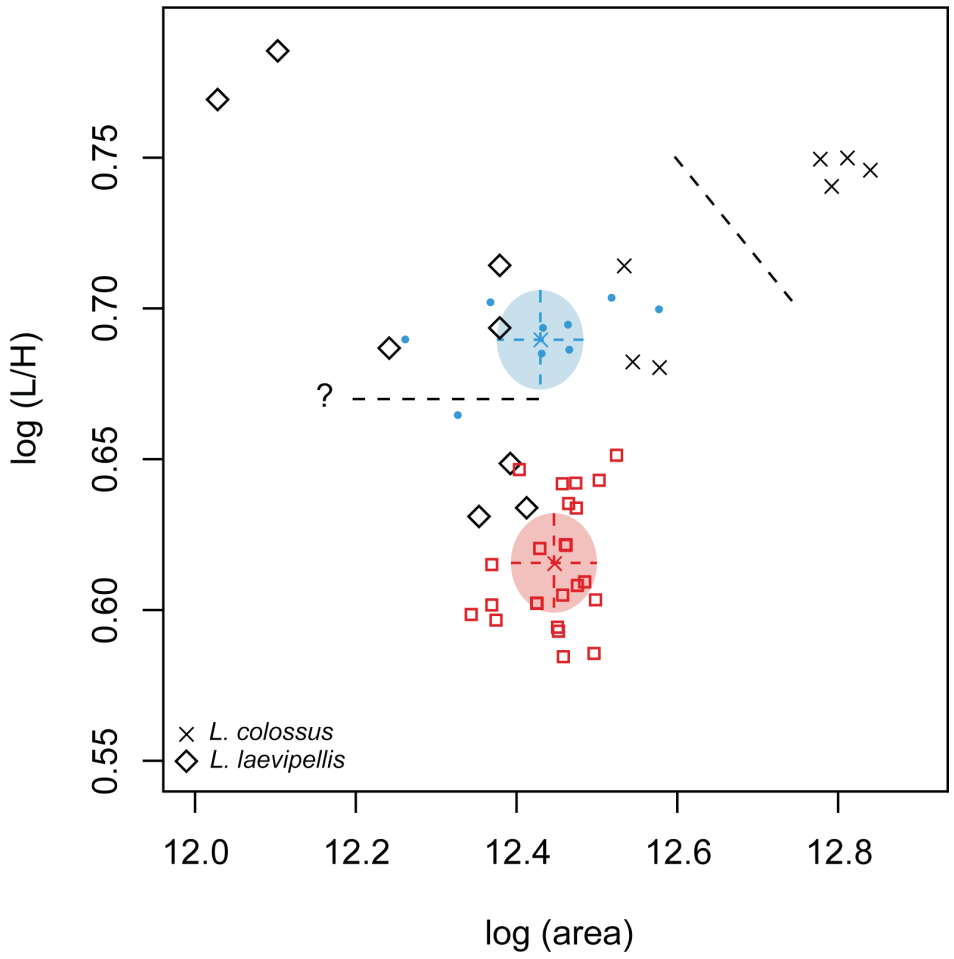

TEXT-FIGURE 13
Size (log area) versus shape (log[L/H]) for *Laevipellacythereis colossus* (X) and *Laevipellacythereis laevipellis* (diamonds). Other points are from larger sample of this species analyzed by Hunt et al. (2017, population ANT_CACU-1-2). Blue circles = male and red squares = female clusters from that analysis, with corresponding colors for the 50% probability ellipses. Dotted line indicates inferred separation between males and females for the specimens figured in this work.

infracurvate; the ventral outline is broadly concave, more so in the RV; the posterior margin in the LV is very broadly rounded, nearly blunt, equicurvate, and becomes nearly straight along the dorsoposterior margin; the ventral part of the posterior margin in the RV is very broadly rounded and the upper part is concave, forming a distinct angle near mid-height; the dorsal silhouette is slightly humped at circa ¾ length due to the bulging of the dorsoposterior lobe above the hinge line. In dorsal view, the carapace has three bulges, each rising progressively higher posteriorly: one just behind the anterior margin, another just in front of mid-length, and the other just behind mid-length; the greatest width is at the third bulge; the anterior and posterior margins are not compressed but rise gently from the ends.

There are four lobes on the lateral part of the carapace: one is dorsoposterior, another is ventral, a third is subcentral, and the fourth is parallel to the anterior margin; the intervening sulci are shallow and more distinct in the male; the dorsoposterior lobe is located at ¾ length and rises above the level of the hinge; the ventral lobe rises gently from the anterior to its maximum height directly below the dorsoposterior lobe; and the subcentral lobe, which is the smallest, corresponds in location to the central muscle scar field.

The eye tubercle is indistinct. The anterior area has very gentle costae that are sub-parallel to the outer margin. The lateral surface is almost smooth except for the small circular fossae that contain the sieve-type normal pore canals; these regions appear to be three-tiered: the external carapace forms the upper tier, which is undercut in many specimens (Pl. 14, fig. 9), the soli of the fossae form the middle tier, and the sieve plate forms the lower tier; the soli surrounding the sieve plate are rimmed.

The hinge is paramphidont (Pl. 14, figs. 5-8); the anterior tooth of the RV has a narrow anterior part that steps up to a taller, multilobate tooth; the subjacent socket is smooth; the median groove is crenulate and widens towards the extremities, and a large posterior tooth that arches across the dorsoposterior angle; the socket in the LV is loculate to accommodate the multilobed complementary tooth; the subjacent tooth is blunt; the median bar is straight, thin and crenulate, and widens very slightly near the posterior terminus; and the posterior socket is loculate, arched across the dorsoposterior angle, and with a ventral rim.

The inner surface is punctuated by scattered pores that correspond to the openings of the sieve-type normal pore canals on the outer surface. The inner margin is relatively wide and distinct; the selvage is a distinct, narrow rim; marginal in-folds are broadest anteriorly and posteriorly. The posterior caudal region of the RV has an interruption of the selvage that forms a double ogee-shaped structure (arrow on Pl. 14, fig. 8), with no complementary structure in the LV. A pair of rimmed internal platforms (Pl. 14, figs. 5, 7 and 8) that corresponds to the inside of the postocular sulcus is located just behind and ventral to the anterior hinge element; the upper platform is larger and acuminate anteriorly and the lower, smaller platform is acuminate posteriorly. The ocular sinus is located just below and anterior to the anterior hinge element.

The muscle scars (Pl. 3, fig. 10; Pl. 14, figs. 6-8 and 10) include a U-shaped F scar, rotated slightly anteriorly; the ovate A-1 scar is oriented at 300° (in RV), acuminate at the upper end, and located above the posterior part of the other adductor scars; the A-2, A-3 and A-4 scars intertwine similar to a yin-yang symbol in the overall form of a circle; the A-2 is large and paisley-shaped, oriented horizontally, and narrows between the A-1 and the lower scars; the A-3 scar is very small and squeezed between the posterior ends of the A-2 and A-4 scars. The A-4 scar is of intermediate size, oblong and oriented at 50° (in LV). A pair of mandibular scars lie directly below the F scar, with the upper, kidney-shaped M-1 being smaller and above the U-shaped M-2, which is close to the ventral margin. The small dorsal scars include one located between the anterior hinge element and the central muscle scars, and a vertical pair located behind the interior platforms (Pl. 14, fig. 7).

Species is sexually dimorphic, with the female more inflated and slightly larger; the male are slimmer, with a very gentle, elongate sulcus along central part of lateral swelling (text-fig. 13).

Remarks: This species differs from the others in the Subfamily Anticytherideinae by having very small, round fossae that encircle the sieve-type normal pore canals. There are, therefore, three tiers at these locations: the outer carapace is the upper tier, which is undercut around the fossae, very narrow soli form the second tier, and the sieve plates form the lower tier.

This species differs from *L. colossus* by being more inflated laterally; by the presence of the four lateral lobes; by having more rounded anterior and posterior margins; and by being very slightly rather than strongly infracurvate. It differs from *Laevipellacythereis* sp. 1, which was found in the Coon Creek Formation of latest Campanian-early Maastrichtian age, by the presence of a smooth and lobate carapace, but differs in having a smooth anterior region, rather than having a depressed line of fossae that parallels the anterior margin and being more elongate.

Range: This species was found in the Owl Creek Formation of Tippah County, Mississippi and in the Providence Sand (both Maastrichtian) of Barbour County, eastern Alabama (text-figs 2 and 4). This is the only species in this study to be found across the field area, ranging from northern Mississippi to eastern Alabama.

***Laevipellacythereis* sp. 1**
Plate 4, figures 7 and 8

Material: Only 9 valves were collected

Remarks: This species is very similar to *Laevipellacythereis colossus* n. gen., n. sp., differing mainly in outline, with a less infracurvate anterior margin, and the carapace is less elongate and more sub-rectangular. As both male and female were collected of both species, the difference between the two species cannot be attributed to sexual dimorphism. It is morphologically intermediate between *L. colossus* and *L. laevipellis*. It is likely that *L.* sp. 1 is the ancestor to both *L. laevipellis* and *L. colossus*.

Range: All specimens were found from a single sample (2010-10-22-1(512)), collected from the latest Campanian-early Maastrichtian Coon Creek Formation of Union County, Mississippi (text-fig. 2).

Genus ***Tumulocythereis*** Puckett and Hunt **n. gen.**

Etymology: This genus is named after the type species, *Tumulocythereis tumulus* sp. nov, in reference to the characteristic lobation of the species.

Type Species: *Tumulocythereis tumulus* n. gen et sp. nov. (Pl. 2, fig. 4; Pl. 3, fig. 14; Pl. 18, figs. 1-14; Text-fig. 15).

Diagnosis: Species of the genus *Tumulocythereis* are characterized by a combination of a diagonal swelling of the carapace that extends from just in front of the dorsoposterior angle to below the subcentral tubercle, with an intervening sulcus; external carapace drops off steeply from lateral swelling to form compressed posterior region; carapace completely reticulated, with subrounded to polygonal fossae.

Species: Species that are assigned to *Tumulocythereis* from this study include the type species from the Owl Creek Formation of northern Mississippi and the Prairie Bluff Chalk from eastern Mississippi and central Alabama, all of Maastrichtian age; *T. priddyi* (Smith 1978) from the Owl Creek Formation and Prairie Bluff Chalk of central Alabama; *T. tiberti* n. sp. from the Coon Creek Formation of northern Mississippi of latest Campanian-earliest Maastrichtian age, the Owl Creek Formation and the Prairie Bluff Chalk; and *T.* sp. 1 from the Coon Creek Formation of northern Mississippi and the Ripley Formation of latest Campanian-Maastrichtian of central Alabama.

Remarks: Species of the genus *Tumulocythereis* differ from species of *Anticythereis* by a more even dorsal outline (without the dorsal shoulder), by the presence of a large ventrolateral lobe, and by the absence of prominent carinae. They differ from species of *Asculdoracythereis* by the presence of lateral lobes and much more inflated carapaces and the smoother dorsal outline uninterrupted by a dorsal carina. They differ from species of *Laevipellacythereis* by the presence of large fossae.

Tumulocythereis incompta Puckett and Hunt **n. sp.**
Plate 2, figure 1; Plate 3, figure 11; Plate 15, figures 1-14; Text-fig. 14

Etymology: incomptus, Latin meaning unadorned, in reference to the lack of reticulation.

Type Specimens: Holotype: USNM PAL 771812, specimen 142-11 (pl. 15, fig. 1, male RV); paratype: USNM PAL 771813, specimen 142-10 (Pl. 15, fig. 3, female RV); both specimens from sample 2011-8-4-1 (water level), Maastrichtian Owl Creek Formation, Tippah County, Mississippi.

Diagnosis: This species is characterized by a relatively smooth carapace except for moderately sized, subcircular fossae associated with sieve pores, very broad muri, and very subtle diagonal sulcus on LV.

Material: 158 valves

Measurements: Holotype L = 0.696 mm, H = 0.309 mm; paratype L = 0.654 mm, H = 0.298 mm.

Description: The carapace is of medium size for the genus, elongate, sub-rectangular, and robust. The greatest height is at the eye tubercle and the greatest length is at or near mid-height. The dorsal outline is slightly undulating, with a hump at the eye tubercle that corresponds to the low stragula; the lateral swelling of the carapace bulges slightly above the hinge behind mid-length; the anterior margin is broadly and evenly rounded and slightly infracurvate; the ventral margin in the RV has the typical concavity at 1/3 length that corresponds to the upturned ventral margin; the ventral margin in the LV is either straight or slightly convex; the posterior margin in the LV is very broadly rounded and equicurvate; in the RV, the ventral half of the posterior margin is very gently convex, but at mid-height, the posterior margin becomes concave to just below the dorsoposterior angle. In dorsal view, the carapace outline rises gently from the anterior margin in a very broad convexity to the greatest width at approximately 4/5 length, then slopes sharply down to the compressed posterior margin.

The eye tubercle is a subtle, smooth area, not bulged. A prominent postocular sulcus extends from just below the dorsal margin to below the eye tubercle, with the dorsal part being horizontal, then bends down below the eye tubercle; in some specimens, the postocular sulcus is broken into sub-rectangular cells defined by apophyses (Pl. 15, fig. 4); a gentle, diagonal sulcus extends from near the dorsal margin behind mid-length, across the middle region to terminate above the ventroanterior angle. The lateral surface of the carapace is almost completely covered by fossae and intervening wide muri; distinctive but small, circular fossa punctuate the smooth zone that is laterally adjacent to the eye tubercle; there is an anterior row of small fossae very close to the anterior margin that is bordered posteriorly by a low carina, with the fossae being slightly elongate parallel to the anterior margin; there is a row of large, sub-rectangular fossae just behind the low anterior carina, with the long axes parallel to the anterior margin; the fossae in the region of the subcentral tubercle are small relative to those behind it; the posterior part of the LV has small, marginal fossae that are very close to the posterior margin and bordered by a low carina, similar to those near the anterior margin; a row of large, subcircular fossae is located in front of the low carina, and extends from the dorsoposterior angle to below the lateral bulge behind mid-length. Sieve-type normal pore canals with raised rims occupy the soli sub-centrally (Pl. 15, figs. 9 and 12), and the margins of the fossae undercut the carapace; the carapace within small fossae appears to be three-tiered, with the upper tier being the muri, the middle tier being the soli, and the lower tier being the sieve plate (Pl. 15. figs. 9 and 11); the sieve pores are uniform in size, despite variation in size of the surrounding fossae; the openings in the sieve plates are of irregular geometry that surround a central opening; in some sieve plates, relatively strong bars connect the central opening to the margins of the plate; the soli are moated, with maximum depth slightly more than half way from the sieve pore rims to the margins (Pl. 15, figs. 9 and 12); the soli display subtle caperation (Pl. 15, fig. 12); the entire lateral surface is punctuated by microstructural tubes within the crystal fabric, with no preferred orientation.

The hinge is paramphidont (Pl. 15, figs. 5-8 and 10); the RV has a stepped anterior tooth, with a low, narrow and lobate anterior part that steps up to a taller multilobate tooth; the postjacent socket is smooth; the median groove is straight, crenulated, and bordered dorsally by a thin bar; the posterior tooth is crenulated and arches across the dorsoposterior angle; in the LV, the anterior socket is grooved in the lower part to accept the complementary tooth; the median bar is crenulate and extends to the dorsal parts of the anterior and posterior sockets; the posterior socket is angled, bordered dorsally by bar and groove, and forms dorsal bulge (stragulum) at the dorsoposterior angle. The anterior, ventral, and posterior margins have a selvage, selvage groove, and list; the ventral margin is typically upturned at 1/3 length; the marginal zone is relatively wide, particularly along the posterior and anterior regions, with no distinct vestibule; the RV has the distinctive double ogee-shaped structure that interrupts the selvage in the caudal region (arrow on Pl. 15, fig. 8), with no corresponding structure in the LV; scattered, large pits in the interior correspond to external sieve-type normal pore canals; the ventroanterior and ventroposterior regions have small, blunt denticles very close to the margins. Two distinctive, elongate, rimmed inverted platforms are located below the anterior part of the median hinge bar (Pl. 15, figs. 10 and 13-14), which may represent attachment points of muscles and tendons; the upper platform is larger and acuminate anteriorly; the upper platform is smaller and acuminate posteriorly. The ocular sinus is at the ventroanterior border of anterior hinge elements.

The muscle scars (Pl. 3, fig. 11; Pl. 15, fig. 14) have a V-shaped F scar; the A-1 scar is elliptical, angled at circa 320° (in RV), and lies above the posterior part of the other adductor scars; the A-2, A-3 and A-4 scars intertwined in the pattern of a yin-yang symbol, with an overall circular shape; the A-2 scar is paisley-shaped, tapers posteriorly over the A-3 scar, and is angled ventroanteriorly; the A-3 scar is small and slightly elongate, and is sandwiched between the posterior ends of the A-2 and A-3 scars; the A-4 scar is elliptical and angled ventroanteriorly; the M-1 scar is located ventrally of the F scar, is elongate and narrow, and is angled ventroposteriorly; the M-2 scar is located near the ventral margin, is narrow and angled ventroposteriorly, and is crescent shaped; the D-1 scar is located below the ocular sinus, is nearly circular and small; the D-2, D-3 and D-4 scars are small, circular, evenly distributed horizontally above the central muscle scar field near dorsal margin; the fulcral point is a depression located in front of the A-1 scar between the adductor scars and the F scar.

The species is sexually dimorphic, with the female being shorter and rounder and the male being more elongate (text-fig. 14). The lateral sulci in the male is slightly deeper than the female, which is more inflated.

Remarks: This species is distinctive in having very wide muri that separate the relatively small, subcircular fossae. Among the species of *Tumulocythereis* n. gen., *T. incompta* is most similar to *T. tumulus*, as *T. priddyi* and *T. tiberti* have well developed reticulation and more elevated lobation. It differs from *T. tumulus* in being less elongate; the anterior and posterior marginal zones are also less compressed. This is the oldest species of the genus and may be the ancestor.

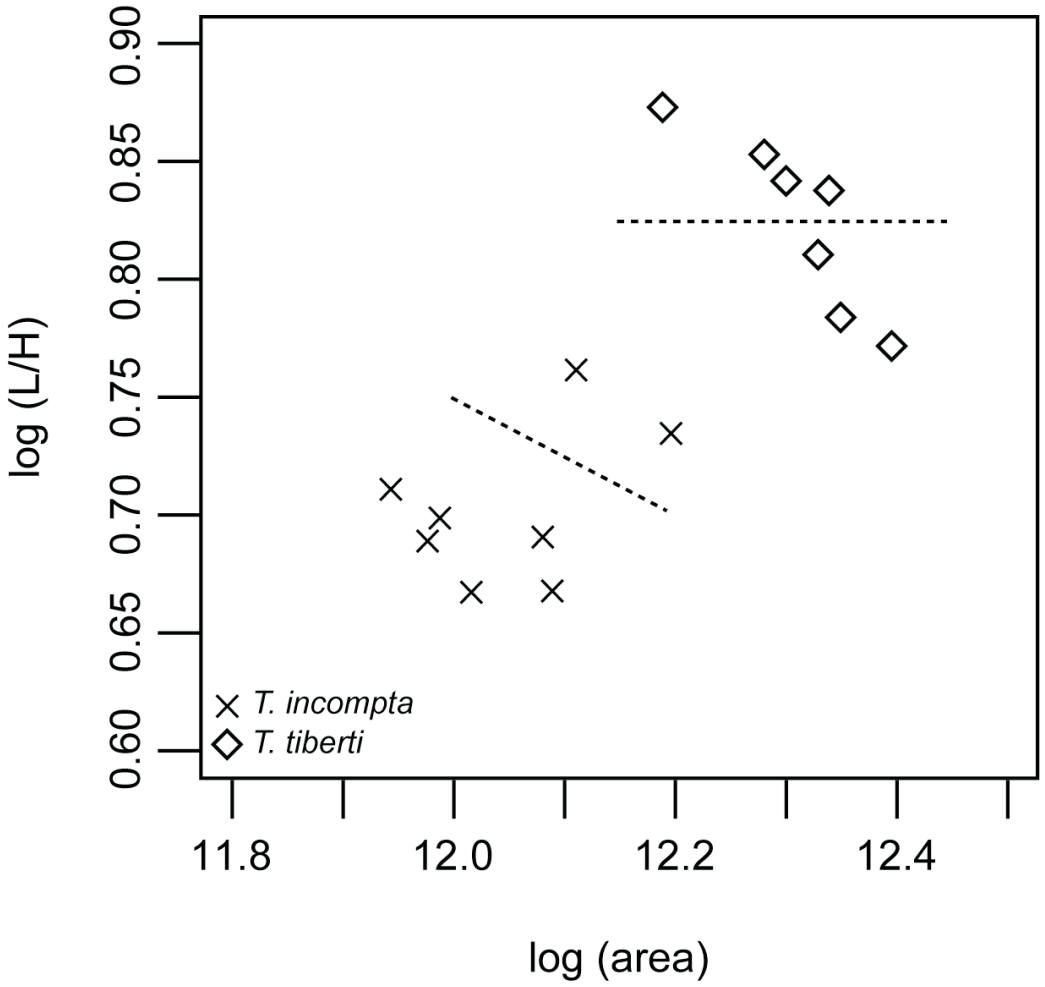

TEXT-FIGURE 14
Size (log area) versus shape (log[L/H]) for *Tumulocythereis incompta* (X) and *Tumulocythereis tiberti* (diamonds). Dotted line indicates inferred separation between males and females for the specimens figured in this work.

Range: This species was found in the Coon Creek Formation (latest Campanian-early Maastrichtian) of northern Mississippi, the Owl Creek Formation (late Maastrichtian) of the type locality in Tippah County, Mississippi, where it may be abundant, and in the Prairie Bluff Chalk (late Maastrichtian) of central Alabama (text-figs 2 and 4).

Tumulocythereis priddyi Smith 1978
Plate 2, figure 3; Plate 3, figure 12; Plate 16, figures 1-13; Text-fig. 15

Carinocythereis (?) *priddyi* SMITH 1978, p. 553-554, pl. 5, figs. 8-10.

Type Specimens: The type specimens were collected from the Prairie Bluff Chalk (Maastrichtian) of Lowndes County, central Alabama. All three type specimens are LVs: holotype (USNM PAL 255717) and paratypes USNM PAL 255718 and USNM PAL 255719 (Pl. 16, fig. 2). Another specimen that is recorded as being from the type locality is catalogued at the USNM PAL as number 642412, which has a broken dorsoposterior margin, and is not illustrated here. In all these specimens, the fossae have considerable adventitious material that obscures their details. Adventitious material covers the ventral and anterior regions of the holotype, which completely obscures the morphology in these regions. Debris also covers the muscle scars in paratype USNM PAL 255418 (not illustrated here).

Diagnosis: None given, but Smith (1978) described the species. Smith stated that the generic assignment was uncertain and suggested that the species may represent a new genus.

Emended Diagnosis: Carapace elongate, sub-rectangular; carapace rises from anterior region to approximately 4/5 length, where it drops off sharply to posterior compressed zone; ventral margin concave in both LV and RV; posterior and anterior margins nearly symmetrical in LV; fossae subrounded, cover entire carapace, with moderately wide muri.

Material: 195 valves

Remarks: The fossae are typically round to highly elliptical; in some case, adjacent fossae seem to have merged, with an apophysis that extends to the raised sieve pores (arrow on Pl. 16, fig. 11), although the single sieve-type normal pore canal within indicates a single, invaginated fossa. The species displays the characters typical of the genus, including the

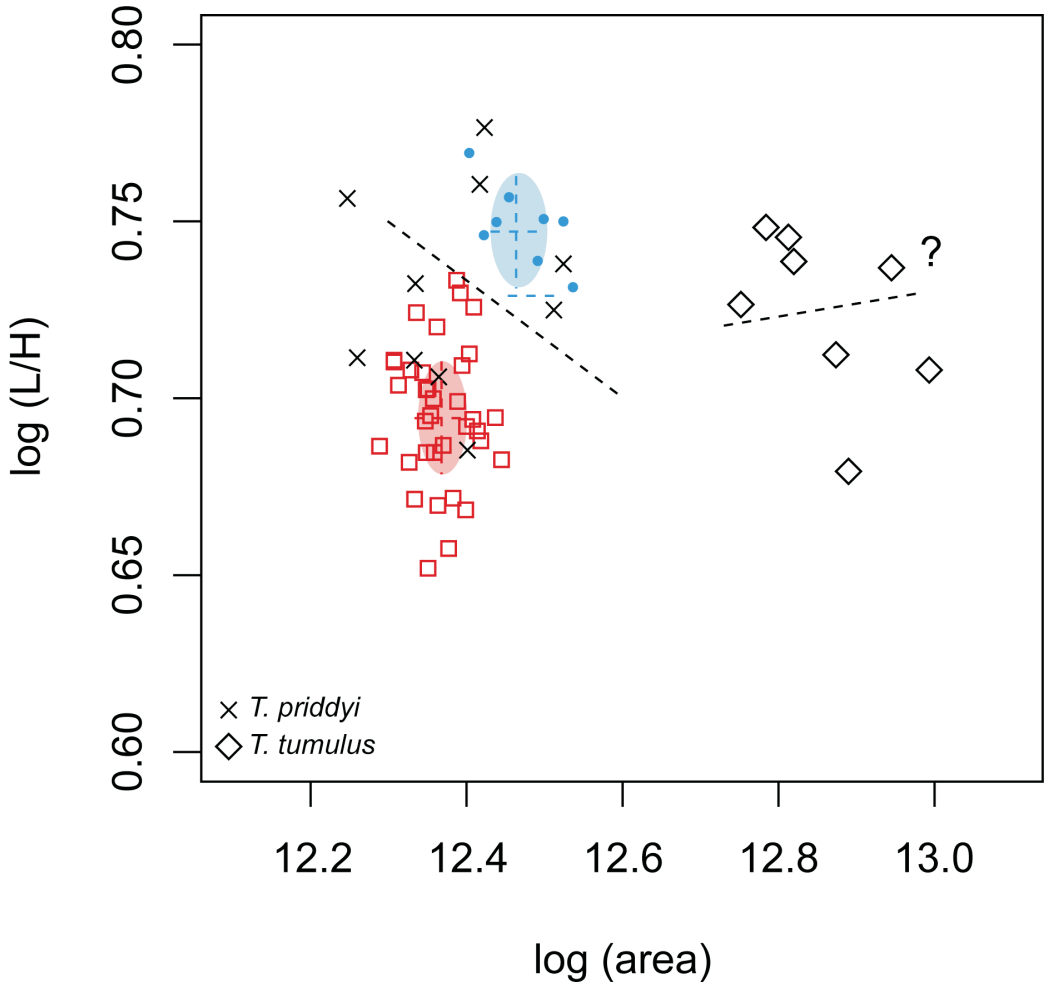

TEXT-FIGURE 15
(A) Size (log area) versus shape (log[L/H]) for *Tumulocythereis priddyi* (X) and *Tumulocythereis tumulus* (diamonds). Other points are from larger sample of this species analyzed by Hunt et al. (2017, population CAR_PRID-1). Blue circles = male and red squares = female clusters from that analysis, with corresponding colors for the 50% probability ellipses.

postocular sulcus that extends from the dorsal margin just anterior of mid-length to below the bulged eye tubercle; the hinge in RV has a stepped anterior tooth, with lower anterior part lobed that steps up to a taller lobed postjacent tooth; the posterior tooth is crenulated and angled arched across the dorsoposterior angle; the selvage is interrupted at the caudal region of the RV by a double ogee-shaped structure (arrow on Pl. 16, fig. 8), with no corresponding structure in the LV; the A-2, A-3 and A-4 scars are intertwined in the shape of yin-yang symbol, with a dorsally offset, elliptical, and tilted A-1. A pair of rimmed, fusiform inverted platforms is located below and ventral of the anterior hinge element, corresponding to the interior of the postocular sulcus, that are possibly related to the attachment point of the inner lamella at the anterior isthmus (arrows on Pl. 16, fig. 10). In this species, the rimmed sieve-type normal pore canals are typically on the margins of fossae, rather than in the center (Pl. 16, fig. 11). Some of the rimmed sieve-type normal pore canals are located on a low murus within a fossa (see arrow on Pl. 16, fig. 11); the small openings of the sieve plate are arranged concentrically around the central opening; the margins of fossae undercut surrounding muri (Pl. 16, figs. 11 and 12). The carapace has foveolate muri, with foveolae being subparallel to the margins of fossae and separated from them by narrow smooth strip (Pl. 16, fig. 11).

T. priddyi is distinctive in being relatively elongate and sub-rectangular. It is very similar to *T. tiberti* n. sp., but is less elongate, less compressed posteriorly, more infracurvate and less constricted vertically near mid-length. It differs from *T. tumulus* in having more dense reticulation, is more sub-rectangular, has more subtle lobation and lacks the strong marginal carinae. The density of the reticulation is variable, with some specimens having narrower intervening muri (i.e., the paratype specimen, Pl. 16, fig. 2) and others having wider intervening muri (Pl. 16, figs. 3-6). Sexual dimorphism is observed with male being more elongate than female (text-fig. 15).

Range: Smith (1978) described this species based on specimens collected from the Prairie Bluff Chalk (Maastrichtian) of Lowndes County, central Alabama. All but one of the specimens collected for this study were from the Owl Creek Forma-

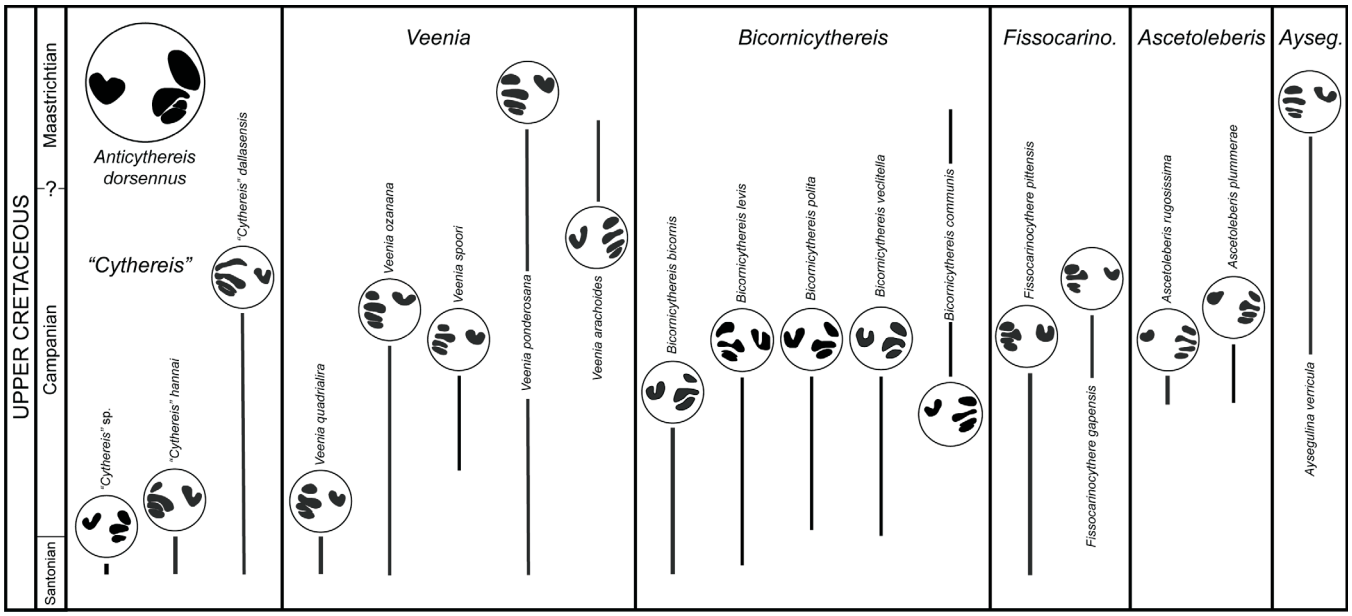

TEXT-FIGURE 16
Comparison of the central muscle scars of representative trachyleberid ostracod species from the U.S. Gulf Coastal Plain. Ranges of the species is based on Puckett (2005) and Puckett (2012). The *Fissocarino* refers to *Fissocarinocythere* and *Ayseg* refers to *Aysegulina*.

tion (Maastrichtian) of Tippah County, northern Mississippi. The lone exception was collected from Smith's type locality (a topotype specimen). This species, therefore, ranges in the Maastrichtian from central Alabama to northern Mississippi and is among the most widespread species of the genus (text-figs. 2 and 4).

Tumulocythereis tiberti Puckett and Hunt **n. sp.**
Plate 2, figure 2; Plate 3, figure 13; Plate 17, figures 1-11; Text-fig. 14

Etymology: Named in honor of Neil Tibert of the University of Mary Washington, who passed away Dec. 20, 2015, for his contributions to the study of Cretaceous ostracods of North America.

Material: 99 valves.

Type Specimens: Holotype: USNM PAL 771814, specimen 130/135-18 (Pl. 17, fig. 3, female RV) from sample 2011-8-4-1 (water level), Maastrichtian Owl Creek Formation, Tippah County, Mississippi.

Diagnosis: Carapace very elongate, medially swollen with dorsal sulcus in the middle in lateral view, widening at the ends; polygonal fossae cover the carapace in leopard-like pattern; carapace highly inflated laterally, rising towards the posterior to drop off abruptly to highly compressed ventroposterior margin, forming a diagonal lobe with median sulcus; configuration of fossae just in front of the central muscle scar field as viewed from outside distinct from rest of carapace, with small, round fossae near the scars and elongate fossae more anteriorly.

Description: The carapace is elongate, with the greatest height at the eye tubercle; the anterior margin is slightly infracurvate and broadly rounded; the posterior margin in the LV is very slightly infracurvate, with an obtusely angled caudal region; the ventroposterior margin in the RV is infracurvate, with an obtuse angle located below mid-height, and a straight dorsoposterior margin. Short, blunt denticles are located just above the margins in the ventroanterior and ventroposterior regions; the venter in the LV of male (Pl. 17, fig. 2) is very slightly concave to about ¾ length where it turns down to form the rounded ventroposterior margin; the dorsal margin is straighter than in the male. In dorsal view, the carapace outline is sagittate; the anterior margin rises to the anterior marginal carina, then tapers at the post-carina sulcus, then rises to the greatest width at approximately 4/5 length; there is a slight bulge at the subcentral tubercle; the posterior margin drops abruptly and convexly from the greatest width to the highly compressed posterior margin.

The eye tubercle is a distinctive smooth area near the dorsoanterior angle but bulges only slightly. There is a very prominent, diagonal, slightly arcuate (concave up) lateral swelling that extends from the dorsoposterior margin and becomes imperceptible near the ventral margin at about 1/3 length; the sub-central tubercle area is on a slight platform; and the posterior part of the carapace behind the lateral swellings is very compressed and forms a nearly vertical step up to the lateral swelling. The external ornamentation is a complex combination of fossae, foveolate muri and rimmed sieve-type normal pore canals. Fossae completely cover the exterior surface; a line of fossae that are subquadrate is located just behind the anterior margin at mid-height that become sub-rectangular near the dorsal and ventral margins; behind that is a line of large subquadrate fossae; the rest of the carapace is generally covered with medium-sized, rounded, polygonal fossae aligned in rows parallel to the outline; the fossae in the subcentral platform are small and more complex, particularly within muscle scar field; muscle scars are often clearly seen in external view (Pl. 17, fig. 11), with muri conforming to the scar outlines. Sola of fossae

are generally smooth but slightly caperate in some fossae (Pl. 17, fig. 7). The muri are foveolated, with foveolae aligned in uni-, bi- and multi-serial rows subparallel to muri (Pl. 17, figs. 8, 10 and 11). Rimmed sieve-type normal pore canals generally are located in the sola of scattered fossae in the central part of carapace but are not present in every fossa.

The hinge is holamphidont (Pl. 17, figs. 5 and 6); the anterior tooth in the RV is stepped, with a lower, grooved anterior part that rises up to a grooved subjacent tooth; the median element is a straight, crenulate groove that widens towards the extremities; the posterior tooth is tilted at circa 45° across the dorsoposterior angle; the LV has an anterior, elongate socket, subjacent and small tooth, straight and crenulate median bar that forms a shelf below the dorsal margin, and a subrounded posterior socket. The inner surface of the carapace is generally smooth except for the openings of the sieve-type normal pore canals; the sieve plate can be observed in internal view in some thin-shelled specimens (Pl. 17, fig. 9). The selvage in the RV is interrupted by a double ogee-shaped structure at the caudal region (which is abraded on the specimen in Pl. 17, fig. 6), with no corresponding structure in the LV. A pair of rimmed, fusiform inverted platforms is located behind and below the anterior hinge elements and directly above the central muscle scar field (arrows on Pl. 17, fig. 9); these platforms are located on the inside of the postocular sulcus; the larger, upper platform is acuminate anteriorly, and the smaller, lower platform is acuminate posteriorly. A large, prominent ocular sinus is subjacent to the anterior hinge element.

The muscle scar field (Pl. 3, fig. 13, Pl. 17, figs. 5-9 and 11) includes an open V-shaped F scar. The adductor set includes a vertical column of four scars; the A-1 scar is ovoid, tilted forward dorsally and lies above the posterior ends of the other adductor scars; the A-2, A-3 and A-4 scars are intertwined like a yin and yang symbol in an overall circular pattern; the A-2 scar is paisley shaped, with the posterior tapering above the A-3 scar; the A-3 scar is very small and circular, and sandwiched between the posterior margins of the A-2 and A-4 scars; the A-4 scar is oblong and points towards the ventroanterior margin. There are two mandibular scars; M-1 lies directly below the F scar in a posteriorly directed parenthesis shape; the M-2 appears to be two small, circular scars that are close to the ventral margin. The dorsal scars include a small subcircular anterior scar (D-1) located directly below the eye tubercle, a pair of small elongate scars (D-2 a and b) that are located behind the tubercle, a small ovoid scar (D-3) that is well back from the D-2 pair, and a small, lower, centrally located sub-rectangular scar (D-4).

The species is sexually dimorphic, with the male being more elongate than the female (text-fig. 14); the ventral margins of the male are more concave than the female (compare Pl. 17, fig. 2 to fig. 4). The male are distinguished from the female also by a constriction in the height of the carapace at mid-length.

PLATE 1

Morphology of fossae and maps of normal pore canals in Anticytherideinae Ostracoda. Note the color scheme that denotes whether the pore was mapped based on an inner view, outer view, combined view (position estimated by mapping a mid-way point between the same pore as viewed from the inside and from the outside), and estimated position based on other specimens.

1 *Oertliella horridula* (Bosquet 1854) showing homologous fossae and conation in upper Maastrichtian tuffaceous chalk of Maastricht from Liebau (1977, fig. 10). Alphanumeric code reflects interpreted homology.

2 *Aysegulina ornata* (Bosquet 1847), coding and locality as above. This species was traditionally placed in the genus *Limburgina* Deroo 1966, but Özdikmen (2010) discovered that the name had previously been used by Laurentiaux (1950) for a genus of Carboniferous insects. Özdikmen then substituted the name *Aysegulina* for *Limburgina*.

3 *Asculdoracythereis lowndesensis* (Smith 1978), LV, based on SEM image of specimen 134-18 (closeup of external morphological features on Pl. 10, fig. 9). Pores mapped on basis of external view only.

4 *Asculdoracythereis asculdora* n. gen., n. sp., LV, based on SEM image of specimen 148-3 (Pl. 8, fig. 4). Pores mapped on basis of external view only.

5 *Asculdoracythereis pseudoalabamensis* n. gen., n. sp., RV, based on SEM image of specimen 147-6 (internal views on Pl. 7, figs. 7 and 8). Pores mapped on basis of external view only.

6 *Asculdoracythereis invicta* n. gen., n. sp., LV, based on SEM images of external view of specimen 147-12 (Pl. 9, figs. 2 and 11) and inner pores (specimen 147-14, Pl. 9, fig. 5).

7 *Laevipellacythereis colossus* n. gen., n. sp., RV, based on SEM images of external view of specimen 148-8 (Pl. 13, figs. 1 and 9).

8 *Laevipellacythereis laevipellis* n. gen., n. sp., LV, based on SEM images of external view of specimen 130-5 (internal view on Pl. 14, fig. 5).

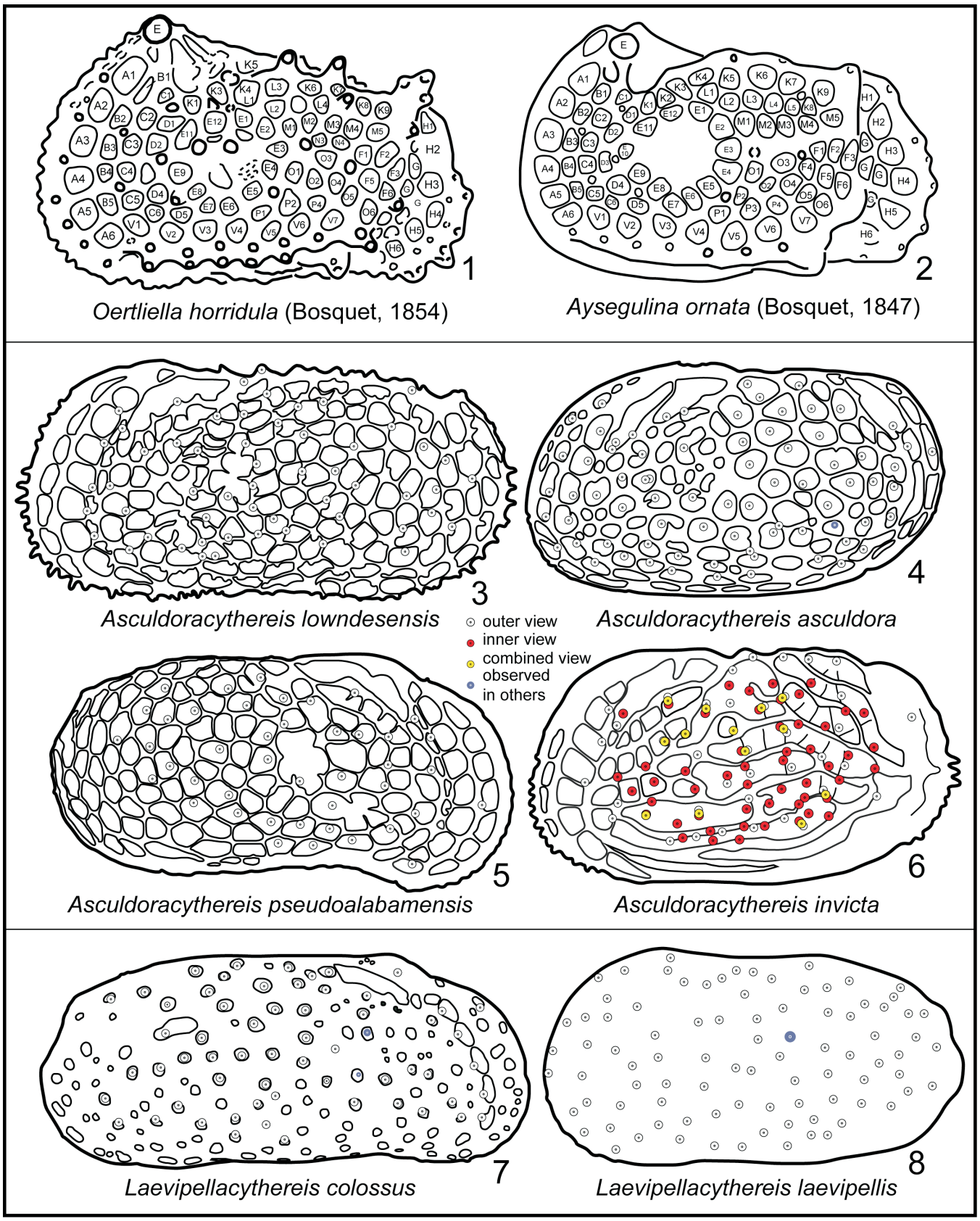
1
Oertliella horridula (Bosquet, 1854)
2
Aysegulina ornata (Bosquet, 1847)
3
Asculdoracythereis lowndesensis
4
Asculdoracythereis asculdora
outer view
inner view
combined view
observed
in others
5
Asculdoracythereis pseudoalabamensis
6
Asculdoracythereis invicta
7
Laevipellacythereis colossus
8
Laevipellacythereis laevipellis

Remarks: This species is distinctive in being highly elongate and constricted medially, creating a sagittate posterior margin, particularly in the LV. The lateral lobes are highly inflated relative to the compressed ventroposterior margin. The reticulation becomes fine and complex above the central muscle scar field, and the muscle scars are often visible in exterior view (Pl. 17, figs. 7-8 and 10). Unfortunately, the carapace of this species is susceptible to breaking, due possibly to a relatively thin carapace and the mid-length constriction. Several specimens were broken in attempts to clean the specimens and during handling. Thus, no paratype has been designated.

Range: This species was observed from the Coon Creek Formation (latest Campanian-early Maastrichtian) of Union County, northern Mississippi, the Owl Creek Formation (late Maastrichtian) type locality in Tippah County, northern Mississippi, and Prairie Bluff Chalk (late Maastrichtian) of Lowndes County, central Alabama (text-figs 2 and 4).

Tumulocythereis tumulus Puckett and Hunt **n. sp.**
Plate 2, figure 4; Plate 3, figure 14; Plate 18, figures 1-14; Text-fig. 15

Etymology: *tumulus*, Latin for mound, barrow, or hillock, in reference to the distinctive lateral swellings of the carapace.

Type Specimens: Holotype: USNM PAL 771815, specimen 143-6 (Pl. 18, figs. 1 and 13, female RV); paratype: USNM PAL 771816, specimen 143-7 (Pl. 18, figs. 4 and 10; male LV); both specimens from sample 2011-5-18-1 (water level), Maastrichtian Owl Creek Formation.

Diagnosis: This species is characterized by three prominent swellings on the lateral carapace: a subcentral tubercle, an arcuate ventral lobe, and a dorsoposterior lobe; the subcentral and dorsoposterior lobes form a shoulder in front of which is the post-ocular depression; the fossae are generally subrounded and with wide muri.

Material: 54 valves

Measurements: Holotype L = 0.738 mm, H = 0.345 mm; paratype L = 0.750 mm, H = 0.369.

Description: The carapace is elongate and robust; the carapace outline is constricted vertically; the anterior margin is broadly and evenly curved, and very slightly infracurvate; the ventral margin is incurved; the posterior margin in the LV is broadly and evenly rounded and slightly supracurvate; the posterior outline in the RV is evenly convex in the lower half, gently concave in the upper half, and angled at mid-height; the dorsal margins are straight, but have stragula above the terminal hinge elements that form a concave mid-dorsum that is eclipsed by the dorsoposterior lobe. There are denticles very close to the ventroanterior and ventroposterior margins. The carapace outline in dorsal view is flat and compressed anteriorly, then rises gently to slight bulge at 1/3 length that corresponds to the subcentral tubercle, drops very slightly at mid-length, then gently rises to the greatest width at approximately 4/5 length that corresponds to the posterior lobe, then drops rapidly and concavely to the compressed posterior zone.

PLATE 2

See Plate 1 for details regarding color coding system for pores.

1 *Tumulocythereis incompta* n. gen., n. sp., RV, based on SEM images of inner and outer views of specimen 141-7, collected from sample 2011-8-4-1 (water level), Owl Creek Formation, Maastrichtian, Tippah County, Mississippi.

2 *Tumulocythereis tiberti* n. gen., n. sp., LV, based on SEM images of inner and outer views of specimen 130/135-9 (closeup of external features on Pl. 17, fig. 10).

3 *Tumulocythereis priddyi* (Smith 1978), RV, based on SEM images of inner and outer views of specimen 130/135-8 (internal view on Pl. 16, fig. 9).

4 *Tumulocythereis tumulus* n. gen., n. sp., LV, based SEM image of external view of specimen 143-18, collected from sample 2011-8-4-1 (water level), Owl Creek Formation, Maastrichtian, Tippah County, Mississippi.

5 *Frodocythereis frodoi* n. gen., n. sp., LV, based on SEM images of external and internal views of specimen 132/136-3, collected from sample 2011-8-4-1 (water level), Owl Creek Formation, Maastrichtian, Tippah County, Mississippi.

6 *Frodocythereis copelandi* (Smith 1978), LV., based on SEM images of external and internal views of specimen 132/136-24 (closeup of muscle scars on Pl. 11, fig. 10).

7 *Anticythereis slipperi* n. sp., LV, based on SEM image of external view of specimen 134-14 (Pl. 6, fig. 2).

8 *Anticythereis dorsennus* n. sp., LV, based on SEM image of external and internal views of specimen 132/136-13 (Pl. 5, figs. 2 and 7).

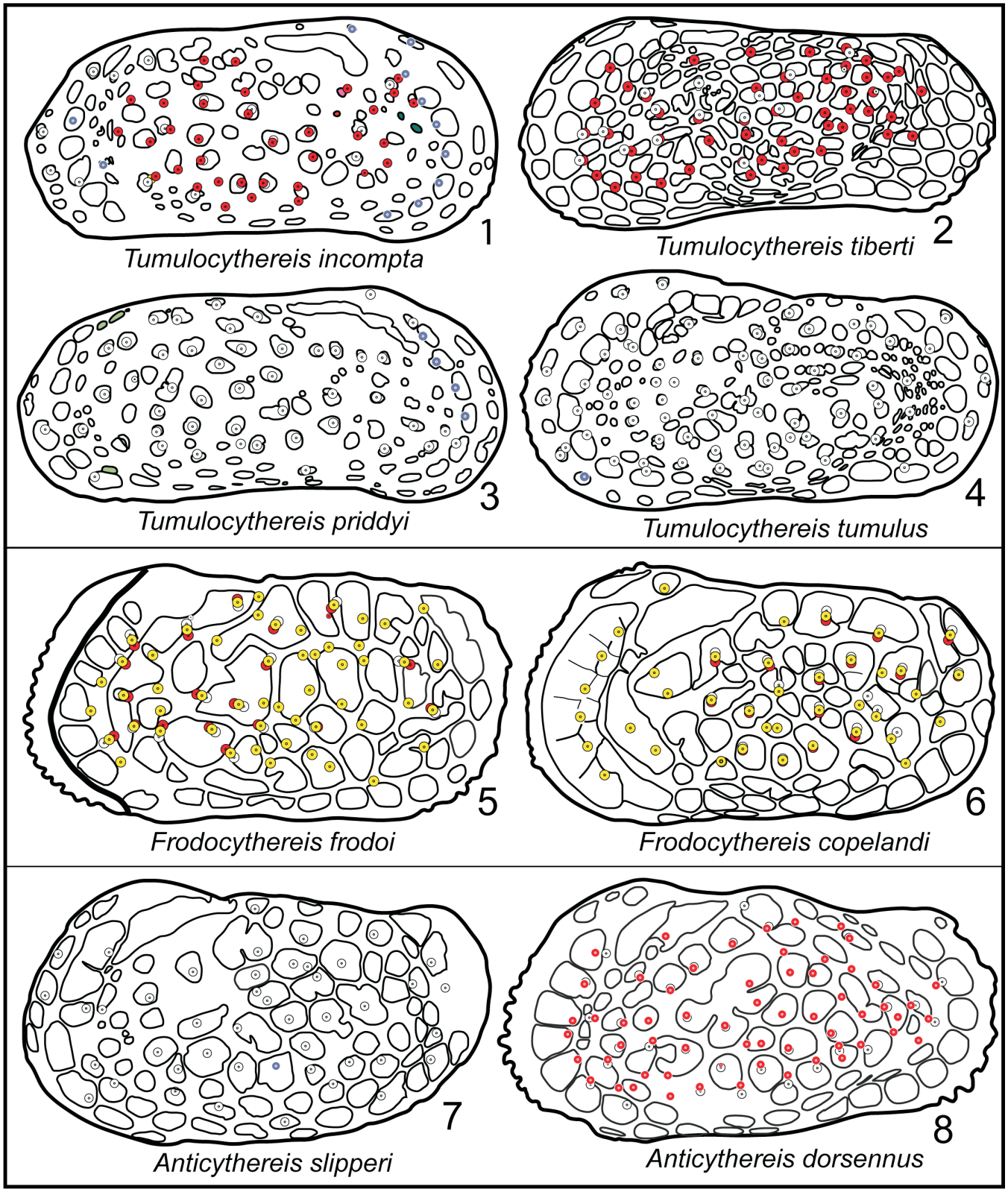
1
Tumulocythereis incompta
2
Tumulocythereis tiberti
3
Tumulocythereis priddyi
4
Tumulocythereis tumulus
5
Frodocythereis frodoi
6
Frodocythereis copelandi
7
Anticythereis slipperi
8
Anticythereis dorsennus

The eye tubercle is a gentle, smooth bulge at the dorsoanterior angle. The external carapace has a combination of large lobes, deep sulci ornamented with fossae of a wide variety of shapes and sizes like a spotted leopard, and wide muri. There are three main lobes: a broad subcentral tubercle is located slightly above and in front of carapace center, a dorsoposterior lobe that extends above the hinge line, and a large arcuate ventrolateral lobe; the subcentral tubercle rises gently from the anterior margin, but drops off more sharply ventrally and posteriorly to the central sulcus; the subcentral tubercle and dorsoposterior lobes are connected by broad ridge; the dorsoposterior lobe terminates just in front of the posterior hinge element; the ventral lobe arises gently out of the anterior region and swells prominently in a curved, concave-up lobe to drop abruptly to the compressed posterior margin below the dorsoposterior lobe; the lower side of the ventral lobe is nearly vertical in lateral view; a broad sulcus is located between the bordering lobes, being horizontal between the dorsal and ventral lobes and curved below the subcentral tubercle to flatten out in the anterior region; a gentle ridge extends downward from the eye tubercle and flattens out in the anterior region. The postocular sulcus is bipartite, with a deeply sculpted, boomerang-shaped sulcus cutting into the thick marginal ridge just below and behind the eye tubercle that points to the lower edge of the eye; this sulcus is floored by shallow, polygonal fossae, with delicate intervening muri (Pl. 18, figs. 3-4); the immediately posterior zone is not quite as deeply sculpted, but curves back to lie immediately below the thick dorsal rim; this latter sulcus cuts deeply into the dorsal rim and the adjacent dorsal lobe, undercutting them. The anterior and posterior margins are thick and prominent and bordered inwardly by equally wide, deeply sculpted regions; within the marginal rims is a single line of 10-11 elongate fossae that extend from just in front of the eye tubercle and continue to the incurved ventral margin; in the RV, a line of elongate fossae ornament the convex ventroposterior margin, but the fossae become small and round along the concave dorsoposterior margin; the fossae behind the anterior rim are deeply sculpted, sub-rectangular, and separated by narrow muri that are tapered in the middle; within each fossa is a single, rimmed sieve-type normal pore canal that is offset towards the center of the carapace (Pl. 18, figs. 1-4), and in some places is connected to the bordering murus by an apophysis (arrow on Pl. 18, fig. 10). The muri that border the fossae are steep and undercut in places (Pl. 18, fig. 14); in some fossae there is a single sieve-type normal pore canal that is surrounded by a moated solum; the sieve plates lie below the level of the soli; the soli are often caperate (arrow on Pl.

PLATE 3

Muscle scar patterns of species of the Subfamily Anticytherideinae. Arrows point anteriorly.
Dashed features represent the fulcral point. Locality information for specimens not given here are in the referenced plate captions.
See text-figure 8 for identification of muscle scars.

1 *Anticythereis dorsennus* n. sp., specimen number 132/136-15, collected from sample 2011-8-4-1 (water level), Maastrichtian Owl Creek Formation, Tippah County, Mississippi.

2 *Anticythereis slipperi* n. sp., specimen number 150-9 (Pl. 6, fig. 7).

3 *Asculdoracythereis asculdora* n. gen., n. sp., specimen 148-5 (Pl. 8, figs. 3 and 9).

4 *Asculdoracythereis invicta* n. gen., n. sp., specimen 147-17 (Pl. 9, figs. 7 and 10).

5 *Asculdoracythereis lowndesensis* (Smith 1978), specimen 146-7 (Pl.10, figs. 5 and 10).

6 *Asculdoracythereis pseudoalabamensis* n. gen., n. sp., specimen 147-7 (Pl. 7, figs. 6 and 11).

7 *Frodocythereis copelandi* (Smith 1978), specimen 132-24 (Pl. 11, fig. 10).

8 *Frodocythereis frodoi* n. gen., n. sp., specimen 132-3, sample 2011-8-4-1 (water level), Maastrichtian Owl Creek Formation, Tippah County, Mississippi.

9 *Laevipellacythereis colossus* n. gen., n. sp., sample 148-11 (Pl. 13, figs. 5 and 11).

10 *Laevipellacythereis laevipellis* n. gen., n. sp., specimen 130-2, sample 2011-5-18-1 (water level), Maastrichtian Owl Creek Formation, Tippah County, Mississippi.

11 *Tumulocythereis incompta* n. gen., n. sp., specimen 145-6 (Pl. 15, figs. 10 and 14).

12 *Tumulocythereis priddyi* (Smith 1978), specimen 133-11, sample 2011-8-4-1 (water level), Maastrichtian Owl Creek Formation, Tippah County, Mississippi.

13 *Tumulocythereis tiberti* n. gen., n. sp., specimen 130-9 (closeup of external surface on Pl. 17, fig. 10).

14 *Tumulocythereis tumulus* n. gen., n. sp., specimen 143-1 (Pl. 18, fig. 13).

15 *Asculdoracythereis pseudoalabamensis* n. gen., n. sp., for reference specimen 147-7 (Pl. 7, figs. 6 and 11).

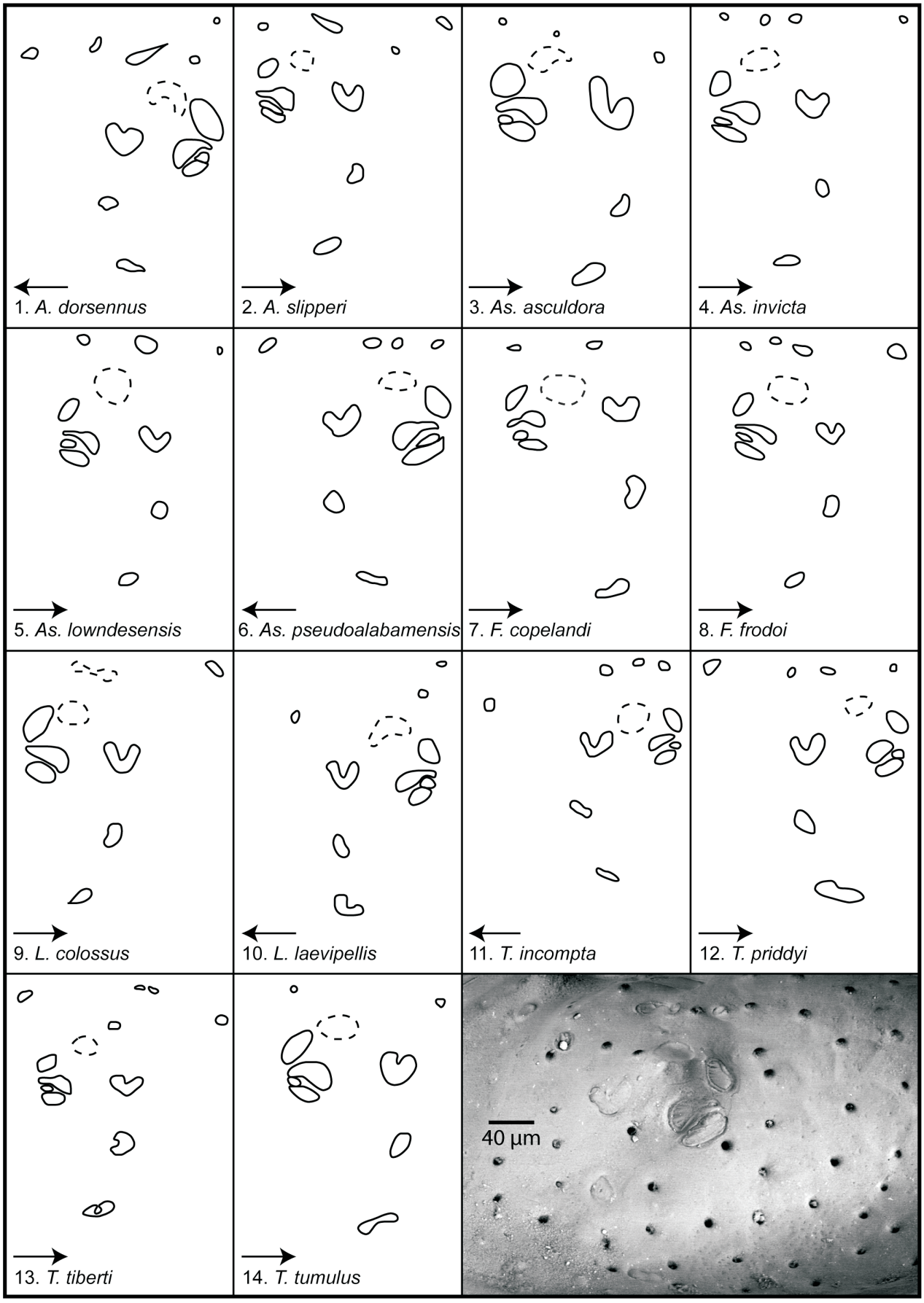
1. A. dorsennus
2. A. slipperi
3. As. asculdora
4. As. invicta
5. As. lowndesensis
6. As. pseudoalabamensis
7. F. copelandi
8. F. frodoi
9. L. colossus
10. L. laevipellis
11. T. incompta
12. T. priddyi
13. T. tiberti
14. T. tumulus
40 µm

18, fig. 11); the fossae on the subcentral tubercle are sparse, small and round; the fossae on the posterior slope are also small and round; most of the fossae in the center of the carapace are of medium size, with wide variety of shapes, and some appear to coalesce, thus forming elongate fossae. The entire carapace except for the fossae is foveolate (Pl. 18, figs. 9-11 and 14).

The hinge is holamphidont (Pl. 18, figs. 5-8 and 12); the anterior tooth in the RV is stepped, with a lower, grooved part in the anterior that steps up posteriorly to a taller tooth and subjacent socket; the middle hinge element is a straight, crenulated groove that widens at the extremities; the posterior tooth is elongate and angled in the middle; the hinge in the LV has a deep anterior socket that extends below the postjacent, vertically elongate tooth; the middle hinge element is a straight crenulate bar; the posterior socket is at the dorsoposterior angle and is tilted ventroposteriorly; low stragula overlie the terminal hinge elements. The inner surface has scattered openings that correspond to the inside of sieve-type normal pore canals. The marginal zone is wide, especially in the anterior; the selvage in the RV is interrupted by a double ogee-shaped structure at the caudal region (Pl. 18, figs. 6 (with arrow) and 8), with no complementary structure in the LV; the anterior selvage has thin, radiating muri that are connected to the anterior margin (Pl. 18, fig. 8). Two parallel, rimmed, fusiform inverted platforms (arrows on Pl. 18, fig. 12) are located just behind and ventral of the anterior hinge elements, with the lower, smaller platform being more acuminate posteriorly and the larger, upper one being more acuminate anteriorly; these structures correspond to the inside of the postocular sulci. The ocular sinus is located just below and anterior of the anterior hinge elements.

The muscle scars (Pl. 3, fig. 14; Pl. 18, figs. 5-8, and 12-13) have a U-shaped F scar that is tilted slightly anteriorly; the A-1 scar is elliptical, tilted slightly dorsoanteriorly from vertical, and is detached above the posterior end of other adductor scars; the A-2, A-3 and A-4 scars are intertwined in a yin-yang symbol with overall circular pattern; the A-2 scar is paisley shaped and curves and tapers over the A-3 scar; the A-3 scar is small, circular, and sandwiched between posterior ends of the A-2 and A-4 scars; the A-4 scar is elongate longitudinally and tilted slightly ventroanteriorly; the M-1 scar is elliptical, points towards the ocular sinus, and lies directly below the F scar; the M-2 scar is below and slightly posterior to the M-1 scar, is very elongate and constricted in the middle; the D-1 scar is elliptical and located directly below the ocular sinus; the D-4 is small, circular, and located above the A-1 scar; the other dorsal scars are small and indistinct; the fulcral point is depressed, slightly elliptical, and located just in front of and above the A-1 scar.

The species is sexually dimorphic, with the male being more elongate than the female (text-fig. 15). The lateral lobes on the male are not as inflated as on the female.

PLATE 4

Type specimens and species of Anticytherideinae left in open nomenclature or described from the Atlantic Coastal Plain
All specimens at same scale. Sexes are uncertain. LV = left valve, RV = right valve

1 Paratype *Anticythereis reticulata* (Jennings 1936), AMNH-FI 37780B, internal LV. Arrow points to inverted platform almost obscured by crystal growth.

2 Same specimen as figure 1.

3 *Anticythereis reticulata* (Jennings, 1936), USNM PAL 129016, Maastrichtian Peedee Formation, Pitt County, North Carolina; this is Brown's (1957) holotype of *Velarocythere eikonata* (USNM PAL 129016).

4 *Tumulocythereis* sp. 1, external LV, specimen 149-1, sample 2019-6-20-1 (185), Maastrichtian Ripley Formation, Lowndes County, Alabama.

5 *Tumulocythereis* sp. 1, external RV, specimen 149-3, sample 2019-6-20-1 (190), Maastrichtian Ripley Formation, Lowndes County, Alabama.

6 *Frodocythereis* sp. 1, external LV, specimen 141-21, sample 2010-10-22-1 (512), latest Campanian-Maastrichtian Coon Creek Formation, Union County, Mississippi.

7 *Laevipellacythereis* sp. 1, external RV, specimen 149-18, sample 2010-10-22-1 (512), latest Campanian-Maastrichtian Coon Creek Formation, Union County, Mississippi.

8 *Laevipellacythereis* sp. 1, external LV, specimen 149-19, sample 2010-10-22-1 (512), latest Campanian-Maastrichtian Coon Creek Formation, Union County, Mississippi.

9 *Asculdoracythereis* sp. 1, external RV, specimen 149-7, sample 2011-5-18-1 (water level), Maastrichtian Owl Creek Formation, Tippah County, Mississippi.

10 *Asculdoracythereis* sp. 1, external LV, specimen 149-9, sample 2011-5-18-1 (water level), Maastrichtian Owl Creek Formation, Tippah County, Mississippi.

11 *Anticythereis* sp. 1, external LV, specimen 149-14, sample 1993-6-11-3 (1), Campanian Cusseta Sand, Barbour County, Alabama.

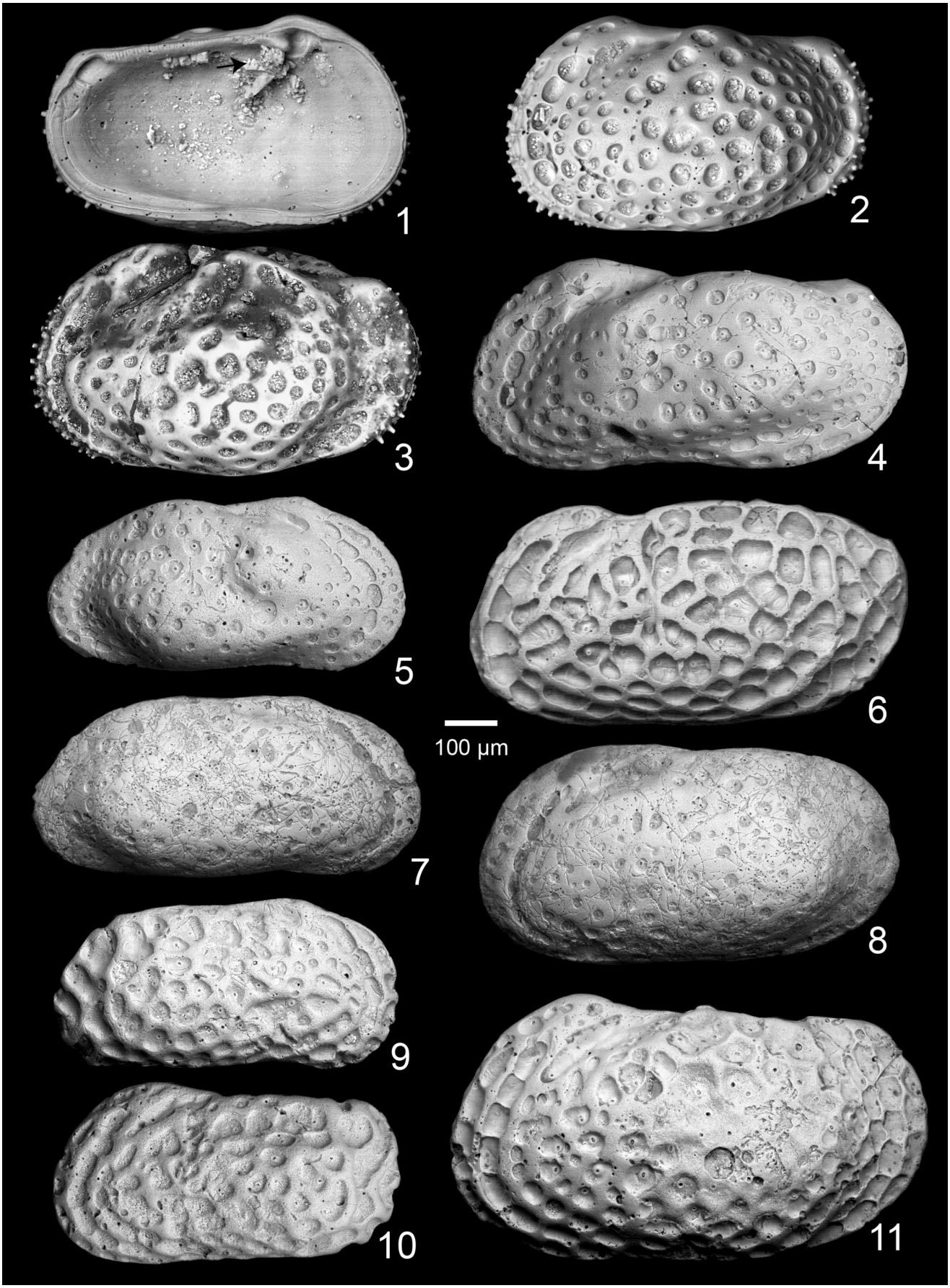
1
2
3
4
5
6
100 µm
7
8
9
10
11

Remarks: This species is relatively thick-shelled and with swollen muri; the carapace is strongly lobate and with marginal carinae; the strongly inflated subcentral tubercle and ventrolateral lobes with intervening sulcus are also distinctive. Among the species of *Tumulocythereis*, it is most similar to *T. incompta* in having broader muri and smaller fossae but has subcircular, rather than polygonal, fossae and is more elongate and constricted medially than *T. incompta*.

Range: This species was found in the Owl Creek Formation type locality, Tippah County, northern Mississippi; in the Prairie Bluff Chalk of Oktibbeha County, eastern Mississippi; and in the Prairie Bluff Chalk of Lowndes County, central Alabama. All samples are of late Maastrichtian age (text-figs. 2 and 4).

Tumulocythereis sp. 1
Plate 4, figures 4-5

Material: 16 valves were collected during this study.

Remarks: This species is very similar to *T. tumulus* n. gen., n. sp., but the lateral outline is less elongate. The posterior margin is more supracurvate and rounded, the anterior lobe is more swollen, the sulcus between the subcentral and ventral lobes is shallower, the anterior and posterior margins are not as compressed, and the subcircular fossae are fewer by the thickened muri.

Range: This species was collected from the Coon Creek Formation of Union County, Mississippi and from the coeval Ripley Formation of Lowndes County, Alabama, both of latest Campanian-early Maastrichtian age. This species could, therefore, be the ancestor of the other species of the genus (text-figs. 2 and 4).

DISCUSSION

Character Evolution and Evolutionary History

Despite many years of study on the Late Cretaceous marine ostracods of the U.S. Gulf Coastal Plain, there remains a considerable amount of work to be done on the taxonomy and systematics of these diverse fossils. This contribution makes several taxonomic proposals to organize and understand many of the species of trachyleberids that occur near the end of the Cretaceous. This section presents some of the taxonomic implications for their study.

The anticytherideinines belong to the Family Trachyleberidae based mainly on their amphidont hinge, presence of ornamentation such as carinae and fossae, and the muscle scar pattern, which includes a single (unsplit) frontal muscle scar and a vertical row of adductor muscle scars. Sylvester-Bradley (1948) originally described the Family Trachyleberidae to include a large number of ornamented ostracods with "…accommodation groove lacking or reduced to a narrow shelf; straight hinge, with subdivided median element; and compressed carapace (especially anteriorly and posteriorly) though sometimes with alae." Sylvester-Bradley (1948) also described the Subfamily Trachyleberinae to include "Ornate Trachyleberidae with compressed sub-rectangular shell, pronounced muscle scar node (='subcentral tubercle' [*sic*]; forms a "muscle scar pit" when viewed from the interior; eye tubercle, posterior and anterior cardinal angles, and posterior and anterior rims. Accommoda-

---

PLATE 5

Anticythereis dorsennus n. sp.
Specimens 1-8 at same scale, as indicated. Scale for figures 9-11 as indicated.
All specimens collected from the Maastrichtian Owl Creek Formation, Tippah County, Mississippi.
LV = left valve, RV = right valve

1 Exterior RV, female, specimen 132/136-21, same figure as 6, 9 and 11, sample 2011-5-18-1 (water level).

2 Holotype (USNM PAL 771796), exterior LV, male, specimen 132/136-13, sample 2011-5-18-1 (water level).

3 Exterior RV, female, specimen 132/136-20, same specimen as figures 8 and 10 sample 2011-5-18-1 (water level).

4 Paratype (USNM PAL 771797), exterior LV, female, specimen 132/136-18, sample 2011-8-4-1 (water level).

5 Interior LV, male, specimen 132/136-14, sample 2011-5-18-1 (water level).

6 Interior RV, male, specimen 132/136-21, same specimen as figures 1, 9 and 11. Arrow points to double ogee-shaped caudal interruption of selvage.

7 Interior LV, same specimen as figure 2.

8 Interior RV, same specimen as figures 3 and 10.

9 Closeup reticulations and sieve pores, same specimen as figures 1 and 6.

10 Closeup muscle scars, RV, same specimen as figure 3 and 8.

11 Closeup muscle scars. RV, same specimen as figures 1, 6 and 9.

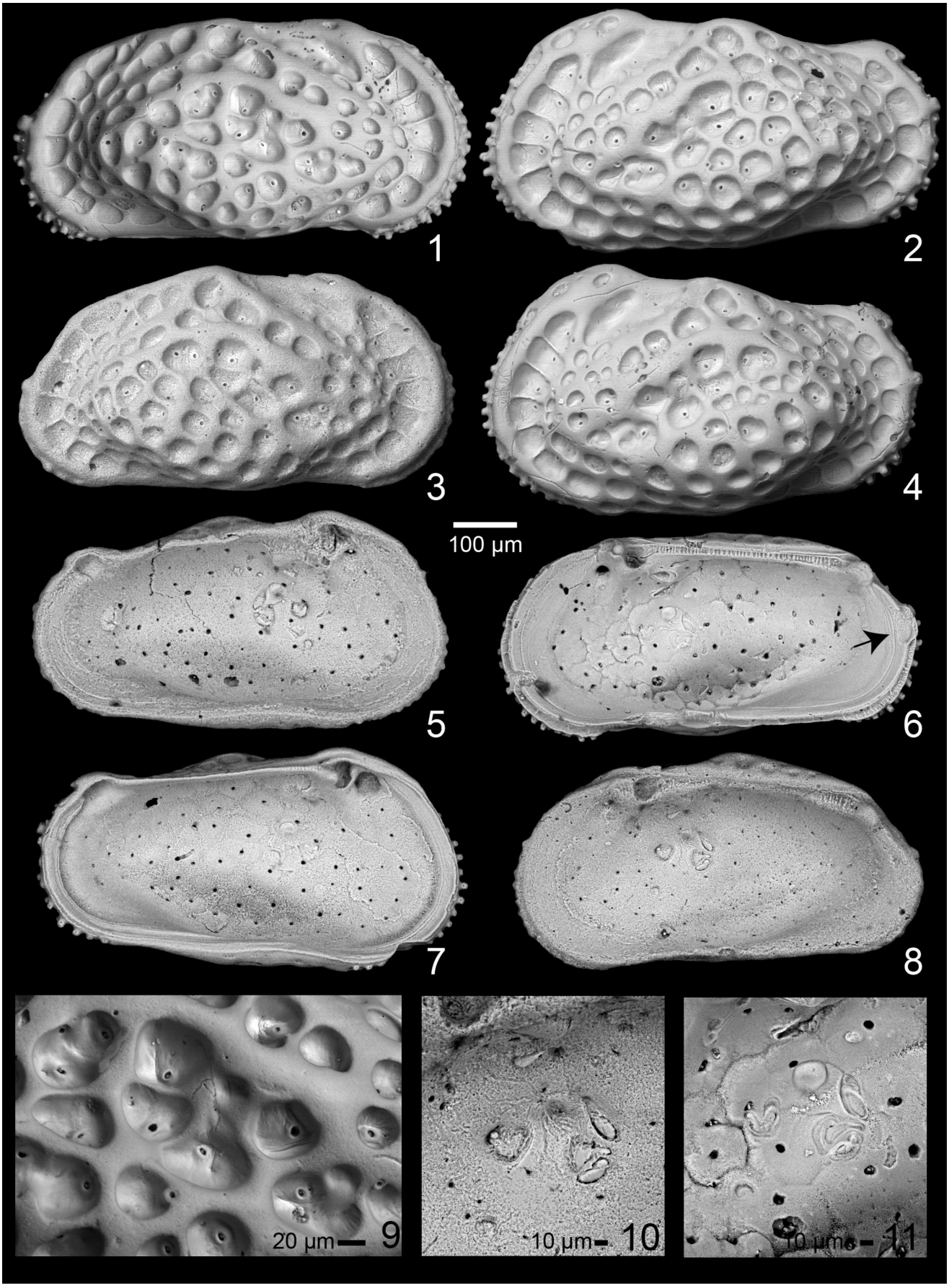
1
2
3
4
100 µm
5
6
7
8
20 µm
9
10 µm
10
10 µm
11

tion groove absent, or present only as a very narrow shelf. No vestibule. Median element of hinge subdivided, smooth or finely denticulate." These definitions included a large number of taxa ranging from the Jurassic to the Recent, and even include taxa, such as *Oligocythereis*, that have a merodont/entomodont hinge. Puri (1953), recognizing that the Family Trachyleberidae included genera that are not closely related to one another, described the Subfamily Hemicytherinae to include genera with a muscle scar pattern consisting of a vertical row of four adductor scars, with additional three or four scars in an oblique row situated anteriorly (i.e., a subdivided frontal scar). Later, van Morkhoven (1963) emended the diagnosis of the Subfamily Trachyleberinae (Family Cytheridae, now Cytheroidea) to put the pattern of the central muscle scars in primary importance: "Central muscle scars consisting of a vertical row of four adductor scars, which are rarely subdivided, and a V-shaped frontal scar." Other diagnostic characters included a wide marginal zone, numerous marginal pore canals, hinge generally amphidont/heterodont (but included some Cretaceous genera with merodont or entomodont hinges), generally well-developed eyespots, heavily calcified carapace that is usually ornamented with strong spines or ridges, and marginal denticulations. Similarly, the Treatise volume on ostracods (Benson et al. 1961) defined the trachyleberids solely on the basis of hard part morphology. Hazel (1967) recognized the importance of the muscle scar patterns in deciphering the phylogenetic history of the trachyleberids and hemicytherids, interpreting the former to be the ancestors of the latter. As more details about the biology of living trachyleberids became known, the soft part morphology was included (Athersuch et al. 1989; Horne et al. 2002).

The paramphidont hinges of the anticytherideinines are not unique to the group, although the combination of the stepped and grooved anterior hinge element and the angled and arched posterior hinge element of the RV are distinctive. In the U.S. Gulf Coastal Plain, species of *Bicornicythereis* also have a stepped anterior hinge element in the RV, although the lower anterior part is not grooved (see Puckett (2009a), Pl. 3, fig. 14, other images unpublished). Species of *Ascetoleberis* also have this knob-like step anterior to the anterior tooth in the RV. Almost all the species described herein have a grooved anterior tooth in the RV (paramphidont), but some appear to be smooth (holamphidont); that may be due, however, to being slightly worn, as the grooves are subtle.

The pattern of the muscle scars, particularly the adductor scars, is one of the most distinctive characters in the new subfamily. Text-figure 16 presents the muscle scar patterns of representative trachyleberid species of the Late Cretaceous of the U.S. Gulf Coast (trachyleberids that are clearly distinctive, such as the brachycytherines, were omitted from the comparison). Whereas all the taxa in text-figure 16 have a single U- or V-shaped frontal scar, most of the taxa have stacked series of four elongate adductor scars (*Ascetoleberis, Aysegulina,* and *Veenia*), rather than the intertwined A-2, A-3 and A-4 scars. The adductor muscle scars of species of *Bicornicythereis* (Puckett 2009a) are the most similar to the new subfamily, although several of the species (*B. bicornis, B. polita* and *B. veclitella*) ap-

---

PLATE 6

Anticythereis slipperi n. sp.

Specimens 1-6, 8 at same scale, as indicated. Scale for figures 7, 9-11 as indicated.

LV = left valve, RV = right valve

1 Exterior RV, presumed male, specimen 148-14, sample 1991-8-15-7, Maastrichtian Ripley Formation, Lowndes County, Alabama.

2 Holotype (USNM PAL 771798), exterior LV, presumed male, specimen 134-14, sample 2011-8-15-1 (15), latest Campanian-Maastrichtian Coon Creek Formation, McNairy County, Tennessee.

3 Paratype (USNM PAL 771799), exterior RV, presumed male, specimen 146-4, sample 2011-8-15-1 (15), latest Campanian-Maastrichtian Coon Creek Formation, McNairy County, Tennessee.

4 Exterior LV, female, specimen 148-18, sample 2010-10-22-1 (512), latest Campanian-Maastrichtian Coon Creek Formation, Union County, Mississippi.

5 Interior LV, presumed male, specimen 150-9, same specimen as figure 7, sample 2019-6-20-1 (180), Maastrichtian Ripley Formation, Lowndes County, Alabama.

6 Interior RV, female, specimen 148-20, sample 2019-6-20-1 (185), Maastrichtian Ripley Formation, Lowndes County, Alabama.

7 Closeup muscle scars, LV, same specimen as figure 5.

8 Exterior LV, male, specimen 134-15, sample 2011-8-15-1 (15), latest Campanian-Maastrichtian Coon Creek Formation, McNairy County, Tennessee.

9 Closeup of muscle scars, reticulation and sieve pores in exterior view, same specimen as figure 1.

10 Closeup reticulation and sieve pores, specimen 148-15, sample 2010-10-22-1 (512), latest Campanian-Maastrichtian Coon Creek Formation, Union County, Mississippi.

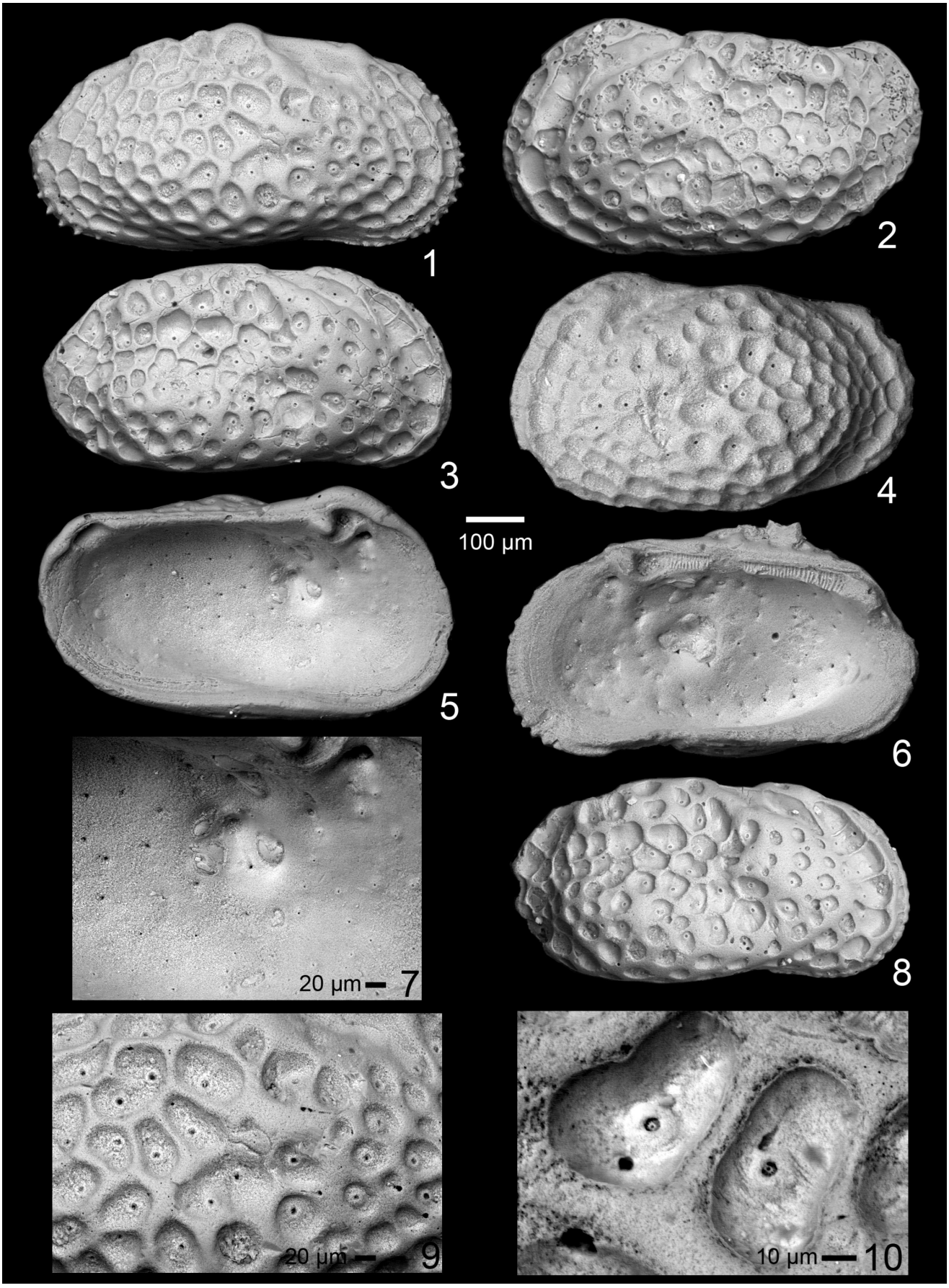
1
2
3
4
100 µm
5
6
20 µm
7
8
20 µm
9
10 µm
10

pear to have only three adductor scars; however, the lowest scar is probably two scars that have fused (in two of the species, *B. communis* and *B. levis*, these can be seen as two scars that are almost fused). The distinctive A-2 scar in *Bicornicythereis*, which bulges anteriorly over the lower scars, is very similar to those of the new subfamily, but the A-3 is either missing, elongate or fused. Puckett and colleagues (Puckett 2009a, Puckett et al. 2016) recognized the close association of paleogeography and distinctive muscle scar patterns in Late Cretaceous trachyleberids and the tremendous amount of information that is conveyed by these patterns. For example, many species in North America, South America, Africa, and Madagascar had been assigned to the genus *Brachycythere.* Puckett (2012) recognized that there is a systematic difference in the muscle scar patterns between those that occur in North America and those that occur elsewhere, as all the species from North America have split second adductor scars, whereas those from elsewhere have a single, elongate second adductor. This difference was the basis of describing a new genus of brachycytherines, *Sapucariella*. Similarly, given an image of the central muscle scar pattern of any of the species described herein, they can be readily assigned to the new genus, and thus are restricted paleogeographically to North America.

Another distinctive character of the new subfamily is the pair of rimmed, fusiform, inverted platforms located on the inside of the carapace that corresponds to the postocular sulcus. As with the muscle scar patterns, this structure is an indication of distinctive soft part morphology, although the exact function is uncertain. It is possible that this structure is an isthmus, which is the area where the inner lamella is connected to the body, or the attachment site for dorsal muscles and tendons that support the soft body and control appendages. Keyser (1990, 2005) described and illustrated both anterior and posterior isthmuses in *Cyprideis torosa* (Jones 1850), and stated that the isthmus is where the connection between the inner epidermal cell layer and the outer epidermal cell layer is lost and the inner cell lining is connected to the body cuticle. Whatever the function was of this structure, the authors are not aware of any other taxa that possess it or any homologous structure.

PLATE 7

Asculdoracythereis pseudoalabamensis n. sp., and *Asculdoracythereis alabamensis* (Smith 1978)
Specimens 1-8 at same scale, as indicated. Scale for figures 9-11 as indicated.
LV = left valve, RV = right valve

1 *Asculdoracythereis pseudoalabamensis*, exterior RV, male, specimen 147-3, sample 2012-01-03-1-2, Maastrichtian Providence Sand, Barbour County, Alabama.

2 Holotype (USNM PAL 771804) *Asculdoracythereis pseudoalabamensis*, exterior LV, male, specimen 147-1, sample 2012-01-03-1-2, Maastrichtian Providence Sand, Barbour County, Alabama.

3 *Asculdoracythereis alabamensis* (Smith 1978) holotype (USNM PAL 255753), exterior RV, male, Maastrichtian Prairie Bluff Formation, Lowndes County, Alabama.

4 Paratype (USNM PAL 771805) *Asculdoracythereis pseudoalabamensis,* exterior LV, female, specimen 147-4, sample 2012-01-03-1-2, Maastrichtian Providence Sand, Barbour County, Alabama.

5 *Asculdoracythereis pseudoalabamensis*, interior LV, female, specimen 147-5, sample 2012-01-03-1-2, Maastrichtian Providence Sand, Barbour County, Alabama.

6 *Asculdoracythereis pseudoalabamensis*, interior RV, female, specimen 147-7, sample 2012-01-03-1-2, Maastrichtian Providence Sand, Barbour County, Alabama.

7 *Asculdoracythereis pseudoalabamensis*, closeup of interior RV, female, specimen 147-6, sample 2012-01-03-1-2, Maastrichtian Providence Sand, Barbour County, Alabama. Note stepped anterior hinge tooth and muscle scars. Arrow on right points to upper inverted platform, arrow on left points to lower platform.

8 *Asculdoracythereis pseudoalabamensis*, same specimen as fig. 7.

9 *Asculdoracythereis pseudoalabamensis*, closeup of sieve-type normal pore canals, same specimen as figure 2.

10 *Asculdoracythereis pseudoalabamensis*, closeup of external ornamentation and muscle scars, same specimen as figure 1.

11 *Asculdoracythereis pseudoalabamensis,* closeup of muscle scars, same specimen as figure 6.

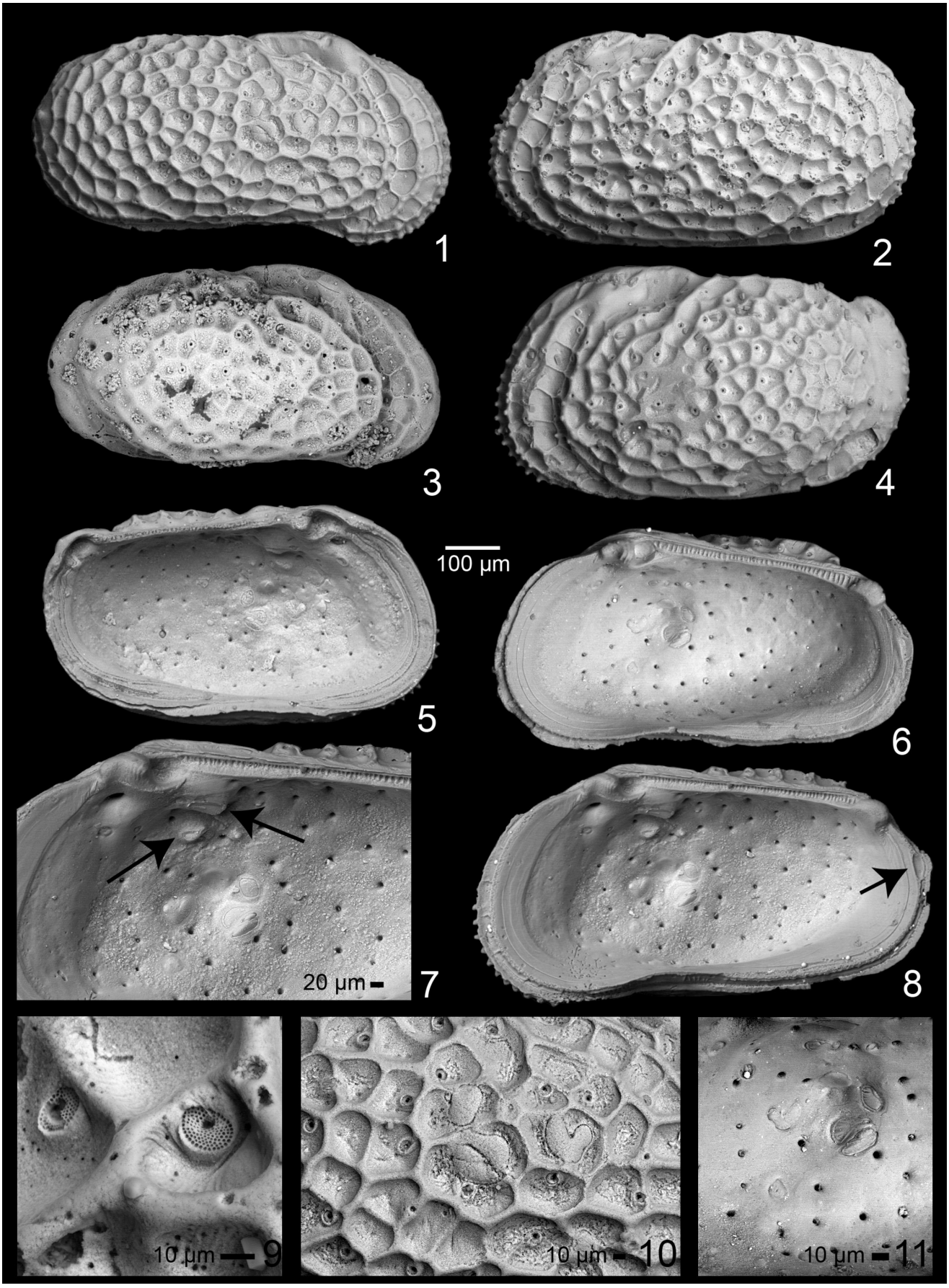
1
2
3
4
100 µm
5
6
20 µm
7
8
10 µm
9
10 µm
10
10 µm
11

All species of the new subfamily have an interruption of the selvage in the RV at the caudal region that is typically shaped like a double ogee or is ovoid (arrows point to this structure on Pl. 5, fig.6; Pl. 7, fig. 8; Pl. 12, fig. 6; Pl. 14, fig. 8; Pl. 15, fig. 8; Pl. 16, fig. 8; and Pl. 18, fig. 6). This structure may be analogous to the posterior siphonate indentations Maddocks (1969) observed in Recent bairdiids, and is the exit for the water that flows over the body of the ostracod so it can breathe with the valves almost closed (Maddocks, personal communication, 2021). This structure is common in the Late Cretaceous ostracods of the U.S. Gulf Coast and has been observed in the following groups:

•brachycytherines, including *Brachycythere asymmetrica* Puckett 1994, *B. crenulata* Crane 1965, *B. plena* Alexander 1934 (Puckett et al. (2016), Pl. 4, fig. 11), *B. rhomboidalis* (Berry 1925), *B. nausiformis* Swain 1952 and *Digmocythere russelli* (Howe and Lea 1936);

•schulerideids (*Schuleridea travisensis* Hazel and Paulson 1964);

•trachyleberids, including species of *Ascetoleberis* (*A. plummeri* (Israelsky 1929) and *A. rugosissima* (Alexander 1929); *Bicornicythereis* (*B. bicornis* (Israelsky 1929); see Puckett (2009a), Pl. 1, fig. 9), *B. communis* (Israelsky 1929); see Puckett (2009a), Pl 5, fig. 6); *B. nodilinea* (Crane 1965), see Puckett (2009a), Pl. 3, fig. 1)); *B. polita* (Crane 1965); see Puckett (2009a), Pl. 3, fig. 12); *Fissocarinocythere* (*F. gapensis* (Alexander 1929) and *F. pidgeoni* (Berry 1925)); *Floricythereis lixula* (Crane 1965); *Planileberis costatana* (Israelsky 1929); *Pterygocythereis (Pterygocythereis) cheethami* Hazel and Paulson 1964; *Praephacorhabdotus pokornyi* (Hazel and Paulson 1964); and *Veenia* (*V. ozanana* (Israelsky 1929); *V. quadrialira* (Swain 1952); *V. spoori* (Israelsky 1929).

All of the aforementioned species have this feature only in the RV; the LV, in contrast, has a flattened area in the caudal region that corresponds to this position (see images in Puckett (2009a), for example, *Bicornicythereis bicornis* (Pl. 1, fig. 9), *B. nodilinea* (Pl. 3, fig. 1), *B. polita* (Pl. 3, fig. 12), *B. communis* (Pl. 5, fig. 6)). This morphology (flattened zone in LV corresponding to the double ogee-shaped structure in RV) is consistent with the interpretation that it is an outlet for water when the valves are nearly closed. The Recent bairdiids have indentations on both valves, however, whereas the anticytherideinines it is only on the RV.

The distribution of the sieve-type normal pore canals and fossae was mapped to answer the following questions: Is there a common pattern for the distribution of the pore canals? Is there a common pattern for some species and not others? If so, what are the taxonomic implications of these patterns? Are there homologous fossae in different species? If so, what are the taxonomic implications? Tsukagoshi and Ikeya (1987) and Tsukagoshi (1990) studied the distribution of normal pore canals in Recent species of *Cythere* to determine their significance in phylogenetics. Tsukagoshi (1990) subdividing the pore canals into five types; types 4 and 5 are pertinent here, as they are sieve-type normal pore canals, differing by Type 4 having a single bristle and Type 5 having a split bristle; the morphology of the sieve pores themselves were approximately the same (in other words, one would not be able to differentiate between Type 4 and Type 5 in fossil material). Tsukagoshi (1990) found that each species has its own distribution of sieve-type normal pore canals, but that these distributions were stable for each species; the distributional patterns for non-sieve-type normal pore canals (that is, simple openings) were stable among closely related species. To make sure that all the normal pore canals were mapped, views from both the inside and outside views were

---

PLATE 8

Asculdoracythereis asculdora n. sp.

Specimens 1-6, 8 at same scale, as indicated. Scale for figures 7, 9-11 as indicated. All specimens from the Maastrichtian Providence Sand of Barbour County, Alabama

LV = left valve, RV = right valve

1 Exterior RV, male, specimen 146-16, sample 2012-01-03-1-2.

2 Holotype (USNM PAL 771800), exterior LV, male, specimen 148-1, sample 2012-01-03-1-2.

3 Interior LV, female, specimen 148-5, sample 2012-01-03-1-2.

4 Paratype (USNM PAL 771801), exterior LV, female, specimen 148-3, sample 2012-01-03-1-2.

5 Exterior RV, A-1 instar, specimen 146-14, sample 2012-01-03-1-2.

6 Exterior LV, A-1 instar, specimen 146-15, sample 2012-01-03-1-2.

7 Closeup showing details of fossae and sieve pores, specimen 146-13, sample 2012-01-03-1-2.

8 Interior RV, male, specimen 146-21, sample 2014-5-28-1-2.

9 Closeup muscle scars, RV, same specimen as figure 3.

10 Closeup muscle scars, same specimen as 8.

11 Closeup fossae and sieve pores, same specimen as figure 6.

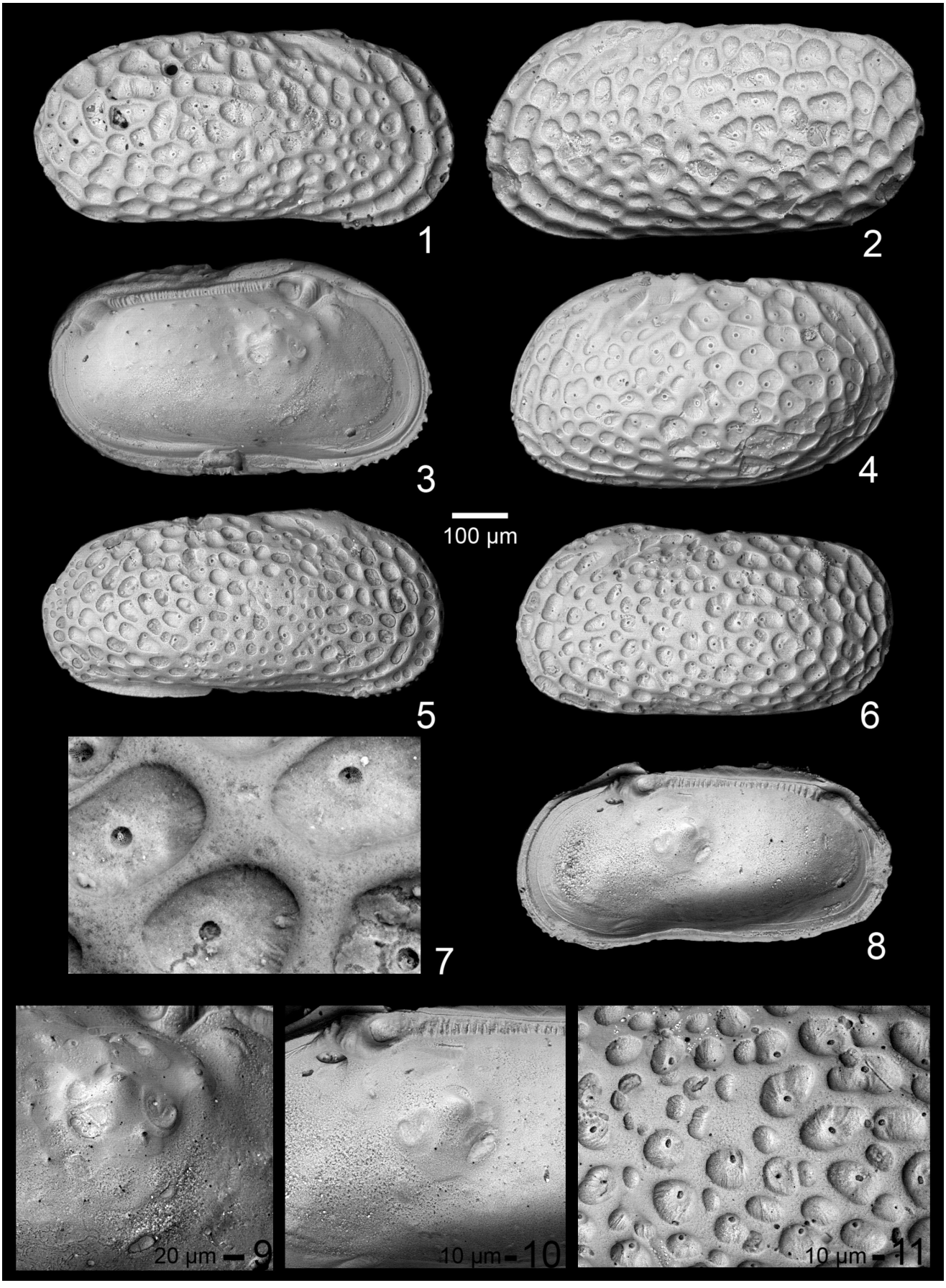
1
2
3
4
100 µm
5
6
7
8
20 µm
9
10 µm
10
10 µm
11

used (Plates 1 and 2) and superimposed on the same images. Each species has a fairly large number of pores, totaling almost 100 in some species. Attempts were made to connect the pores by lines, such as was done by Tsukagoshi (1990), but the patterns seemed to be different for each species. Mapping the sieve-type normal pore canals in the present study indicates that only the pore canals in the anterior and posterior regions could be determined to be homologous and their positions are stable. This indicates that the patterns of distribution of the sieve-type normal pore canals among the species of the anticytherideinines are species specific and cannot be used as a synapomorphic character to unite species within genera.

Similarly, the patterns of fossae were mapped in order to 1.) determine if homologous patterns of fossae could be determined among species, and 2.) assist in recognizing homologous patterns of sieve-type normal pore canals. Okada (Okada 1981, 1982b, 1982a) demonstrated that there is a correlation between epidermal cells and cuticular reticulation of the Recent species *Bicornucythere bisanensis*, with the cells correlating to the fossae and the cell walls corresponding to the muri. Okada (1981) observed the same cell-polygon in species of *Loxoconcha*. Similar correlation has been discovered in other fossil groups as well, including the recent discovery in scalidophoran worms of Cambrian age (Wang et al. 2020). The pattern of reticulation of the ostracods is stable in the last two instars within species, indicating a genetic control (Okada 1981, 1982b, 1982a). Clearly, then, the pattern of reticulation in the species that Liebau (1977) studied, for which he was able to track homologous fossae, must have had a nearly identical arrangement of epicuticle cells, and it was hypothesized that at least some of the species studies herein would have similar patterns as well. Except for the fossae along the anterior and posterior margins, however, the patterns of fossae are unique to each species (Pl. 1 and 2). Even within a species there is variability, and no two specimens are exactly the same, even from the same sample, and the exact patterns are different for females and males; compare, for example, the male on Plate 16, fig. 4 and the female on Plate 16, fig. 6, which were collected at the same level at the same outcrop. These differences indicate the possibility that there are cryptic species among those described herein. In any case, these observations indicate that homologous patterns of fossae and carinae cannot be used as a synapomorphic character to unite species into higher taxa within the anticytherideinines.

Overall, the anticytherideinines first appear in the later Campanian planktonic foraminiferal *Radotruncana calcarata* Taxon Range Zone (*Anticythereis* sp. 1, which was found in the Cusseta Sand of Barbour County, eastern Alabama). *Anticythereis slipperi*, which occurs in the latest Campanian-early Maastrichtian Coon Creek Formation and Ripley Formation of central Alabama, was among the oldest species to occur abundantly. Other species that appear at this level include *Tumulocythereis incompta* and *T. tiberti.* Several other species occurred at this time but were rare and left in open nomenclature (*Frodocythereis* sp. 1, *Laevipellacythereis* sp. 1, *Tumulocythereis* sp. 1). By the Maastrichtian, the subfamily reached its highest diversity, but became extinct at the K/Pg boundary. The ancestors to the subfamily are uncertain. Among the most similar morphologically are the species of *Bicornicythereis*, which has a similar muscle scar pattern and a small knob just anterior to the anterior tooth in the RV. One of those species, *B. communis*, is a long-ranging, widespread and com-

---

PLATE 9

Asculdoracythereis invicta n. sp.

Specimens 1-8 at same scale, as indicated. Scale for figures 9-11 as indicated. All specimens collected from the Maastrichtian Providence Sand of Barbour County, Alabama.

LV = left valve, RV = right valve

1 Holotype (USNM PAL 771802), exterior RV, male, specimen 147-10, sample 2012-01-03-1-2.

2 Exterior LV, female, specimen 147-12, sample 2012-01-03-1-2. Arrow points to distinctive circular fossa.

3 Exterior RV, female, specimen 147-11, sample 2012-01-03-1-2.

4 Paratype (USNM PAL 771803), exterior LV, female, specimen 147-13, sample 2012-01-03-1-2.

5 Interior LV, female, specimen 147-14, sample 2012-01-03-1-2.

6 Interior RV, female, specimen 147-16, sample 2012-01-03-1-2.

7 Interior LV, female, specimen 147-17, sample 2014-5-28-1-2.

8 Interior RV, male, specimen 147-18, sample 2014-5-28-1-2.

9 Closeup muscle scars, same specimen as figure 8.

10 Closeup muscle scars, same specimen as figure 7.

11 Closeup fossae and sieve pores, same specimen as figure 2.

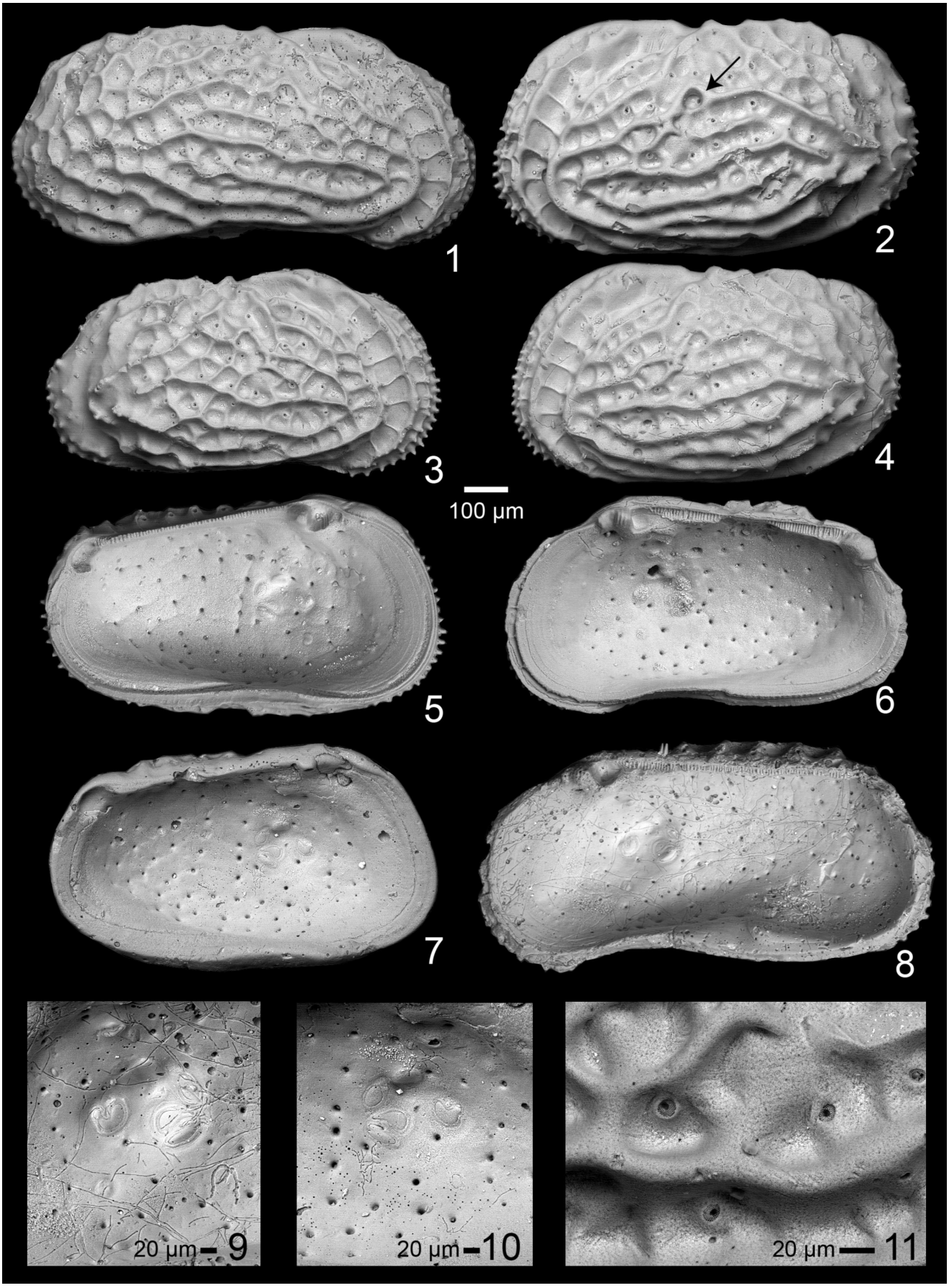
1
2
3
4
100 µm
5
6
7
8
20 µm 9
20 µm 10
20 µm 11

mon species in the Late Cretaceous deposits of the Gulf Coastal Plain and was living at the time of the appearance of the new subfamily. There is no indication, however, of the inverted platforms nor the related extended and deep postocular sulcus in that genus (see images in Puckett (2009a)).

Biogeographic Implications

The results of this study demonstrate that shallow marine, ornamented and sighted ostracods have a remarkable capacity to evolve indigenously. This makes them a powerful group for testing plate tectonic reconstructions and for studying evolutionary patterns uncomplicated by immigration and emigration. The newly defined Subfamily Anticytherideinae is a good example of such endemism, but so are several other genera that are restricted to these Late Cretaceous deposits of the North American coastal plain, including *Acuminobrachycythere, Antibythocypris, Ascetoleberis, Bicornicythereis,* and *Fissocarinocythere*. There are still species in these deposits that are assigned to catch-all genera such as *Cythereis* that should probably be assigned to an as-yet undescribed endemic genera (e.g., *C. caudata* Butler and Jones 1957*,* and *C. hannai* Israelsky 1929). The present study was undertaken to clean up the taxonomy of a relatively large number of species that one of the authors (TMP) has been collecting for many years.

On a regional scale, Puckett et al. (2012) discovered an indigenous shallow marine ostracod fauna from the Maastrichtian of Jamaica, and later discovered a very similar fauna in Chiapas, Mexico (Puckett 2009b, 2013). These observations, plus plate tectonic models, indicate that Jamaica was connected to Chiapas during the Late Cretaceous and rifted away during the Paleocene. On a much larger scale, Seeling et al. (2004) performed cluster analysis, ordination by nonmetric multidimensional scaling analysis and area cladograms on the global occurrences of 218 genera of ostracods from the Campanian to demonstrate an association of genera with paleogeography. The results showed an overall close alignment of generic assemblages with paleogeographic areas. There were, however, some anomalies. For example, Mexico clustered with Middle Eastern countries, Jamaica clustered with West Africa and Brazil, and the U.S. Gulf Coast clustered with European Georgia. A close inspection of that dataset reveals considerable noise in the signal due, in part, to incorrect generic assignments in the original published literature. The analysis also included all known genera in the various regions, including wide-ranging, apparently blind taxa such as *Argilloecia*, *Bairdia, Bythocypris* and many others, and single occurrences of genera at many localities. Deep water is not a barrier to blind taxa like it can be for sighted taxa, so it would not be unexpected for blind taxa to occur on more than one continent, and thus they would not be as useful for determining paleogeography as the sighted taxa that are restricted to shallow water. Genera located at a single locality cannot be used to infer former connectedness of habitats, just as an apomorphic character cannot be used in a phylogenetic analysis to determine relatedness of taxa—synapomorphic characters must be used. Further, and more crucial to the present arguments, there were several genera that were reported from different continents where species had been assigned to inappropriate genera. For example, the genera *Brachycythere* and *Curfsina* were reported from several continents, but analysis of the internal morphology reveals that the muscle scar patterns differ systematically according to region (Puckett 2002, 2009a). One of the authors of this paper (TMP) took the dataset of Seeling et al. (2004), eliminated the blind, ubiquitous genera, and the taxa that occur at a single area, and updated the generic assignments, resulting in a dataset of only 118 genera, and re-ran the analysis. The results show a closer association of genera and paleogeography and eliminated the anomalies. These observa-

---

PLATE 10

Asculdoracythereis lowndesensis (Smith 1978)

Specimens 1-6 at same scale, as indicated. Scale for figures 7-10 as indicated. All specimens collected from the Maastrichtian Providence Sand in Alabama.

LV = left valve, RV = right valve

1 Exterior RV, female, specimen 146-10, sample 2012-01-03-1-2, Barbour County.

2 Exterior LV, female, specimen 146-8 6216, sample 2012-01-03-1-2, Barbour County.

3 Exterior RV, male, specimen 134-17, sample 1991-8-14-1, Bullock County.

4 Exterior LV, female, specimen 146-11, sample 2014-5-28-1-1, Barbour County.

5 Interior LV, female, specimen 146-7, sample 2012-01-03-1-2, Barbour County.

6 Interior RV, male, specimen 146-5, sample 2012-01-03-1-2, Barbour County.

7 Closeup elevated pores, specimen 146-9, sample 2012-01-03-1-2, Barbour County.

8 Closeup muscle scars, external view RV, same specimen as figure 3.

9 Closeup sieve pores and ornamentation, specimen 134-18, sample 1991-8-14-1, Bullock County. Arrow points to knob-like conjunctive spine.

10 Closeup muscle scars, LV, same specimen as figure 5.

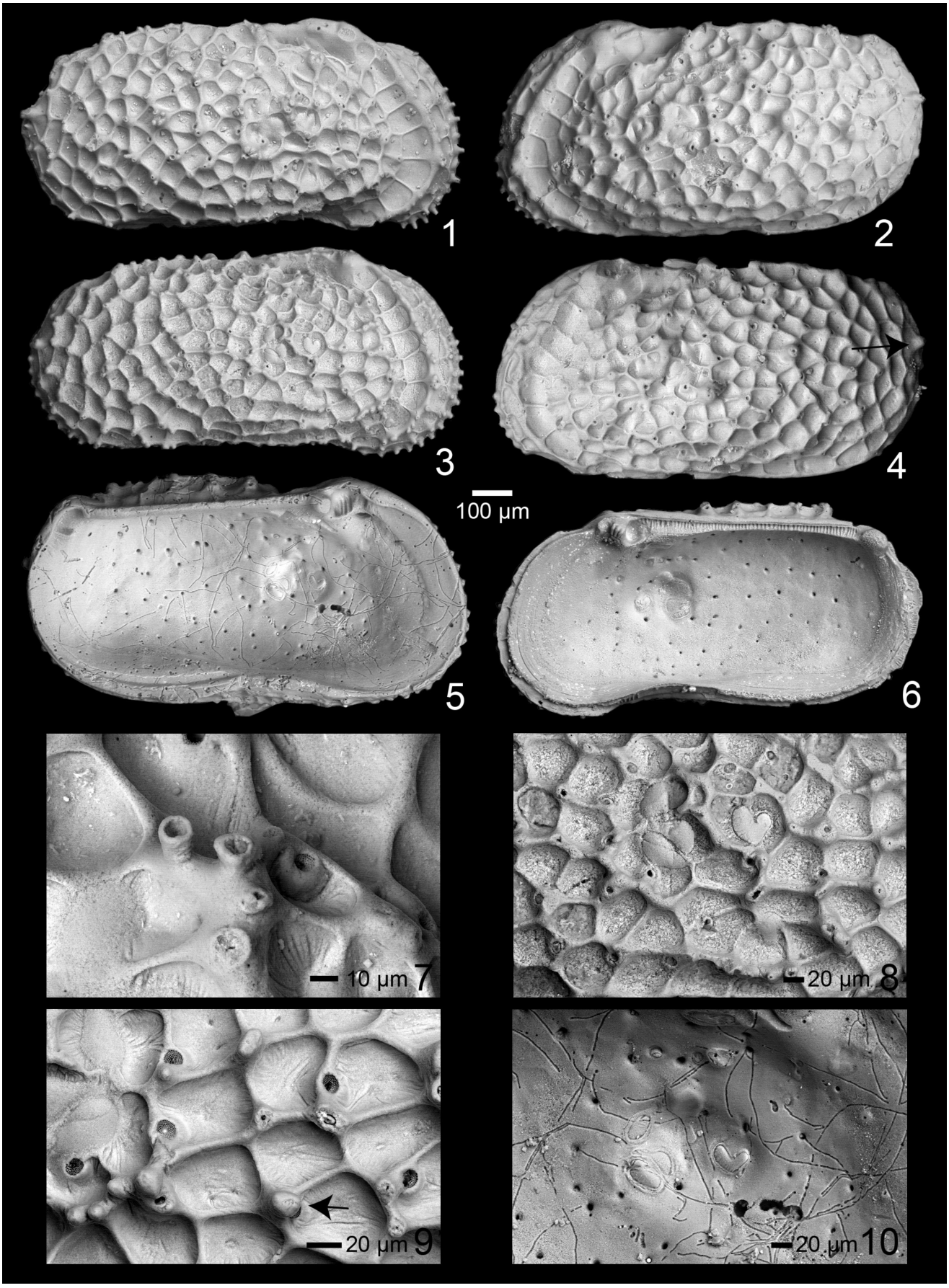
1
2
3
4
100 µm
5
6
10 µm 7
20 µm 8
20 µm 9
20 µm 10

tions indicate that uncritically assigning shallow marine, sighted ostracods from different continents to the same genera undermines their use in paleogeographic studies, including plate tectonics, and should, therefore, be regarded as an opportunity for re-evaluation. As indicated in this discussion, the internal features, particularly the central muscle scars, are critical for accurate assignment of species to genera. Ideally, a phylogenetic analysis combining character cladograms and area cladograms, such as discussed by Lieberman (2000), would result in viable hypotheses regarding the evolution of the faunas through time.

Another implication of the present study is the rapidity with which ostracods can evolve and diversify. Several species have been observed only at a single outcrop, despite sampling of coeval deposits elsewhere. Species of the Subfamily Anticytherideinae first appear in eastern Alabama in the Cusseta Sand (planktonic foraminiferal *Radotruncana calcarata* Taxon Range Zone, early part of the Upper Campanian) and diversify relatively slowly until the Maastrichtian, when their numbers surge to more than 20 species. Its high Maastrichtian diversity did not protect the subfamily from the Cretaceous-Paleogene mass extinction, which marked the end of this clade after approximately 10 million years of evolution.

ACKNOWLEDGMENTS

The authors are grateful to several individuals who contributed to this work. Rosalie Maddocks, Professor at the University of Houston, is sincerely thanked for informative discussions on many aspects of ostracod morphology and biology; her review of the manuscript resulted in vast improvements. Bushra Hussaini, Senior Museum Specialist at the American Museum of Natural History, is thanked for the loan of the type specimens of *Pseudocythereis reticulata* Jennings 1936. Michael Blanton, Research Associate/Team Leader at the University of Southern Mississippi School of Polymer Science and Engineering, is thanked for the extensive use of the Zeiss scanning electron microscope. Amy Stephenson, then undergraduate student at the University of North Alabama, is thanked for picking many specimens and for field assistance. Molly Pasco-Pranger, Associate Professor and Chair of Classics, University of Mississippi, is thanked for her help with the Latin names. Conner and Nathan Puckett are thanked for their assistance in the field.

PLATE 11

Frodocythereis copelandi (Smith 1978)

Specimens 1-7 at same scale, as indicated. Scale for figures 8-11 as indicated.

LV = left valve, RV = right valve

1 Holotype (USNM PAL 255757), exterior RV, female, sample 15A, Maastrichtian Prairie Bluff Formation, Lowndes County, Alabama.

2 Exterior LV, female, specimen 132/136-28, sample 2011-5-18-1 (water level), Maastrichtian Owl Creek Formation, Tippah County, Mississippi.

3 Exterior RV, female, specimen 143-22, sample 2011-8-4-1 (water level), Maastrichtian Owl Creek Formation, Tippah County, Mississippi.

4 Exterior LV, female, specimen 132/136-23, sample 2011-5-18-1 (water level), Maastrichtian Owl Creek Formation, Tippah County, Mississippi.

5 Interior LV, male, specimen 132/136-27, sample 2011-8-4-1 (water level), Maastrichtian Owl Creek Formation, Tippah County, Mississippi.

6 Interior RV, male, specimen 142-9, sample 2011-5-18-1 (water level), Maastrichtian Owl Creek Formation, Tippah County, Mississippi.

7 Exterior RV, male, specimen 28-6a, sample 1994-8-12-4b, Maastrichtian Prairie Bluff Chalk, Lowndes County, Alabama.

8 Closeup external valve, specimen 142-17, sample 2011-8-4-1 (water level), Maastrichtian Owl Creek Formation, Tippah County, Mississippi.

9 Closeup muscle scars, RV, specimen 132/136-26, sample 2011-8-4-1 (water level), Maastrichtian Owl Creek Formation, Tippah County, Mississippi.

10 Closeup muscle scars, LV, specimen 132/136-24, sample 2011-8-4-1 (water level), Maastrichtian Owl Creek Formation, Tippah County, Mississippi.

11 Closeup fossae, punctation and sieve pore, specimen 103-2, sample 2011-5-18-1 (water level), Maastrichtian Owl Creek Formation, Tippah County, Mississippi.

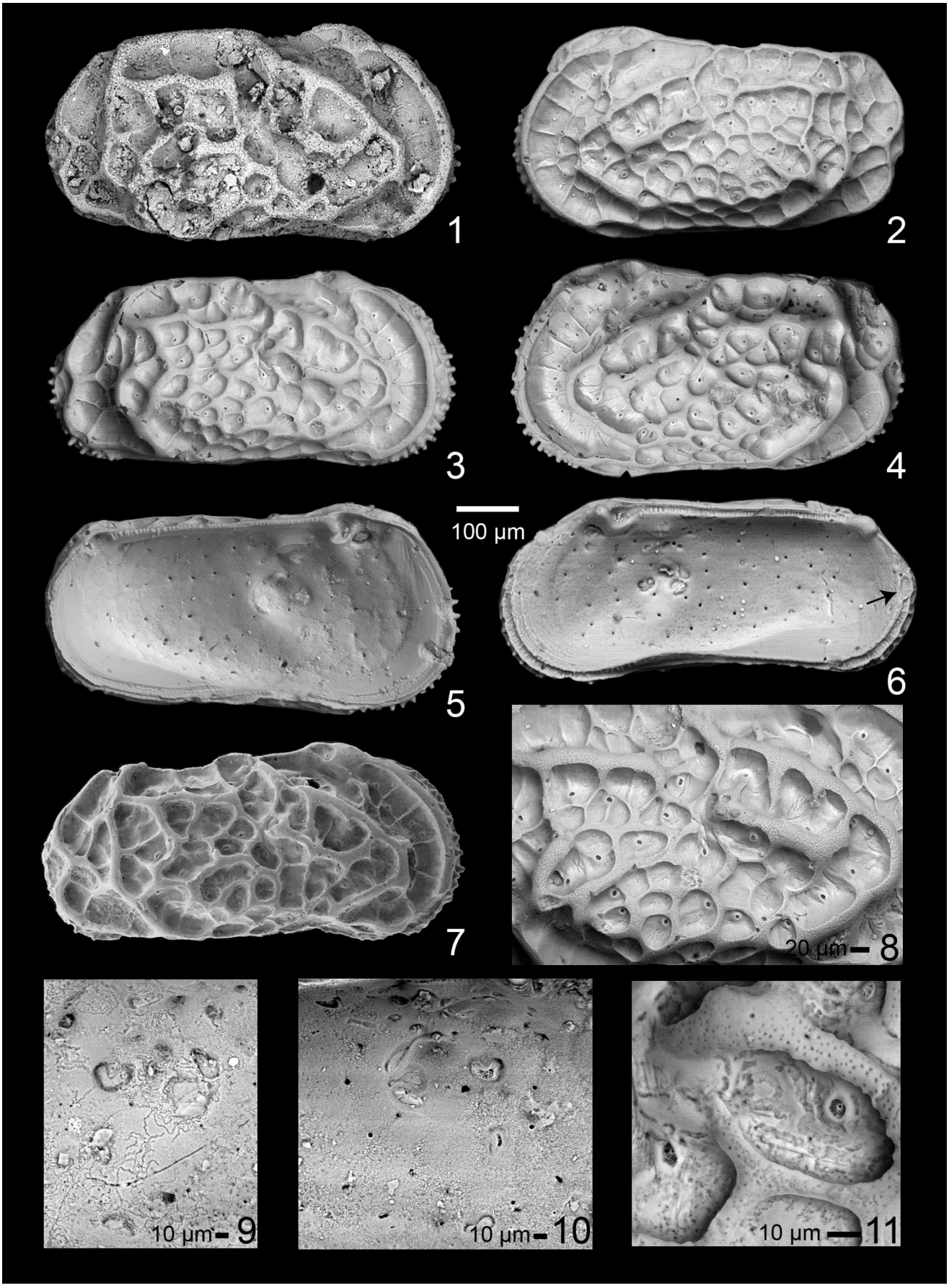
1
2
3
4
100 µm
5
6
7
20 µm
8
10 µm
9
10 µm
10
10 µm
11

REFERENCES

AL-FURAIH, A. A. F., 1980. *Upper Cretaceous and lower Tertiary Ostracoda (Superfamily Cytheracea) from Saudi Arabia.* University of Riyadh, 211 pp.

APOSTOLESCU, V., 1961. Contribution a l'étude paléontoloque (Ostracodes) et stratigraphique des bassins Crétacé et Tertiares de l'Afrique occidentale. *Revue de l'Institut Français du Pétrole,* 16: 779–867.

ATHERSUCH, J., HORNE, D. J. and WHITTAKER, J. E., 1989. *Marine and Brackish Water Ostracods,* London: E.J. Brill.

BAIRD, W., 1850. *The Natural History of the British Entomostraca,* London: The Ray Society.

BARSOTTI, G., 1963. Paleocenic ostracods of Libya (Sirte Basin) and their wide African distribution. *Revue de l'Institut Français du Pétrole,* 18: 1520–1535.

BENSON, R. H., 1972. The *Bradleya* problem, with descriptions of two new psychorospheric genera, *Agrenocythere* and *Poseidonamicus* (Ostracoda: Crustacea). *Smithsonian Contributions to Paleobiology,* 12: 1–138.

BENSON, R. H., BERDAN, J. M., VAN DEN BOLD, W. A. and MOORE, R. C., 1961. *Treatise on Invertebrate Paleontology: Part Q: Crustacea, Ostracoda,* Lawrence, Geological Society of America, 422 pp.

BERTELS, A., 1973. Ostracodes of the type locality of the lower Tertiary (lower Danian) Rocanian Stage and Roca Formation of Argentina. *Micropaleontology,* 19: 308–340.

———, 1975a. Upper Cretaceous (middle Maastrichtian) ostracodes of Argentina. *Micropaleontology,* 21: 97–130.

———, 1975b. Ostracode ecology during the Upper Cretaceous and Cenozoic in Argentina. In: Swain, F. M., Kornicker, L. S. and Lundin, R. F. Eds. *Biology and Paleobiology of Ostracoda, Bulletins of American Paleontology.* Ithaca: Paleontological Research Institute, 317–351.

———, 1976. Evolutionary lineages of some Upper Cretaceous and Tertiary ostracodes of Argentina. *Abhandlungen und Verhandlungen des naturwissenschaftlichen Vereins Hamburg (NF), Supplement,* 18/19: 175–190.

———, 1977. Cretaceous Ostracoda—South Atlantic. In: Swain, F. M. Ed. *Stratigraphic Micropaleontology of Atlantic Basins and Borderlands.* Amsterdam: Elsevier. Developments in Palaeontology and Stratigraphy, 6: 271–303.

BOSQUET, J., 1854. Les crustacés fossiles du terrain crétacé du Limbourg. *Verhandelingen uitgegeven door de Commis sie belast met het vervaardigen eener geologische beschrijving en kaart van Nederland,* 2: 1–127.

BRANDÃO, S. and KARANOVIC, I., 2021. *World Ostracoda Database* [Online]. Available: http://www.marinespecies.org/ostracoda [Accessed 2021-02-02].

BROUWERS, E. and HAZEL, J. E., 1978. Ostracoda and correlation of the Severn Formation (Navarroan; Maestrichtian) of Maryland. *Society of Economic Paleontologists and Mineralogists, Paleontological Monograph,* 1: 1–52.

PLATE 12

Frodocythereis frodoi n. sp.
Specimens 1-8 at same scale, as indicated. Scale for figures 9-12 as indicated.
All specimens collected from the Maastrichtian Owl Creek Formation type locality, Tippah County, Mississippi.
LV = left valve, RV = right valve

1 Exterior RV, female, specimen 132-4, sample 2011-8-4-1 (water level).

2 Exterior LV, female, specimen 29-12, sample 94-5-11-7a.

3 Exterior RV, female, specimen 134-10, sample 2011-8-4-1 (water level).

4 Holotype (USNM PAL 771806), exterior LV, male, specimen 134-2, sample 2011-8-4-1 (water level).

5 Exterior RV, male, specimen 132-9, sample 2011-5-18-1 (water level).

6 Paratype (USNM PAL 771807), exterior LV, female, specimen 104-6, sample 2011-5-18-1 (water level).

7 Interior RV, male, specimen 134-4, sample 2011-8-4-1 (water level).

8 Interior LV, male, specimen 134-1, sample 2011-8-4-1 (water level).

9 Closeup muscle scars, LV, same specimen as figure 8.

10 Closeup muscle scars, RV, specimen 134-8, sample 2011-8-4-1 (water level).

11 Closeup muscle scars, RV, same specimen as figure 7. Note the pair of inverted platforms near the top of the image.

12 Closeup of muscle scars, exterior view, same specimen as figure 4.

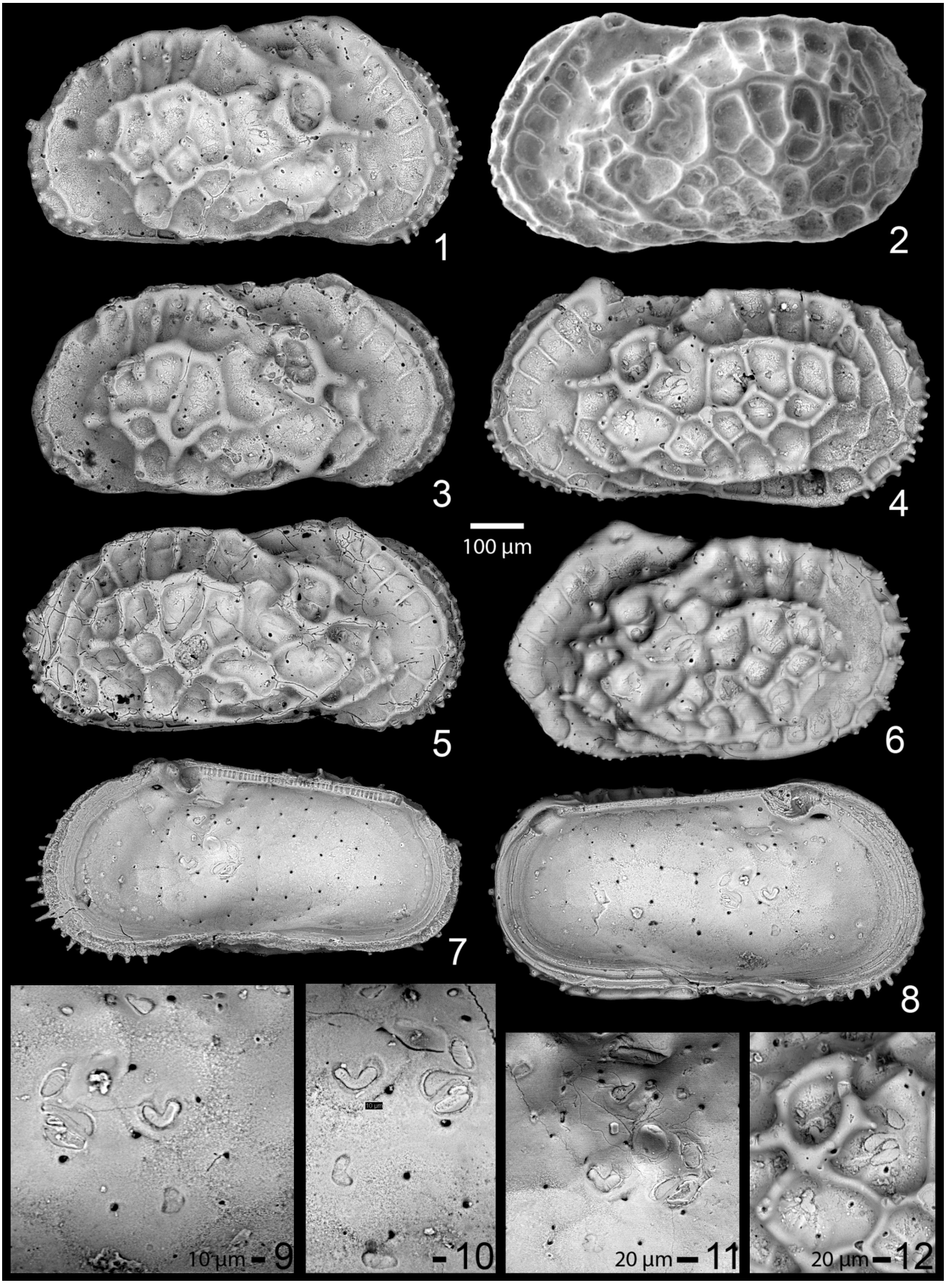
1
2
3
4
100 µm
5
6
7
8
10 µm
9
10
20 µm
11
20 µm
12

BROWN, P. M., 1957. Upper Cretaceous Ostracoda from North Carolina. *North Carolina Department of Conservation and Development, Division of Mineral Resources, Bulletin,* 70: 1–28.

———, 1958. Well logs from the Coastal Plain of North Carolina. *North Carolina Department of Conservation and Development, Division of Mineral Resources, Bulletin*, 72: 1–68.

CARBONNEL, G., 1986. Ostracodes Tertiaires (Paléogène a Néogène) du bassin sénégalo-guinéen. *Documents du Bureau de Recherches Géologiques et Minières,* 101: 33–243.

———, 1988. Les écozones d'ostracodes paléogènes dans les bassins côtiers d'Afrique (Togo, Guinée-Bissau, Sénégal, Mauritanie): un révélateur biogéographique. *Newsletters on Stratigraphy,* 20: 59–72.

CRONIN, T. M. and KHALIFA, H., 1979. Middle and Late Eocene Ostracoda from Gebel El Mereir, Nile Valley, Egypt. *Micropaleontology,* 25: 397–411.

DAMOTTE, R., 1982. Ostracodes Maestrichtiens et Paléocenes du Togo. *Cahiers de Micropaléontologie,* 2: 47–63.

DEROO, G., 1966. Cytheracea (Ostracodes) du Maastrichtien de Maastricht (Pays-Bas) et des régions voisines; résultats stratigraphiques de leur étude. *Mededelingen Van de Geologische Stichting, Serie C, Uitgevers-Maatschappij "Ernst Van Aest", Maastricht,* 2: 1–197.

EL-NADY, H., 2002. Upper Cretaceous ostracods from northeastern Sinai, Egypt: taxonomy and paleobiogeography. *Revue de Paléobiologie, Genève,* 21: 587–638.

GALE, A. S., MUTTERLOSE, J. and BATENBURG, S., 2020. The Cretaceous Period. In: Gradstein, F. M., Ogg, J. G., Schmitz, M. D. and Ogg, G. M. Eds. *Geologic Time Scale 2020.* Amsterdam: Elsevier, 1023–1086.

GEBHARDT, H., 1999. Cenomanian to Coniacian biogeography and migration of North and West African ostracods. *Cretaceous Research,* 20: 215–229.

GOHN, G. S., 1992. Distribution of selected Campanian and Maastrichtian Ostracoda in stratigraphic test holes of the New Jersey Coastal Plain. *U. S. Geological Survey Open File Report, 92-399*: 1–25.

GREKOFF, N., 1964. Étude biostratigraphique des Ostracodes du Crétacé et de l'Eocène inférieur d'Algerie. In: Pétrole, I. F. D. Ed., *Branche Recherche et Exploitation du Pétrole Division Géologie.*

GROSDIDIER, E., 1973. Associations d'Ostracodes de Crétacé d'Iran. *Revue de l'Institut Français du Pétrole,* 28: 131–169.

––––––, 1979. Principaux ostracodes marins de l'intervalle Aptien-Turonien du Gabon (Afrique occidentale). *Bulletin des Centres de Recherches Exploration-Production Elf-Aquitaine,* 3: 1–35.

GUBER, A. L. and JAANUSSON, V., 1964. Ordovician ostracodes with posterior domiciliar dimorphism. *Uppsala University, Geological Institutions Bulletin,* 43: 1–41.

HABIB, D., MOSHKOVITZ, S. and KRAMER, C., 1992. Dinoflagellate and calcareous nannofossil response to sea-level changes in Cretaceous-Tertiary boundary sections. *Geology,* 20: 165–168.

HABIB, D., OLSSON, R. K., LIU, C. and MOSHKOVITZ, S., 1996. High-resolution biostratigraphy of sea-level low, biotic extinction, and chaotic sedimentation at the Cretaceous-Tertiary boundary in Alabama, north of the Chixculub crater. In: Ryder, G., Fastovsky, D. E. and Gartner, S. Eds. *The Cretaceous-Tertiary Event and Other Catastrophes in Earth History.* Boulder: Geological Society of America, 243–252.

HART, M. B., HARRIES, P. J. and CÁRDENAS, A. L., 2013. The Cretaceous/Paleogene boundary events in the Gulf Coast: comparisons

---

PLATE 13

Laevipellacythereis colossus n. sp.
Specimens 1-6, 8 at same scale, as indicated. Scale for figures 7, 9-11 as indicated.
All specimens from sample 2012-01-03-1-2, Maastrichtian Providence Sand of Barbour County, Alabama.
LV = left valve, RV = right valve

1 Exterior RV, male, specimen 148-8.

2 Holotype (USNM PAL 771808), exterior LV, male, specimen 148-7.

3 Interior LV, female, specimen 148-10.

4 Paratype (USNM PAL 771809), exterior LV, female, specimen 148-9. Arrow points to outline of upper internal inverted platform as seen on the exterior of the carapace.

5 Interior LV, male, specimen 148-11.

6 Interior RV, male, specimen 148-13. Left arrows point to upper and lower inverted platforms and right arrow points to interruption of selvage at caudal region.

7 Closeup muscle scars, same specimen as figure 8.

8 Interior RV, female, specimen 148-12.

9 Closeup muscle scars, exterior view, RV, same specimen as figure 1.

10 Closeup sieve pores, RV, same specimen as figure 3.

11 Closeup muscle scars, LV, same specimen as figure 5.

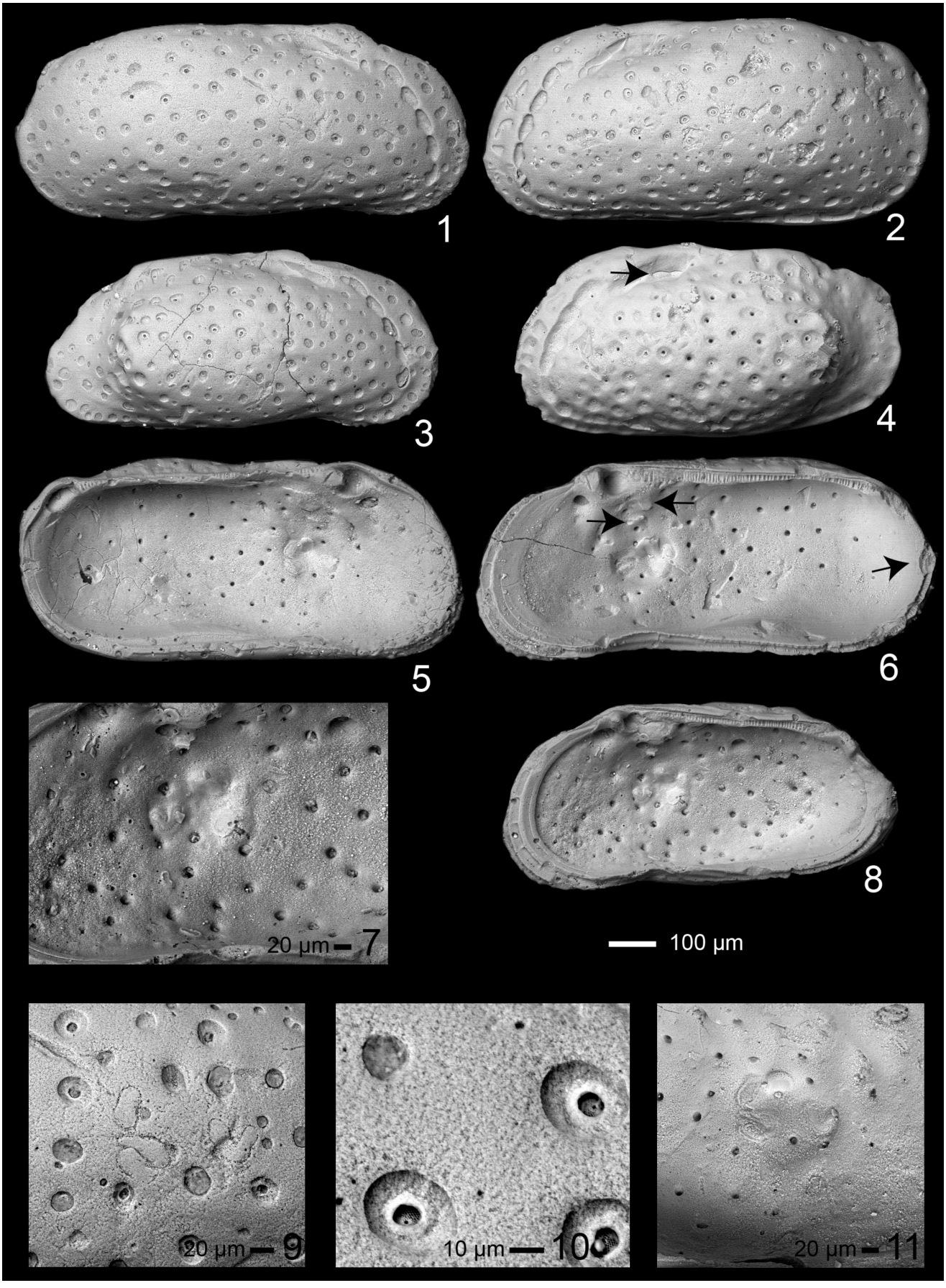
1
2
3
4
5
6
8
20 µm
7
100 µm
20 µm
9
10 µm
10
20 µm
11

between Alabama and Texas. *Transactions of the Gulf Coast Association of Geological Societies,* 63: 235–255.

HAZEL, J. E., 1967. Classification and distribution of the Recent Hemicytheridae and Trachyleberididae (Ostracoda) off northeastern North America. *U.S. Geological Survey Professional Paper,* 564: 1–49.

HAZEL, J. E. and BROUWERS, E. M., 1982. Biostratigraphic and chronostratigraphic distribution of ostracodes in the Coniacian-Maastrichtian (Austinian-Navarroan) in the Atlantic and Gulf Coastal Provinces. *Guidebook of excursions and related papers for the 8th International Symposium on Ostracoda*, 166–198.

HONIGSTEIN, A., 1984. Senonian ostracodes from Israel. *Geological Survey of Israel, Bulletin,* 78: 1–48.

HONIGSTEIN, A., RAAB, M. and ROSENFELD, A., 1985. Manual of Cretaceous ostracodes from Israel. *Geological Survey of Israel, Special Publication,* 5: 1–25.

HORNE, D. J., COHEN, A. and MARTENS, K., 2002. Taxonomy, morphology and biology of Quaternary and living Ostracoda. *Geophysical Monograph,* 131, The Ostracoda: Applications on Quaternary Research, 5–139.

HOWE, H. V. and LAURENCICH, L., 1958. *Introduction to the Study of Cretaceous Ostracoda,* Baton Rouge: Louisiana State University Press, 1–536.

HUANG, H.-H. M., YASUHARA, M., CRONIN, T. M., HISAYO, O. and HUNT, G., 2022. *Poseidonamicus* (Ostracoda) from the North Atlantic Ocean. *Micropaleontology,* 68: 257–271.

HUNT, G., 2007. Morphology, ontogeny, and phylogenetics of the Genus *Poseidonamicus* (Ostracoda: Thaerocytherinae). *Journal of Paleontology,* 81: 607–631.

HUNT, G., FERNANDES MARTINS, J., PUCKETT, T. M., LOCKWOOD, R., SWADDLE, J. P., HALL, C. M. S. and STEDMAN, J., 2017. Sexual dimorphism and sexual selection in cytheroidean ostracodes from the Late Cretaceous of the U.S. Gulf Coastal Plain. *Paleobiology,* 43: 620–641.

ISMAIL, A. A. and SOLIMAN, S. I., 1997. Cenomanian-Santonian foraminifera and ostracodes from Horus Well-1, North Western Desert, Egypt. *Micropaleontology,* 43: 165–183.

JENNINGS, P. H., 1936. A microfauna from the Monmouth and basal Rancocas Groups of New Jersey. *Bulletins of American Paleontology,* 23: 1–77.

KENNEDY, W. J., LANDMAN, N. H., COBBAN, W. A. and JOHNSON, R. O., 2000. Additions to the ammonite fauna of the Upper Cretaceous Navesink Formation of New Jersey. *American Museum Novitates*, 1–30.

KESLING, R. V., 1951. Terminology of ostracod carapaces. *Contributions from the Museum of Paleontology University of Michigan,* 9: 93–171.

KEYSER, D., 1990. Morphological changes and function of the inner lamella of podocopid Ostracoda. In: Whatley, R. and Maybury, C. Eds. *Ostracoda and Global Events.* London: Chapman and Hall, 401–410.

———, 2005. Histological peculiarities of the noding process in *Cyprideis torosa* (Jones) (Crustacea, Ostracoda). *Hydrobiologia,* 538: 95–106.

PLATE 14

Laevipellacythereis laevipellis n. sp.

Specimens 1-8 at same scale, as indicated. Scale for figures 9-11 as indicated.

All specimens collected from the type locality of the Maastrichtian Owl Creek Formation, Tippah County, Mississippi.

LV = left valve, RV = right valve

1 Exterior RV, female, specimen 130/135-22, sample 2011-8-4-1 (water level).

2 Holotype (USNM PAL 771810), exterior LV, female, specimen 130/135-23, sample 2011-8-4-1 (water level).

3 Paratype (USNM PAL 771811), exterior RV, male, specimen 130/135-28, sample 2011-8-4-1 (water level).

4 Exterior LV, male, specimen 130/135-10, possible juvenile, sample 2011-5-18-1 (water level).

5 Interior LV, female, specimen 130/135-5, sample 2011-5-18-1 (water level).

6 Interior RV, female, specimen 130/135-6, sample 2011-5-18-1 (water level).

7 Interior LV, male, specimen 130/135-7, possible juvenile, sample 2011-8-4-1 (water level).

8 Interior RV, male, specimen 130/135-20, sample 2011-8-4-1 (water level). Arrow points to interruption of selvage at caudal region.

9 Closeup sieve pores, specimen 130/135-31, sample 2011-8-4-1 (water level).

10 Closeup muscle scars, specimen 130/135-8, sample 2011-8-4-1 (water level).

11 Closeup sieve pore, same specimen as figure 6.

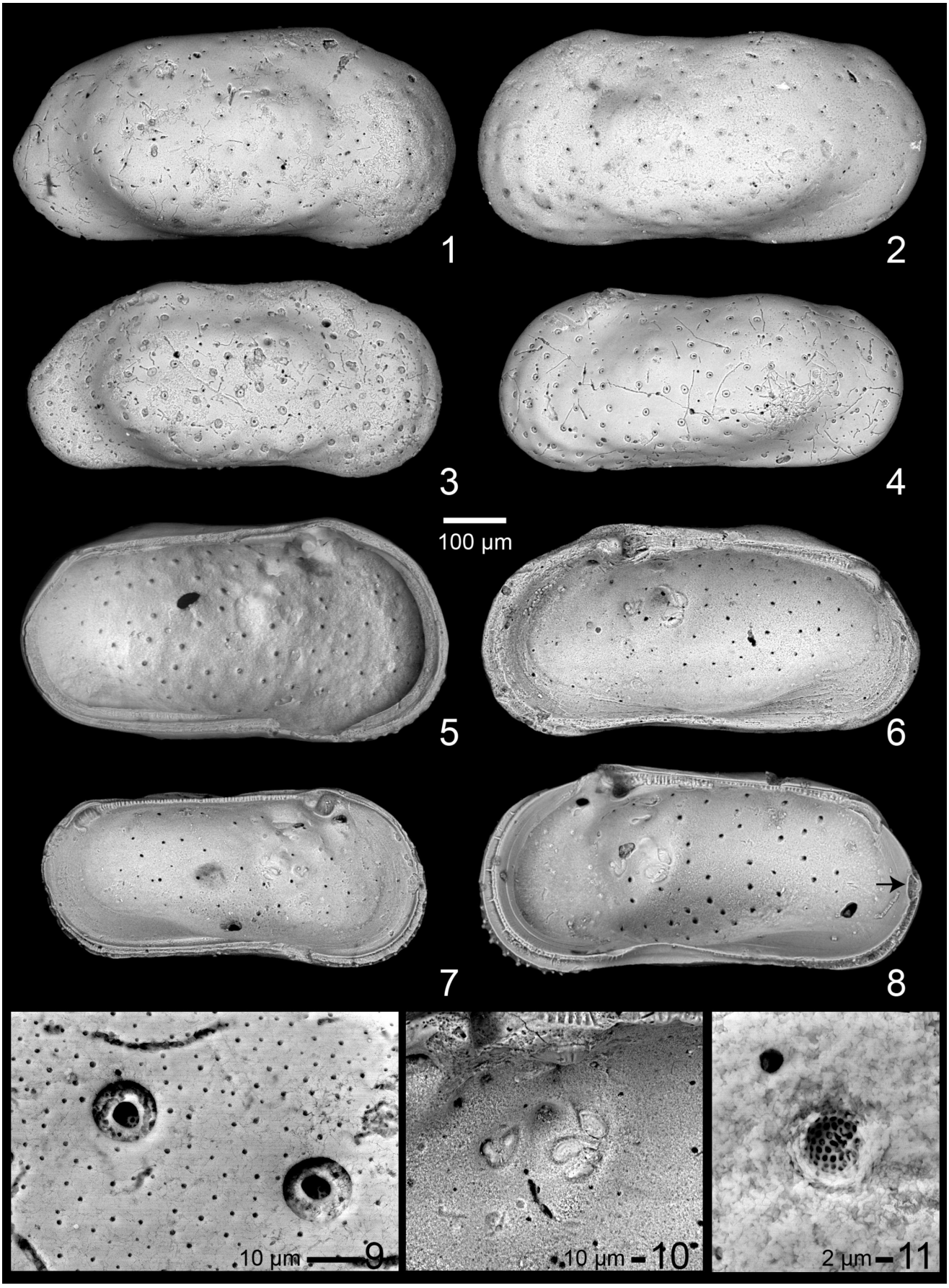
1
2
3
4
100 µm
5
6
7
8
10 µm
9
10 µm
10
2 µm
11

KHALIFA, H. and CRONIN, T. M., 1979. Ostracodes de l'Éocène moyen de El Sheikh Fadl, est de Beni Mazar, Haute-Égypte. *Revue de Micropaléontologie,* 22: 172–185.

LARINA, E., GARB, M., LANDMAN, N., DASTAS, N., THIBAULT, N., EDWARDS, L., PHILLIPS, G., ROVELLI, R., MYERS, C. and NAUJOKAITYTE, J., 2016. Upper Maastrichtian ammonite biostratigraphy of the Gulf Coastal Plain (Mississippi Embayment USA). *Cretaceous Research,* 60: 128–151.

LATREILLE, P. A., 1802. Histoire naturelle, générale et particulière des Crustacés et des Insectes. *Histoire des Cypris et des Cytherées,* 8: 232–254.

LAURENTIAUX, C., 1950. Les insectes Houillers du Limbourg hollandais. *Mededelingen Van de Geologische Stichting, Serie C, Uitgevers-Maatschappij "Ernst Van Aest", Maastricht,* 4: 13–22.

LIEBAU, A., 1977. *Homologous sculpture patterns in Trachyleberididae and related ostracods,* Belgrade: Nolit Publishing House.

LIEBERMAN, B. S., 2000. *Paleobiogeography: Using Fossils to Study Global Change, Plate Tectonics, and Evolution,* New York: Kluwer Academic/Plenum Publishers.

LORD, A. R., CABRAL, M. C. and DANIELOPOL, D. L., 2020. Sieve-type normal pore canals in Jurassic ostracods: A review with description of a new genus. *Acta Palaeontologica Polonica,* 65: 313–349.

MADDOCKS, R. F., 1969. Revision of Recent Bairdiidae (Ostracoda). *United States National Museum Bulletin,* 295: 1–126.

MANCINI, E. A. and PUCKETT, T. M., 2005. Jurassic and Cretaceous transgressive-regressive (T-R) cycles, northern Gulf of Mexico, USA. *Stratigraphy,* 2: 31–48.

MANCINI, E. A., TEW, B. H. and PUCKETT, T. M., 1996a. Comparison of Upper Cretaceous and Paleocene depositional sequences in the eastern Gulf Coastal Plain. *Transactions of the Gulf Coast Association of Geological Societies,* 46: 281–286.

MANCINI, E. A., PUCKETT, T. M. and TEW, B. H., 1996b. Integrated biostratigraphic and sequence stratigraphic framework for Upper Cretaceous strata of the eastern Gulf Coastal Plain. *Cretaceous Research,* 17: 645–669.

MANCINI, E. A., PUCKETT, T. M., TEW, B. H. and SMITH, C. C., 1995a. Upper Cretaceous sequence stratigraphy of the Missis-

PLATE 15

Tumulocythereis incompta n. sp.
Specimens 1-8 at same scale, as indicated. Scale for figures 9-14 as indicated.
LV = left valve, RV = right valve

1 Holotype (USNM PAL 771812), exterior RV, male, specimen 142-11, sample 2011-8-4-1 (water level), Maastrichtian Owl Creek Formation, Tippah County, Alabama.

2 Exterior LV, female, specimen 134-19, 2010-10-22-1 (505), Maastrichtian Coon Creek Formation, Tippah County, Mississippi.

3 Paratype (USNM PAL 771813), exterior RV, female, specimen 142-10, sample 2011-8-4-1, latest Campanian-Maastrichtian Owl Creek Formation, Tippah County, Mississippi.

4 Exterior LV, female, specimen 141-9, sample 2011-8-4-1 (water level), Maastrichtian Owl Creek Formation, Tippah County, Mississippi.

5 Interior LV, female, same specimen as figure 4.

6 Interior RV, female, specimen 145-4, sample 1994-5-11-7a, Maastrichtian Owl Creek Formation, Tippah County, Mississippi.

7 Interior LV, male, specimen 145-5, sample 2011-8-4-1, Maastrichtian Owl Creek Formation, Tippah County, Mississippi.

8 Interior RV, male, specimen 142-9, sample 2011-8-4-1 (water level), Maastrichtian Owl Creek Formation, Tippah County, Mississippi. Arrow points to interruption of selvage at caudal region.

9 Closeup sieve pores, specimen 145-10, sample 2011-5-18-1 (water level), Maastrichtian Owl Creek Formation, Tippah County, Mississippi.

10 Closeup hinge area, specimen 145-6, sample 2011-8-4-1, Maastrichtian Owl Creek Formation, Tippah County, Mississippi.

11 Closeup sieve pores, specimen 145-7, sample 1994-5-11-7 (18' below shell bed), Maastrichtian Owl Creek Formation, Tippah County, Mississippi.

12 Closeup fossae and sieve pores, same specimen as figure 3.

13 Closeup muscle scars, same specimen as figure 7.

14 Closeup muscle scars, same specimen as figure 10.

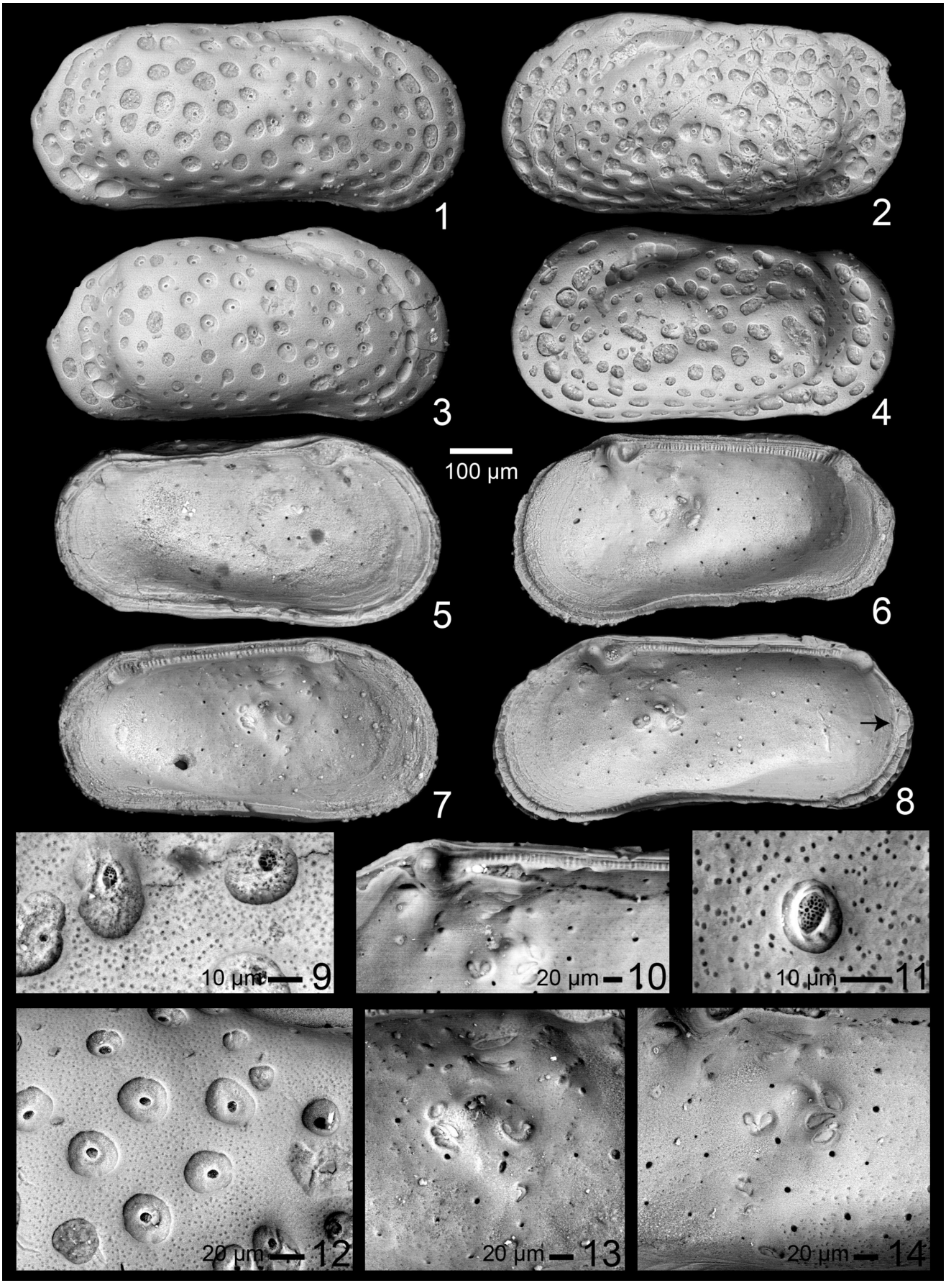
1
2
3
4
100 µm
5
6
7
8
10 µm 9
20 µm 10
10 µm 11
20 µm 12
20 µm 13
20 µm 14

sippi-Alabama area. *Transactions of the Gulf Coast Association of Geological Societies,* 44: 377–384.

———, 1995b. Upper Cretaceous sequence stratigraphy of the Mississippi-Alabama area. *Transactions of the Gulf Coast Association of Geological Societies,* 45: 377–384.

MASOLI, M., 1965. Sur quelques ostracodes fossiles Mésozoiques (Crétacé) du Bassin Côtier de Tarfaya (Maroc méridional). *Bulletin du Bureau de recherches géologiques et minières, Memoire*, 32: 119–128.

MINARD, J. P., SOHL, N. F. and OWENS, J. P., 1976. Re-introduction of the Severn Formation (Upper Cretaceous) to replace Monmouth Formation in Maryland. *U.S. Geological Survey Bulletin,* 1435-A: 132–133.

MOSHKOVITZ, S. and HABIB, D., 1993. Calcareous nannofossil and dinoflagellate stratigraphy of the Cretaceous-Tertiary boundary, Alabama and Georgia. *Micropaleontology,* 39: 167–191.

OKADA, Y., 1981. Development of cell arrangement in ostracod carapaces. *Paleobiology,* 7: 276–280.

———, 1982a. Ultrastructure and pattern of the carapace of *Bicornucythere bisanensis* (Ostracoda, Crustacea). In: Hanai, T. Ed. *Studies on Japanese Ostraoda.* Tokyo: University of Tokyo Press, 229–267.

———, 1982b. Structure and cuticle formation of the reticulated carapace of the ostracode *Bicornucythere bisanensis*. *Lethaia,* 15: 85–101.

OSBORNE, W. E., SZABO, M., COPELAND, C. W., JR. and NEATHERY, T. L., 1989. Geologic Map of Alabama. Tuscaloosa: Geological Survey of Alabama.

ÖZDIKMEN, H., 2010. Substitute names for three genera of Ostracoda (Crustacea). *Munis Entomology & Zoology,* 5: 315–316.

PEYPOUQUET, J.-P., DUCASSE, O., GAYET, J. and PRATVEIL, L., 1980. "Agradation et dégradation" des tests d'ostracodes. Intéret pour la connaissance de l'évolution paléohydrologique des domaines margino-littoraux carbonates. *Actes Réunion "Cristallisation-Déformation-Dissolution des carbonates*, 357–369.

PEYPOUQUET, J.-P., CARBONEL, P., DUCASSE, O., TÖLDERER-FARMER, M. and LÉTÉ, C., 1988. Environmentally cued polymorphism of ostracods. *Developments in Palaeontology and Stratigraphy,* 11: 1003–1019.

PITAKPAIVAN, K., 1994. *Ostracoda of the latest Cretaceous and earliest Tertiary of the Gulf Coastal Plain: biostratigraphy, paleoenvironments and systematics.* unpublished Ph.D. dissertation, Louisiana State University.

PLATE 16

Tumulocythereis priddyi (Smith 1978)

Specimens 1-10 at same scale, as indicated. Scale for figures 11-13 as indicated.

LV = left valve, RV = right valve

1 Exterior RV, male, specimen 130/135-16, sample 2011-8-4-1 (water level), Maastrichtian Owl Creek Formation, Tippah County, Mississippi.

2 Paratype (USNM PAL 255719), sex uncertain, sample 15A, Maastrichtian Prairie Bluff Formation, Lowndes County, Alabama.

3 Exterior RV, female, specimen 143-20, sample 2011-8-4-1 (water level), Maastrichtian Owl Creek Formation, Tippah County, Mississippi.

4 Exterior LV, male, specimen 104-11, sample 2011-5-18-1 (5'), Maastrichtian Owl Creek Formation, Tippah County, Mississippi.

5 Exterior RV, female, specimen 133/137-13, sample 2011-8-4-1 (water level), Maastrichtian Owl Creek Formation, Tippah County, Mississippi.

6 Exterior LV, female, specimen 133/137-6, sample 2011-8-4-1 (water level), Maastrichtian Owl Creek Formation, Tippah County, Mississippi.

7 Interior LV, male, specimen 143-12, sample 2011-8-4-1 (water level), Maastrichtian Owl Creek Formation, Tippah County, Mississippi.

8 Interior RV, male, specimen 145-16, sample 2011-8-4-1 (water level), Maastrichtian Owl Creek Formation, Tippah County, Mississippi. Arrow points to interruption of selvage at caudal region.

9 Interior LV, female, specimen 133/137-8, sample 2011-8-4-1 (water level), Maastrichtian Owl Creek Formation, Tippah County, Mississippi.

10 Interior RV, male, specimen 143-14, sample 2011-8-4-1 (water level), Maastrichtian Owl Creek Formation, Tippah County, Mississippi. Arrows point to upper and lower fusiform inverted platforms.

11 Closeup fossae, specimen 142-13, sample 2011-8-4-1 (water level), Maastrichtian Owl Creek Formation, Tippah County, Mississippi.

12 Closeup sieve pore, same specimen as figure 7.

13 Closeup muscle scars, specimen 103-15, sample 2011-5-18-1 (water level), Maastrichtian Owl Creek Formation, Tippah County, Mississippi.

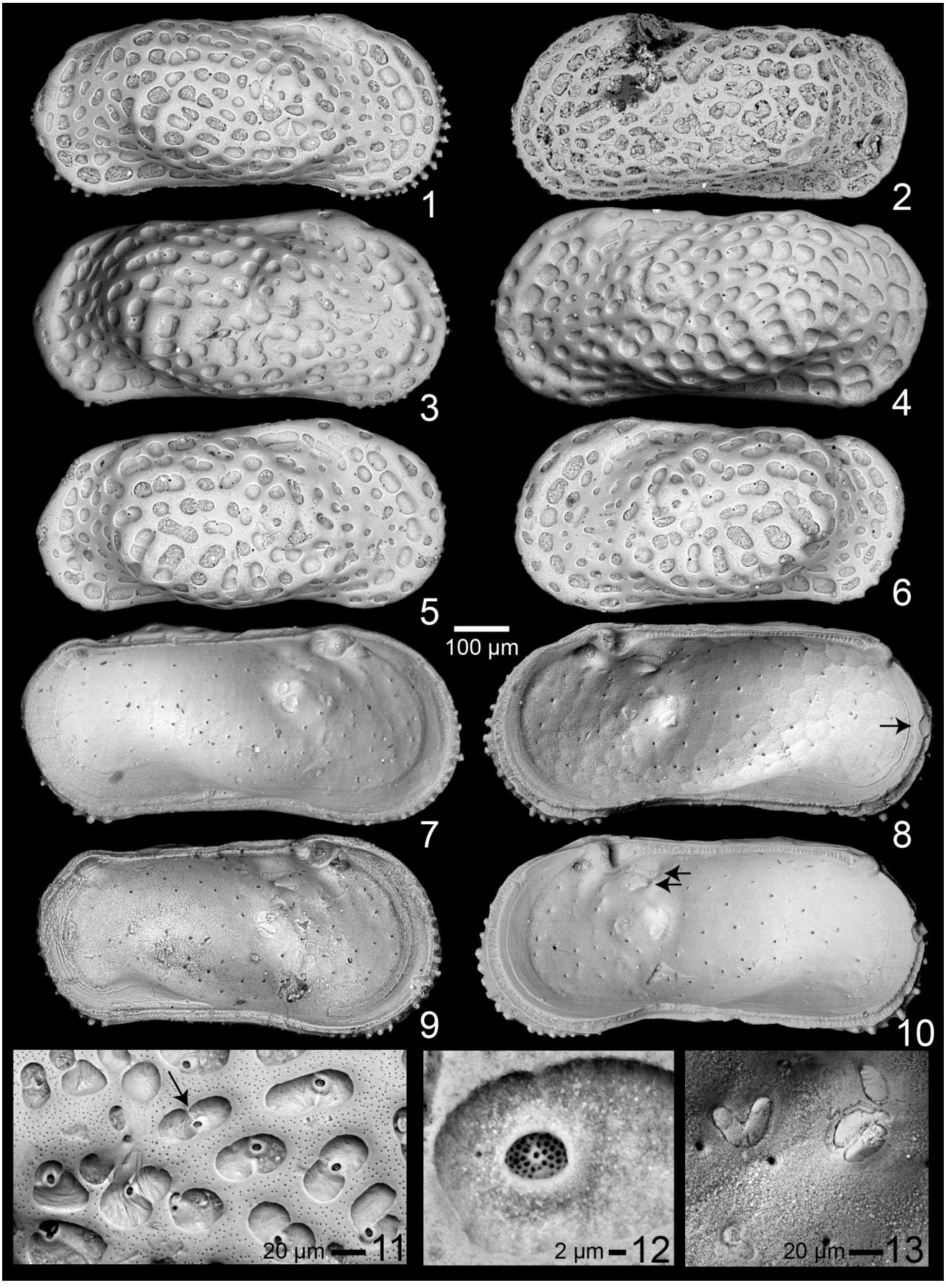
1
2
3
4
5
6
100 µm
7
8
9
10
20 µm
11
2 µm
12
20 µm
13

POKORNÝ, V., 1969a. The Genus *Radimella* Pokorný 1969 (Ostracoda, Crustacea). *Acta Universitatis Carolinae,* 4: 293–334.

———, 1969b. *Radimella*, gen. n.: a new genus of the Hemicytherinae (Ostracoda, Crustacea). *Acta Universitatis Carolinae,* 4: 359–373.

PUCKETT, T. M., 1992. Distribution of ostracodes in the Upper Cretaceous (late Santonian through middle Maastrichtian) of Alabama and Mississippi. *Transactions of the Gulf Coast Association of Geological Societies,* 42: 613–631.

———, 1994. Planktonic foraminiferal and ostracode biostratigraphy of upper Santonain through lower Maastrichtian strata in central Alabama. *Transactions of the Gulf Coast Association of Geological Societies,* 44: 585–595.

———, 1995a. Upper Cretaceous ostracode paleoecology, SE USA. In: Ríha, J. Ed. *Ostracoda and Biostratigraphy.* Rotterdam: A.A. Balkema, 141–151.

———, 1995b. Planktonic foraminiferal and ostracode biostratigraphy of lat Santonian through early Maastrichtian strata in Dallas County, Alabama. *Geological Survey of Alabama Bulletin,* 164: 1–59.

———, 1996. Ecologic atlas of Upper Cretaceous ostracodes of Alabama. *Geological Survey of Alabama Monograph,* 14: 1–176.

———, 2002. Systematics and paleobiogeography of brachycytherine Ostracoda. *Micropaleontology,* 48, supplement no. 2: 1–87.

———, 2005. Santonian-Maastrichtian planktonic foraminiferal and ostracode biostratigraphy of the northern Gulf Coastal Plain, USA. *Stratigraphy,* 2: 117–146.

———, 2009a. On the global distribution of Late Cretaceous ostracodes: the Genus *Bicornicythereis* (n. gen.), with notes on *Curfsina*. *Micropaleontology,* 55: 345–364.

———, 2009b. On the relationship between plate tectonics and phylogeny in ostracodes. *North American Micropaleontological Section—SEPM, Geologic Problem Solving with Microfossils II.* Houston: SEPM.

———, 2012. Paleogeographic significance of muscle scars in global populations of Late Cretaceous ostracodes. *Micropaleontology,* 58: 259–271.

———, 2013. Ostracodes and plate tectonics: a case from the latest Cretaceous of the Caribbean region. *North American Micropaleontological Section—SEPM, Geological Problem Solving with Mircofossils III.* Houston: SEPM.

PUCKETT, T. M. and MANCINI, E. A., 1998. Planktonic foraminiferal *Globotruncanita calcarata* total range zone: its significance and importance to chronostratigraphic correlation in the Gulf Coastal Plain, USA. *Journal of Foraminiferal Research,* 28: 124–134.

PUCKETT, T. M., COLIN, J.-P. and MITCHELL, S., 2012. New species and genera of Ostracoda from the Maastrichtian (Late Cretaceous) of Jamaica. *Micropaleontology,* 58: 397–455.

PUCKETT, T. M., ANDREU, B. and COLIN, J.-P., 2016. The evolution of the Brachycytheride Ostracoda in the context of the breakup of Pangea. *Revue de Micropaléontologie,* 59: 97–167.

PURI, H. S., 1953. The ostracode genus *Hemicythere* and its allies. *Journal of the Washington Academy of Sciences,* 43: 169–179.

PLATE 17

Tumulocythereis tiberti n. sp.
Specimens 1-7 at same scale, as indicated. Scale for figures 8-11 as indicated.
All specimens collected from the type locality of the Maastrichtian Owl Creek Formation, Tippah County, Mississippi.
LV = left valve, RV = right valve

1 Exterior RV, female, specimen 130/135-13, sample 2011-5-18-1 (water level).

2 Exterior LV, male, specimen 130/135-14, sample 2011-5-18-1 (water level).

3 Holotype (USNM PAL 771814), exterior RV, female, specimen 130/135-18, sample 2011-5-18-1 (water level).

4 Exterior LV, presumed female, specimen 103-13, sample 2011-5-8-1 (water level).

5 Interior LV, female, specimen 142-2, sample 2011-8-4-1 (water level).

6 Interior RV, female, specimen 150-6, sample 2011-8-4-1 (water level).

7 Interior LV, presumed male, specimen 130-12, sample 2011-5-18-1 (water level).

8 Closeup muscle scars, external view, same specimen as figure 1.

9 Closeup of muscle scars, LV, specimen 142-1, sample 2011-8-4-1 (water level). Arrows point to fusiform inverted platforms.

10 Closeup of sieve pore and punctation, specimen 130/135-9, sample 2011-5-8-1 (water level).

11 Closeup external ornamentation, specimen 151-6, sample 2011-8-4-1 (water level).

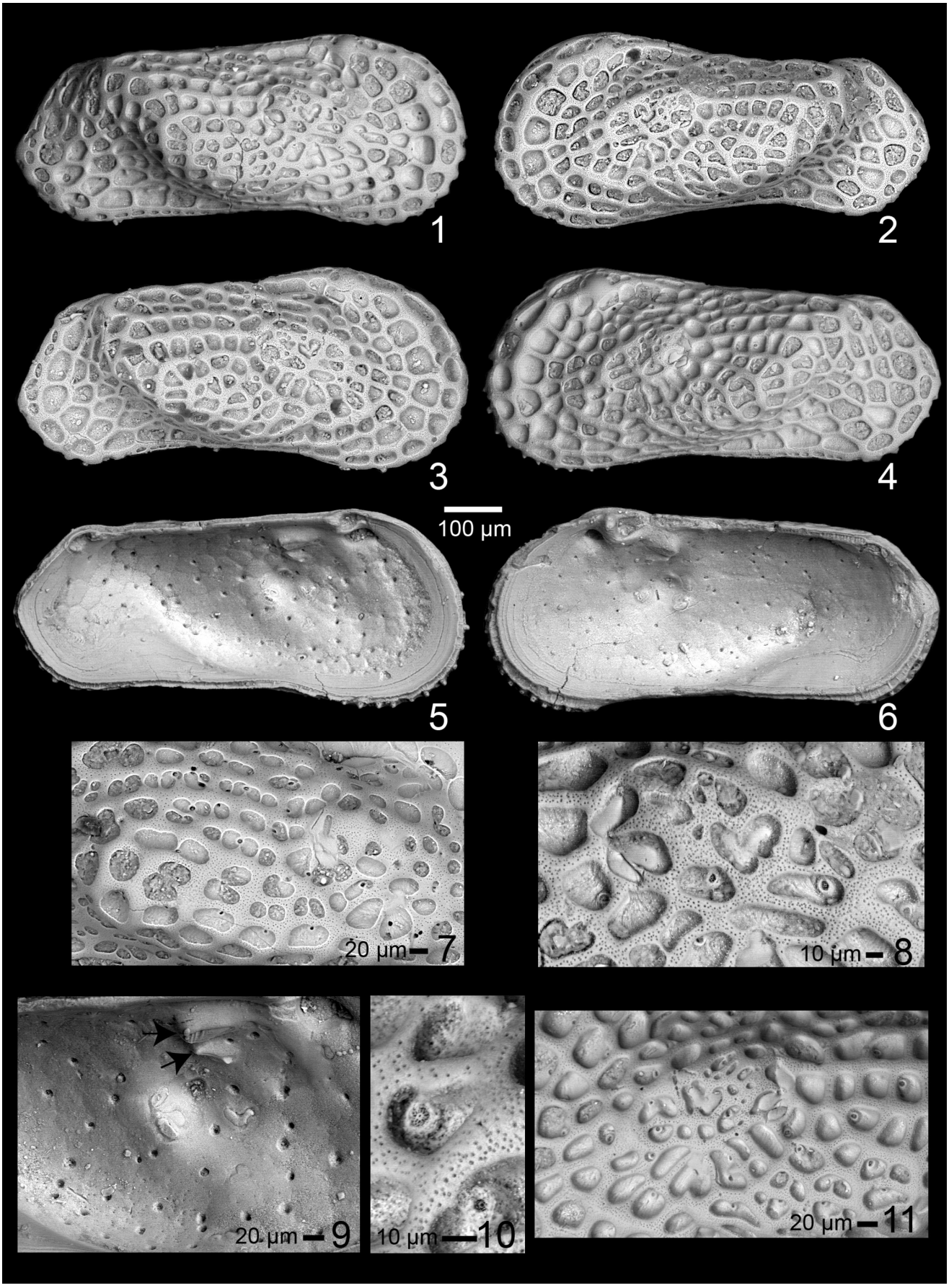
1
2
3
4
100 µm
5
6
20 µm
7
10 µm
8
20 µm
9
10 µm
10
20 µm
11

PURI, H. S. and DICKAU, B. E., 1969. Use of normal pores in taxonomy of Ostracoda. *Transactions of the Gulf Coast Association of Geological Societies,* 29: 353–367.

REYMENT, R. A., 1980. Biogeography of the Saharan Cretaceous and Paleocene epicontinental transgressions. *Cretaceous Research,* 1: 299–327.

REYMENT, R. A. and REYMENT, E. R., 1980. The Palaeocene trans-Saharan transgression and its ostracod fauna. In: Salem, M. J. and Busrewil, M. T. Eds. *The Geology of Libya.* London: Academic Press, 245–254.

ROHLF, F. J., 2013. tpsDIG. 2.17 ed. SUNY Stoneybrook.

RUSSELL, E. E. and PARKS, W. S., 1975. Stratigraphy of the outcropping Upper Cretaceous, Paleocene, and Lower Eocene in western Tennessee including description of younger fluvial deposits. *Tennesse Geological Survey Bulletin*, 76: 1–111.

SAMES, B., WHATLEY, R. and SCHUDACK, M., 2010. *Praecypridea*: A new non-marine ostracod genus from the Jurassic and Early Cretaceous of Europe, North and South America, and Africa. *Journal of Micropalaeontology,* 29: 163–176.

SARS, G. O., 1866. Oversigt af Norges marine Ostracoder. *Forhandlinger i Videnskabs-Selskabet,* 1965, 1–130.

SCHALLREUTER, R. E. L., 1977. On *Miehlkella cribroporata* Schallreuter gen. et sp. nov. *A Stereo-Atlas of Ostracod Shells,* 4: 9–16.

SEELING, J., COLIN, J.-P. and FAUTH, G., 2004. Global Campanian (Upper Cretaceous) ostracod paleobiogeography. *Palaeogeography, Palaeoclimatology, Palaeoecology,* 213: 379–398.

SHAHIN, A., 2005. Maastrichtian to middle Eocene ostracodes from Sinai, Egypt: systematics, biostratigraphy and paleobiogeography. *Revue de Paléobiologie,* 24: 749–779.

SKOGSBERG, K. J. T., 1928. Studies on marine ostracods. Part 2. External morphology of the genus *Cythereis* with descriptions of twenty-one new species. *Occasional Papers California Academy of Science,* 15: 1–155.

SLIPPER, I., 2019. Ostracoda from the Turonian of South-East England. Part 1. *Monographs of the Palaeontographical Society,* 655: 1–75.

———, 2021. Ostracoda from the Turonian of South-East England Part 2. Cytherocopina. *Monographs of the Palaeontological Society,* 657: 47–168.

SMITH, J. K., 1978. Ostracoda of the Prairie Bluff Chalk, Upper Cretaceous (Maestrichtian) and the Pine Barren Member of the Clayton Formation, lower Paleocene (Danian) from exposures along Alabama State Highway 263 in Lowndes County, Alabama. *Transactions of the Gulf Coast Association of Geological Societies,* 28: 539–580.

SUGARMAN, P. J., MILLER, K. G., BUKRY, D. and FEIGENON, M. D., 1995. Uppermost Campanian-Maastrichtian strontium isotopic, biostratigraphic, and sequence stratigraphic framework of the New

---

PLATE 18

Tumulocythereis tumulus n. sp.
Specimens 1-8 at same scale, as indicated. Scale for figures 9-14 as indicated.
All specimens collected from sample 2011-5-18-1 (water level), Maastrichtian Owl Creek Formation
LV = left valve, RV = right valve

1 Holotype (USNM PAL 771815), exterior RV, female, specimen 143-6.

2 Exterior LV, male, specimen 143-11.

3 Exterior RV, presumed male, specimen 103-14.

4 Paratype (USNM PAL 771816), exterior LV, presumed male, specimen 143-7.

5 Interior LV, same specimen as figure 2.

6 Interior RV, female, specimen 143-4. Arrow points to interruption of selvage at caudal region.

7 Interior LV, male, specimen 143-2.

8 Interior RV, female, specimen 143-13.

9 Closeup sieve pore, specimen 143-10.

10 Closeup fossae, same specimen as figure 4. Arrow points to apophysis extending across fossa.

11 Closeup fossae and punctation, specimen 143-17. Note caperate solum (arrow), undercut muri, and apophyses connecting invaginations of muri to puckered sieve-type normal pore canals (upper left of image).

12 Closeup hinge and inverted platform, same specimen as figure 8. Note two fusiform inverted platforms (arrows).

13 Closeup muscle scars LV, specimen 143-1, sample 2011-5-18-1.

14 Closeup fossae and punctation, same specimen as figure 1. Note apophysis extending into fossa (arrow).

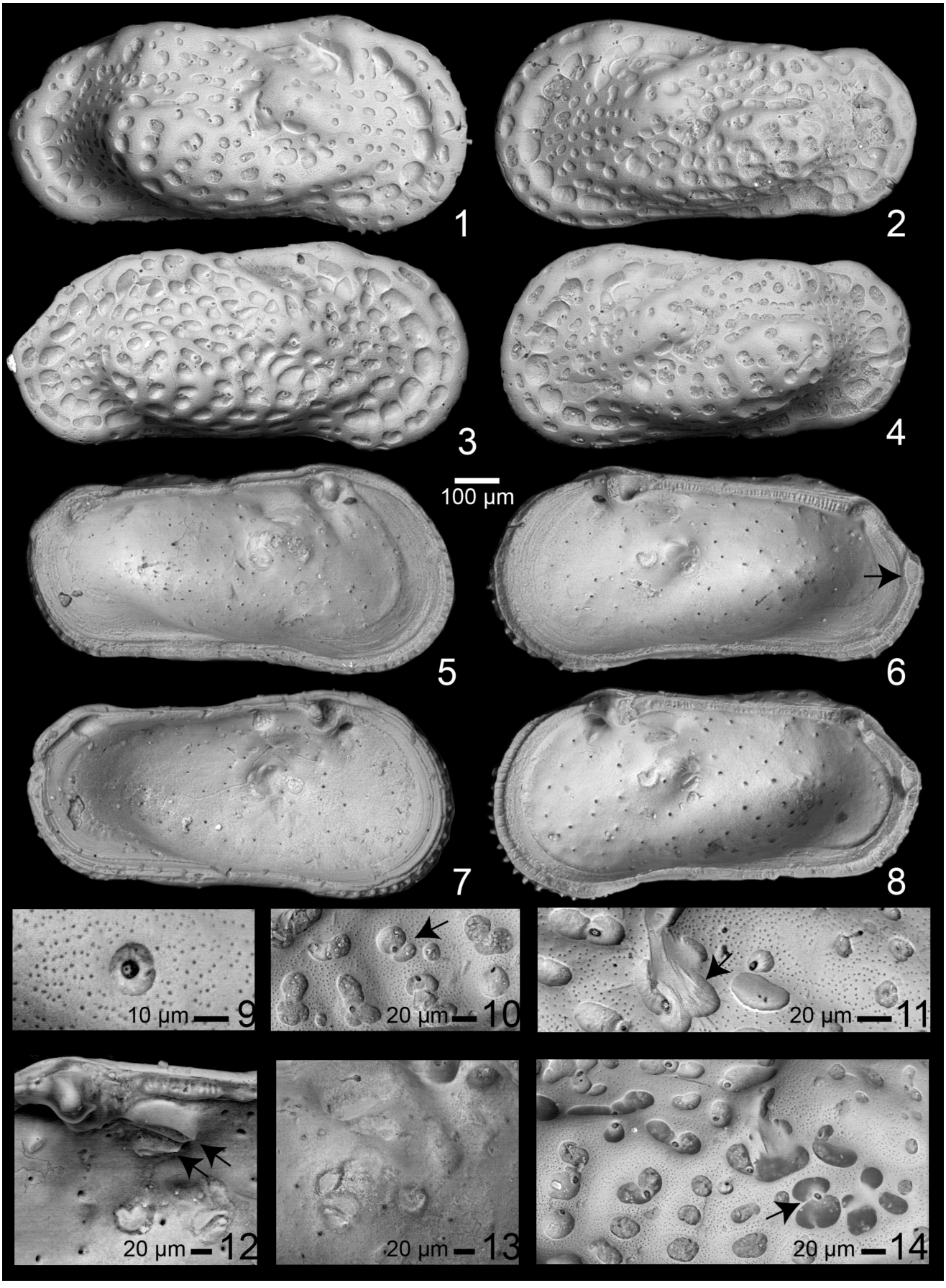
1
2
3
4
100 µm
5
6
7
8
10 µm
9
20 µm
10
20 µm
11
20 µm
12
20 µm
13
20 µm
14

Jersey coastal plain. *Geological Society of America Bulletin,* 107: 19–37.

SWAIN, F. M., unpublished. *Biostratigraphy of Cretaceous Ostracoda from wells in South Carolina* [Online]. Available: http://www.geo.umn.edu/people/profs/swain/ostra_scarolina.pdf [Accessed 2 July 2008].

SYLVESTER-BRADLEY, P. C., 1948. The ostracode genus *Cythereis*. *Journal of Paleontology,* 22: 792–797.

SYLVESTER-BRADLEY, P. C. and BENSON, R. H., 1971. Terminology for surface features in ornate ostracodes. *Lethaia,* 4: 249–286.

THOMPSON, D. E., 2011. Geologic Map of Mississippi. Jackson, MS: Mississippi Department of Environmental Quality.

TRIEBEL, E., 1940. Die Ostracoden der deutschen Kreide. III. Cytherideinae und Cytherinae aus der Unteren Kreide. *Senckenbergiana,* 22: 160–227.

TSUKAGOSHI, A., 1990. Ontogenetic change of distributional patterns of pore systems in *Cythere* species and its phylogenetic significance. *Lethaia,* 23: 225–241.

TSUKAGOSHI, A. and IKEYA, N., 1987. The ostracod genus *Cythere* O. F. Müller, 1785 and its species. *Transactions and Proceedings of the Palaeontological Society of Japan,* 148: 197–222.

VAN DEN BOLD, W. A., 1946. *Contribution to the Study of Ostracoda, with special reference to the Tertiary and Cretaceous microfauna of the Caribbean region,* Amsterdam: J. H. DeBussy.

———, 1964. Ostracoden aus der Oberkreide von Abu Rawash, Ägypten. *Palaeontographica Abteilung, Stuttgart,* 123: 111–136.

VAN MORKHOVEN, F. P. C. M., 1963. *Post-Paleozoic Ostracoda,* Amsterdam: Elsevier Publishing Company, 1–478.

VAN NIEUWENHUISE, D. and KAMES, W. H., 1976. Lithology and ostracode assemblages of the Peedee Formation at Burches Ferry, South Carolina. *South Carolina Division of Geology, Geologic Note,* 20: 73–87.

VAN VEEN, J. E., 1936. Die Cytheridae der Maastrichter Tuffkreide und der Kunrader Korallenkalkes von süd-Limburg. IV. Die gattungen *Cythereis, Archicythereis* und *Cytherideis*. *Natuurjistorisch Maandblad, Jaargang,* 25: 131–168.

WANG, D., VANNIER, J., YANG, X.-G., SUN, J., SUN, Y.-F., HAO, W.-J., TANG, Q.-Q., LIU, P. and HAN, J., 2020. Cuticular pattern replicates the pattern of epidermal cells in lowermost Cambrian scalidophoran worms. *Proceedings of the Royal Society B,* 287: 20200470.

APPENDIX 1
Sample localities.

Coon Creek Fm										
StationNumber	SampleID	Section	Tnship	Range	County	State	Quad	lat	long	Comments
2011-8-15-1	11-8-15-1 (15)	C. E/2 sec. 7	04S	04E	McNairy	TN	Ripley	35° 20' 04"	88° 25' 50"	Coon Creek type locality approximately 4.4 mile WSW of Milledgeville, TN, on west-facing bluff on Coon Creek. Sample collected approximately 15 ft above water level (very shallow).
2010-10-22-1	10-10-22-1 (505)	NW1/4 sec. 16	08S	04E	Union	MS	Sherman	34° 25' 32"	88° 53' 01"	"Blue Springs" section about 5 miles ENE of Tupelo. Section is large exposure about 1/4 mile NW of intersection of MS HWY 178 and HWY 9. Sample collected at elevation approximately 505 a.m.s.l.
Owl Creek Formation										
StationNumber	SampleID	Section	Tnship	Range	County	State	Quad	lat	long	Comments
94-5-11-7	94-5-11-7a	C. E/2 sec. 7	04S	04E	Tippah	MS	Ripley	34° 44' 53"	88° 54' 42"	Owl Creek type locality; sample collected from water level in lower part of section.
94-5-11-7	94-5-11-7 (18' below shell bed)	C. E/2 sec. 7	04S	04E	Tippah	MS	Ripley	34° 44' 53"	88° 54' 42"	Owl Creek type locality; sample collected 18 feet below shell bed in Owl Creek Formation.
2011-5-18-1	11-5-18-1 (water level)	C. E/2 sec. 7 C. E/2 sec.	04S	04E	Tippah	MS	Ripley	34° 44' 53"	88° 54' 42"	Owl Creek type locality; sample collected from water level in lower part of section.
2011-5-18-1	11-5-18-1 (5 ft)	C. E/2 sec. 7	04S	04E	Tippah	MS	Ripley	34° 44' 53"	88° 54' 42"	Owl Creek type locality; sample collected from 5 ft above water level in lower part of section.
2011-5-18-1	11-5-18-1 (15 ft)	C. E/2 sec. 7	04S	04E	Tippah	MS	Ripley	34° 44' 53"	88° 54' 42"	Owl Creek type locality; sample collected from 15 ft above water level in lower part of section.
2011-8-4-1	11-8-4-1 (water level)	C. E/2 sec. 7	04S	04E	Tippah	MS	Ripley	34° 44' 53"	88° 54' 42"	Owl Creek type locality. Sample collected from water level at main section.
Prairie Bluff Formation										
StationNumber	SampleID	Section	Tnship	Range	County	State	Quad	lat	long	Comments
94-8-12-4	94-8-12-4b	SW 1/4 sec. 15	13E	12N	Lowndes	AL	Braggs	32° 00' 37"	86° 45' 20"	Sample collected about 24 feet above road surface.
Providence Sand										
StationNumber	SampleID	Section	Tnship	Range	County	State	Quad	lat	long	Comments
91-8-14-1	91-8-14-1	NW 1/4 sec. 25	01N	23E	Bullock	AL	Perote	31° 54' 07"	85° 42' 08"	Sample collected from road cut on east side of Alabama Highway 29, approximately 1200 feet south of bridge over Double Creek, near base of hill, approximately 20 feet above elevation of bridge. Elevation of bottom of section 365 ft. a.m.s.l.

APPENDIX 1
Sample localities, continued.

2012-01-03-1	2012-01-03-1 (1)	SE 1/4 SE 1/4 sec. 15	10N	28E	Barbour	AL	Eufaula South	31° 50' 26"	85° 13' 16"	Same section as 14-5-28-1, collected on north-facing bank of Cheneyhatchee Creek.
2014-5-28-1	2014-5-28-1 (1)	SE 1/4 SE 1/4 sec. 15	10N	28E	Barbour	AL	Eufaula South	31° 50' 26"	85° 13' 16"	Same section as 12-01-03-1. Elevation of bottom of section 195 ft. a.m.s.l.
Ripley Formation										
StationNumber	SampleID	Section	Tnship	Range	County	State	Quad	lat	long	Comments
91-8-15-7	91-8-15-7	NC 1/2 sec. 26	13N	12E	Lowndes	AL	Braggs	32° 04' 34"	86° 49' 48"	Sample collected directly under bridge over Dry Cedar Creek approximately 2 feet above bottom of creek at ~ 168 ft. a.m.s.l., in lower Ripley Formation.
2019-6-20-1	2019-6-20-1 (180)	S.C. NE/4 sec. 25	13N	13E	Lowndes	AL	Braggs	32° 04' 20"	86° 48' 44"	Upper part of Ripley Fm. ~25-30 ft section, but could only reach 15 ft for samples. Elevation of bottom of section approximately 175 ft a.m.s.l. Sample collected from 180 ft a.m.s.l.
2019-6-20-1	2019-6-20-1 (185)	S.C. NE/4 sec. 25	13N	13E	Lowndes	AL	Braggs	3°2 04' 20"	86° 48' 44"	Upper part of Ripley Fm.. ~25-30 ft section, but could only reach 15 ft for samples. Elevation of bottom of section approximately 175 ft amsl. Sample collected from 185 ft a.m.s.l.
2019-6-20-1	2019-6-20-1 (190)	S.C. NE/4 sec. 25	13N	13E	Lowndes	AL	Braggs	32° 04' 20"	86° 48' 44"	Upper part of Ripley Fm. ~25-30 ft section, but could only reach 15 ft for samples. Elevation of bottom of section approximately 175 ft amsl. Sample collected from 190 ft a.m.s.l.